To be or not to be?

Mechanisms for inhibitory bouton formation and stabilization

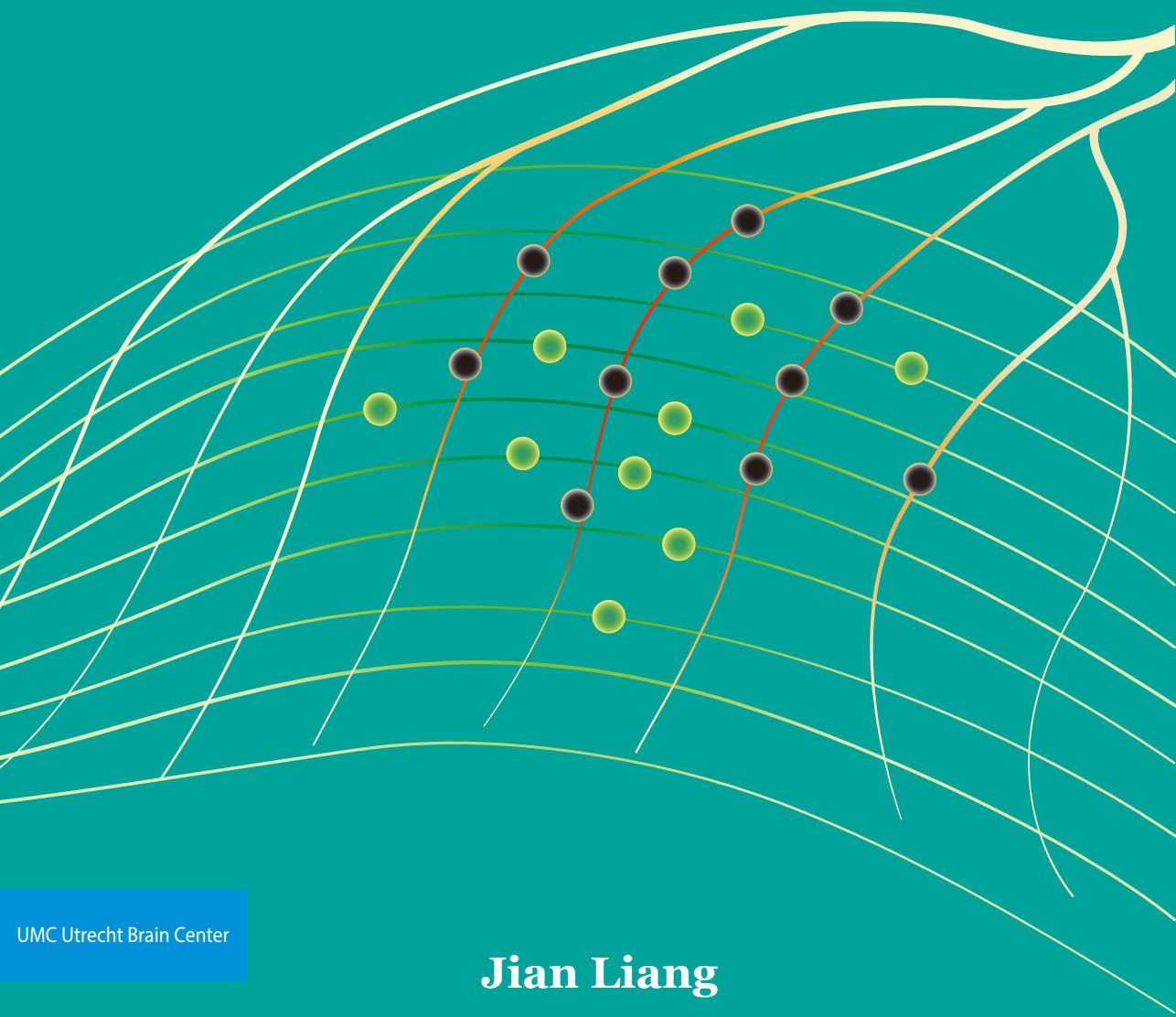

UMC Utrecht Brain Center

Jian Liang

To be or not to be?

Mechanisms for inhibitory bouton formation and stabilization

Jian Liang

ISBN: 978-94-6458-148-5

The studies described in the thesis were performed at the division of Cell Biology at the Faculty of Science of Utrecht University, The Netherlands.

Cover Desigh by Dahua and Jian Liang
Print by Ridderprint | www.ridderprint.nl

To be or not to be?

Mechanisms for inhibitory bouton formation and stabilization

Zijn of niet zijn?

Mechanismen voor de vorming en stabilisatie van remmende boutons

(met een samenvatting in het Nederlands)

Proefschrift

ter verkrijging van de graad van doctor aan de
Universiteit Utrecht
op gezag van de
rector magnificus, prof.dr. H.R.B.M. Kummeling,
ingevolge het besluit van het college voor promoties
in het openbaar te verdedigen op

woensdag 13 april 2022 des ochtends te 10.15 uur

door

Jian Liang

geboren op 5 december 1989
te Sichuan, China

Promotor:
Prof. dr. **Anna Akhmanova**

Copromotor:
Dr. **Corette J. Wierenga**

Table of Contents

Chapter 1

General introduction

Jian Liang

Cell Biology, Department of Biology, Faculty of Science, Utrecht University, 3584 CH Utrecht, The Netherlands

The mammalian brain is the most fascinating organ. It consists of billions of neurons (Herculano-Houzel, 2009), which are specialized cells with long and thin branched structures: dendrites and axons. Neurons receive synaptic input signals from other neurons via their dendrites and send signals via their axons. This unidirectional signal transduction makes neurons so unique. The large majority of neurons in the brain are excitatory neurons which mostly use glutamate as neurotransmitter, while around 10-20% of the neurons are inhibitory neurons, and they mainly use GABA as neurotransmitter. Despite being clearly outnumbered by the excitatory neurons, the inhibitory neurons play several important roles in shaping brain network activity and neuronal connectivity (Flores and Méndez, 2014; Chiu et al., 2019; Herstel and Wierenga, 2021). Dysfunction of inhibitory neurons is at the basis of many brain diseases, including autism spectrum disorders, intellectual disability, Fragile X syndrome and schizophrenia (Lewis et al., 2005; Mullins et al., 2016).

Communication between neurons is compartmentalized in synapses. Synapses consist of three parts: a presynaptic terminal - from here on called bouton - , the synaptic cleft, and a postsynaptic terminal (Sheng and Hoogenraad, 2007). When a presynaptic neuron fires an action potential, chemical neurotransmitters are released from the presynaptic axonal terminal. The released neurotransmitter diffuses across the synaptic cleft and activates receptors in the postsynaptic dendrite. Postsynaptic receptors are ligand-gated ion channels which transform the chemical neurotransmission signal into an electric signal, a small alteration of the membrane potential of the postsynaptic neuron. In case of excitatory transmission, the membrane potential of the postsynaptic neuron depolarizes. Thereby the postsynaptic neuron is more likely to fire an action potential. In contrast, inhibitory neurotransmitters hyperpolarize the membrane of the postsynaptic neuron, reducing the probability to fire an action potential.

The strength of both inhibitory and excitatory synaptic transmission is not fixed but can be adapted in an activity-dependent manner. This capacity for adaptation, generally termed synaptic plasticity, is thought to be the principal mechanism in the brain for learning and memory formation. Synaptic plasticity includes changes in synaptic strength and structure, including changes in the number of synapses. Therefore, understanding the mechanism underlying synapse formation and synaptic plasticity is essential for unraveling basic biological processes such as learning and memory formation, and will provide

important insight in neurodevelopmental diseases.

The structure of inhibitory synapses

Although neurons are capable of forming electrical synapses via gap junctions, the majority of synapses in the brain are chemical (Pereda, 2014). 80-90% of chemical synapses are excitatory synapses, which use glutamate as neurotransmitter and serve to activate the postsynaptic neuron. In contrast, inhibitory synapses utilize gamma-aminobutyric acid (GABA) as neurotransmitter and serve to decrease the membrane potential, and thereby inhibit activation of the postsynaptic neurons. Inhibitory synapses are typically formed directly onto the dendritic shaft of the postsynaptic neuron (Rudy et al., 2011; Kubota et al., 2016; Wamsley and Fishell, 2017), while excitatory synapses are often formed on small dendritic protrusions called spines (Wierenga et al., 2008). Excitatory synapses can be recognized under the electron microscope from their asymmetric axonic-dendritic spine ultrastructure, which contains a dense, mesh-like postsynaptic density (Harris and Weinberg, 2012; Tao et al., 2018). In contrast, inhibitory synapses have a symmetric ultrastructure, with weaker, sheet-like, presynaptic boutons and postsynaptic densities (Harris and Weinberg, 2012; Nakamoto et al., 2014; Tao et al., 2018).

The presynaptic bouton is a small specialized subcellular structure, which can be recognized as a swelling of the axon. An average bouton made by pyramidal cells is around 1 µm in diameter, and around 2-3 µm in Purkinje cells (Kawaguchi, 2019). A single bouton contains hundreds of synaptic vesicles and other organelles (De Paola et al., 2003, 2006). Morphology of axonal boutons is highly diverse: some axons show high density of small boutons, while other axons have a lower bouton density, but larger boutons. These differences may result from the diversity neuron cell types and neuronal developmental stages (Morimoto et al., 2018).

Axonal boutons are filled with synaptic neurotransmitter vesicles and contain active zone proteins, scaffolding proteins and the neurotransmitter release machinery (Fig. 1). Excitatory and inhibitory presynaptic terminals have a similar molecular organization of the active zone, except for the neurotransmitter (glutamate versus GABA) inside the synaptic vesicles (Murthy and De Camilli, 2003; Takamori et al., 2006; Südhof, 2012). The arrival of an action potential triggers synaptic vesicle fusion, and release of

neurotransmitters. The presence of a cluster of synaptic vesicles is the most prominent feature of presynaptic terminals, and they can be subdivided into three 'pools' of vesicles: resting pool, recycling pool and readily releasable pool (Alabi and Tsien, 2012). These vesicles are located at the active zone, which is discernable with electron microscopy as an electron-dense area of the presynaptic membrane (Siksou et al., 2007; Harris and Weinberg, 2012). The active zone is the specialized structure for docking, priming, and release of synaptic vesicles. Bassoon and piccolo are the most abundant active zone proteins (Waites et al., 2013; Ackermann et al., 2015). The molecular composition of the active zone is regulated by neuronal activity. For instance, neuronal inactivity results in the diffusion of bassoon clusters within the active zone and actin depolymerization at the active zone to strengthen neurotransmitter release machinery (Glebov et al., 2017). The actin cytoskeleton is highly dynamic and displays ongoing polymerization and depolymerization, which mediates presynaptic structural plasticity (Cingolani and Goda, 2008). In addition, boutons can be the site for microtubule nucleation, which may be important for presynaptic organization and synapse maturation (Qu et al., 2019). Several cellular organelles are located at presynaptic terminals, including mitochondria, endosomes, and polyribosomes. These organelles can move along the axonal shaft and can move between synaptic boutons, which can be monitored with live imaging (Frias and Wierenga, 2013; Wierenga, 2017; Lees et al., 2020). These cellular organelles are important for synaptic plasticity (Smit-Rigter et al., 2016), or axonal regeneration (Han et al., 2016; Patrón and Zinsmaier, 2016).

The synaptic cleft is organized by trans-synaptic adhesion molecules, including neurexins and neuroligins, leucine-rich repeat proteins, immunoglobulin (Ig) family proteins, receptor phosphotyrosine kinases and phosphatases (Chua et al., 2010; Missler et al., 2012; De Wit and Ghosh, 2016). Pairs of these proteins bind and connect the pre- and postsynaptic compartments. This binding, which is often highly specific, is thought to be important not only for synapse formation, but also for modulating synaptic maturation and function (Elia et al., 2006; Mendez et al., 2010; Nikitczuk et al., 2014). Synaptic adhesion proteins play important roles in inhibitory synapse formation and development (Fig. 1). For instance, neuroligin 2 (NL2) is specifically expressed at the postsynaptic side of inhibitory synapses (Varoqueaux et al., 2004; Craig and Kang, 2007). When neurons are cocultured with non-neuron cells expressing NL2, NL2 is sufficient to induce presynaptic terminal differentiation, and synaptic inhibition is impaired in neurons that lack NL2

(Scheiffele et al., 2000; Liang et al., 2015).

The $GABA_A$ receptors are pentameric ligand-gated ion channels located at inhibitory postsynaptic terminal to mediate fast inhibition (Fig. 1). With the help of electron microscopy and super-resolution microscopy, the architecture of the postsynaptic terminal has been largely resolved. Directly underneath the postsynaptic membrane scaffold proteins are highly enriched. Gephyrin is the main scaffold protein at inhibitory synapses. Gephyrin closely regulates the number, location and clustering of postsynaptic $GABA_A$ receptors (Essrich et al., 1998; Kneussel et al., 1999). The crucial role of the number and nano-organization of postsynaptic neurotransmitter receptors for synapse function and plasticity has been studied in greatest detail at excitatory synapses. For instance, it was shown that AMPARs are more localized towards the periphery of the postsynaptic density (PSD) at excitatory synapses, while NMDARs have a more central location (Kharazia and Weinberg, 1997; Chen et al., 2008; Tang et al., 2016). This distribution facilitates the rapid trafficking of AMPARs from PSD periphery to its center during long-term potentiation. After translocation, more receptors will become activated when glutamate is released from the presynaptic active zone, resulting in a larger postsynaptic response. More recently, super-resolution microscopy has revealed that AMPARs display a clustered distribution within the PSD, forming postsynaptic nanodomains (MacGillavry et al., 2013; Nair et al., 2013). Additionally, presynaptic release machinery and postsynaptic receptors can form trans-synaptic nanocolumn to fast the efficiency of neuronal signal transduction (Tang et al., 2016). These nanodomains are important for efficient neuronal communication and the distribution of these nanodomains can be modulated. Like glutamate receptors, $GABA_A$ receptors and gephyrin also form nanodomains and trans-synaptic nanocolumns to prompt information transfer efficiency (Specht et al., 2013; Crosby et al., 2019). Changes in $GABA_A$ receptors play an important role in shaping brain network activity (Luscher et al., 2011; Pennacchietti et al., 2017; Yamasaki et al., 2017; Crosby et al., 2019; Scott and Aricescu, 2019).

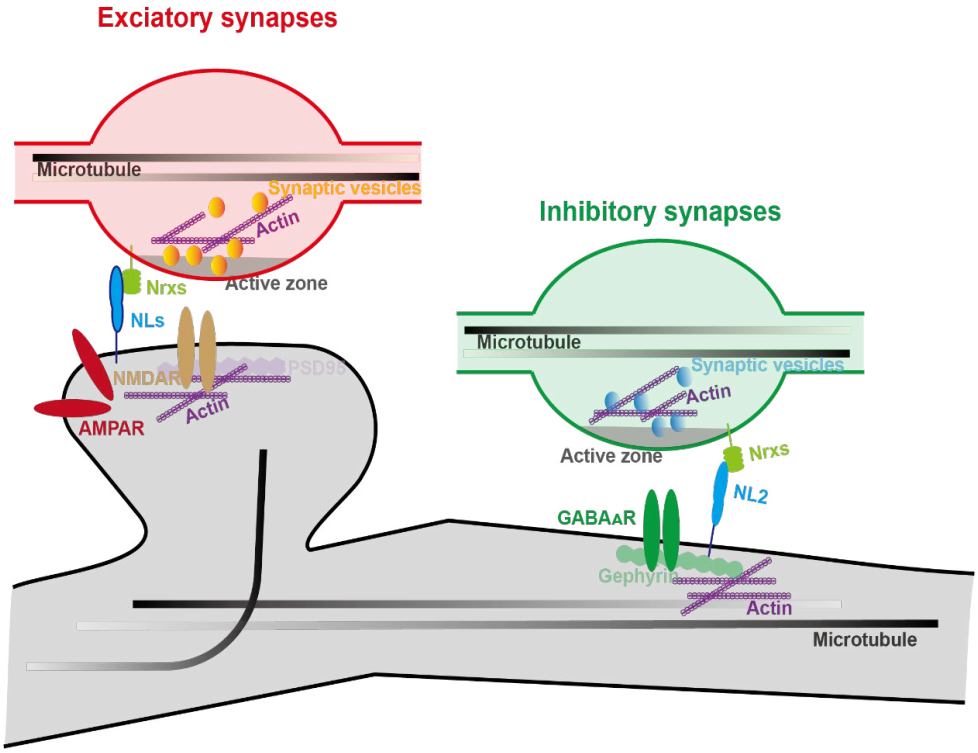

Figure 1 Molecular components of excitatory and inhibitory synapses
The schematic diagram shows a subset of proteins which decorate the excitatory synapse (left, red) and inhibitory synapse (right, green). These proteins include presynaptic active zone proteins, synaptic vesicles, neurotransmitter release machinery (not shown here); synaptic adhesion proteins, like the neurexins-neuroligins complex; postsynaptic receptors for neurotransmitters, scaffold proteins, and cytoskeleton proteins in both pre and postsynaptic terminals.

Inhibitory synapse formation and dynamics

As described above, inhibitory synapses are specialized cellular structures with complex molecular components. Building these structures is not a plug-and-play process, but follows a dynamic, multiple-step process, which is tightly orchestrated temporally and spatially (Sytnyk et al., 2004; Dobie and Craig, 2011; Wierenga, 2017; Favuzzi and Rico, 2018). Whereas some types of inhibitory neurons make synapses specifically with the soma, others target the axonal initial segments or dendrites of their target neurons (Pelkey et al., 2017). New inhibitory synapses can be formed at dendritic locations where an inhibitory axon is crossing. This requisite for a pre-existing contact site is very different from excitatory synapses, where new synapses can be formed by outgrowth of dendritic filopodia (Sytnyk et al., 2004; Wierenga

et al., 2008). The newly formed bouton is first unstable (it can disappear and reappear several times), but it can eventually stabilize and recruit postsynaptic proteins to grow out to a functional, mature inhibitory synapse. More and more proteins and signaling molecules are being uncovered that play a role in inhibitory synapse formation, stabilization, and maturation, and this was also the main focus of the research described in this thesis.

Synaptic adhesion proteins are well-known organizers for initiating synaptic recognition and promoting synapse development (Craig and Kang, 2007; De Wit and Ghosh, 2016; Lu et al., 2017; Favuzzi and Rico, 2018). Adhesion molecules recruit synaptic vesicles and neurotransmitter release machinery on the presynaptic side, and scaffold proteins and receptors on the postsynaptic side. Many synaptic adhesion proteins complexes are involved in regulating inhibitory synapse development (Graf et al., 2004; Craig and Kang, 2007; De Wit and Ghosh, 2016). As mentioned above, Neuroligin 2 (NL2) is specific for the postsynaptic membrane and mediates inhibitory synapse formation (Varoqueaux et al., 2004; Craig and Kang, 2007). Conditional knockout of NL2 impairs inhibitory synaptic transmission and induces anxiety-like behavior (Varoqueaux et al., 2004; Blundell et al., 2009; Gibson et al., 2009). Other synaptic proteins like Slitrk3 (ST3) cooperate with NL2 to promote inhibitory synapse development (Li et al., 2017).

Whereas the dendrite is actively involved in excitatory synapse formation, the inhibitory axon is the central player in the formation of inhibitory synapses (Wierenga et al., 2008). Live imaging studies, including from our lab, revealed that inhibitory boutons are highly dynamic structures. During time lapse imaging, boutons are appearing and disappearing over a time course of tens of minutes to hours (Frias and Wierenga, 2013; Schuemann et al., 2013; Wierenga, 2017). Bouton dynamics vary widely between cell types, developmental stage, and brain region. For instance, catecholaminergic axonal boutons have higher bouton turnover than pyramidal neurons (Morimoto et al., 2018). In general, boutons are more dynamic in younger brain tissue and less dynamic in adulthood (Ruiter et al., 2021). Interestingly, aging mice show high bouton turnover rate in excitatory axons (Grillo et al., 2013). Not all boutons form functional synapses. Only stable boutons that contain presynaptic markers, and are associated with postsynaptic receptors, represent functional synapses (Wierenga et al., 2008; Schuemann et al., 2013). The non-stable boutons presumably present a state transition between bouton initiation, pruning or maturation. This will be further described in this thesis.

Inhibitory synapse structural plasticity

Neuronal plasticity refers to the capacity of the nervous system to change its function and structure in response to internal and external cues, including environmental influences and pathological conditions. Neuronal plasticity comprises the genesis and death of neurons, the remodeling of axons and dendrites, the removal and addition of synapses, and the plasticity of neuronal excitability and synaptic strength (Frick and Johnston, 2005). Synaptic plasticity is perhaps the most important aspect of neuronal plasticity and may be the fundamental basis for learning and memory. Synaptic plasticity is an overarching term which include Hebbian processes such as long-term or short-term potentiation and depression and homeostatic plasticity processes such as synaptic scaling. (Turrigiano, 2008, 2017; Castillo et al., 2011; Lee and Kirkwood, 2019). Although the excitatory synapses have received the bulk of the attention of neuroscience research in the past, it is now clear that learning also involves critical changes in inhibitory synapses and impaired inhibitory plasticity is linked to several neuronal disorders (Flores and Méndez, 2014; Chiu et al., 2019; Herstel and Wierenga, 2021).

Inhibitory synapses are capable to adapt via structural modifications as remodeling of inhibitory axons or dendrites, and as inhibitory synapse formation or elimination or via short or long term modulations in functional changes in synaptic strength (Lee et al., 2008; Knodel et al., 2011; Wierenga, 2017; Boivin and Nedivi, 2018; Eavri et al., 2018). Synaptic strength can be modulated by short-term or long-term regulation of GABA release (Castillo et al., 2011; Méndez and Bacci, 2011; Capogna et al., 2020), as well as by activity-dependent postsynaptic reorganization (Flores and Méndez, 2014; Chiu et al., 2019; Herstel and Wierenga, 2021). This involves the regulation of intracellular trafficking and membrane diffusion of receptors, for instance via scaffold proteins (Muir et al., 2010; Petrini et al., 2014). Structural plasticity at the inhibitory presynapses remains relatively less explored (Frias and Wierenga, 2013; Schuemann et al., 2013).

Though it is widely recognized that learning involves structural plasticity of spines, where excitatory synapses are located (Caroni et al., 2012; Fu et al., 2012; Yang et al., 2018), inhibitory synapses change during learning as well. During learning dendritically located inhibitory boutons are decreased in number, and perisomatic inhibitory bouton density increases (Chen et al., 2015). Also in other studies, coordinated changes in excitatory and inhibitory synapses are found during learning (Keck et al., 2011; Donato et

al., 2013; D'amour and Froemke, 2015; Keller et al., 2020). This demonstrates that structural plasticity at excitatory and inhibitory synapses are tightly coordinated to facilitate learning.

A previous study from our lab has shown that strong local excitatory activity can trigger the formation of a new inhibitory bouton at the same dendrite (Hu et al., 2019) (Fig. 2). This process is mediated by the endogenous cannabinoid 2-AG, which is synthesized by the dendrite and activates endocannabinoid type 1 (CB1) receptors at the inhibitory axon. This shows that the dendrite can actively regulate the local coordination of excitatory and inhibitory synaptic inputs. However, the underlying molecular mechanism and signal cascades after receptor activation remained unclear and this was an important part of my PhD research. In the following part, I will introduce the endocannabinoid signal system.

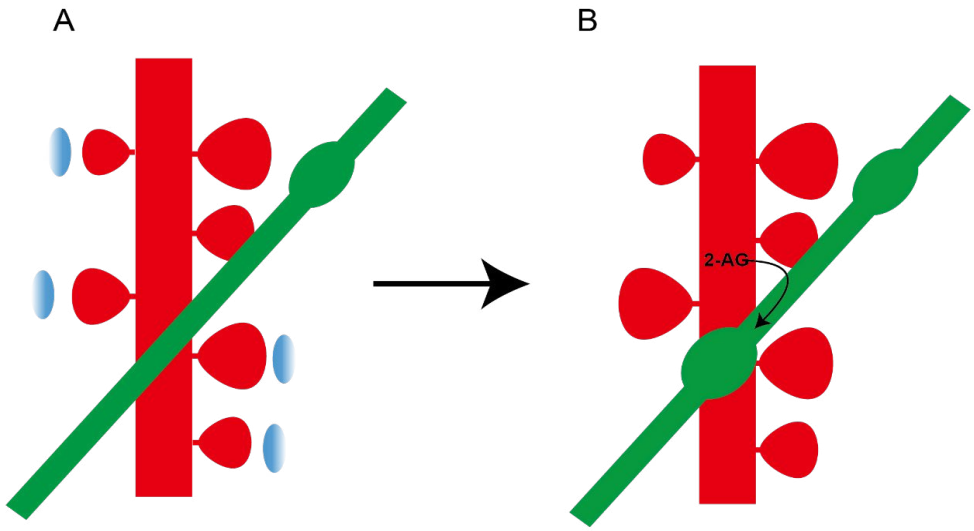

Figure 2. Endocannabinoid 2-AG promotes new bouton formation
This cartoon shows that local activation of spines in excitatory neurons induces inhibitory bouton formation at the axon-dendrite crossing site This process is mediated by the endocannabinoid 2-AG. Glutamate uncaging at 4 spines (indicated in blue, A), results in the formation of a new bouton occurs at the crossing site (B). Endogenous cannabinoid 2-AG is synthesized and released from the dendrite upon stimulation of spines to trigger nearby inhibitory bouton formation. Adapted from (Hu et al., 2019).

The endocannabinoid system

Endocannabinoids are probably the most well-known neuromodulators

of brain function, acting at the synaptic, neuronal and behavioral level (Kano et al., 2009; Castillo et al., 2012a; Busquets-Garcia et al., 2018). The endocannabinoid system includes enzymes for endocannabinoid synthesis and degradation, receptors and downstream effectors (Turu and Hunyady, 2010; Lu and MacKie, 2016). Dysfunction of the endocannabinoid system affects synaptic plasticity and can trigger abnormal behavior (Karhson et al., 2016; Busquets-Garcia et al., 2018; Hurd et al., 2019). Endocannabinoid signaling is implicated in various neuronal degeneration diseases, including Parkinson's disease and Huntington's disease (Hashimotodani et al., 2007; Mulder et al., 2011; Aso and Ferrer, 2014; Dhopeshwarkar and Mackie, 2014; Basavarajappa et al., 2017; Kendall and Yudowski, 2017).

The endocannabinoid system is named after its best-known exogenous ligand, which is cannabis. Humans have a long history of using plant cannabis, also known as marijuana. As it was found to be functional to reduce pain, nausea, and anxiety, helpful to promote appetite and sleep and to relax muscles, marijuana has been widely applied for medical purpose already in ancient times (Mechoulam and Hanuš, 2001). The primary psychoactive ingredient of the plant cannabis is Δ^9-tetrahydrocannabinol (THC), which was isolated in the 60's (Mechoulam and Gaoni, 1965), and is currently also used in clinical trials. In addition to THC, many more cannabinoids have been discovered. Because its psychoactive effects limit the clinical application for THC, cannabidiol (CBD), the major non-psychoactive cannabinoid in cannabis plants is often used for medical purposes in various disorders (Kicman and Toczek, 2020).

The discovery of endogenous cannabinoids and their receptors in the late 80's and 90's increased the attention on the endocannabinoids system. The endocannabinoid system consists of the two major endogenous cannabinoids- 2-AG and anandamide (AEA), the endocannabinoid receptors CB1 and CB2 and the enzymes for synthesis and degradation (Fig. 3). AEA (Anandamide) was the first endogenous cannabinoid that was discovered (Devane et al., 1992). However, as it could not replicate THC's effect, further studies revealed a second endogenous cannabinoid, 2-AG (2-Arachidonoylglycerol) (Mechoulam et al., 1995; Sugiura et al., 1995). Already before, the endocannabinoid receptor type 1 (CB1R) was cloned by Lisa A. Matsuda and colleges in 1990, followed by the type 2 receptor (CB2R) by Sean Munro and colleges in 1993 (Matsuda et al., 1990; Munro et al., 1993). In addition to CB1 and CB2 receptors, the endocannabinoid AEA can also interact with other receptors, like the transient receptor potential

TRPV1, and peroxisome proliferator-activated receptor γ (PPARγ) (Bouaboula et al., 2005; O'Sullivan, 2007; Chávez et al., 2010; Muller et al., 2019). Pharmacological and biochemical characterization demonstrated that AEA is a high-affinity ligand for CB1R, while it binds with lower affinity to CB2R. In contrast, 2-AG activates both CB1R and CB2R with roughly equal affinity. 2-AG is more abundant compared with AEA in the brain, indicating that 2-AG is the primary endogenous cannabinoids (Freund et al., 2003; Murataeva et al., 2014). Furthermore, several synthetic cannabinoids have been generated. For instance, CP 55940, and WIN55212-2 are widely used chemical agonists for endocannabinoids receptors, which have high binding affinity, and are stable in biological conditions. The diversity of ligands and receptors make endocannabinoid signaling in the brain quite complex (Zygmunt et al., 1999; Bouaboula et al., 2005; O'Sullivan, 2007; Chávez et al., 2010; Muller et al., 2019).

The components of endocannabinoid system

In the following, I mainly focus on 2-AG and CB1 receptors, which is most relevant for my PhD research. For a complete overview of the endocannabinoid system, many excellent reviews are available (Kano et al., 2009; Turu and Hunyady, 2010; Castillo et al., 2012b; Lu and MacKie, 2016; Zou and Kumar, 2018).

2-AG is produced by the enzyme diacylglycerol lipase (DAGL) from 2-arachidonoyl-containing phospholipids in the membrane (Bisogno et al., 2003; Gao et al., 2010). Importantly, 2-AG is synthesized on demand, in response to cell depolarization or neuronal activity (Hashimotodani et al., 2007, 2013; Kano et al., 2009; Castillo et al., 2012b). Endocannabinoids are lipids and therefore highly hydrophilic, which severely limits diffusion, especially extracellularly. It remains unclear how endocannabinoids are transported from the postsynaptic dendrite to the presynaptic axon, until recently data shows that synuclein mediated endocannabinoids exocytosis and depended on SNARE complex (Albarran et al., 2021) However, it is clear that dendritically produced endocannabinoids can activate CB1 receptors that are located at the presynaptic terminals and axons of other neurons (Castillo et al., 2012b). After being produced, endocannabinoids are rapidly degraded via several 2-AG hydrolysis enzymes including monoacylglycerol lipase (MGL), alpha/beta domain containing hydrolase 6 (ABHD6), and alpha/beta domain containing hydrolase 12 (ABHD12) (Blankman et al., 2007), terminating the endocannabinoid signaling. In addition, 2-AG can be

oxidized by cyclooxygenase-2 (COX-2) which is also followed by hydrolysis (Hermanson et al., 2014). Interestingly, the different 2-AG degradation enzymes have different subcellular locations, which indicates that there are multiple mechanisms to regulate the endocannabinoids signal. Thereby, MGL is mostly located at presynaptic terminals to control 2-AG modulation of synaptic release properties. For instance, activity of MGL strongly regulates tonic activation of presynaptic CB1 receptors at perisomatic inhibitory synapses in the hippocampal CA1 area (Lee et al., 2015; Lenkey et al., 2015). This suggests that dendritic endocannabinoid signaling is tightly regulated by local synthesis and degradation.

The CB1 receptor is the major endogenous cannabinoid receptor mediating retrograde modulation of synaptic transmission. CB1 receptor is coded by the *CNR1* gene and contains ~470 amino acids in humans and more than 95% of the amino acid sequence is identical to other species (Agrawal and Lynskey, 2009; Hartman et al., 2009). Interestingly, CB1 receptors have different isoforms from alternative splicing, with possible different functions (Ryberg et al., 2005; Marti-Solano et al., 2020). CB1 receptors are mainly expressed in the central nervous system, including in brain regions involved in cognition and motivation behavior, such as, hippocampus, cerebellum, cortex, and basal ganglia (Herkenham et al., 1990; Mackie, 2005). The expression of CB1 receptors in the brain is not homogenous. For instance, CB1 receptors are enriched in the cell layers of CA1 and CA3 in the hippocampus (Lenkey et al., 2015). At the cellular level, CB1 receptor is highly expressed by a specific subtype of inhibitory neurons, which also express cholecystokinin (CCK). In these neurons, CB1 receptors are localized to the axonal shaft and presynaptic terminals (Katona et al., 1999; Dudok et al., 2015). In addition, CB1 receptors are also expressed by excitatory neurons, although the expression level is much lower compared to inhibitory neurons (Katona et al., 2006). Furthermore, CB1 receptors at astrocytes may also regulate synaptic plasticity and memory formation (Navarrete and Araque, 2008; Han et al., 2012). With super-resolution microscopy, the precise location and dynamics of CB1 receptor were resolved. This revealed that CB1 receptors are homogenously distributed at boutons and axonal shaft of inhibitory axons, even after receptor activation (Dudok et al., 2015). The localization of axonal CB1 receptors is highly corelated with membrane-associated periodic skeleton (MPS), which is proposed to help signal transduction (Zhou et al., 2019; Li et al., 2020). Intriguingly, CB1 receptors are not only localized in the cell membrane, but also in intracellular membranes of mitochondria and endosomes (Bénard et al., 2012; Hebert-Chatelain et al., 2016; Busquets-

Garcia et al., 2018; Zou and Kumar, 2018).

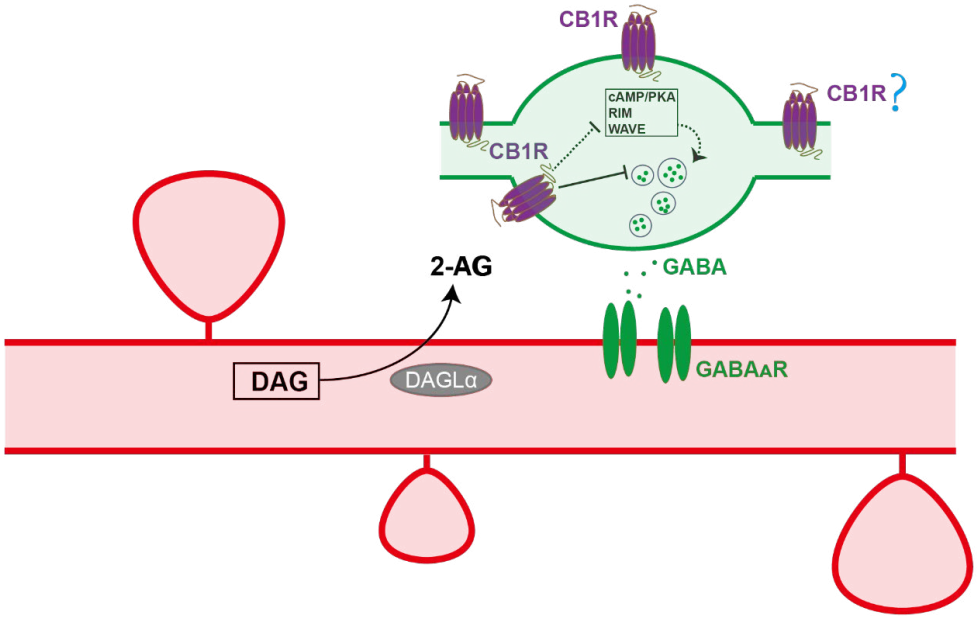

Figure 3 Endocannabinoid signaling at inhibitory synapses
Overview of endocannabinoid (2-AG) signal in inhibitory synapse. Endogenous cannabinoid 2-AG is synthesized from diacylglycerol (DAG) via diacylglycerol lipase (DAGL). Upon activity-dependent synthesis and release from the postsynaptic dendrite, it can retrogradely activate presynaptic endocannabinoid type 1 (CB1) receptors and recruit various downstream effectors to inhibit GABA release (inhibitory synapse). The functions and signaling pathways downstream of axonal shaft located CB1 receptors (blue question mark) are the focus of chapter 3 in my PhD thesis.

Endocannabinoid signaling at synapses

The most well-known function of endocannabinoids is to serve as retrograde messenger to reduce neurotransmitter release. Endocannabinoids are synthesized and released from postsynaptic dendrites in response to elevated intracellular calcium levels (Ohno-Shosaku et al., 2001), for instance after synaptic activation. Released endocannabinoids activate presynaptic CB1 receptors (Kano et al., 2009; Castillo et al., 2012b). CB1 receptors are G-protein coupled receptors (GPCRs). Heterotrimeric G proteins contain three subunits, α, and βγ. Upon endocannabinoid binding, the Gα subunit gets activated via a transition from the guanosine diphosphate (GDP) state to the guanosine triphosphate (GTP) state. Active Gα will dissociate from the heteromeric G protein complex, and affect multiple downstream

effectors, including enzymes and ion channels. Typically, the CB1 receptor is a $G_{i/o}$ coupled receptor. Activated $G\alpha_{i/o}$ reduces cellular cyclic adenosine monophosphate (cAMP) levels, and thereby inhibits RIM phosphorylation and neurotransmitter release. In parallel, CB1 receptor activation can also inhibit voltage-dependent calcium channels (VGCC) and activate inward-rectifying K+ channels via their Gβγ subunits. All these presynaptic pathways converge to weakening of synaptic transmission (Kano et al., 2009; Castillo et al., 2012a).

In addition, activated CB1 receptors can also interact with other G proteins, and can signal via G-protein independent pathways. For instance, CB1 receptor can couple with G_s protein, which directly opposes the typical CB1-G_i signal pathway, by increasing intracellular cAMP levels and PKA activity (Cui et al., 2016; Finlay et al., 2017; Wang et al., 2017)(. Stimulated CB1 receptors can also interact with G_q proteins to increase intracellular calcium concentration and they can interact with $G_{12/13}$ to guide axon growth (Lauckner et al., 2005; Roland et al., 2014). Persistent activation of CB1 receptors results in receptor uncoupling from G proteins, inducing receptor internalization and desensitization via G-protein-coupled receptor (GPCR) kinases (GRKs) and β-arrestins mediated process. Internalized CB1 receptors can interact with β-arrestins and exert G-protein independent signal cascades (Nguyen et al., 2012; Delgado-Peraza et al., 2016).

Endocannabinoid-mediated synaptic plasticity

The best-known physiological effect of the endocannabinoid system is to inhibit neurotransmitters release for several minutes (Kreitzer and Regehr, 2001; Ohno-Shosaku et al., 2001). Depolarization-induced suppression of inhibition (DSI) is the earliest verified function of endocannabinoids as a retrograde signal. The mechanism of DSI is via βγ subunits, which inhibit calcium influx via voltage-gated calcium channels (VGCCs) (Wilson et al., 2001), as described in more detail above. Later, it was also shown that depolarization-induced suppression of excitation (DSE) is also mediated by endocannabinoids, although excitatory synapses appear less sensitive (Kreitzer and Regehr, 2001). DSI and DSE are present in many brain regions and therefore represent a general form of short-term modulation of synaptic strength (Castillo et al., 2012b).

Endocannabinoids also induce long-term suppression of GABA transmission (eCB-LTD, but the mechanism is not fully understood (Castillo et al., 2012b;

Monday et al., 2020). The downstream effectors involved in eCB-LTD include the active zone protein RIM1a, presynaptic cAMP/PKA activity and protein synthesis (Chevaleyre and Castillo, 2003; Chevaleyre et al., 2007; Hashimotodani et al., 2017).

Normally, endocannabinoids are synthesized and released by principal excitatory neurons, and act as a retrograde signal to regulate synaptic transmission of incoming inputs. Interestingly, it was also shown that interneurons including CCK-expressing neurons can synthesize endocannabinoids to hyperpolarize itself via activation of G-protein-coupled inward rectifier potassium (GIRK) conductance (Bacci et al., 2004). This phenomenon is called slow-self inhibition, as it results from repeated firing by the CCK-neurons themselves (Glickfeld and Scanziani, 2005; Marinelli et al., 2008).

Scope of this thesis

During my PhD, I have focused on the mechanisms of inhibitory synapses formation upon CB1 receptors activation. I have used high-resolution two photon microscopy to monitor the appearance, disappearance, and reappearance of boutons on inhibitory axons in living brain slices. In these live imaging experiments, we followed inhibitory bouton dynamics over several hours and demonstrated that inhibitory boutons are highly dynamic structures. I have used a combination of pharmacological, viral and chemogenetic approaches to manipulate inhibitory bouton dynamics and to unravel underlying pathways. **In chapter 2**, I describe that Sema4D, the class 4 semaphorin, is necessary for inhibitory bouton stabilization. We showed that Sema4D-induced bouton stabilization requires activation of the receptor tyrosine kinase MET and involves activity-dependent actin remodeling. **In chapter 3**, I discovered that activation of CB1 receptor triggers new inhibitory bouton formation via an increase in intracellular cAMP/PKA activity, which suggests that axonal CB1 receptors are coupled to G_s rather than G_i protein signaling. **In chapter 4**, I found that repeated activation of CB1 receptor with WIN, but not 2-AG, can induce CB1 receptor internalization, and alter membrane expression of CB1 receptors. Interestingly, WIN-induced CB1 receptor internalization and expression pattern changes occur in slices, but they appear absent in cultured primary neurons. **In chapter 5**, I discuss the molecular identity of inhibitory boutons and factors which may be involved in regulating inhibitory bouton dynamics. Furthermore, I further discuss the multiple downstream signal cascades upon CB1 receptors activation, and functional selectivity of endocannabinoid signaling.

Reference

Ackermann F, Waites CL, Garner CC (2015) Presynaptic active zones in invertebrates and vertebrates. EMBO Rep 16:923–938.

Agrawal A, Lynskey MT (2009) Candidate genes for cannabis use disorders: Findings, challenges and directions. Addiction 104:518–532.

Alabi ARA, Tsien RW (2012) Synaptic vesicle pools and dynamics. Cold Spring Harb Perspect Biol 4.

Albarran E, Sun Y, Liu Y, Raju K, Dong A, Li Y, Wang S, Südhof TC, Ding JB (2021) Postsynaptic synucleins mediate vesicular exocytosis of endocannabinoids. bioRxiv:2021.10.04.462870 Available at: https://www.biorxiv.org/content/10.1101/2021.10.04.462870v1%0Ahttps://www.biorxiv.org/content/10.1101/2021.10.04.462870v1.abstract.

Aso E, Ferrer I (2014) Cannabinoids for treatment of alzheimer's disease: Moving toward the clinic. Front Pharmacol 5 MAR:1–11.

Bacci A, Huguenard JR, Prince DA (2004) Long-lasting self-inhibition of neocortical interneurons mediated by endocannabinoids. Nature 431:312–316.

Basavarajappa BS, Shivakumar M, Joshi V, Subbanna S (2017) Endocannabinoid system in neurodegenerative disorders. J Neurochem 142:624–648.

Bénard G et al. (2012) Mitochondrial CB 1 receptors regulate neuronal energy metabolism. Nat Neurosci 15:558–564.

Bisogno T, Howell F, Williams G, Minassi A, Cascio MG, Ligresti A, Matias I, Schiano-Moriello A, Paul P, Williams EJ, Gangadbaran U, Hobbs C, Di Marzo V, Doherty P (2003) Cloning of the first sn1-DAG lipases points to the spatial and temporal regulation of endocannabinoid signaling in the brain. J Cell Biol 163:463–468.

Blankman JL, Simon GM, Cravatt BF (2007) A Comprehensive Profile of Brain Enzymes that Hydrolyze the Endocannabinoid 2-Arachidonoylglycerol. Chem Biol 14:1347–1356.

Blundell J, Tabuchi K, Bolliger MF, Blaiss CA, Brose N, Liu X, Südhof TC, Powell CM (2009) Increased anxiety-like behavior in mice lacking the inhibitory synapse cell adhesion molecule neuroligin 2. Genes, Brain Behav 8:114–126.

Boivin JR, Nedivi E (2018) Functional implications of inhibitory synapse placement on signal processing in pyramidal neuron dendrites. Curr Opin Neurobiol 51:16–22 Available at: https://doi.org/10.1016/j.conb.2018.01.013.

Bouaboula M, Hilairet S, Marchand J, Fajas L, Le Fur G, Casellas P (2005) Anandamide induced PPARγ transcriptional activation and 3T3-L1 preadipocyte differentiation. Eur J Pharmacol 517:174–181.

Busquets-Garcia A, Bains J, Marsicano G (2018) CB 1 Receptor Signaling in the Brain: Extracting Specificity from Ubiquity. Neuropsychopharmacology 43:4–20 Available at: http://dx.doi.org/10.1038/npp.2017.206.

Capogna M, Castillo PE, Maffei A (2020) The ins and outs of inhibitory synaptic plasticity: Neuron types, molecular mechanisms and functional roles. Eur J Neurosci:1–20.

Caroni P, Donato F, Muller D (2012) Structural plasticity upon learning: Regulation and functions. Nat Rev Neurosci 13:478–490.

Castillo PE, Chiu CQ, Carroll RC (2011) Long-term plasticity at inhibitory synapses. Curr Opin Neurobiol 21:328–338 Available at: http://dx.doi.org/10.1016/j.conb.2011.01.006.

Castillo PE, Younts TJ, Chávez AE, Hashimotodani Y (2012a) Endocannabinoid Signaling and Synaptic Function. Neuron 76:70–81.

Castillo PE, Younts TJ, Chávez AE, Hashimotodani Y (2012b) Endocannabinoid Signaling and Synaptic Function. Neuron 76:70–81.

Chávez AE, Chiu CQ, Castillo PE (2010) TRPV1 activation by endogenous anandamide triggers postsynaptic long-term depression in dentate gyrus. Nat Neurosci 13:1511–1519 Available at: http://dx.doi.org/10.1038/nn.2684.

Chen SX, Kim AN, Peters AJ, Komiyama T (2015) Subtype-specific plasticity of inhibitory circuits in motor cortex during motor learning. Nat Neurosci 18:1109–1115.

Chen X, Winters C, Azzam R, Li X, Galbraith JA, Leapman RD, Reese TS (2008) Organization of the core structure of the postsynaptic density. Proc Natl Acad Sci U S A 105:4453–4458.

Chevaleyre V, Castillo PE (2003) Heterosynaptic LTD of hippocampal GABAergic synapses: A novel role of endocannabinoids in regulating excitability. Neuron 38:461–472.

Chevaleyre V, Heifets BD, Kaeser PS, Südhof TC, Purpura DP, Castillo PE (2007) Endocannabinoid-Mediated Long-Term Plasticity Requires cAMP/PKA Signaling and RIM1α. Neuron 54:801–812.
Chiu CQ, Barberis A, Higley MJ (2019) Preserving the balance: diverse forms of long-term GABAergic synaptic plasticity. Nat Rev Neurosci 20:272–281 Available at: http://dx.doi.org/10.1038/s41583-019-0141-5.
Chua JJE, Kindler S, Boyken J, Jahn R (2010) The architecture of an excitatory synapse. J Cell Sci 123:819–823.
Cingolani LA, Goda Y (2008) Actin in action: The interplay between the actin cytoskeleton and synaptic efficacy. Nat Rev Neurosci 9:344–356.
Craig AM, Kang Y (2007) Neurexin-neuroligin signaling in synapse development. Curr Opin Neurobiol 17:43–52.
Crosby KC, Gookin SE, Garcia JD, Hahm KM, Dell'Acqua ML, Smith KR (2019) Nanoscale Subsynaptic Domains Underlie the Organization of the Inhibitory Synapse. Cell Rep 26:3284-3297.e3 Available at: https://doi.org/10.1016/j.celrep.2019.02.070.
Cui Y, Prokin I, Xu H, Delord B, Genet S, Venance L, Berry H (2016) Endocannabinoid dynamics gate spike- timing dependent depression and potentiation. Elife 5:1–32.
D'amour JA, Froemke RC (2015) Inhibitory and excitatory spike-timing-dependent plasticity in the auditory cortex. Neuron 86:514–528 Available at: http://dx.doi.org/10.1016/j.neuron.2015.03.014.
De Paola V, Arber S, Caroni P (2003) AMPA receptors regulate dynamic equilibrium of presynaptic terminals in mature hippocampal networks. Nat Neurosci 6:491–500.
De Paola V, Holtmaat A, Knott G, Song S, Wilbrecht L, Caroni P, Svoboda K (2006) Cell type-specific structural plasticity of axonal branches and boutons in the adult neocortex. Neuron 49:861–875.
De Wit J, Ghosh A (2016) Specification of synaptic connectivity by cell surface interactions. Nat Rev Neurosci 17:22–35.
Delgado-Peraza F, Ahn KH, Nogueras-Ortiz C, Mongrue IN, Mackie K, Kendall DA, Yudowski GA (2016) Erratum: Mechanisms of biased β-arrestin-mediated signaling downstream from the cannabinoid 1 receptor (Molecular Pharmacology (2016) 89 (618-629)). Mol Pharmacol 90:62.
Devane W, Hanus L, Breuer A, Pertwee R, Stevenson L, Griffin G, Gibson D, Mandelbaum A, Etinger A, Mechoulam R (1992) Isolation and structure of a brain constituent that binds to the cannabinoid receptor. Science (80-) 258.
Dhopeshwarkar A, Mackie K (2014) CB2 Cannabinoid Receptors as a Therapeutic Target—What.pdf. :430–437.
Dobie FA, Craig AM (2011) Inhibitory synapse dynamics: Coordinated presynaptic and postsynaptic mobility and the major contribution of recycled vesicles to new synapse formation. J Neurosci 31:10481–10493.
Donato F, Rompani SB, Caroni P (2013) Parvalbumin-expressing basket-cell network plasticity induced by experience regulates adult learning. Nature 504:272–276 Available at: http://dx.doi.org/10.1038/nature12866.
Dudok B et al. (2015) Cell-specific STORM super-resolution imaging reveals nanoscale organization of cannabinoid signaling. Nat Neurosci 18:75–86.
Eavri R, Shepherd J, Welsh CA, Flanders GH, Bear MF, Nedivi E (2018) Interneuron simplification and loss of structural plasticity as markers of aging-related functional decline. J Neurosci 38:8421–8432.
Elia LP, Yamamoto M, Zang K, Reichardt LF (2006) p120 Catenin Regulates Dendritic Spine and Synapse Development through Rho-Family GTPases and Cadherins. Neuron 51:43–56.
Essrich C, Lorez M, Benson JA, Fritschy JM, Lüscher B (1998) Postsynaptic clustering of major GABAA receptor subtypes requires the γ2 subunit and gephyrin. Nat Neurosci 1:563–571.
Favuzzi E, Rico B (2018) Molecular diversity underlying cortical excitatory and inhibitory synapse development. Curr Opin Neurobiol 53:8–15.
Finlay DB, Cawston EE, Grimsey NL, Hunter MR, Korde A, Vemuri VK, Makriyannis A, Glass M (2017) Gαs signalling of the CB1 receptor and the influence of receptor number. Br J Pharmacol 174:2545–2562.
Flores CE, Méndez P (2014) Shaping inhibition: Activity dependent structural plasticity of GABAergic synapses. Front Cell Neurosci 8:1–13.
Freund TF, Katona I, Piomelli D (2003) Role of endogenous cannabinoids in synaptic signaling. Physiol Rev 83:1017–1066.

Frias CP, Wierenga CJ (2013) Activity-dependent adaptations in inhibitory axons. Front Cell Neurosci 7:1–16.
Frick A, Johnston D (2005) Plasticity of dendritic excitability. J Neurobiol 64:100–115.
Fu M, Yu X, Lu J, Zuo Y (2012) Repetitive motor learning induces coordinated formation of clustered dendritic spines in vivo. Nature 483:92–96.
Gao Y et al. (2010) Loss of retrograde endocannabinoid signaling and reduced adult neurogenesis in diacylglycerol lipase knock-out mice. J Neurosci 30:2017–2024.
Gibson JR, Huber KM, Südhof TC (2009) Neuroligin-2 deletion selectively decreases inhibitory synaptic transmission originating from fast-spiking but not from somatostatin-positive interneurons. J Neurosci 29:13883–13897.
Glebov OO, Jackson RE, Winterflood CM, Owen DM, Barker EA, Doherty P, Ewers H, Burrone J (2017) Nanoscale Structural Plasticity of the Active Zone Matrix Modulates Presynaptic Function. Cell Rep 18:2715–2728 Available at: http://dx.doi.org/10.1016/j.celrep.2017.02.064.
Glickfeld LL, Scanziani M (2005) Self-administering cannabinoids. 28.
Graf ER, Zhang X, Jin SX, Linhoff MW, Craig AM (2004) Neurexins induce differentiation of GABA and glutamate postsynaptic specializations via neuroligins. Cell 119:1013–1026.
Grillo FW, Song S, Teles-Grilo Ruivo LM, Huang L, Gao G, Knott GW, MacO B, Ferretti V, Thompson D, Little GE, De Paola V (2013) Increased axonal bouton dynamics in the aging mouse cortex. Proc Natl Acad Sci U S A 110.
Han J, Kesner P, Metna-Laurent M, Duan T, Xu L, Georges F, Koehl M, Abrous DN, Mendizabal-Zubiaga J, Grandes P, Liu Q, Bai G, Wang W, Xiong L, Ren W, Marsicano G, Zhang X (2012) Acute cannabinoids impair working memory through astroglial CB1 receptor modulation of hippocampal LTD. Cell 148:1039–1050 Available at: http://dx.doi.org/10.1016/j.cell.2012.01.037.
Han SM, Baig HS, Hammarlund M (2016) Mitochondria Localize to Injured Axons to Support Regeneration. Neuron 92:1308–1323 Available at: http://dx.doi.org/10.1016/j.neuron.2016.11.025.
Harris KM, Weinberg RJ (2012) Ultrastructure of synapses in the mammalian brain. Cold Spring Harb Perspect Biol 4:7.
Hartman CA, Hopfer CJ, Haberstick B, Rhee SH, Crowley TJ, Corley RP, Hewitt JK, Ehringer MA (2009) The association between cannabinoid receptor 1 gene (CNR1) and cannabis dependence symptoms in adolescents and young adults. Drug Alcohol Depend 104:11–16.
Hashimotodani Y, Nasrallah K, Jensen KR, Chávez AE, Carrera D, Castillo PE (2017) LTP at Hilar Mossy Cell-Dentate Granule Cell Synapses Modulates Dentate Gyrus Output by Increasing Excitation/Inhibition Balance. Neuron 95:928-943.e3.
Hashimotodani Y, Ohno-Shosaku T, Kano M (2007) Endocannabinoids and synaptic function in the CNS. Neuroscientist 13:127–137.
Hebert-Chatelain E et al. (2016) A cannabinoid link between mitochondria and memory. Nature 539:555–559.
Herculano-Houzel S (2009) The human brain in numbers: A linearly scaled-up primate brain. Front Hum Neurosci 3:1–11.
Herkenham M, Lynn AB, Little MD, Johnson MR, Melvin LS, De Costa BR, Rice KC (1990) Cannabinoid receptor localization in brain. Proc Natl Acad Sci U S A 87:1932–1936.
Hermanson DJ, Gamble-George JC, Marnett LJ, Patel S (2014) Substrate-selective COX-2 inhibition as a novel strategy for therapeutic endocannabinoid augmentation. Trends Pharmacol Sci 35:358–367 Available at: http://dx.doi.org/10.1016/j.tips.2014.04.006.
Herstel LJ, Wierenga CJ (2021) Network control through coordinated inhibition. Curr Opin Neurobiol 67:34–41 Available at: https://doi.org/10.1016/j.conb.2020.08.001.
Hu HY, Kruijssen DLH, Frias CP, Rózsa B, Hoogenraad CC, Wierenga CJ (2019) Endocannabinoid Signaling Mediates Local Dendritic Coordination between Excitatory and Inhibitory Synapses. Cell Rep 27:666-675.e5.
Hurd YL, Manzoni OJ, Pletnikov M V., Lee FS, Bhattacharyya S, Melis M (2019) Cannabis and the developing brain: Insights into its long-lasting effects. J Neurosci 39:8250–8258.
Kano M, Ohno-Shosaku T, Hashimotodani Y, Uchigashima M, Watanabe M (2009) Endocannabinoid-mediated control of synaptic transmission. Physiol Rev 89:309–380.
Karhson DS, Hardan AY, Parker KJ (2016) Endocannabinoid signaling in social functioning: An RDoC perspective. Transl Psychiatry 6.
Katona I, Sperlágh B, Sík A, Käfalvi A, Vizi ES, Mackie K, Freund TF (1999) Presynaptically located CB1 cannabinoid receptors regulate GABA release from axon terminals of specific hippocampal

interneurons. J Neurosci 19:4544–4558.
Katona I, Urban GM, Wallace M, Ledent C, Jung K-M, Piomelli D, Mackie K, Freund TF (2006) Molecular Composition of the Endocannabinoid System at Glutamatergic Synapses. J Neurosci 26:5628–5637.
Kawaguchi SY (2019) Dynamic factors for transmitter release at small presynaptic boutons revealed by direct patch-clamp recordings. Front Cell Neurosci 13:1–6.
Keck T, Scheuss V, Jacobsen RI, Wierenga CJ, Eysel UT, Bonhoeffer T, Hübener M (2011) Loss of sensory input causes rapid structural changes of inhibitory neurons in adult mouse visual cortex. Neuron 71:869–882.
Keller AJ, Roth MM, Scanziani M (2020) Feedback generates a second receptive field in neurons of the visual cortex. Nature 582:545–549 Available at: http://dx.doi.org/10.1038/s41586-020-2319-4.
Kendall DA, Yudowski GA (2017) Cannabinoid receptors in the central nervous system: Their signaling and roles in disease. Front Cell Neurosci 10:1–10.
Kharazia VN, Weinberg RJ (1997) Tangential synaptic distribution of NMDA and AMPA receptors in rat neocortex. Neurosci Lett 238:41–44.
Kicman A, Toczek M (2020) The effects of cannabidiol, a non-intoxicating compound of cannabis, on the cardiovascular system in health and disease.
Kneussel M, Brandstätter JH, Laube B, Stahl S, Müller U, Betz H (1999) Loss of postsynaptic GABA(A) receptor clustering in gephyrin-deficient mice. J Neurosci 19:9289–9297.
Knodel M, Queisser G, Bucher D, Geiger R, Ge LH, Grillo A, Schuster C, Wittum G (2011) Synaptic bouton sizes are tuned to best fit their physiological performances. BMC Neurosci 12:1–2.
Kreitzer AC, Regehr WG (2001) Retrograde inhibition of presynaptic calcium influx by endogenous cannabinoids at excitatory synapses onto Purkinje cells. Neuron 29:717–727.
Kubota Y, Karube F, Nomura M, Kawaguchi Y (2016) The diversity of cortical inhibitory synapses. Front Neural Circuits 10:1–15.
Lauckner JE, Hille B, Mackie K (2005) The cannabinoid agonist WIN55,212-2 increases intracellular calcium via CB1 receptor coupling to Gq/11 G proteins. Proc Natl Acad Sci U S A 102:19144–19149.
Lee HK, Kirkwood A (2019) Mechanisms of Homeostatic Synaptic Plasticity in vivo. Front Cell Neurosci 13:1–7.
Lee SH, Ledri M, Tóth B, Marchionni I, Henstridge CM, Dudok B, Kenesei K, Barna L, Szabó SI, Renkecz T, Oberoi M, Watanabe M, Limoli CL, Horvai G, Soltesz I, Katona I (2015) Multiple forms of endocannabinoid and endovanilloid signaling regulate the tonic control of GABA release. J Neurosci 35:10039–10057.
Lee WCA, Chen JL, Huang H, Leslie JH, Amitai Y, So PT, Nedivi E (2008) A dynamic zone defines interneuron remodeling in the adult neocortex. Proc Natl Acad Sci U S A 105:19968–19973.
Lees RM, Johnson JD, Ashby MC (2020) Presynaptic Boutons That Contain Mitochondria Are More Stable. Front Synaptic Neurosci 11:1–13.
Lenkey N, Kirizs T, Holderith N, Máté Z, Szabó G, Vizi ES, Hájos N, Nusser Z (2015) Tonic endocannabinoid-mediated modulation of GABA release is independent of the CB1 content of axon terminals. Nat Commun 6.
Lewis DA, Hashimoto T, Volk DW (2005) Cortical inhibitory neurons and schizophrenia. Nat Rev Neurosci 6:312–324.
Li H, Yang J, Tian C, Diao M, Wang Q, Zhao S, Li S, Tan F, Hua T, Qin Y, Lin CP, Deska-Gauthier D, Thompson GJ, Zhang Y, Shui W, Liu ZJ, Wang T, Zhong G (2020) Organized cannabinoid receptor distribution in neurons revealed by super-resolution fluorescence imaging. Nat Commun 11 Available at: http://dx.doi.org/10.1038/s41467-020-19510-5.
Li J, Han W, Pelkey KA, Duan J, Mao X, Wang YX, Craig MT, Dong L, Petralia RS, McBain CJ, Lu W (2017) Molecular Dissection of Neuroligin 2 and Slitrk3 Reveals an Essential Framework for GABAergic Synapse Development. Neuron 96:808-826.e8 Available at: https://doi.org/10.1016/j.neuron.2017.10.003.
Liang J, Xu W, Hsu YT, Yee AX, Chen L, Südhof TC (2015) Conditional neuroligin-2 knockout in adult medial prefrontal cortex links chronic changes in synaptic inhibition to cognitive impairments. Mol Psychiatry 20:850–859.
Lu HC, MacKie K (2016) An introduction to the endogenous cannabinoid system. Biol Psychiatry 79:516–525 Available at: http://dx.doi.org/10.1016/j.biopsych.2015.07.028.
Lu W, Bromley-Coolidge S, Li J (2017) Regulation of GABAergic synapse development by postsynaptic

membrane proteins. Brain Res Bull 129:30–42 Available at: http://dx.doi.org/10.1016/j.brainresbull.2016.07.004.
MacGillavry HD, Song Y, Raghavachari S, Blanpied TA (2013) Nanoscale scaffolding domains within the postsynaptic density concentrate synaptic ampa receptors. Neuron 78:615–622 Available at: http://dx.doi.org/10.1016/j.neuron.2013.03.009.
Mackie K (2005) Distribution of cannabinoid receptors in the central and peripheral nervous system. Handb Exp Pharmacol 168:299–325.
Marinelli S, Pacioni S, Bisogno T, Di Marzo V, Prince DA, Huguenard JR, Bacci A (2008) The endocannabinoid 2-arachidonoylglycerol is responsible for the slow self-inhibition in neocortical interneurons. J Neurosci 28:13532–13541.
Marti-Solano M, Crilly SE, Malinverni D, Munk C, Harris M, Pearce A, Quon T, Mackenzie AE, Wang X, Peng J, Tobin AB, Ladds G, Milligan G, Gloriam DE, Puthenveedu MA, Babu MM (2020) Combinatorial expression of GPCR isoforms affects signalling and drug responses. Nature 587:650–656 Available at: http://dx.doi.org/10.1038/s41586-020-2888-2.
Matsuda LA, Lolait SJ, Brownstein MJ, Young AC, Bonner TI (1990) Structure of a cannabinoid receptor and functional expression of the cloned cDNA. Nature 346:561–564.
Mechoulam R, Ben-Shabat S, Hanus L, Ligumsky M, Kaminski NE, Schatz AR, Gopher A, Almog S, Martin BR, Compton DR, Pertwee RG, Griffin G, Bayewitch M, Barg J, Vogel Z (1995) Identification of an endogenous 2-monoglyceride, present in canine gut, that binds to cannabinoid receptors. Biochem Pharmacol 50:83–90.
Mechoulam R, Gaoni Y (1965) A Total Synthesis of dl-Δ1-Tetrahydrocannabinol, the Active Constituent of Hashish. J Am Chem Soc 87:3273–3275.
Mechoulam R, Hanuš L (2001) The cannabinoids: An overview. Therapeutic implications in vomiting and nausea after cancer chemotherapy, in appetite promotion, in multiple sclerosis and in neuroprotection. Pain Res Manag 6:67–73.
Méndez P, Bacci A (2011) Assortment of GABAergic plasticity in the cortical interneuron melting pot. Neural Plast 2011.
Mendez P, De Roo M, Poglia L, Klauser P, Muller D (2010) N-cadherin mediates plasticity-induced long-term spine stabilization. J Cell Biol 189:589–600.
Missler M, Südhof TC, Biederer T (2012) Synaptic cell adhesion. Cold Spring Harb Perspect Biol 4.
Monday HR, Bourdenx M, Jordan BA, Castillo PE (2020) Cb1-receptor-mediated inhibitory ltd triggers presynaptic remodeling via protein synthesis and ubiquitination. Elife 9:1–25.
Morimoto MM, Tanaka S, Mizutani S, Urata S, Kobayashi K, Okabe S (2018) In vivo observation of structural changes in neocortical catecholaminergic projections in response to drugs of abuse. eNeuro 5:1–11.
Muir J, Arancibia-Carcamo IL, MacAskill AF, Smith KR, Griffin LD, Kittler JT (2010) NMDA receptors regulate GABAA receptor lateral mobility and clustering at inhibitory synapses through serine 327 on the γ2 subunit. Proc Natl Acad Sci U S A 107:16679–16684.
Mulder J, Zilberter M, Pasquaré SJ, Alpár A, Schulte G, Ferreira SG, Köfalvi A, Martín-Moreno AM, Keimpema E, Tanila H, Watanabe M, MacKie K, Hortobágyi T, De Ceballos ML, Harkany T (2011) Molecular reorganization of endocannabinoid signalling in Alzheimer's disease. Brain 134:1041–1060.
Muller C, Morales P, Reggio PH (2019) Cannabinoid ligands targeting TRP channels. Front Mol Neurosci 11:1–15.
Mullins C, Fishell G, Tsien RW (2016) Unifying Views of Autism Spectrum Disorders: A Consideration of Autoregulatory Feedback Loops. Neuron 89:1131–1156 Available at: http://dx.doi.org/10.1016/j.neuron.2016.02.017.
Munro S, Thomas KL, Abu-Shaar M (1993) Molecular characterization of a peripheral receptor for cannabinoids. Nature 365:61–65.
Murataeva N, Straiker A, MacKie K (2014) Parsing the players: 2-arachidonoylglycerol synthesis and degradation in the CNS. Br J Pharmacol 171:1379–1391.
Murthy VN, De Camilli P (2003) Cell biology of the presynaptic terminal. Annu Rev Neurosci 26:701–728.
Nair D, Hosy E, Petersen JD, Constals A, Giannone G, Choquet D, Sibarita JB (2013) Super-resolution imaging reveals that AMPA receptors inside synapses are dynamically organized in nanodomains regulated by PSD95. J Neurosci 33:13204–13224.
Nakamoto KT, Mellott JG, Killius J, Storey-Workley ME, Sowick CS, Schofield BR (2014) Ultrastructural

characterization of GABAergic and excitatory synapses in the inferior colliculus. Front Neuroanat 8:1–13.
Navarrete M, Araque A (2008) Endocannabinoids Mediate Neuron-Astrocyte Communication. Neuron 57:883–893.
Nguyen PT, Schmid CL, Raehal KM, Selley DE, Bohn LM, Sim-Selley LJ (2012) β-Arrestin2 regulates cannabinoid CB 1 receptor signaling and adaptation in a central nervous system region-dependent manner. Biol Psychiatry 71:714–724 Available at: http://dx.doi.org/10.1016/j.biopsych.2011.11.027.
Nikitczuk JS, Patil SB, Matikainen-Ankney BA, Scarpa J, Shapiro ML, Benson DL, Huntley GW (2014) N-cadherin regulates molecular organization of excitatory and inhibitory synaptic circuits in adult hippocampus in vivo. Hippocampus 24:943–962.
O'Sullivan SE (2007) Cannabinoids go nuclear: Evidence for activation of peroxisome proliferator-activated receptors. Br J Pharmacol 152:576–582.
Ohno-Shosaku T, Maejima T, Kano M (2001) Endogenous cannabinoids mediate retrograde signals from depolarized postsynaptic neurons to presynaptic terminals. Neuron 29:729–738.
Patrón LA, Zinsmaier KE (2016) Mitochondria on the Road to Power Axonal Regeneration. Neuron 92:1152–1154.
Pelkey KA, Chittajallu R, Craig MT, Tricoire L, Wester JC, McBain CJ (2017) Hippocampal gabaergic inhibitory interneurons. Physiol Rev 97:1619–1747.
Pereda AE (2014) Electrical synapses and their functional interactions with chemical synapses. Nat Rev Neurosci 15:250–263.
Petrini EM, Ravasenga T, Hausrat TJ, Iurilli G, Olcese U, Racine V, Sibarita JB, Jacob TC, Moss SJ, Benfenati F, Medini P, Kneussel M, Barberis A (2014) Synaptic recruitment of gephyrin regulates surface GABA A receptor dynamics for the expression of inhibitory LTP. Nat Commun 5:1–19 Available at: http://dx.doi.org/10.1038/ncomms4921.
Qu X, Kumar A, Blockus H, Waites C, Bartolini F (2019) Activity-Dependent Nucleation of Dynamic Microtubules at Presynaptic Boutons Controls Neurotransmission. Curr Biol 29:4231-4240.e5 Available at: https://doi.org/10.1016/j.cub.2019.10.049.
Roland AB, Ricobaraza A, Carrel D, Jordan BM, Rico F, Simon A, Humbert-Claude M, Ferrier J, McFadden MH, Scheuring S, Lenkei Z (2014) Cannabinoid-induced actomyosin contractility shapes neuronal morphology and growth. Elife 3:e03159.
Rudy B, Fishell G, Lee SH, Hjerling-Leffler J (2011) Three groups of interneurons account for nearly 100% of neocortical GABAergic neurons. Dev Neurobiol 71:45–61.
Ruiter M, Lützkendorf C, Liang J, Wierenga CJ (2021) Amyloid-β Oligomers Induce Only Mild Changes to Inhibitory Bouton Dynamics. J Alzheimer's Dis Reports 5.
Ryberg E, Vu HK, Larsson N, Groblewski T, Hjorth S, Elebring T, Sjögren S, Greasley PJ (2005) Identification and characterisation of a novel splice variant of the human CB1 receptor. FEBS Lett 579:259–264.
Scheiffele P, Fan J, Choih J, Fetter R, Serafini T (2000) Neuroligin expressed in nonneuronal cells triggers presynaptic development in contacting axons. Cell 101:657–669.
Schuemann A, Klawiter A, Bonhoeffer T, Wierenga CJ (2013) Structural plasticity of GABAergic axons is regulated by network activity and GABAA receptor activation. Front Neural Circuits 7:1–16.
Sheng M, Hoogenraad CC (2007) The postsynaptic architecture of excitatory synapses: A more quantitative view. Annu Rev Biochem 76:823–847.
Siksou L, Rostaing P, Lechaire JP, Boudier T, Ohtsuka T, Fejtová A, Kao HT, Greengard P, Gundelfinger ED, Triller A, Marty S (2007) Three-dimensional architecture of presynaptic terminal cytomatrix. J Neurosci 27:6868–6877.
Smit-Rigter L, Rajendran R, Silva CAP, Spierenburg L, Groeneweg F, Ruimschotel EM, van Versendaal D, van der Togt C, Eysel UT, Heimel JA, Lohmann C, Levelt CN (2016) Mitochondrial Dynamics in Visual Cortex Are Limited In Vivo and Not Affected by Axonal Structural Plasticity. Curr Biol 26:2609–2616 Available at: http://dx.doi.org/10.1016/j.cub.2016.07.033.
Specht CG, Izeddin I, Rodriguez PC, ElBeheiry M, Rostaing P, Darzacq X, Dahan M, Triller A (2013) Quantitative nanoscopy of inhibitory synapses: Counting gephyrin molecules and receptor binding sites. Neuron 79:308–321 Available at: http://dx.doi.org/10.1016/j.neuron.2013.05.013.
Südhof TC (2012) The presynaptic active zone. Neuron 75:11–25.
Sugiura T, Kondo S, Sukagawa A, Nakane S, Shinoda A, Itoh K, Yamashita A, Waku K (1995) 2-arachidonoylglycerol: A possible endogenous cannabinoid receptor ligand in brain. Biochem

Biophys Res Commun 215:89–97.
Sytnyk V, Leshchyns'ka I, Dityatev A, Schachner M (2004) Trans-Golgi network delivery of synaptic proteins in synaptogenesis. J Cell Sci 117:381–388.
Takamori S et al. (2006) Molecular Anatomy of a Trafficking Organelle. Cell 127:831–846.
Tang AH, Chen H, Li TP, Metzbower SR, MacGillavry HD, Blanpied TA (2016) A trans-synaptic nanocolumn aligns neurotransmitter release to receptors. Nature 536:210–214 Available at: http://dx.doi.org/10.1038/nature19058.
Tao CL, Liu YT, Sun R, Zhang B, Qi L, Shivakoti S, Tian CL, Zhang P, Lau PM, Hong Zhou Z, Bi GQ (2018) Differentiation and characterization of excitatory and inhibitory synapses by cryo-electron tomography and correlative microscopy. J Neurosci 38:1493–1510.
Turrigiano GG (2008) The Self-Tuning Neuron: Synaptic Scaling of Excitatory Synapses. Cell 135:422–435.
Turrigiano GG (2017) The dialectic of hebb and homeostasis. Philos Trans R Soc B Biol Sci 372:4–6.
Turu G, Hunyady L (2010) Signal transduction of the CB1 cannabinoid receptor. J Mol Endocrinol 44:75–85.
Varoqueaux F, Jamain S, Brose N (2004) Neuroligin 2 is exclusively localized to inhibitory synapses. Eur J Cell Biol 83:449–456.
Waites CL, Leal-Ortiz SA, Okerlund N, Dalke H, Fejtova A, Altrock WD, Gundelfinger ED, Garner CC (2013) Bassoon and Piccolo maintain synapse integrity by regulating protein ubiquitination and degradation. EMBO J 32:954–969 Available at: http://dx.doi.org/10.1038/emboj.2013.27.
Wamsley B, Fishell G (2017) Genetic and activity-dependent mechanisms underlying interneuron diversity. Nat Rev Neurosci 18:299–309 Available at: http://dx.doi.org/10.1038/nrn.2017.30.
Wang W, Jia Y, Pham DT, Palmer LC, Jung K-M, Cox CD, Rumbaugh G, Piomelli D, Gall CM, Lynch G (2017) Atypical endocannabinoid signaling initiates a new form of memory-related plasticity at a cortical input to hippocampus. Cereb Cortex:1–14.
Wierenga CJ (2017) Live imaging of inhibitory axons: Synapse formation as a dynamic trial-and-error process. Brain Res Bull 129:43–49 Available at: http://dx.doi.org/10.1016/j.brainresbull.2016.09.018.
Wierenga CJ, Becker N, Bonhoeffer T (2008) GABAergic synapses are formed without the involvement of dendritic protrusions. Nat Neurosci 11:1044–1052.
Wilson RI, Kunos G, Nicoll RA (2001) Presynaptic specificity of endocannabinoid signaling in the hippocampus. Neuron 31:453–462.
Yang Y, Lu J, Zuo Y (2018) Changes of Synaptic Structures Associated with Learning, Memory and Diseases. Brain Sci Adv 4:99–117.
Zhou R, Han B, Xia C, Zhuang X (2019) Membrane-associated periodic skeleton is a signaling platform for RTK transactivation in neurons. Science (80-) 365:929–934.
Zou S, Kumar U (2018) Cannabinoid receptors and the endocannabinoid system: Signaling and function in the central nervous system. Int J Mol Sci 19.
Zygmunt PM, Petersson J, Andersson DA, Chuang HH, Sørgård M, Di Marzo V, Julius D, Högestätt ED (1999) Vanilloid receptors on sensory nerves mediate the vasodilator action of anandamide. Nature 400:452–457.

Chapter 2

Semaphorin4D induces inhibitory synapse formation by rapid stabilization of presynaptic boutons via MET co-activation

Abbreviated title: Sema4D stabilizes inhibitory boutons via MET

Authors: Cátia P. Frias[1,2], **Jian Liang**[1], Tom Bresser[1], Lisa Scheefhals[1], Matthijs van Kesteren[1], René van Dorland[1], Hai Yin Hu[1], Anna Bodzeta[1], Paul M. P. van Bergen en Henegouwen[1], Casper C. Hoogenraad[1] and Corette J. Wierenga[1*]

Affiliation: [1]Cell Biology, Department of Biology, Science4Life, Utrecht University, 3584 CH Utrecht, the Netherlands

[2]Current address: Department of Bionanoscience, Kavli Institute of Nanoscience, Delft University of Technology, 2629 HZ Delft, The Netherlands

*Corresponding author: Corette J. Wierenga

This chapter has been published in the Journal of Neuroscience, Vol. 39, Issue 22, 29 May 2019

ABSTRACT

Changes in inhibitory connections are essential for experience-dependent circuit adaptations. Defects in inhibitory synapses are linked to neurodevelopmental disorders, but the molecular processes underlying inhibitory synapse formation are not well understood. Here we use high resolution two-photon microscopy in organotypic hippocampal slices from GAD65-GFP mice of both sexes to examine the signaling pathways induced by the postsynaptic signaling molecule Semaphorin4D (Sema4D) during inhibitory synapse formation. By monitoring changes in individual GFP-labeled presynaptic boutons, we found that the primary action of Sema4D is to induce stabilization of presynaptic boutons within tens of minutes. Stabilized boutons rapidly recruited synaptic vesicles, followed by accumulation of postsynaptic gephyrin and were functional after 24 hours, as determined by electrophysiology and immunohistochemistry. Inhibitory boutons are only sensitive to Sema4D at a specific stage during synapse formation and sensitivity to Sema4D is regulated by network activity. We further examined the intracellular signaling cascade triggered by Sema4D and found that bouton stabilization occurs through rapid remodeling of the actin cytoskeleton. This could be mimicked by the actin-depolymerizing drug Latrunculin B or by reducing ROCK activity. We discovered that the intracellular signaling cascade requires activation of the receptor tyrosine kinase MET, which is a well-known autism risk factor. By using a viral approach to reduce MET levels specifically in inhibitory neurons, we found that their axons are no longer sensitive to Sema4D signaling. Together, our data yield important insights into the molecular pathway underlying activity-dependent Sema4D-induced synapse formation and reveal a novel role for presynaptic MET at inhibitory synapses.

Significance Statement

GABAergic synapses provide the main inhibitory control of neuronal activity in the brain. We wanted to unravel the sequence of molecular events that take place when formation of inhibitory synapses is triggered by a specific signaling molecule, Sema4D. We find that this signaling pathway depends on network activity and involves specific remodeling of the intracellular actin cytoskeleton. We also reveal a previously unknown role for MET at inhibitory synapses. Our study provides novel insights into the dynamic process of inhibitory synapse formation. As defects in GABAergic synapses have been implied in many brain disorders, and mutations in MET are strong risk factors for autism, our findings urge for a further investigation of the role of MET at inhibitory synapses.

INTRODUCTION

GABAergic synapses provide the main inhibitory control over neuronal activity in the brain and are indispensable for shaping network function (Isaacson and Scanziani, 2011). Although the majority of synaptic connections are formed during development, synapse turnover is still ongoing in postnatal brain tissue to allow for continuous adaptation and learning (Caroni et al., 2012). Recent studies have indicated that activity-dependent formation and disassembly of inhibitory synapses are crucial in experience-dependent circuit adaptation (Hensch, 2005; Keck et al., 2011; Chen et al., 2015; Froemke, 2015; Sprekeler, 2017), and defects in GABAergic synapses have been observed in many neurodevelopmental disorders (Marín, 2012; Cellot and Cherubini, 2014; Nelson and Valakh, 2015). We and others have shown that inhibitory synapses are dynamic structures with presynaptic boutons and postsynaptic scaffolds forming and disappearing with apparently stochastic dynamics (Wierenga et al., 2008; Fu and Huang, 2010; Dobie and Craig, 2011; Kuriu et al., 2012; Schuemann et al., 2013; Villa et al., 2016). These dynamics allow quick adaptation of connections in response to changes in the neuronal circuitry (Staras, 2007; Keck et al., 2011; Frias and Wierenga, 2013; Chen et al., 2015).

Previous work has shown that the formation of inhibitory synapses is a highly dynamic process, which starts with the formation of a new bouton by the presynaptic axon and takes several hours, up to 1-2 days, to be complete (Wierenga et al., 2008; Dobie and Craig, 2011; Schuemann et al., 2013; Flores et al., 2015). In recent years, enormous progress has been made by the identification and characterization of proteins that are involved in the formation of inhibitory synapses (Siddiqui and Craig, 2011; Lu et al., 2016; Krueger-Burg et al., 2017), but the precise molecular events that take place when new synapses are formed are not yet clear. For instance, boutons do not emerge randomly, but appear and reappear at specific axonal locations (Staras, 2007; Dobie and Craig, 2011; Schuemann et al., 2013), which seem to be predefined by a currently unknown mechanism. Furthermore, only some boutons get stabilized at these locations to form mature synapses (Wierenga et al., 2008; Fu et al., 2012; Schuemann et al., 2013; Villa et al., 2016) and it is currently not clear what determines the decision to ‘stay or go’.

The class 4 semaphorin Sema4D, originally identified as an axon guidance factor (Kolodkin et al., 1993; Pasterkamp, 2012), was shown to be specifically required for the formation of GABAergic, but not glutamatergic, synapses

in primary cultures as well as in vivo (Paradis et al., 2007). It was further shown that activation of the Sema4D signaling pathway rapidly induces the formation of inhibitory synapses (Kuzirian et al., 2013). Sema4D is a postsynaptic membrane protein and induces inhibitory synapse formation via presynaptic PlexinB1 receptors (Raissi et al., 2013; McDermott et al., 2018), but the precise molecular events that take place during Sema4D-induced inhibitory synapse formation are not known. The observation that somatic and dendritic inhibitory synapses respond equally to Sema4D signaling (Kuzirian et al., 2013) suggests that it acts at the majority of (or perhaps all) inhibitory synapses, making Sema4D signaling an interesting starting point to study the process of inhibitory synapse formation.

We used high resolution two-photon microscopy in organotypic hippocampal slices to characterize the molecular events during Sema4D-induced formation of inhibitory synapses in intact tissue. We found that Sema4D signaling does not induce the formation of de novo synapses, but specifically promotes the rapid stabilization of inhibitory boutons along the axon in an activity-dependent manner. Rapid presynaptic changes are followed by subsequent slower recruitment of postsynaptic gephyrin, and maturation to functional inhibitory synapses completes over the course of several hours. The intracellular pathway for bouton stabilization involves specific remodeling of the actin cytoskeleton. We demonstrate that Sema4D-induced inhibitory bouton stabilization requires the activation of the receptor tyrosine kinase MET. Our data unravel an important regulatory pathway of activity-dependent inhibitory synapse formation and reveal a novel role for presynaptic MET in Sema4D-induced formation of inhibitory synapses.

RESULTS

We performed time-lapse two-photon microscopy in organotypic hippocampal cultures from GAD65-GFP mice to monitor the dynamics of inhibitory boutons in the CA1 region of the hippocampus (Wierenga et al., 2008; Schuemann et al., 2013). In GAD65-GFP mice, the majority of GFP-labeled interneurons are dendritically targeting CGE-derived interneurons, while MGE-derived parvalbumin and somatostatin interneurons are not labeled (López-Bendito et al., 2004; Wierenga et al., 2010). This results in GFP-labeling of approximately 20% of CA1 interneurons, allowing monitoring of individual axons over time. High-resolution image stacks of GFP-labeled inhibitory axons were acquired every 10 minutes, for a total period of 140 minutes (15 time points).

As previously reported (Wierenga et al., 2008; Dobie and Craig, 2011; Fu et al., 2012; Schuemann et al., 2013), inhibitory boutons are remarkably dynamic and many boutons appeared, disappeared and reappeared during the course of the imaging period. To bias our analysis towards synaptic events, we only included boutons that were present for at least 2 time points at the same location during the imaging period (Schuemann et al., 2013). We distinguished two main classes of boutons: persistent boutons, which were present during all time points (Fig. 1A), and non-persistent boutons, which were absent during one or more time points during the imaging session (Fig. 1B). In our slices, the majority of GFP-labeled boutons (77%, with standard deviation of 12%) were persistent (Fig. 1C) and they reflect mature inhibitory synapses (Wierenga et al., 2008; Müllner et al., 2015). Non-persistent boutons reflect locations where inhibitory synapses are 'in transition', e.g. where synapses are being formed or disassembled in an apparent trial-and-error fashion (Wierenga et al., 2008; Dobie and Craig, 2011; Fu et al., 2012; Schuemann et al., 2013).

We assume that synapse formation is reflected in subsequent transitions of boutons from absent (A) to non-persistent (NP) to persistent (P) (A → NP → P) and synapse disassembly in the reverse order. We identify these transitions by comparing the dynamics of individual boutons in a baseline and wash-in period and we define 5 subgroups of non-persistent boutons: new (A → NP), lost (NP → A), stabilizing (NP → P), destabilizing (P → NP) and intermittent (always NP) boutons (Fig. 1B,D; details are given in the methods section). We could observe transitions between developmental bouton stages in ~50% of non-persistent boutons (Fig. 1E). After live imaging, slices were

fixed and immunostained for the presynaptic vesicular GABA transporter (VGAT) and the postsynaptic scaffold gephyrin to correlate bouton dynamics of individual boutons with their molecular composition. We found that boutons that were non-persistent at the end of the imaging period (new, destabilizing and intermittent boutons) showed a lower percentage of association with VGAT and gephyrin compared to persistent boutons, reflecting that these boutons usually do not (yet) form synapses (Fig. 1F). Stabilizing boutons, which had been present for at least 90 minutes before fixation, showed similar association with VGAT and gephyrin to persistent boutons (Fig. 1F), indicating that they represent nascent inhibitory synapses that have started to recruit pre- and postsynaptic proteins within this period. Association of non-persistent boutons with VGAT and gephyrin increased with their total lifetime, suggesting a gradual recruitment of proteins over the imaging period (Fig. 1G). Recruitment of gephyrin was delayed compared to VGAT, consistent with earlier reports that synaptic proteins are recruited in a presynaptic before postsynaptic order (Wierenga et al., 2008; Dobie and Craig, 2011). These data demonstrate that inhibitory presynaptic boutons are continuously being formed and disassembled along axons. By monitoring the dynamics of individual inhibitory boutons over time we can distinguish boutons at different stages of synapse assembly and disassembly.

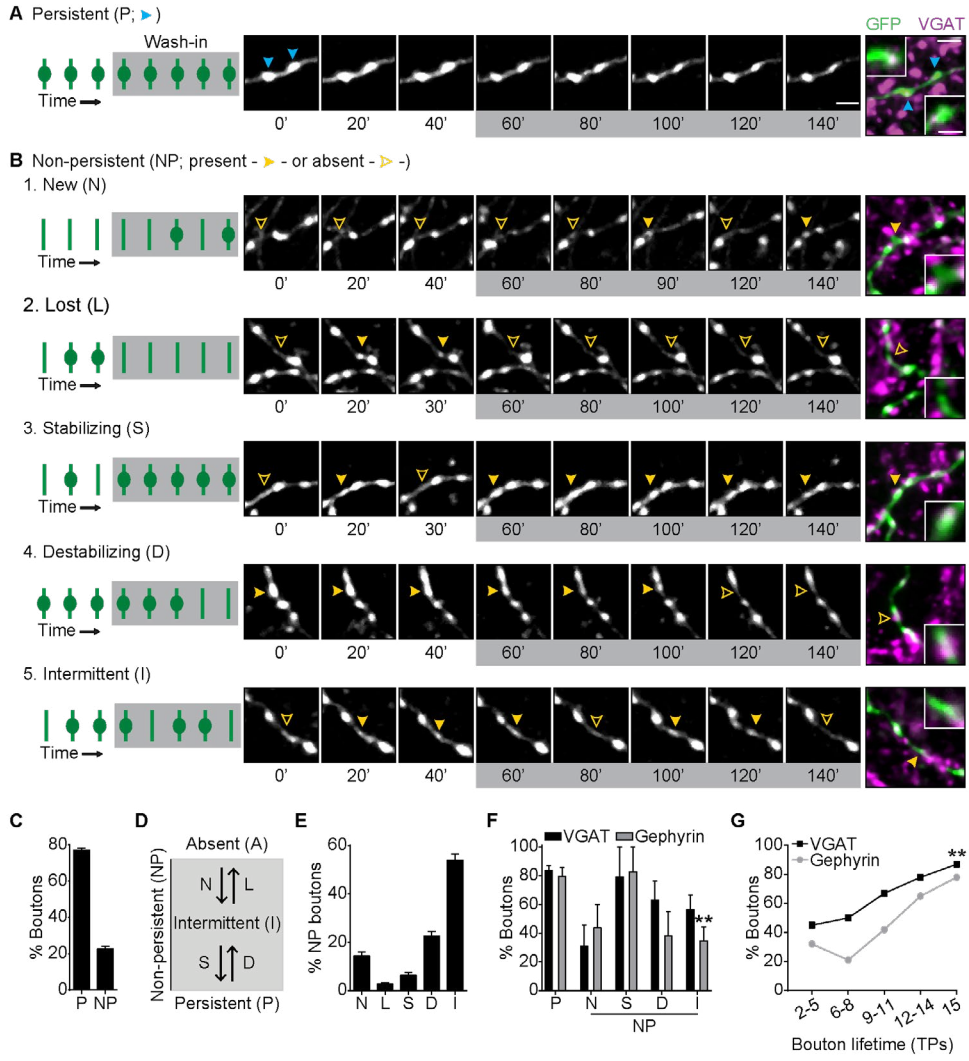

Figure 1. Classification of presynaptic inhibitory boutons by their dynamics.

(A) Time-lapse two-photon images of two inhibitory boutons (blue arrowheads) along a GAD65-GFP-labeled axon in the CA1 region of the hippocampus. These boutons were present at all time points, and were therefore categorized as persistent boutons. Only every second image is shown for clarity. On the right, the same region is shown after fixation and staining against vesicular GABA transporter (VGAT, magenta). The zoom shows a single optical plane through the bouton to demonstrate overlap (white) of VGAT and GFP boutons (green). Time in minutes. Scale bars 2 µm and 1 µm (zoom).

(B1-5) Same as in A, showing examples of new (B1; absent during baseline), lost (B2; absent during wash-in), stabilizing (B3; non-persistent during baseline, persistent during wash-in), destabilizing (B4; persistent during baseline, non-persistent during wash-in) and intermittent (B5; non-persistent during both baseline and wash-in) boutons. Filled yellow arrowheads indicate that the bouton is present, and empty yellow arrowheads indicate that

the bouton is absent at the time point shown.
(C) Average fraction of persistent (P) and non-persistent (NP) boutons at any given time point.
(D) Schematic illustration of bouton classification. We consider 3 developmental stages of inhibitory boutons at axon-dendrite crossings: absent (A), non-persistent (NP) or persistent (P). Within the group of NP boutons, we define 5 subgroups, reflecting transitions between these stages: N: new (A → NP), L: lost (NP → A), S: stabilizing (NP → P), D: destabilizing (P → NP) and I: intermittent (always NP) boutons.
(E) Average fraction of the 5 subgroups of non-persistent (NP) boutons normalized to the total number of NP boutons (N – new; L – lost; S – stabilizing; D – destabilizing; I – intermittent).
(F) Fraction of boutons positive for VGAT and gephyrin per axon. Two-way ANOVA analysis showed a significant effect on bouton type ($p = 0.008$). For gephyrin, P vs I, $p = 0.001$ (Sidak's multiple comparisons test).
(G) Fraction of boutons co-localizing with VGAT or gephyrin as a function of bouton lifetime (total number of time points (TPs) present during the imaging period). Lost boutons ('L' in D) were not included. χ^2: TP2-5, $p = 0.36$; TP6-8, $p = 0.11$; TP9-11, $p = 0.15$; TP12-14, $p = 0.33$: TP15, $p = 0.008$.

Sema4D treatment induces stabilization of inhibitory boutons

We used our live imaging method to examine if Sema4D signaling affects a specific step in the process of inhibitory synapse formation. We bath applied the extracellular domain of mouse Sema4D conjugated to the Fc region of mouse IgG2A (Sema4D; 1 nM) and compared inhibitory bouton dynamics during a baseline period of 5 time points and during Sema4D treatment in the subsequent 10 time points (Fig. 2A). We used Fc (1 nM) as a control treatment (Kuzirian et al., 2013). Bath application of Sema4D did not affect axonal morphology (Fig. 2A) and did not change the overall density of inhibitory boutons (Fig. 2B). However, when we analyzed the different subgroups of non-persistent boutons, we found that Sema4D treatment resulted in an enhanced fraction of stabilizing boutons from 6 ± 2% to 16 ± 3% (Fig. 2C). The absolute density of stabilizing boutons was increased by >2-fold, while the other subgroups of boutons were unaffected by Sema4D (Fig. 2D-H). Noticeably, new boutons were unaffected (Fig. 2D), indicating that Sema4D treatment did not induce de novo bouton formation. To examine how bouton stabilization developed over time, we quantified the number of boutons that were present for 5 consecutive time points during the baseline and the wash-in period. Sema4D induced a marked increase in bouton stabilization over the course of the wash-in period (Fig. 2I), and strongly increased the number of boutons that were stabilized by the end of the imaging period (Fig. 2J). Stabilizing boutons were relatively rare in our slices, as under control conditions most axons display no, or at most one, stabilizing bouton (Fig. 2K). Treatment with Sema4D significantly increased

the fraction of axons with one or more stabilizing boutons (Fig. 2K). Longer Sema4D treatment (6 h) did not increase bouton stabilization beyond the 2 h level (Fig. 2L), indicating that only a limited number of inhibitory boutons can be stabilized by Sema4D. Altogether, these data show that Sema4D treatment in intact tissue does not induce de novo bouton formation, but rather specifically promotes the stabilization of inhibitory presynaptic boutons, without affecting synapse elimination.

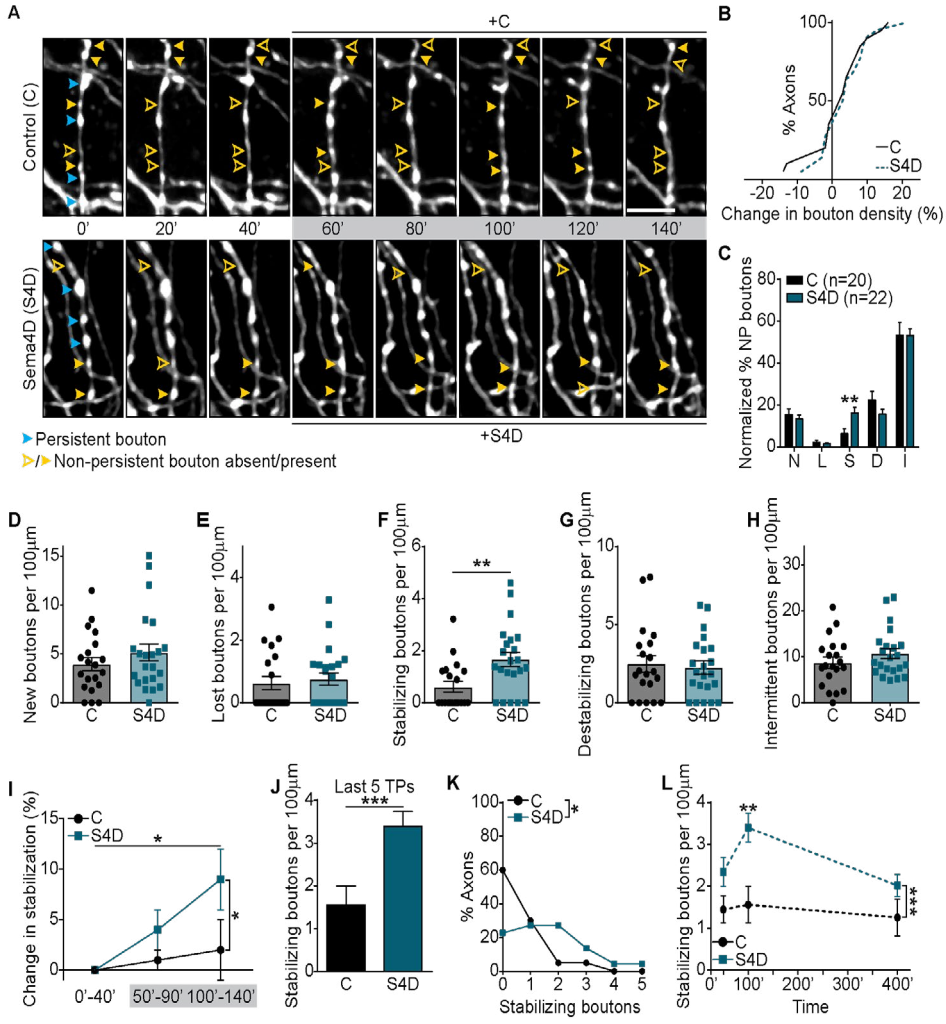

Figure 2. Sema4D treatment promotes inhibitory bouton stabilization.
(A) Time-lapse two-photon images of GFP-labeled inhibitory axons in the CA1 region of

the hippocampus during baseline (5 time points) and wash-in (10 time points; gray box) of 1 nM Fc - control (C; upper panel) or 1 nM Sema4D-Fc (S4D; bottom panel). Only every second image is shown for clarity. Persistent (blue) and non-persistent (yellow) boutons are indicated by arrowheads. Filled arrowheads indicate that the bouton is present, and empty arrowheads indicate that the bouton is absent at that time point. Images are maximum intensity projections of 11-18 z stacks. Time in minutes. Scale bar 5 μm.
(B) Cumulative distribution of the change in mean bouton density during the wash-in period compared to baseline after wash-in of C or S4D (MW, p = 0.83).
(C) Average fraction of subgroups of non-persistent boutons in C- and S4D-treated axons: N – new (MW, p = 0.86); L – lost (MW, p = 0.93); S – stabilizing (MW, p = 0.003); D – destabilizing (MW, p = 0.25); I – intermittent (MW, p = 0.89).
(D-H) Density of new (D; MW, p = 0.41), lost (E; MW, p = 0.61), stabilizing (F; MW, p = 0.003), destabilizing (G; MW, p = 0.84) and intermittent (H; MW, p = 0.34) boutons in axons treated with 1 nM Fc (C) and 1 nM Sema4D-Fc (S4D). Each dot represents an individual axon.
(I) Stabilization of inhibitory boutons, as determined by the change (compared to baseline) in density of boutons that were present at 5 consecutive time points during the imaging period: 0'-40' (baseline), 50'-90' (wash-in, gray box) and 100'-140' (wash-in, gray box). Two-way ANOVA analysis showed a significant effect of both treatment (p = 0.04) and time (p = 0.03).
(J) Density of boutons that stabilized in the last 5 time points (TPs) (MW, p = 0.0008).
(K) Frequency distribution of the stabilizing bouton density in C- and S4D-treated axons (χ^2, p = 0.03).
(L) Density of stabilizing boutons after treatment with Fc or S4D for 50, 100 and 400 minutes. Two-way ANOVA analysis showed that S4D increased bouton density independent of time (p = 0.0002). At 100', p = 0.005 (Sidak's multiple comparisons test).
Data are represented as mean ± SEM. Data from 20 control axons (N=6) and 22 S4D-treated axons (N=5). Data in L at 400' from 15 control axons (N=4) and 17 S4D-treated axons (N=4)

Sema4D-induced stabilization of inhibitory boutons is the first step of inhibitory synapse formation

We wanted to verify that Sema4D-induced inhibitory bouton stabilization leads to the formation of functional synapses in our slices. We treated organotypic hippocampal slices with 1 nM Fc or 1 nM Sema4D for 24 h, and recorded miniature inhibitory postsynaptic currents (mIPSCs) (Fig. 3A). Treatment with Sema4D increased the mIPSC frequency by 37% (from 5.2 ± 0.5 to 7.1 ± 0.5 Hz), while mIPSC amplitude was not affected (Fig. 3B,C). We also determined overall inhibitory synapse density by co-localizations of presynaptic VGAT and postsynaptic gephyrin (Fig. 3D,E). Consistent with the electrophysiology results, Sema4D induced a clear 24 ± 7% increase in the density of inhibitory synapses (Fig. 3F). These results demonstrate that the bouton stabilization observed within 2 h after Sema4D treatment leads to the formation of new functional synapses after 24 h.

A previous study has shown that Sema4D can induce rapid changes in

postsynaptic gephyrin in primary neurons (Kuzirian et al., 2013), but it was not addressed if these postsynaptic changes preceded or followed presynaptic changes. To determine the time course of the recruitment of pre- and postsynaptic elements during Sema4D-induced synapse formation, we quantified VGAT and gephyrin immunostaining after 2, 6 and 24 h treatments. Treatment with Sema4D induced an increase in the area of VGAT puncta, without affecting their density (Fig. 3G-I), consistent with an effect on stabilization, and not de novo formation, of inhibitory boutons. For gephyrin, Sema4D treatment caused an increase in puncta density, but not in their size (Fig. 3J-L), suggesting that stabilizing boutons were recruiting gephyrin. The average puncta intensity was not affected (at 24 h, VGAT: 107 ± 4% of control, $p = 0.35$ (MW); gephyrin: 106 ± 5% of control, $p = 0.51$ (MW)). Interestingly, the time course for presynaptic and postsynaptic changes was different. Whereas an increase in presynaptic VGAT area could already be detected after 6 h (Fig. 3G), the increase in postsynaptic gephyrin density was only evident after 24 h (Fig. 3K). This suggests that Sema4D signaling induced a gradual increase in presynaptic vesicle content in stabilized boutons and subsequent acquisition of postsynaptic scaffolds to form new inhibitory synapses. Our data indicate that Sema4D signaling primarily acts via the presynaptic axon and that the changes in postsynaptic gephyrin are secondary.

The previously reported rapid increase in postsynaptic gephyrin clusters after Sema4D treatment in primary cultures (Kuzirian et al., 2013) may be well explained by an overall difference in neuronal maturation level compared to our experiments. In young neurons, new gephyrin clusters can be rapidly induced by local GABA signaling (Oh et al., 2016), while in mature neurons prolonged or additional signaling appears to be required. In our slices, Sema4D treatment increased inhibitory synapse density by ~25% after 24 hours (Fig. 3F), which is comparable to experience-dependent changes in inhibitory synapses observed in vivo (Keck et al., 2011; Chen et al., 2015; Villa et al., 2016).

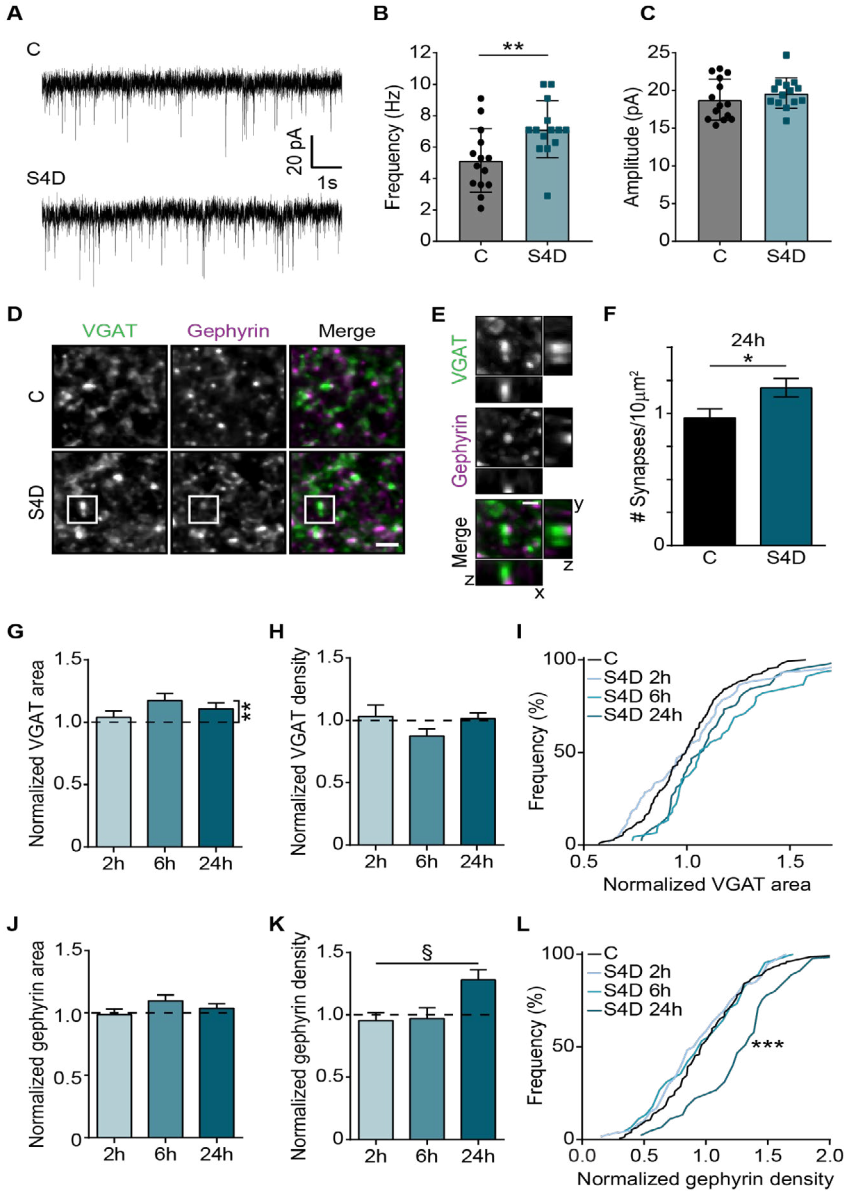

Figure 3. Sema4D increases overall inhibitory synaptic density.

(A) Representative whole-cell voltage-clamp recordings of miniature inhibitory postsynaptic currents (mIPSCs) from CA1 pyramidal cells in organotypic hippocampal slices treated for 24 h with 1 nM Fc (C) or 1 nM S4D (S4D).

(B) Mean mIPSC frequency after 24 h treatment with C or S4D (MW, p = 0.008).

(C) Mean mIPSC amplitude after 24 h treatment with C or S4D (MW, p = 0.35).

(D) Representative images of CA1 dendritic area of GAD65-GFP hippocampal slices treated with 1 nM Fc (C) or 1 nM Sema4D-Fc (S4D) for 24 h, and immunostained for

presynaptic vesicular GABA transporter (VGAT, green) and gephyrin (magenta). Images are average intensity projections of 5 z stacks. Scale bar 2 µm.
(E) Example of an inhibitory synapse (white box in D), identified as the apposition of VGAT (green) and gephyrin (magenta) puncta. The respective xz and yz projections show the close apposition of the two markers. Images are maximum intensity projections of 6 z stacks. Scale bar 1 µm.
(F) Density of inhibitory synapses in slices treated with Fc or S4D for 24 h (MW, $p = 0.03$).
(G) Normalized area of VGAT puncta (after treatment with 1 nM S4D for 2 h, 6 h and 24 h). Two-way ANOVA analysis showed that S4D treatment increased VGAT area independent of time ($p = 0.005$).
(H) Normalized density of VGAT puncta, after treatment with 1 nM S4D for 2 h, 6 h and 24 h.
(I) Cumulative distributions of the normalized area of VGAT after treatment with 1 nM S4D for 2, 6 and 24 h. Black line represents the normalized control values. $p = 0.81$, $p = 0.08$ and $p = 0.14$ (KS) for 2, 6 and 24 h, respectively.
(J-K) Same as G-H, but for normalized area (J) and density (K) of postsynaptic gephyrin puncta. In K, two-way ANOVA analysis showed a significant effect of time ($p = 0.04$) and an interaction between treatment and time (§; $p = 0.04$).
(L) Same as in I, but for normalized gephyrin density. $p = 0.99$, $p = 0.99$ and $p < 0.0001$ (KS) for 2, 6 and 24 h, respectively.
Data are represented as mean ± SEM. Data in A-C from 14 control cells (N=5) and 14 S4D-treated cells (N=7), data in F from 15 control images (N=3) and 15 S4D images (N=3), and data in G-L from 15-20 control images (N=3-4) and 15-20 S4D images (N=3-4) per time point. Dashed lines in G, H and J, K represent control values (treatment with 1nM Fc for 2 h, 6 h and 24 h). In B and C, dots represent individual cells.

Local application of Sema4D suggests competition between presynaptic boutons

Under physiological conditions, Sema4D is a membrane-attached protein acting locally at the synapse (Pasterkamp, 2012; Raissi et al., 2013), which is very different from the bath-applied Sema4D treatment that we use in our experiments. To examine possible differences between local and global Sema4D signaling, we locally applied Sema4D to short stretches (~40 µm) of GFP-labeled inhibitory axons (Fig. 4A). Local application with control solution slightly reduced local bouton stabilization (compare control curves in 4B and 2I), possibly because of mechanical pressure. In contrast, local application of Sema4D induced robust stabilization of inhibitory boutons in these axons (Fig. 4B). In fact, local application of Sema4D induced a significant increase in local bouton density (Fig. 4C), whereas bath application had failed to induce a change in overall bouton density (Fig. 2B). Presynaptic boutons are known to share presynaptic proteins and vesicles along the axon (Staras, 2007; Bury and Sabo, 2016). Our data suggest that stabilizing boutons compete for presynaptic components within individual axons when Sema4D is bath applied, limiting an increase in overall bouton density.

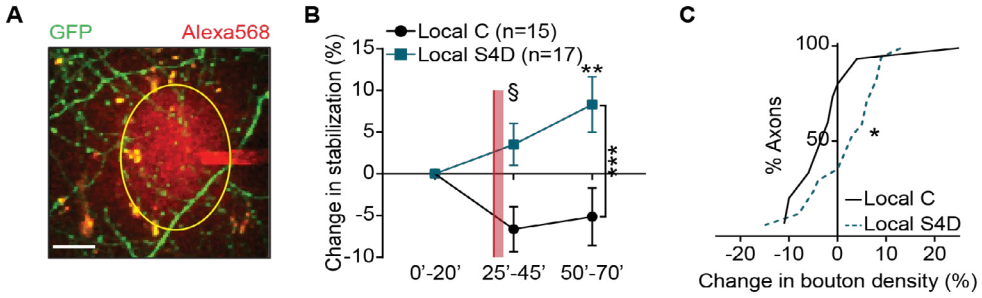

Figure 4. Sema4D induces local stabilization of inhibitory boutons.
(A) Representative image of the local treatment of GFP-labeled inhibitory axons in the CA1 region of the hippocampus. Alexa568 (red) was added to the pipette to visualize the area of the puff (yellow circle). Scale bar 10 µm.
(B) Stabilization of inhibitory boutons, as determined by the change (compared to baseline) in density of boutons that were present at 5 consecutive time points during the imaging period after local treatment with 10 nM Fc (C) or 10 nM Sema4D (S4D). Red line marks the puffing. Two-way ANOVA analysis showed a significant effect of treatment ($p = 0.0002$) and an interaction between treatment and time (§; $p = 0.02$). At 50'-70', $p = 0.003$ (Sidak's multiple comparisons test).
(C) Cumulative distribution of the change in mean bouton density after local treatment with C or S4D compared to baseline (MW, $p = 0.045$).
Data are represented as mean ± SEM. Data from 15 control axons (N=6) and 17 S4D-treated axons (N=6).

Actin remodeling by low dosis of LatrunculinB promotes stabilization of inhibitory boutons

Induction of inhibitory synapses in response to Sema4D was previously shown to be mediated by presynaptic PlexinB1 receptors (Kuzirian et al., 2013; McDermott et al., 2018). Bouton stabilization is presumably induced by local changes in the intracellular actin cytoskeleton via Sema4D/PlexinB1 signaling pathways, which are well described in non-neuronal cells (Zhou et al., 2008; Cagnoni and Tamagnone, 2014). Interestingly, it was reported that Sema4D/PlexinB1 signaling can induce either polymerization or depolymerization of actin via RhoA regulation, depending on the co-activation of receptor tyrosine kinases MET and ErbB-2, which act as co-receptors for PlexinB1 (Swiercz et al., 2008; Sun et al., 2012). To examine how the actin cytoskeleton is involved in inhibitory bouton stabilization, we studied the effect of two actin remodeling drugs in our system with intended opposite effects: the actin monomer sequestering drug LatrunculinB (100 nM LatB), which promotes actin depolymerization, and the actin stabilizer Jasplakinolide (200

nM Jasp), which promotes actin polymerization. None of these actin drugs affected overall axon morphology (Fig. 5A). We analyzed bouton dynamics in the presence of these actin drugs and found that LatB treatment, and not Jasp treatment, increased the fraction of stabilizing boutons (Fig. 5B,C). The effect of LatB was highly specific for stabilizing boutons, as the other bouton subgroups were not affected (Fig. 5C). Indeed, we found that LatB specifically increased the absolute density of stabilizing boutons by almost 2-fold (Fig. 5D) and increased the fraction of axons with stabilizing boutons (Fig. 5E), while Jasp did not change overall inhibitory bouton dynamics. The changes in bouton dynamics after LatB treatment were rapid and were surprisingly similar to Sema4D treatment (compare Fig. 5D-E with Fig. 2F and 2K). At these low concentrations, actin drugs do not affect synaptic function (Honkura et al., 2008; Rex et al., 2009), and we therefore assume that the observed effects reflect the direct action of the actin drugs on the local actin cytoskeleton. Our findings suggest that inhibitory bouton stabilization is promoted by conditions favoring local actin depolymerization, rather than polymerization.

The striking similarity between stabilization of inhibitory boutons induced by treatment with LatB or Sema4D suggests that both treatments induce a comparable effect on intracellular actin. As we found that only a specific subset of inhibitory boutons was stabilized by Sema4D treatment, we tested if these were the same boutons that responded to LatB. We treated slices with a combination of LatB and Fc or LatB and Sema4D. We found that bouton stabilization by LatB occluded a further increase by co-application with Sema4D (Fig. 5F,G). These results suggest that LatB and Sema4D treatment act to stabilize a specific, overlapping, subset of inhibitory boutons.

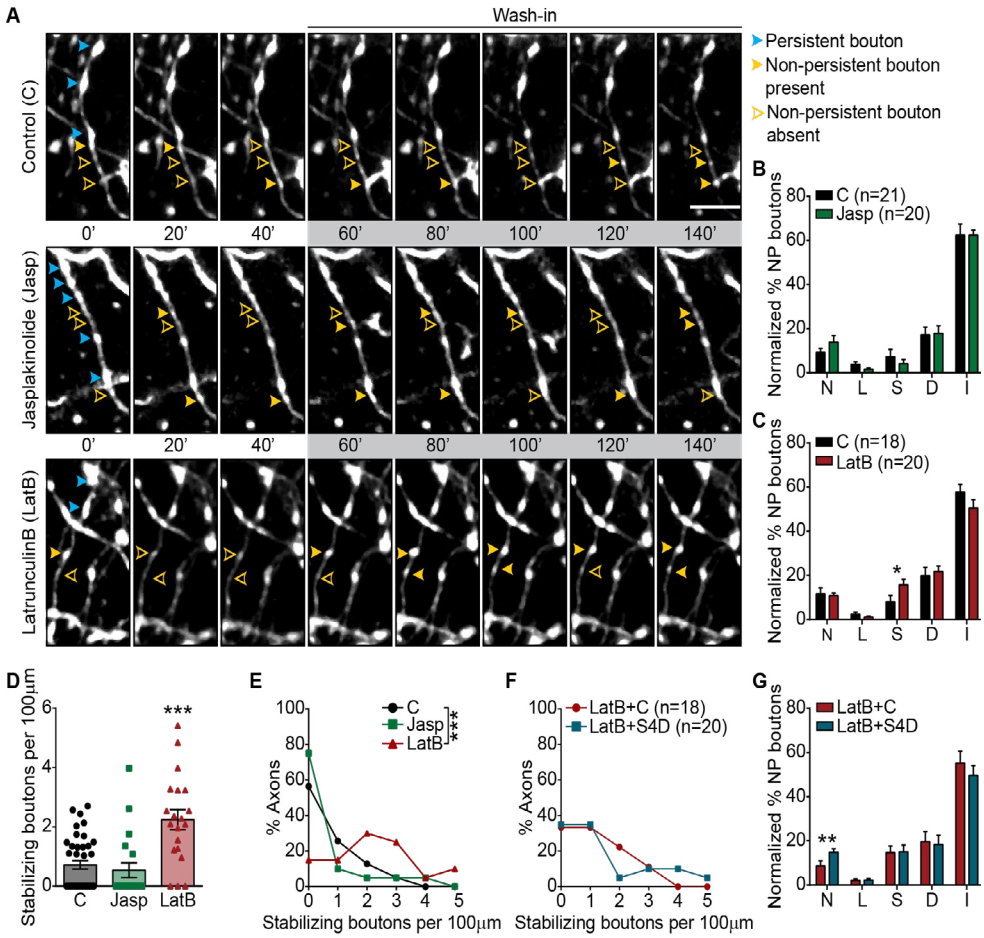

Figure 5. Inhibitory bouton dynamics are regulated by actin.

(A) Time-lapse two-photon images of GAD65-GFP-labeled axons in the CA1 region of the hippocampus during baseline (5 time points) and wash-in (10 time points; gray box) of DMSO - control (C; upper panel), 200 nM Jasplakinolide (Jasp; middle panel) or 100 nM LatrunculinB (LatB; bottom panel). Only every second image is shown for clarity. Persistent and non-persistent boutons are indicated as in Figure 2. Images are maximum intensity projections of 12-14 z stacks. Time in minutes. Scale bar 5 µm.

(B) Fraction of non-persistent (NP) boutons in C and Jasp-treated axons: N – new (MW, $p = 0.37$); L – lost (MW, $p = 0.18$); S – stabilizing (MW, $p = 0.49$); D – destabilizing (MW, $p = 0.95$); I – intermittent (MW, $p = 0.93$).

(C) Same as in B, but for C and LatB-treated axons (N: MW, $p = 0.99$; L: MW, $p = 0.66$; S: MW, $p = 0.01$; D: MW, $p = 0.6$; I: MW, $p = 0.29$).

(D) Density of stabilizing boutons in C, Jasp- (MW: $p = 0.28$) and LatB-treated axons (MW: $p < 0.0001$). Dots represent individual axons.

(E) Frequency distribution of the stabilizing bouton density in C, Jasp- and LatB-treated axons (χ^2; C vs Jasp, $p = 0.31$; C vs LatB, $p = 0.0005$).

(F) Same as E, but for combined treatment with 100 nM LatB/1 nM Fc (LatB+C) or 100 nM

LatB/1 nM Sema4D (LatB+S4D) (χ^2, p = 0.37).
(G) Same as B, but for combined treatment with LatB+C or LatB+S4D (N: MW, p = 0.005; L: MW, p = 0.58; S: MW, p = 0.96; D: MW, p = 0.82; I: MW, p = 0.52).
Data are represented as mean ± SEM. Data in B from 21 control axons (N=6) and 20 Jasp-treated axons (N=5), in C from 18 control axons (N=5) and 20 LatB-treated axons (N=5) and in F-G from 18 LatB+Fc- (N=4) and 20 LatB+S4D-treated axons (N=5).

We then wondered if treatment with the actin depolymerizing drug LatB would be sufficient to induce inhibitory synapse formation, similar to Sema4D signaling (Fig. 3F). Interestingly, we observed that although LatB induced changes in VGAT area and gephyrin puncta density after 2 h (Fig. 6A-F), these changes were not coordinated and did not result in an increase in the density of inhibitory synapses (Fig. 6G). The changes in gephyrin and VGAT staining returned to baseline with longer LatB treatment. Together, our data suggest that LatB and Sema4D induce rapid stabilization of the same subgroup of inhibitory boutons, but that only Sema4D signaling leads to coordinated pre- and postsynaptic changes resulting in inhibitory synapse formation. This indicates that presynaptic bouton stabilization alone is not enough to induce inhibitory synapse formation, which requires further signaling mechanisms.

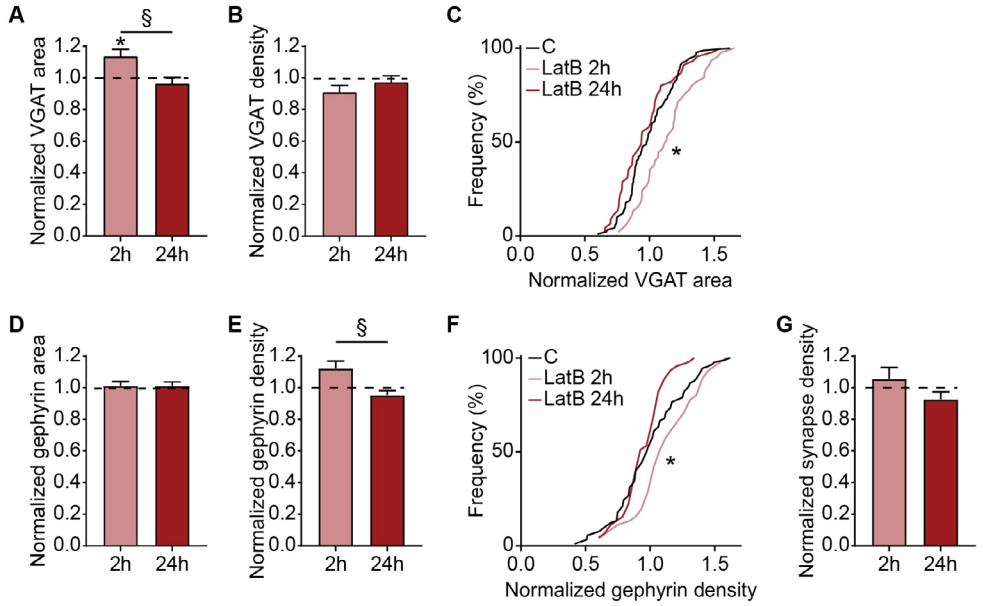

Figure 6. Latrunculin B treatment does not promote inhibitory synapse formation.
(A) Normalized area of presynaptic vesicular GABA transporter (VGAT) puncta after treatment with 100 nM LatB for 2 h and 24 h. Two-way ANOVA analysis indicated a significant effect of time (p = 0.02) and an interaction between treatment and time (§, p = 0.02).

(B) Normalized density of VGAT, after treatment with 100 nM LatB for 2 h and 24 h.
(C) Cumulative distributions of the normalized area of VGAT after treatment with 100 nM LatB for 2 and 24 h. Black line represents the normalized control values. p = 0.047 and 0.33 (KS) for 2 and 24 h, respectively.
(D-E) Same as in A-B, but for the area (D) and density (E) of postsynaptic gephyrin puncta. In E, Two-way ANOVA analysis showed a significant effect of time (p =0.04) and interaction between treatment and time (§, p =0.04).
(F) Same as in C, but for normalized gephyrin density. p = 0.047 and 0.33 (KS) for 2 and 24 h, respectively.
(F) Normalized density of inhibitory synapses.
Data are represented as mean ± SEM. Data from 15 control images (N=3) and 15 LatB images (N=3) per time point. Dashed line represents control values (treatment with DMSO for 2 h and 24 h).

Inhibitory bouton stabilization by Sema4D requires MET activation

Our observation that LatB could mimic the Sema4D-induced stabilization of inhibitory boutons points to a possible involvement of MET, as co-activation of MET mediates the actin depolymerization pathway downstream of Sema4D/PlexinB1 signaling (Swiercz et al., 2008). We therefore assessed if MET activation is necessary for the Sema4D-induced bouton stabilization by making use of the highly specific MET inhibitor PHA-665752 (PHA) (Christensen et al., 2003; Lim and Walikonis, 2008). We first verified that adding PHA alone did not affect bouton dynamics (Fig. 7A) or spontaneous inhibitory postsynaptic currents (Fig. 7B-D), indicating that MET is not very active under baseline conditions in our slices. Next, we treated our slices with Sema4D to induce bouton stabilization and compared bouton dynamics in the presence or absence of PHA (Fig. 7E). Blocking MET with PHA completely abolished the Sema4D-induced increase in the density of stabilizing boutons, while the other bouton subgroups were hardly affected (Fig. 7F). In fact, blocking MET in combination with Sema4D treatment almost entirely abolished the occurrence of stabilizing boutons in our slices (Fig. 7G,H). Consistent with the live imaging data, inhibiting MET with PHA also blocked the increase in VGAT staining intensity (Fig. 7I,J) and mIPSC inter-event interval (Fig. 7K) triggered by Sema4D treatment. Taken together, these data indicate that activation of MET is required for the Sema4D-induced stabilization of inhibitory boutons.
As the actin depolymerization pathway downstream of Sema4D/PlexinB1 signaling via MET is mediated via a reduction of intracellular RhoA activity (Swiercz et al., 2008; Sun et al., 2012), we tested if stabilization of inhibitory boutons could also be achieved by directly reducing ROCK activity, a well-known downstream effector of RhoA (Amano et al., 2010). We found that treatment with the specific ROCK inhibitor Y-27632 (Deguchi et al., 2016) resulted in an increase in the density of stabilizing boutons in our slices

(Fig. 7L), without affecting the other subclasses of boutons. These findings are consistent with an intracellular pathway induced by Sema4D/PlexinB1 signaling via co-activation of MET and reduction of ROCK activity to promote stabilization of inhibitory boutons.

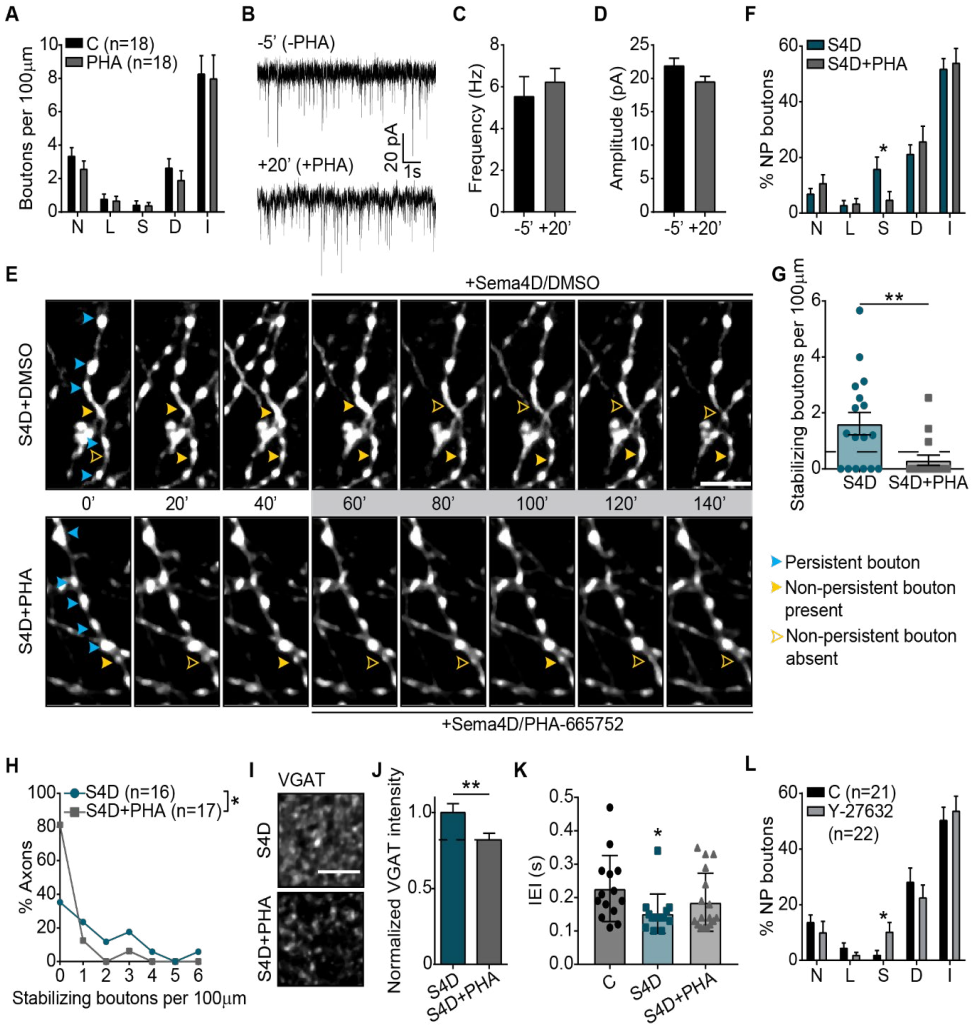

Figure 7. Inhibitory bouton stabilization by Sema4D requires MET activation.
(A) Density of non-persistent boutons in slices treated with DMSO (C) and 1 µM PHA-665752 (PHA): N – new (MW, p = 0.28); L – lost (MW, p = 0.77); S – stabilizing (MW, p = 0.98); D – destabilizing (MW, p = 0.24); I – intermittent (MW, p = 0.67).
(B) Representative whole-cell voltage-clamp recordings of spontaneous IPSCs (sIPSCs) from CA1 pyramidal cells in organotypic hippocampal slices before (-5') and after treatment (+20') with PHA-665752 (PHA; 1 µM). Time in minutes.
(C-D) Mean sIPSC frequency (C) and amplitude (D) before (-5') and after (+20') treatment

with PHA. Time in minutes. One-way ANOVA for multiple time points: p = 0.97 (C); p = 0.19 (D).
(E) Time-lapse two-photon images of GAD65-GFP-labeled axons in organotypic hippocampal slices during wash-in (gray box) of combination of 1 nM Sema4D and DMSO (S4D; upper panel) or combination of 1 nM Sema4D with 1 µM PHA-665752 (S4D+PHA; bottom panel). Only every second image is shown for clarity. Persistent and non-persistent boutons are indicated as in Figure 2. Images are maximum intensity projections of 15-16 z stacks. Scale bar 5 µm.
(F) Fraction of non-persistent (NP) boutons in S4D- and S4D+PHA-treated axons: N: MW, p = 0.34; L: MW, p = 0.74; S: MW, p = 0.01; D: MW, p = 0.64; I: MW, p = 0.53.
(G) Density of stabilizing boutons in slices treated with S4D or S4D+PHA (MW, p = 0.006). Dashed line represents control values. Dots represent individual axons.
(H) Frequency distribution of the stabilizing bouton density in S4D- and S4D+PHA-treated axons (χ^2, p = 0.048).
(I) Representative images of hippocampal slices treated with S4D (upper panel) or S4D+PHA (bottom panel) for 100', and stained for presynaptic VGAT. Images are average intensity projections of 5 z stacks. Scale bar 5 µm.
(J) Normalized mean staining intensity for VGAT in S4D- and S4D+PHA-treated slices (MW, p = 0.009). Control value is indicated with dashed line.
(K) Inter-event interval (IEI) of mIPSCs from CA1 pyramidal cells in organotypic slices after treatment with 1 nM Fc/DMSO (C), 1 nM S4D/DMSO (S4D) or 1nM S4D/1 µM PHA-665752 (S4D+PHA) for 24 h (KW, C vs S4D, p = 0.04; C vs PHA, p = 0.19). Dots represent individual cells.
(L) Fraction of non-persistent boutons in axons treated with MQ (control; C) or 10 µM ROCK inhibitor Y-27632: N: MW, p = 0.05; L: MW, p = 0.39; S: MW, p = 0.02; D: MW, p = 0.38; I: MW, p = 0.78.
Data are represented as mean ± SEM. Data in A from 18 control axons (N=4) and 18 PHA-treated axons (N=4), in C-D from 5 CA1 pyramidal cells (N=5), in F-H from 17 S4D-treated axons (N=4) and 16 S4D+PHA-treated axons (N=4), in J from 16 images of S4D-treated slices (N=3) and 23 images of S4D+PHA-treated slices (N=4), in K from 14 control cells (N=5), 14 S4D-treated cells (N=7) and 17 S4D+PHA-treated cells (N=6), and in L from 21 control axons (N=5) and 22 Y-27632-treated axons (N=5).

MET is required in presynaptic inhibitory axons

Our pharmacological experiments do not address if the Sema4D-induced changes in actin occur in the pre- or postsynaptic compartment. MET was reported to be expressed predominantly in axons, where it is present in small puncta in the axonal shaft and small presynaptic terminals (Judson et al., 2009; Eagleson et al., 2013). However, studies on MET have focused on glutamatergic synapses (Tyndall and Walikonis, 2006; Xie et al., 2016) and MET localization in GABAergic axons has never been directly addressed. We made use of an antibody (Qiu et al., 2014) and a nanobody (Heukers et al., 2014) with demonstrated specificity for MET to localize MET in our slices. We first confirmed that MET was present at synapses in primary hippocampal cultures (Fig. 8A,B). In line with previous reports (Tyndall and Walikonis,

2006; Eagleson et al., 2013; Xie et al., 2016), the majority of MET puncta overlapped with excitatory synapses (Fig. 8A,B), but clear association of MET with inhibitory presynapses was also observed in these cultures (Fig. 8B). This was further confirmed with STED microscopy (Fig. 8C). We then used the MET nanobody and antibody to label MET in our hippocampal slices of GAD65-GFP mice (Fig. 8D). Although there was a quantitative difference presumably reflecting a difference in labeling affinity, both methods clearly showed that a subset of GFP-labeled inhibitory boutons was enriched for MET (Fig. 8E). Comparison between the MET staining pattern with staining for postsynaptic gephyrin (compare Figs. 8F and 3E) suggests a presynaptic localization of MET at these inhibitory synapses, as MET puncta were often completely enclosed by the GFP-labeled bouton. These data indicate that MET is present at inhibitory axons and terminals, where it can mediate Sema4D signaling to induce bouton stabilization.

To directly test if presynaptic MET is required for Sema4D-induced bouton stabilization we reduced MET specifically in presynaptic inhibitory axons using a miRNA-based knock down approach. We first verified that the miRNA construct effectively reduced MET levels in primary hippocampal neurons (Fig. 8G-H) and HEK cells (Fig. 8I). We then injected Cre-dependent Lentiviruses in hippocampal slices from VGAT-Cre mice at DIV 1 to infect a few GABAergic cells per slice. We either used a construct with GFP (control), or GFP with miRNA against MET (MET-miRNA), and we performed similar two-photon experiments at >DIV 14 as previously described. We first confirmed that Sema4D promoted bouton stabilization in GFP-positive axons in VGAT-Cre slices (Fig. 8J). As GFP-labeled axons in VGAT-Cre slices comprise all inhibitory axons (compared to only a subset in GAD65-GFP slices), this suggests that many, if not all, inhibitory axons are sensitive to Sema4D signaling. In MET-miRNA axons, in which MET levels were reduced for several days, overall bouton dynamics appeared slightly enhanced (fraction of non-persistent boutons in MET-miRNA axons was 20.9 ± 1.6% compared to 15.5 ± 1.7% in control GFP axons; $p = 0.04$). In contrast to GFP-positive axons, Sema4D was not able to increase the density of stabilizing boutons along MET-miRNA axons (Fig. 8K). These data demonstrate that Sema4D-induced inhibitory bouton stabilization requires the co-activation of presynaptic MET in inhibitory axons.

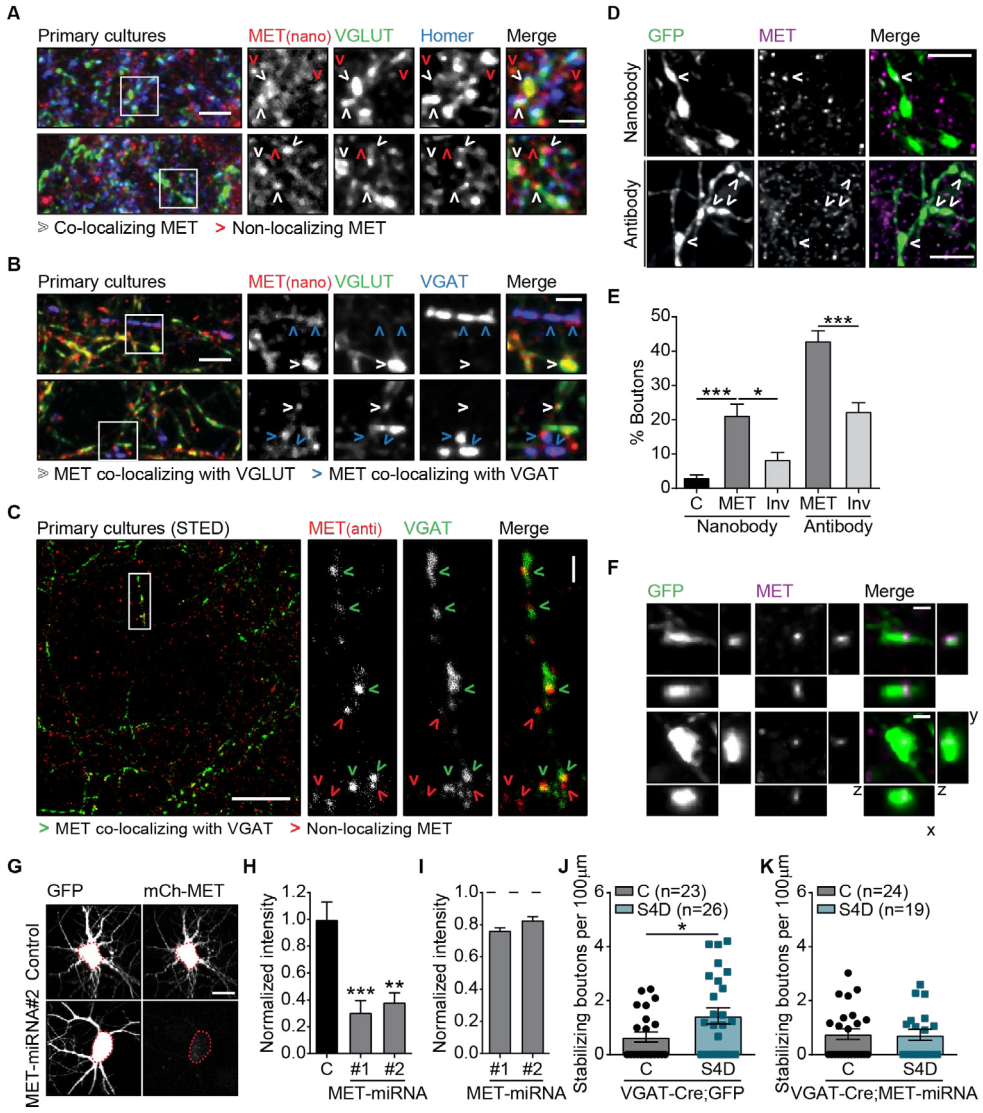

Figure 8. MET is required at inhibitory presynaptic boutons.

(A) Images of primary cultures of hippocampal neurons immunostained with MET nanobody (red) and markers for excitatory synapses: presynaptic vesicular glutamate transporter (VGLUT; green) and postsynaptic Homer (blue). The majority of MET puncta co-localize with one or both markers (white arrows), but some MET puncta do not co-localize (red arrows). Images are maximum intensity projections of 13 stacks. Scale bar 5 µm (overview) and 2 µm (zoom).

(B) Same as A, but neurons were stained with MET nanobody (red) and markers for excitatory presynapses (VGLUT; green) and inhibitory presynapses (vesicular GABA transporter VGAT; blue). White arrows indicate MET co-localizing with VGLUT and blue arrows indicate MET co-localizing with VGAT. Images are maximum intensity projections of 12 stacks. Scale bar 5

µm (overview) and 2 µm (zoom).
(C) Representative STED images (single optical sections) of primary cultures of hippocampal neurons immunostained with MET antibody (red) and VGAT (green). Green arrows highlight MET puncta co-localizing with VGAT, while red arrows indicate MET puncta that do not co-localize with VGAT. Scale bar 10 µm (overview) and 1 µm (zoom).
(D) Representative images of GFP-labeled inhibitory boutons (green) in hippocampal slices, stained with a nanobody (upper panel) and an antibody (lower panel) against MET (magenta). Images are maximum intensity projections of 5-6 z stacks. White arrows indicate MET enrichment in GFP-labeled boutons. Scale bar 5 µm.
(E) Fraction of GFP boutons positive for MET. Aspecific staining was determined by anti-myc staining without nanobody ('C'; black) and random co-localization was determined by inverting the MET channel ('Inv'; light gray) (Nanobody - KW, C vs MET: $p = 0.0002$, MET vs Inv: $p = 0.04$; Antibody: MW, $p < 0.0001$).
(F) Example of two inhibitory boutons (green) in hippocampal slices showing enrichment in MET (magenta), and the respective xz and yz projections. Images are maximum intensity projections of 6 z stacks. Scale bar 1 µm.
(G) Representative images of primary hippocampal neurons (DIV 11) transfected at DIV 9 with mCherry-MET (mCh-MET) together with GFP (control) or MET-miRNA#2+GFP (MET-miRNA#2). Red dashed line highlights the neuronal cell body. Scale bar 20 µm.
(H) Normalized intensity of mCherry-MET in primary hippocampal neurons co-transfected with GFP (control) or MET-miRNA constructs (KW: Cvs#1, $p < 0.0001$; Cvs#2, $p = 0.001$).
(I) Western blot analysis of MET levels in HEK293 cell extracts upon transfection with mCherry-MET and MET-miRNA constructs normalized to control (GFP). Dashed line represents control.
(J) Density of stabilizing boutons in GFP-positive axons treated with 1 nM Fc (C) and 1 nM Sema4D-Fc (S4D) in VGAT-Cre slices (MW; $p = 0.05$).
(K) Same as in J, but in MET-miRNA-expressing axons (MW; $p = 0.88$).
Data are represented as mean ± SEM. Data in E from 10 control images (N=2), 12 images in MET and inverted group (N=3) for the nanobody staining and 15 images in MET and inverted group (N=3) for the antibody staining, in H from 45 control cells (N=3), 40 MET-miRNA#1 cells (N=2) and 43 MET-miRNA#2 cells (N=3), in I from 2 independent Western blot experiments, in J from 23 control axons (N=6) and 26 S4D-treated axons (N=7), and in K from 24 control axons (N=6) and 19 S4D-treated axons (N=5). In J and K, dots represent individual axons.

Sema4D-induced bouton stabilization relies on network activity

Finally, we asked whether Sema4D-induced stabilization of inhibitory boutons depends on the level of neuronal activity. As previously reported (Schuemann et al., 2013), blocking activity by bath application of tetrodotoxin (TTX) mildly decreased overall bouton dynamics in our slices (data not shown). We found that in the presence of TTX, Sema4D treatment no longer induced stabilization of inhibitory boutons, and that Sema4D treatment even led to a reduction in bouton stabilization compared to control (Fig. 9A,B). Whereas under control conditions Sema4D treatment increased the fraction of axons that displayed stabilizing boutons, it led to a decrease in the presence of TTX (Fig. 9C,D). Interestingly, bouton stabilization by LatB was

not affected by TTX (Fig. 9A-D), indicating that activity-dependent changes in the actin cytoskeleton cannot explain this result. These findings suggest that the activity-dependent sensitivity to Sema4D is regulated upstream of the changes induced at the presynaptic actin cytoskeleton.

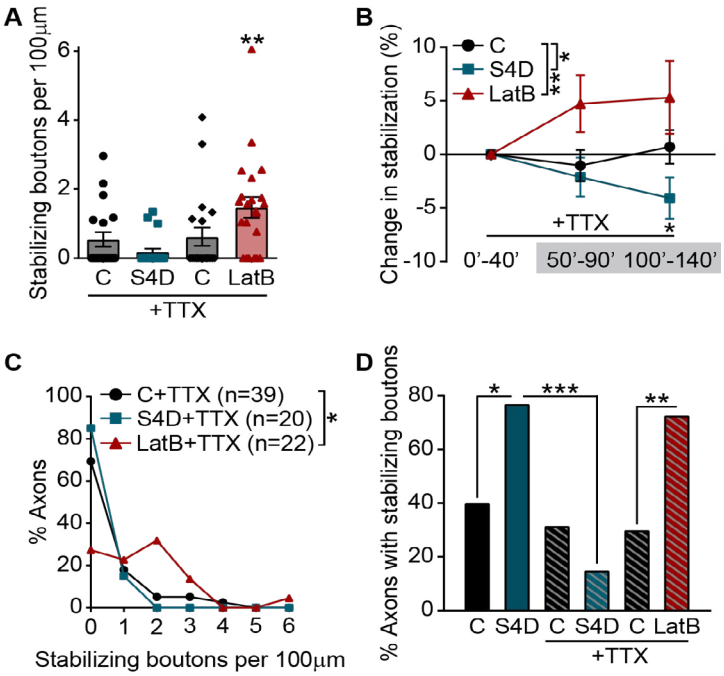

Figure 9. Sema4D-induced bouton stabilization is activity-dependent.

(A) Density of stabilizing boutons in axons treated with 1 nM Fc (C, circles) or DMSO (C, diamonds), 1 nM Sema4D-Fc (S4D), and 100 nM LatrunculinB (LatB) in the presence of 0.5 µM TTX (MW: C vs S4D, p = 0.17; C vs LatB, p = 0.008). Dots represent individual axons.

(B) Stabilization of inhibitory boutons upon treatment with C, S4D or LatB in the presence of 0.5 µM TTX, determined by the change (compared to baseline) in density of boutons that were present at 5 consecutive time points during the imaging period: 0'-40' (baseline), 50'-90' (wash-in) and 100'-140' (wash-in). Two-way ANOVA analysis showed a significant effect of treatment (C vs S4D, p = 0.01; C vs LatB, p = 0.0095). At 100'-140', C vs S4D, p = 0.04 (Sidak's multiple comparisons test).

(C) Frequency distribution of the stabilizing bouton density in C-, S4D- and LatB-treated axons, in the presence of 0.5 µM TTX (χ^2: C vs S4D, p = 0.32; C vs LatB, p = 0.01).

(D) Fraction of axons with stabilizing boutons in axons treated with C or S4D, in control or activity-depleted slices with TTX (χ^2 (p-values are Bonferroni-corrected): C vs S4D, p = 0.01; C vs C+TTX, p = 0.58; C+TTX vs S4D+TTX, p = 0.22; S4D vs S4D+TTX, p < 0.0001; C+TTX vs LatB+TTX, p = 0.006).

Data from 19 control (Fc) axons (N=5), 20 S4D-treated axons (N=5), 20 control (DMSO) axons (N=6) and 22 LatB-treated axons (N=6). The two controls groups are pooled for clarity in B and C, but statistics were performed between treatment and its own control.

DISCUSSION

Research on synapse formation is traditionally dominated by excitatory synapses and has been focused on the postsynaptic side. Inhibitory synapses are formed in a fundamentally different manner, with a more prominent role for the presynaptic axon (Wierenga et al., 2008). Our live imaging experiments provide unique insight into the dynamics of inhibitory synapse formation in brain slices, which remain undetected with methods using stationary comparisons before and after treatment. We used Sema4D-induced inhibitory synapse formation as a model system to study the molecular events happening during presynaptic bouton formation. Rather than being specific for a certain subtype of inhibitory cell, our observations indicate that Sema4D acts at a specific molecular step during inhibitory synapse formation. Our current data put the presynaptic inhibitory axon in the spotlight and highlights the importance of understanding the precise presynaptic changes and signaling events that occur during the formation of new inhibitory synapses.

We demonstrate that the primary action of Sema4D is on the presynaptic side. During the formation of inhibitory synapses, synaptic changes generally occur in a pre-before-post sequence (Wierenga et al., 2008; Dobie and Craig, 2011), but it was recently reported that the formation of inhibitory synapses can also be induced by postsynaptic gephyrin clustering (Flores et al., 2015). A previous observation of rapid formation of new gephyrin clusters after Sema4D treatment in primary cultures (Kuzirian et al., 2013) suggested that Sema4D may promote inhibitory synapse formation via postsynaptic gephyrin. However, our data clearly argue against a triggering mechanism of Sema4D via postsynaptic gephyrin and indicates that the primary action of Sema4D is at the presynaptic bouton. We found that Sema4D signaling does not induce de novo inhibitory synapse formation, but it specifically stabilizes non-persistent boutons within tens of minutes, without affecting bouton disassembly. Initial presynaptic bouton stabilization is followed by a slower postsynaptic recruitment of gephyrin and the entire synapse maturation process takes several (up to 24) hours. Our results highlight the importance of the presynaptic changes that occur during inhibitory synapse formation.

Our observations that longer Sema4D treatment does not further enhance bouton stabilization and that LatB and Sema4D stabilize an overlapping bouton population suggests that only a specific set of boutons is responsive to Sema4D. This indicates that Sema4D acts at a specific, early step during

the synapse formation process and inhibitory boutons which are more mature or too immature are irresponsive to Sema4D. Bouton stabilization and gephyrin recruitment was also induced by LatB, but in an uncoordinated manner, such that LatB failed to induce new inhibitory synapses after bouton stabilization (Figure 6). This suggests that Sema4D signaling coordinates pre- and postsynaptic changes and that independent signaling pathways exist for pre- and postsynaptic changes during inhibitory synapse formation. This is in line with two recent studies, which show that impairing clustering of postsynaptic gephyrin does not affect presynaptic bouton stabilization (Yamasaki et al., 2017; Wu et al., 2018). Gephyrin clustering at synapses is a complex process, which is regulated via phosphorylation-dependent interactions with multiple postsynaptic proteins and $GABA_A$ receptors (Petrini et al., 2014; Tyagarajan and Fritschy, 2014; Flores et al., 2015; Oh et al., 2016; Yamasaki et al., 2017; Wu et al., 2018). It is currently not known how presynaptic bouton stabilization triggers subsequent recruitment of postsynaptic proteins, but this may involve the recruitment of presynaptic organizers such as neurexins (Fu and Huang, 2010; Siddiqui and Craig, 2011; Neupert et al., 2015).

Stabilization of inhibitory boutons involves specific actin remodeling via actin depolymerization downstream of Sema4D signaling. This might seem counterintuitive at first sight, but a similar rapid actin depolymerization was implied in building specific actin structures during spine growth (Bosch et al., 2014; Meyer et al., 2014) and in the formation of immunological synapses (Ritter et al., 2015; De La Roche et al., 2016). Actin remodeling likely involves a qualitative switch in the combined action of many actin-regulating proteins (Lomakin et al., 2015; Rotty et al., 2015; Suarez et al., 2015). Our data suggest that the actin cytoskeleton at stabilizing boutons is different from other compartments and specifically sensitive to LatB. Recent nanoscopy studies have revealed several actin-based structures in axons (Xu et al., 2013; Ganguly et al., 2015; Leterrier et al., 2017), but the precise actin structure in presynaptic boutons remains unresolved. It is currently not known which actin-regulating factors are involved in presynaptic bouton stabilization, but promising candidates include cortactin (Alicea et al., 2017), cofilin (Bosch et al., 2014; Piccioli and Littleton, 2014) and Mical (Orr et al., 2017).

Our experiments uncovered an unexpected role for the receptor tyrosine kinase MET in inhibitory synapses. Human imaging and genetic studies have identified mutations in the MET gene as a risk factor for autism spectrum disorder (ASD) (Peng et al., 2013), but the exact role of MET in ASD is not

yet understood (Eagleson et al., 2017). Previous studies in neurons have implicated MET in regulating postsynaptic strength in excitatory neurons (Qiu et al., 2014; Lo et al., 2016), excitatory synapse formation (Xie et al., 2016) and interneuron migration (Martins et al., 2011). We found that reducing MET levels specifically in inhibitory axons blocked Sema4D-induced inhibitory bouton stabilization, suggesting that presynaptic MET acts as a co-receptor with PlexinB1 (or other family members (McDermott et al., 2018)) to mediate actin remodeling in the presynaptic bouton. This novel role for MET in inhibitory axons could shed new light on its role in neurodevelopmental diseases such as ASD.

Finally, we found that the sensitivity to Sema4D signaling is regulated by activity. Several members of the Semaphorin and Plexin family have been shown to be regulated by neuronal activity (Orr et al., 2017; Wang et al., 2017). Our experiments suggest that intracellular actin is not changed, but that the sensitivity for Sema4D is altered in the axon, possibly by activity-dependent regulation of surface expression or complex formation of receptors. It will be important to further address the activity-dependent regulation of the Sema4D signaling pathway, including PlexinB and MET receptors, in future studies. Changes in inhibitory synapses play an important role in the rewiring of neural circuits during development and in response to behavioral demands in adulthood (Keck et al., 2011; Chen et al., 2015; Froemke, 2015) and defects in inhibitory synapses are associated with many neurodevelopmental diseases (Hensch, 2004; Marín, 2012). Our data emphasize that inhibitory synapses are not plug-and-play devices, but that the activity-dependent formation of new inhibitory synapses requires a complex series of molecular events. A better understanding of the signaling pathways that regulate these events will be crucial to understand circuit adaptation processes during learning and in brain diseases.

EXPERIMENTAL PROCEDURES

Animals

All animal experiments were performed in compliance with the guidelines for the welfare of experimental animals issued by the Federal Government of The Netherlands. All animal experiments were approved by the Animal Ethical Review Committee (DEC) of Utrecht University.

Hippocampal slice cultures

Hippocampal slice cultures (400 µm thick) were prepared from postnatal day 5-7 male and female GAD65-GFP mice (López-Bendito et al., 2004) as previously described (Müllner et al., 2015). In short, the hippocampi were dissected in ice-cold HEPES-GBSS (containing 1.5 mM $CaCl_2$, 0.2 mM KH_2PO_4, 0.3 mM $MgSO_4$, 5 mM KCl, 1 mM $MgCl_2 \cdot 6H_2O$, 137 mM NaCl, 0.85 mM Na_2HPO_4 and 12.5 mM HEPES) supplemented with 1 mM kynurenic acid and 25 mM glucose, and plated in a MEM-based medium (MEM supplemented with 25% HBSS, 25% horse serum, 30 mM glucose and 12.5 mM HEPES).
In GAD65-GFP mice, approximately 20% of the CA1 interneurons express GFP from early embryonic developmental stage into adulthood (López-Bendito et al., 2004; Wierenga et al., 2010). The majority of GFP-labeled interneurons expresses reelin and VIP, while parvalbumin and somatostatin expression is nearly absent (Wierenga et al., 2010). For our study, the relatively low number of GFP-positive axons is crucial for the proper analysis of individual boutons.
The slices were kept in culture for at least one week before the experiments (range 7-29 days *in vitro*) at 35°C in 5% CO_2. For live imaging experiments, slices were transferred to an imaging chamber, where they were continuously perfused with carbogenated artificial cerebrospinal fluid (ACSF; containing 126 mM NaCl, 3 mM KCl, 2.5 mM $CaCl_2$, 1.3 mM $MgCl_2$, 1.25 mM NaH_2PO_4, 26 mM $NaHCO_3$, 20 mM glucose and 1mM Trolox). The temperature of the chamber was maintained at 35-37°C. Treatment and control experiments were conducted in slices from the same culture.

Pharmacological treatments

The following pharmacological treatments were used: 0.1/0.2 % DMSO, 1 nM Fc and Sema4D-Fc (amino acids 24-711) (both R&D Systems), 100 nM Latrunculin B (Santa Cruz Biotechnology), 200 nM Jasplakinolide (Tocris Bioscience), 1 µM PHA-665752 (Sigma-Aldrich), 10 µM Y-27632 (Sigma-Aldrich), tetrodotoxin citrate (TTX; Tocris Bioscience), 20 µM

6,7-dinitroquinoxaline-2,3-dione disodium salt (DNQX; Tocris Bioscience) and 50 µM DL-2-Amino-5-phosphonopentanoic acid (APV; Tocris Bioscience). We used the small molecule PHA-665752 (PHA), a highly specific MET inhibitor (Christensen et al., 2003), to decrease endogenous phosphorylation of MET without affecting MET expression or neuronal cell viability (Christensen et al., 2003; Lim and Walikonis, 2008).
For treatments that were followed by immunostaining of inhibitory synapses, 1 nM Fc or Sema4D-Fc was added to the culturing medium and slices were left in the incubator for 2, 6 or 24 h before fixation.

Two-photon imaging

Time-lapse two-photon microscopy images were acquired on a Femtonics 2D two-photon laser-scanning microscope (Budapest, Hungary), with a Nikon CFI Apochromat 60X NIR water-immersion objective. GFP was excited using a laser beam tuned to 910 nm (Mai Tai HP, Spectra Physics). The 3D images (93.5 µm x 93.5 µm in xy, 1124 x 1124 pixels) consisted of 29-33 z stacks (0.5 µm step size in z). Small misalignments due to drift were manually corrected during the acquisition.
For acute treatments, drugs were added to the perfusion ACSF after a baseline period of 40 minutes (5 time points) and we continued imaging for an additional 10 time points in the wash-in period (total imaging period is 140 minutes). In longer treatments, we treated the slices for 6 hours after the baseline period (5 imaging time points) at the microscope and restarted imaging for 5 time points, for a total treatment period of 6 hours and 40 minutes (400 minutes). Morphology of the axons did not change during this period, indicating slice health was well preserved. For activity blockade, 0.5 µM TTX was added to the perfusion ACSF prior to the transfer of the slice to the imaging chamber.

Two-photon image analysis

The analysis of inhibitory bouton dynamics was performed semi-automatically using ImageJ (US National Institute of Health) and Matlab-based software (Mathworks). The 3D coordinates of individual axons were selected at every time point using the CellCounter plugin (Kurt De Vos, University of Sheffield, Academic Neurology). For each image, 1-5 axons (average length 78 µm with standard deviation 18 µm, with average of 31 boutons per axon with standard deviation 10; for local treatment experiments, average length 39 µm with standard deviation 8 µm, with average of 14 boutons per axon with standard deviation of 4) were selected for analysis.
A 3D intensity profile along the selected axons was constructed at each time

point, and individual boutons were identified in a two-step process using custom-made Matlab software (Schuemann et al., 2013). In brief, an axon threshold was calculated to differentiate the axon from the background (2 standard deviations above mean intensity); subsequently, a local threshold (0.5 standard deviation above mean axon intensity) identified the boutons along the selected axon. Only boutons with at least 5 pixels above bouton threshold were included. Each image stack was visually examined, and false positives and negatives were corrected manually. Only raw data was analyzed; images were median-filtered for illustration purposes only.

Boutons were classified as persistent when they were present during all time points, and non-persistent when they were absent during one or more time points during the imaging session. Per axon, we calculated the average fraction of persistent and non-persistent boutons by normalization to the average number of boutons for each time point. To bias our analysis towards synaptic events (Schuemann et al., 2013), we restricted our analysis to boutons that appeared for at least 2 time points at the same location during the imaging period. We verified that our main conclusions did not change when this restriction was released. Based on their presence during baseline and treatment periods, we defined five subgroups of non-persistent boutons: new boutons (not present during baseline), lost boutons (not present during wash-in), stabilizing boutons (non-persistent during baseline, persistent during wash-in), destabilizing boutons (persistent during baseline, non-persistent during wash-in), and intermittent boutons (non-persistent in baseline and wash-in) (Fig. 1). The average fraction of each subgroup of boutons was normalized to the total average number of non-persistent (NP) boutons per axon. Bouton density was calculated as the average number of boutons at all time points divided by the 3D axon length.

Local treatment experiments

For the local treatment experiments, we used HEPES-ACSF (containing 126 mM NaCl, 3 mM KCl, 2.5 mM $CaCl_2$, 1.3 mM $MgCl_2$, 1.25 mM NaH_2PO_4, 20 mM glucose, and 10 mM HEPES; pH 7.4) with 20 µM Alexa 568 (Invitrogen), in order to visualize the spread of the local application. Sema4D or Fc was added to the HEPES-ACSF to a final concentration of 10 nM. We increased the concentration in comparison to bath application experiments to account for fast dilution. The solution was loaded into a patch pipette (4-6 MΩ), and was locally applied to a GFP-labeled axon using a Picospritzer II (General Valve). Time-lapse two photon microscopy imaging was performed as described previously, except that a second laser (Mai Tai HP, Spectra Physics) was used at 840 nm to visualize the area of the puff and images were taken

at every 5 minutes. The 3D images (51.3 µm x 51.3 µm in xy, 620 x 620 pixels) consisted of 18-22 z stacks (0.5 µm step size in z). After a baseline period of 20 minutes (5 TPs), the pipette was put into position before the stimulation. The stimulation consisted of 300 puffs of 20-50 ms at 2 Hz. The pipette was carefully retracted before continuing the time series for 10 additional time points (total imaging period of 70 minutes). Images were analyzed as described in the previous section.

Electrophysiology

During the experiment, the slice was placed in a recording chamber perfused with carbogenated ACSF at a rate of 1 ml/min. The recording ACSF consisted of 126 mM NaCl, 3 mM KCl, 2.5 mM $CaCl_2$, 1.3 mM $MgCl_2$, 1.25 mM $Na_2H_2PO_4$, 26 mM $NaHCO_3$, and 20 mM glucose. Whole cell voltage clamp recordings were performed at 35°C in CA1 cells of GAD65-GFP slice cultures at DIV 13-19. Recordings were made on a Multiclamp 700B amplifier (Molecular Devices) and stored using pClamp 10 software. To isolate sIPSCs, 20 µM DNQX and 50 µM APV were added to the recording ACSF. For mIPSCs, 0.5 µM TTX was added as well. Thick-walled borosilicate pipettes of 3-6 MΩ were filled with an internal solution containing 70 mM K-gluconate, 70 mM KCl, 0.5 mM EGTA, 10 mM HEPES, 4 mM MgATP, 0.4 mM NaGTP, and 4 mM Na_2Phosphocreatine. Cells were excluded from analysis if the series resistance increased more than 35% over the course of the experiment. IPSCs were automatically detected in Clampfit and further analyzed in custom Matlab scripts. Detected events within 3 ms of each other were merged and events smaller than 3 times the RMS of the signal were excluded.

Immunohistochemistry, confocal imaging and image analysis

For *post hoc* immunohistochemistry, an autofluorescent laser "scar" was made after live imaging by performing a line scan at high intensity to mark the imaged region. Organotypic hippocampal slices were fixed in 4% (w/v) paraformaldehyde for 30 minutes at room temperature. Slices were rinsed in phosphate buffer (PBS) and permeabilized with 0.5% TritonX-100 in phosphate buffer for 15 minutes. Slices were then blocked with 0.2% TritonX-100 and 10% normal goat serum (ab7481, Abcam) in PBS for 60 minutes. Primary antibodies were applied overnight at 4°C in blocking solution. After washing, slices were incubated with secondary antibodies in blocking solution for 4 h at room temperature. Slices were washed and mounted on slides in Vectashield mounting medium (Vector Labs).

The following primary and secondary antibodies were used: rabbit α-VGAT (1:1000; Synaptic Systems, 131 003, RRID: AB_887869), mouse α-gephyrin

(1:1000; Synaptic Systems, 147 011, RRID: AB_887717), guinea pig α-VGLUT1 (1:400; Millipore, AB5905, RRID: AB_2301751), rabbit α-Homer1 (1:1000; Synaptic Systems, 160 002, RRID: AB_2120990), mouse α-myc (1:100; Oncogene Research Products, OP10), mouse α-MET (1:500; Santa Cruz Biotechnology, sc-8057, RRID: AB_673755), Alexa405-, Alexa-488 and Alexa-568 conjugated secondary antibodies (Invitrogen). For staining MET, we also used a previously described myc-tagged nanobody, which was shown to recognize MET with low nanomolar affinity (Heukers et al., 2014). We visualized the nanobody with an antibody against the C-terminal myc tag. We validated the MET staining in primary hippocampal cultures using a previously described immunostaining protocol (Esteves da Silva et al., 2015). For immunostainings, high resolution confocal laser scanning microscopy was performed on a Zeiss LSM-700 system with a Plan-Apochromat 63x 1.4 NA oil immersion objective. Each image was a z-series of 11-35 images (0.3 µm z step size), each averaged 4 times. The imaging area in the CA1 region was 78 x 78 µm (1024 x 1024 pixels). Settings were kept the same to compare fluorescence intensities between slices.

To account for within-slice variability, we took confocal images from separate regions (maximally 5 per slice) as independent measurements. For the quantification of VGAT and gephyrin intensities per image, we determined the mean intensity of 3 randomly chosen areas of 10 x 10 µm of the average projection image from the 5 middle z-stacks. For the cumulative plots individual values (per area) were used. Synaptic puncta size and number of the same image areas were determined using the PunctaAnalyzer plugin, and inhibitory synapses were defined as overlapping VGAT and gephyrin puncta. For determining co-localization of GFP-labeled boutons with synaptic markers VGAT or gephyrin, or with MET, we manually inspected individual boutons through all z-sections. A bouton was only considered positive when at least one z stack of the bouton overlapped with VGAT or MET staining. Images were median-filtered for illustration purposes only. To check for random overlap between MET puncta and GFP boutons, co-localization was determined in images in which the MET channel was inverted.

STED imaging

Dual-color STED imaging was performed in primary neurons with a Leica TCS SP8 STED 3X microscope using a HC PL APO 100 × / 1.4 oil immersion STED WHITE objective. Primary hippocampal neurons were prepared as previously described (Esteves da Silva et al., 2015). Neurons (DIV 18) were fixed with 4% PFA and 4% sucrose in PBS for 10 minutes at room temperature and washed three times with PBS supplemented with 100 mM glycine (PBS/

Gly). Next, cells were permeabilized and blocked with 100 mM glycine, 0.1% Triton-X and 10% normal goat serum in PBS for 1 h at 37°C. Neurons were then incubated for 2-3 h at room temperature with primary antibodies diluted in PBS supplemented with 100 mM glycine, 0.1% Triton-X and 5% normal goat serum. Next, cells were washed three times with PBS/Gly and incubated for 1 h at room temperature with secondary antibodies diluted in PBS supplemented with 100 mM glycine, 0.1% Triton-X and 5% normal goat serum. Cells were then washed three times with PBS/Gly and mounted in Mowiol mounting medium. Abberior STAR 580 was excited with 561 nm and Abberior STAR 635P with 633 nm pulsed laser light (80 MHz). Both Abberior STAR 580 and 635P were depleted with a 775 nm pulsed depletion laser. Fluorescence emission was detected using Leica HyD hybrid detector.

The following primary and secondary antibodies were used: rabbit α-VGAT (1:1000; Synaptic Systems, 131 003, RRID: AB_887869), mouse α-MET (1:500; Santa Cruz Biotechnology, sc-8057, RRID: AB_673755), Abberior STAR 635P α-mouse (1:200; Abberior GmbH, 2-0002-007-5) and Abberior STAR 580 α-rabbit (1:200; Abberior GmbH, 2-0012-005-8).

miRNA and DNA constructs

The miRNA sequences targeting the ORF of mouse full-length MET cDNA (NM_008591) were designed with the BLOCK-iT™ RNAi Designer (Sequence #1: 5'-GCAGTGAATTAGTTCGCTATG-3'; Sequence #2: 5'-GCTTGTTGACACATACTATGA-3'). Sequence #1 was based on a previously published shRNA (Qiu et al., 2014). A scrambled sequence was generated with the siRNA Sequence Scrambler from Genscript (Sequence: 5'-ACTATAGTAATGCTCGTGCAT-3'). A loop sequence was added (5'-GTTTTGGCCACTGACTGAC-3') and oligos were annealed and cloned into pSM155-GFP (Du et al., 2006). The miRNA cassette was then cloned into a lentiviral plasmid (FUGW, RRID: Addgene_14883), which also contains GFP. A double-floxed (lox2272/loxp) inverse orientation version of these plasmids was created for Cre-dependent expression of the miRNA and GFP.

cDNA for overexpression of MET was obtained from pBabe puro MET WT (RRID:Addgene_17493). A PCR was performed with forward primer 5'-AAGGCGCGCCGCCACCATGAAGGCTCCCACCGT-3' and reverse primer 5'-AAGGATCCATGTGTTCCCCTCGCC-3'. This fragment was ligated into a pGW2-mCherry vector resulting in a C-terminal tagged MET.

Verification of knock down

Endogenous MET levels were too low to detect reliably with Western blot and we therefore relied on MET overexpression to verify our miRNA constructs.

Primary hippocampal neurons were transfected using Lipofectamine 2000 (Invitrogen) at DIV 9. Briefly, MET-mCherry and miRNA or GFP only constructs (~ total 2.1 µg/well, for a 12-well plate) were mixed with 3.3 µL Lipofectamine 2000 in 100 µL Neurobasal medium (NB), incubated for 25 minutes, and then added to the neurons in NB with 0.5 mM glutamine at 37°C in 5% CO_2 for 40 minutes. Next, neurons were washed in preheated NB and transferred back to their original medium for 48 h. Neurons were fixed with 4% PFA + 4% sucrose for 10 minutes and mounted on microscope slides with Vectashield mounting medium (Vector Labs). Images were acquired using a Zeiss LSM-700 confocal laser scanning microscope. The imaging settings were kept the same between experiments to compare fluorescence intensity in the soma.

HEK293 cells (American Type Culture Collection, CRL-1573, RRID:CVCL_0045) were grown in 10-cm dishes at 37°C and 5% CO_2, and transfected with MET-mCherry and miRNA or GFP only constructs using polyethylenimine (1 µg/µL; PEI, Polysciences) to assess MET levels by Western blot analysis. After 24-48 h, HEK293 cells were lysed in Laemmli sample buffer (10% glycerol, 2% SDS, 100 mM DTT, 50 mM Tris-HCl pH 6.8 and 0.004% bromophenol blue) and scrapped, and samples were then boiled for 10 minutes. Samples were loaded equally and run on a 10% SDS-PAGE gel. Proteins were transferred to Nitrocellulose membranes (BIO-RAD, #1620115) and blocked in 2% (w/v) bovine serum albumin in PBS/0.1 % (v/v) Tween 20 for 1 h at room temperature. Primary antibodies were diluted in the blocking solution and applied overnight at 4°C. Membranes were washed 3 times in PBS/0.1 % Tween 20 and incubated with secondary IRDye antibodies for 1 h at room temperature. Afterwards, membranes were washed 3 times in PBS/0.1 % Tween 20, and scanned using an Odyssey Infrared Imaging System (LI-COR Biosciences). MET intensity was corrected for tubulin loading control, and values for miRNAs were normalized to GFP control values.

The following primary and secondary antibodies were used: mouse α-MET (1:250; Santa Cruz Biotechnology, sc-8057, RRID: AB_673755), rabbit α-tubulin (1:10000; Abcam, ab52866, RRID: AB_869989), IRdye 680LT α-mouse (1:20000, LI-COR Biosciences, 926-68020, RRID:AB_10706161) and IRdye 800CW α-rabbit (1:15000, LI-COR Biosciences, 926-32211, RRID:AB_621843).

Lentivirus production and infection

HEK293 cells were grown in DMEM supplemented with 10% FBS and 1% penicillin/streptomycin (Pen/Strep) at 37°C and 5% CO_2. A confluent 10-cm dish of HEK293 cells was split 1:4 the day before transfection. Per 10-cm dish the following mixture was used for transfection: 2 µg

pMD2.G (RRID:Addgene_12259), 4 µg psPAX2 (RRID:Addgene_12260), 6 µg FUGW (RRID: Addgene_14883), 500 µl OptiMEM and 36 µl PEI (1 µg/µL; Polysciences). After 15 minutes incubation at room temperature, the mixture was added to the cells. Culture medium was replaced with 5 mL OptiMEM supplemented with 1% Pen-Strep 4-6 h later. Lentivirus containing supernatant was harvested after 48-60 h. Virus were concentrated with Amicon spin filters (Millipore), aliquoted and stored at -80°C.
Cre-dependent expression of miRNA (sequence #2) and GFP was induced in organotypic slices of VGAT-Cre mice (RRID:IMSR_JAX:028862). Stereotactic injections of Lentiviral constructs (miRNA sequence #2 + GFP) were performed in DIV 1 slices using a microinjector (Eppendorf FemtoJet) and stereoscopic microscope (Leica M80). Per slice, 6-8 injections were done in the CA1 stratum radiatum with ~50 Pa pressure (< 1 µL virus solution per slice). For control, we used a lentiviral construct for Cre-dependent GFP expression without miRNA sequence. Imaging and analysis of GFP-labeled axons in VGAT-Cre slices was performed at DIV 14-29 as described above.

Experimental design and statistical analysis

All data analysis was performed blind to the treatment. Live imaging experiments were performed in pairs (control + treatment) per batch of slices, and for each pair of experiments, slices from different animals were used. Data are represented as mean values ± standard error of the mean, unless stated otherwise. Statistical analysis was performed using GraphPad Prism software. Results from treatment and control experiments were compared using the Mann-Whitney U test (MW). The Chi-Square test (χ^2) was used for comparing the fraction of axons with/without stabilizing boutons and the fraction of boutons with synaptic markers VGAT and gephyrin. For comparing multiple groups, we used the Kruskal-Wallis test (KW) followed by a posthoc Dunn's comparison test. We used a One-Way ANOVA followed by a Dunnett's multiple comparison test (One-Way ANOVA) to compare the effect of wash-in of PHA over time during the electrophysiological recordings. Treatment effects at multiple time points were compared using Two-Way ANOVA followed by a Sidak's multiple comparisons test (Two-Way ANOVA). For the comparison of cumulative distributions, we used the Kolmogorov-Smirnov (KS) test. We have indicated the tests and p-values in the figure legends. Differences between control and treatment were considered significant when $p < 0.05$ (*, $p < 0.05$; **, $p < 0.01$; ***, $p < 0.001$). In all figure legends and text, N indicates the number of independent experiments (slices or neuronal cultures), and n indicates the number of axons/images analyzed.

Acknowledgements:
We would like to thank G. Szábo for kindly providing the GAD65-GFP mice and S. Paradis for helpful comments and scientific discussions. This work was supported by the People Programme (Marie Curie Actions) of the European Union's Seventh Framework Programme FP7/2007-2013/ under REA grant agreement 289581 (CPF), a Marie Curie Reintegration Grant 256284 (CJW), the Chinese Science Council (JL) and the Netherlands Organization for Scientific Research (VIDI, CJW, HYH; VICI, CCH; FOM #15PR3178-1, RvD).

Author contributions
CPF and CJW designed the experiments. CPF performed and analyzed most experiments, with specific contributions by JL (Fig. 8J-K), TB (Fig. 9, Sema4D), LS (Fig. 5, Jasp) and MvK (Fig. 9, LatB). HYH performed electrophysiology and local treatment experiments; AB performed super-resolution microscopy. RvD provided technical support and produced and verified the miRNA constructs. PBH and CCH provided reagents. CPF and CJW wrote the manuscript with critical input from all other authors. CJW conceived and supervised the research.

Conflict of Interest:

The authors declare no competing financial interests.

REFERENCES

Alicea D, Perez M, Maldonado C, Dominicci-Cotto C, Marie X (2017) Cortactin Is a Regulator of Activity-Dependent Synaptic Plasticity Controlled by Wingless. J Neurosci 37:2203–2215 Available at: http://www.jneurosci.org/content/jneuro/37/8/2203.full.pdf.

Amano M, Nakayama M, Kaibuchi K (2010) Rho-kinase/ROCK: A key regulator of the cytoskeleton and cell polarity. Cytoskeleton 67:545–554 Available at: http://www.ncbi.nlm.nih.gov/pubmed/20803696 [Accessed December 4, 2017].

Bosch M, Castro J, Saneyoshi T, Matsuno H, Sur M, Hayashi Y (2014) Structural and Molecular Remodeling of Dendritic Spine Substructures during Long-Term Potentiation. Neuron 82:444–459 Available at: http://www.ncbi.nlm.nih.gov/pubmed/24742465 [Accessed April 28, 2014].

Bury LA, Sabo SL (2016) Building a Terminal: Mechanisms of Presynaptic Development in the CNS. Neurosci 22:372–391 Available at: http://www.ncbi.nlm.nih.gov/pubmed/26208860.

Cagnoni G, Tamagnone L (2014) Semaphorin receptors meet receptor tyrosine kinases on the way of tumor progression. Oncogene 33:4795–4802 Available at: http://dx.doi.org/10.1038/onc.2013.474.

Caroni P, Donato F, Muller D (2012) Structural plasticity upon learning: regulation and functions. Nat Rev Neurosci 13:478–490 Available at: http://dx.doi.org/10.1038/nrn3258.

Cellot G, Cherubini E (2014) GABAergic signaling as therapeutic target for autism spectrum disorders. Front Pediatr 2.

Chen SX, Kim AN, Peters AJ, Komiyama T (2015) Subtype-specific plasticity of inhibitory circuits in motor cortex during motor learning. Nat Neurosci 18:1109–1115 Available at: http://www.nature.com/neuro/journal/v18/n8/full/nn.4049.html?WT.ec_id=NEURO-201508&spMailingID=49196618&spUserID=MTMyMDY4MzI3NDgzS0&spJobID=723694367&spReportId=NzIzNjk0MzY3S0%5Cnhttp://www.nature.com/neuro/journal/v18/n8/pdf/nn.4049.pdf.

Christensen JG, Schreck R, Burrows J, Kuruganti P, Chan E, Le P, Chen J, Wang X, Ruslim L, Blake R, Lipson KE, Ramphal J, Do S, Cui JJ, Cherrington JM, Mendel DB (2003) A Selective Small Molecule Inhibitor of c-Met Kinase Inhibits c-Met-Dependent Phenotypes in Vitro and Exhibits Cytoreductive Antitumor Activity in Vivo. Cancer Res 63:7345–7355.

De La Roche M, Asano Y, Griffiths GM (2016) Origins of the cytolytic synapse. Nat Rev Immunol 16:421–432.

Deguchi Y, Harada M, Shinohara R, Lazarus M, Cherasse Y, Urade Y, Yamada D, Sekiguchi M, Watanabe D, Furuyashiki T, Narumiya S (2016) mDia and ROCK Mediate Actin-Dependent Presynaptic Remodeling Regulating Synaptic Efficacy and Anxiety. Cell Rep 17:2405–2417 Available at: http://dx.doi.org/10.1016/j.celrep.2016.10.088.

Dobie FA, Craig AM (2011) Inhibitory synapse dynamics: coordinated presynaptic and postsynaptic mobility and the major contribution of recycled vesicles to new synapse formation. J Neurosci 31:10481–10493 Available at: http://www.jneurosci.org/cgi/doi/10.1523/JNEUROSCI.6023-10.2011 [Accessed July 20, 2011].

Du G, Yonekubo J, Zeng Y, Osisami M, Frohman MA (2006) Design of expression vectors for RNA interference based on miRNAs and RNA splicing. FEBS J 273:5421–5427.

Eagleson KL, Milner TA, Xie Z, Levitt P (2013) Synaptic and extrasynaptic location of the receptor tyrosine kinase met during postnatal development in the mouse neocortex and hippocampus. J Comp Neurol 521:3241–3259 Available at: http://www.pubmedcentral.nih.gov/articlerender.fcgi?artid=3942873&tool=pmcentrez&rendertype=abstract [Accessed November 21, 2014].

Eagleson KL, Xie Z, Levitt P (2017) The Pleiotropic MET Receptor Network: Circuit Development and the Neural-Medical Interface of Autism. Biol Psychiatry 81:424–433 Available at: http://linkinghub.elsevier.com/retrieve/pii/S0006322316327780.

Esteves da Silva M, Adrian M, Schätzle P, Lipka J, Watanabe T, Cho S, Futai K, Wierenga CJ, Kapitein LC, Hoogenraad CC (2015) Positioning of AMPA Receptor-Containing Endosomes Regulates Synapse Architecture. Cell Rep 13:933–943 Available at: http://www.ncbi.nlm.nih.gov/pubmed/26565907 [Accessed November 16, 2015].

Flores CE, Nikonenko I, Mendez P, Fritschy J-M, Tyagarajan SK, Muller D (2015) Activity-dependent inhibitory synapse remodeling through gephyrin phosphorylation. Proc Natl Acad Sci 112:E65–E72 Available at: http://www.pnas.org/lookup/doi/10.1073/pnas.1411170112.

Frias CP, Wierenga CJ (2013) Activity-dependent adaptations in inhibitory axons. Front Cell Neurosci

7:219 Available at: http://www.ncbi.nlm.nih.gov/pubmed/24312009 [Accessed December 12, 2013].
Froemke RC (2015) Plasticity of cortical excitatory-inhibitory balance. Annu Rev Neurosci 38:195–219 Available at: http://www.ncbi.nlm.nih.gov/pubmed/25897875 [Accessed April 30, 2015].
Fu Y, Huang ZJ (2010) Differential dynamics and activity-dependent regulation of α- and β-neurexins at developing GABAergic synapses. Proc Natl Acad Sci U S A 107:22699–22704 Available at: http://www.ncbi.nlm.nih.gov/pubmed/21149722 [Accessed January 3, 2011].
Fu Y, Wu X, Lu J, Huang ZJ (2012) Presynaptic GABAB Receptor Regulates Activity-Dependent Maturation and Patterning of Inhibitory Synapses through Dynamic Allocation of Synaptic Vesicles. Front Cell Neurosci 6:1–20 Available at: http://www.frontiersin.org/Cellular_Neuroscience/10.3389/fncel.2012.00057/abstract [Accessed December 10, 2012].
Ganguly A, Tang Y, Wang L, Ladt K, Loi J, Dargent B, Leterrier C, Roy S (2015) A dynamic formin-dependent deep F-actin network in axons. J Cell Biol 210:401–417 Available at: http://www.jcb.org/cgi/doi/10.1083/jcb.201506110.
Hensch TK (2004) Critical Period Regulation. Annu Rev Neurosci 27:549–579 Available at: http://www.annualreviews.org/doi/10.1146/annurev.neuro.27.070203.144327.
Hensch TK (2005) Critical period plasticity in local cortical circuits. Nat Rev Neurosci 6:877–888 Available at: http://www.ncbi.nlm.nih.gov/pubmed/16261181.
Heukers R, Altintas I, Raghoenath S, De Zan E, Pepermans R, Roovers RC, Haselberg R, Hennink WE, Schiffelers RM, Kok RJ, Van Bergen en Henegouwen PMP (2014) Targeting hepatocyte growth factor receptor (Met) positive tumor cells using internalizing nanobody-decorated albumin nanoparticles. Biomaterials 35:601–610 Available at: http://dx.doi.org/10.1016/j.biomaterials.2013.10.001.
Honkura N, Matsuzaki M, Noguchi J, Ellis-Davies GCR, Kasai H (2008) The subspine organization of actin fibers regulates the structure and plasticity of dendritic spines. Neuron 57:719–729 Available at: http://www.ncbi.nlm.nih.gov/pubmed/18341992 [Accessed July 4, 2011].
Isaacson JS, Scanziani M (2011) How inhibition shapes cortical activity. Neuron 72:231–243 Available at: http://www.ncbi.nlm.nih.gov/pubmed/22017986 [Accessed July 14, 2012].
Judson MC, Bergman MY, Campbell DB, Eagleson KL, Levitt P (2009) Dynamic gene and protein expression patterns of the autism-associated met receptor tyrosine kinase in the developing mouse forebrain. J Comp Neurol 513:511–531.
Keck T, Scheuss V, Jacobsen RI, Wierenga CJ, Eysel UT, Bonhoeffer T, Hübener M (2011) Loss of sensory input causes rapid structural changes of inhibitory neurons in adult mouse visual cortex. Neuron 71:869–882 Available at: http://linkinghub.elsevier.com/retrieve/pii/S0896627311005642 [Accessed September 9, 2011].
Kolodkin AL, Matthes DJ, Goodman CS (1993) The semaphorin genes encode a family of transmembrane and secreted growth cone guidance molecules. Cell 75:1389–1399.
Krueger-Burg D, Papadopoulos T, Brose N (2017) Organizers of inhibitory synapses come of age. Curr Opin Neurobiol 45:66–77 Available at: http://dx.doi.org/10.1016/j.conb.2017.04.003.
Kuriu T, Yanagawa Y, Konishi S (2012) Activity-dependent coordinated mobility of hippocampal inhibitory synapses visualized with presynaptic and postsynaptic tagged-molecular markers. Mol Cell Neurosci 49:184–195 Available at: http://www.ncbi.nlm.nih.gov/pubmed/22146684 [Accessed December 12, 2011].
Kuzirian MS, Moore AR, Staudenmaier EK, Friedel RH, Paradis S (2013) The class 4 semaphorin Sema4D promotes the rapid assembly of GABAergic synapses in rodent hippocampus. J Neurosci 33:8961–8973 Available at: http://www.ncbi.nlm.nih.gov/pubmed/23699507 [Accessed May 22, 2013].
Leterrier C, Dubey P, Roy S (2017) The nano-architecture of the axonal cytoskeleton. Nat Rev Neurosci 18:713–726 Available at: http://www.nature.com/doifinder/10.1038/nrn.2017.129.
Lim CS, Walikonis RS (2008) Hepatocyte growth factor and c-Met promote dendritic maturation during hippocampal neuron differentiation via the Akt pathway. Cell Signal 20:825–835 Available at: http://linkinghub.elsevier.com/retrieve/pii/S0898656807004019 [Accessed December 4, 2017].
Lo F-S, Erzurumlu RS, Powell EM (2016) Insulin-Independent GABAA Receptor-Mediated Response in the Barrel Cortex of Mice with Impaired Met Activity. J Neurosci 36:3691–3697 Available at: http://www.ncbi.nlm.nih.gov/pubmed/27030755 [Accessed May 18, 2016].
Lomakin AJ, Lee KC, Han SJ, Bui DA, Davidson M, Mogilner A, Danuser G (2015) Competition for actin

between two distinct F-actin networks defines a bistable switch for cell polarization. Nat Cell Biol 17:1435–1445.

López-Bendito G, Sturgess K, Erdélyi F, Szabó G, Molnár Z, Paulsen O (2004) Preferential origin and layer destination of GAD65-GFP cortical interneurons. Cereb Cortex 14:1122–1133 Available at: http://www.ncbi.nlm.nih.gov/pubmed/15115742.

Lu W, Bromley-Coolidge S, Li J (2016) Regulation of GABAergic synapse development by postsynaptic membrane proteins. Brain Res Bull 129:30–42 Available at: http://linkinghub.elsevier.com/retrieve/pii/S0361923016301563.

Marín O (2012) Interneuron dysfunction in psychiatric disorders. Nat Rev Neurosci 13:107–120 Available at: http://www.ncbi.nlm.nih.gov/pubmed/22251963 [Accessed October 9, 2012].

Martins GJ, Shahrokh M, Powell EM (2011) Genetic disruption of Met signaling impairs GABAergic striatal development and cognition. Neuroscience 176:199–209 Available at: http://dx.doi.org/10.1016/j.neuroscience.2010.12.058 [Accessed May 18, 2016].

McDermott JE, Goldblatt D, Paradis S (2018) Class 4 Semaphorins and Plexin-B receptors regulate GABAergic and glutamatergic synapse development in the mammalian hippocampus. Mol Cell Neurosci 92:50–66 Available at: https://doi.org/10.1016/j.mcn.2018.06.008.

Meyer D, Bonhoeffer T, Scheuss V (2014) Balance and Stability of Synaptic Structures during Synaptic Plasticity. Neuron 82:430–443 Available at: http://dx.doi.org/10.1016/j.neuron.2014.02.031 [Accessed April 28, 2014].

Müllner FE, Wierenga CJ, Bonhoeffer T (2015) Precision of inhibition: dendritic inhibition by individual GABAergic synapses on hippocampal pyramidal cells is confined in space and time. Neuron 87:576–589.

Nelson SB, Valakh V (2015) Excitatory/Inhibitory Balance and Circuit Homeostasis in Autism Spectrum Disorders. Neuron 87:684–698 Available at: http://linkinghub.elsevier.com/retrieve/pii/S0896627315006753.

Neupert C, Schneider R, Klatt O, Reissner C, Repetto D, Biermann B, Niesmann K, Missler M, Heine M (2015) Regulated Dynamic Trafficking of Neurexins Inside and Outside of Synaptic Terminals. J Neurosci 35:13629–13647 Available at: http://www.jneurosci.org/cgi/doi/10.1523/JNEUROSCI.4041-14.2015%5Cnhttp://www.ncbi.nlm.nih.gov/pubmed/26446217.

Oh WC, Lutzu S, Castillo PE, Kwon H (2016) De novo synaptogenesis induced by GABA in the developing mouse cortex. Science (80-) 353:1037–1040.

Orr BO, Fetter RD, Davis GW (2017) Retrograde semaphorin–plexin signalling drives homeostatic synaptic plasticity. Nature 550:109–113 Available at: http://www.nature.com/doifinder/10.1038/nature24017.

Paradis S, Harrar DB, Lin Y, Koon AC, Hauser JL, Griffith EC, Zhu L, Brass LF, Chen C, Greenberg ME (2007) An RNAi-based approach identifies molecules required for glutamatergic and GABAergic synapse development. Neuron 53:217–232 Available at: http://linkinghub.elsevier.com/retrieve/pii/S0896627306009974.

Pasterkamp RJ (2012) Getting neural circuits into shape with semaphorins. Nat Rev Neurosci 13:605–618 Available at: http://dx.doi.org/10.1038/nrn3302.

Peng Y, Huentelman M, Smith C, Qiu S (2013) MET Receptor Tyrosine Kinase as an Autism Genetic Risk Factor. Int Rev Neurobiol 113:135–165.

Petrini EM, Ravasenga T, Hausrat TJ, Iurilli G, Olcese U, Racine V, Sibarita J-B, Jacob TC, Moss SJ, Benfenati F, Medini P, Kneussel M, Barberis A (2014) Synaptic recruitment of gephyrin regulates surface GABAA receptor dynamics for the expression of inhibitory LTP. Nat Commun 5:3921 Available at: http://www.pubmedcentral.nih.gov/articlerender.fcgi?artid=4059940&tool=pmcentrez&rendertype=abstract [Accessed December 2, 2014].

Piccioli ZD, Littleton JT (2014) Retrograde BMP signaling modulates rapid activity-dependent synaptic growth via presynaptic LIM kinase regulation of cofilin. J Neurosci 34:4371–4381 Available at: http://www.ncbi.nlm.nih.gov/pubmed/24647957.

Qiu S, Lu Z, Levitt P (2014) MET Receptor Tyrosine Kinase Controls Dendritic Complexity, Spine Morphogenesis, and Glutamatergic Synapse Maturation in the Hippocampus. J Neurosci 34:16166–16179 Available at: http://www.jneurosci.org/cgi/doi/10.1523/JNEUROSCI.2580-14.2014.

Raissi AJ, Staudenmaier EK, David S, Hu L, Paradis S (2013) Sema4D localizes to synapses and regulates GABAergic synapse development as a membrane-bound molecule in the mammalian hippocampus. Mol Cell Neurosci 57:23–32 Available at: http://www.ncbi.nlm.nih.gov/

pubmed/24036351 [Accessed September 20, 2013].
Rex CS, Chen LY, Sharma A, Liu J, Babayan AH, Gall CM, Lynch G (2009) Different Rho GTPase-dependent signaling pathways initiate sequential steps in the consolidation of long-term potentiation. J Cell Biol 186:85–97.
Ritter AT, Asano Y, Stinchcombe JC, Dieckmann NMG, Chen BC, Gawden-Bone C, van Engelenburg S, Legant W, Gao L, Davidson MW, Betzig E, Lippincott-Schwartz J, Griffiths GM (2015) Actin Depletion Initiates Events Leading to Granule Secretion at the Immunological Synapse. Immunity 42:864–876 Available at: http://dx.doi.org/10.1016/j.immuni.2015.04.013.
Rotty JD, Wu C, Haynes EM, Suarez C, Winkelman JD, Johnson HE, Haugh JM, Kovar DR, Bear JE (2015) Profilin-1 Serves as a gatekeeper for actin assembly by Arp2/3-Dependent and - Independent pathways. Dev Cell 32:54–67 Available at: http://dx.doi.org/10.1016/j.devcel.2014.10.026.
Schuemann A, Klawiter A, Bonhoeffer T, Wierenga CJ (2013) Structural plasticity of GABAergic axons is regulated by network activity and GABAA receptor activation. Front Neural Circuits 7:1–16 Available at: http://journal.frontiersin.org/article/10.3389/fncir.2013.00113/abstract.
Siddiqui TJ, Craig AM (2011) Synaptic organizing complexes. Curr Opin Neurobiol 21:132–143 Available at: http://www.pubmedcentral.nih.gov/articlerender.fcgi?artid=3016466&tool=pmcentrez&rendertype=abstract [Accessed August 15, 2013].
Sprekeler H (2017) Functional consequences of inhibitory plasticity: homeostasis, the excitation-inhibition balance and beyond. Curr Opin Neurobiol 43:198–203 Available at: http://dx.doi.org/10.1016/j.conb.2017.03.014.
Staras K (2007) Share and share alike: trading of presynaptic elements between central synapses. Trends Neurosci 30:292–298 Available at: http://www.ncbi.nlm.nih.gov/pubmed/17467066.
Suarez C, Carroll RT, Burke TA, Christensen JR, Bestul AJ, Sees JA, James ML, Sirotkin V, Kovar DR (2015) Profilin regulates F-Actin network homeostasis by favoring formin over Arp2/3 complex. Dev Cell 32:43–53.
Sun T, Krishnan R, Swiercz JM (2012) Grb2 mediates semaphorin-4D-dependent RhoA inactivation. J Cell Sci 125:3557–3567 Available at: http://www.ncbi.nlm.nih.gov/pubmed/22505611 [Accessed August 19, 2013].
Swiercz JM, Worzfeld T, Offermanns S (2008) ErbB-2 and Met reciprocally regulate cellular signaling via plexin-B1. J Biol Chem 283:1893–1901 Available at: http://www.ncbi.nlm.nih.gov/pubmed/18025083 [Accessed August 19, 2013].
Tyagarajan SK, Fritschy J-M (2014) Gephyrin: a master regulator of neuronal function? Nat Rev Neurosci 15:141–156 Available at: http://www.ncbi.nlm.nih.gov/pubmed/24552784.
Tyndall SJ, Walikonis RS (2006) The receptor tyrosine kinase met and its ligand hepatocyte growth factor are clustered at excitatory synapses and can enhance clustering of synaptic proteins. Cell Cycle 5:1560–1568.
Villa KL, Berry KP, Subramanian J, Cha JW, Oh WC, Kwon H-B, Kubota Y, So PTC, Nedivi E (2016) Inhibitory synapses are repeatedly assembled and removed at persistent sites in vivo. Neuron 89:756–769 Available at: http://linkinghub.elsevier.com/retrieve/pii/S0896627316000118.
Wang Q, Koropouli E, Chiu S, Hong I, Ginty DD, Huganir RL, Kolodkin AL (2017) Neuropilin-2 / PlexinA3 Receptors Associate with GluA1 and Mediate Sema3F-dependent Homeostatic Scaling in Cortical Neurons. Neuron 96:1–15.
Wierenga CJ, Becker N, Bonhoeffer T (2008) GABAergic synapses are formed without the involvement of dendritic protrusions. Nat Neurosci 11:1044–1052 Available at: http://www.ncbi.nlm.nih.gov/pubmed/18711391.
Wierenga CJ, Müllner FE, Rinke I, Keck T, Stein V, Bonhoeffer T (2010) Molecular and electrophysiological characterization of GFP-expressing CA1 interneurons in GAD65-GFP mice. PLoS One 5:e15915 Available at: http://www.pubmedcentral.nih.gov/articlerender.fcgi?artid=3013138&tool=pmcentrez&rendertype=abstract [Accessed March 10, 2012].
Wu M, Tian HL, Liu X, Lai JHC, Du S, Xia J (2018) Impairment of Inhibitory Synapse Formation and Motor Behavior in Mice Lacking the NL2 Binding Partner LHFPL4/GARLH4. Cell Rep 23:1691–1705 Available at: https://doi.org/10.1016/j.celrep.2018.04.015.
Xie Z, Eagleson KL, Wu H-H, Levitt P (2016) Hepatocyte Growth Factor Modulates MET Receptor Tyrosine Kinase and β-Catenin Functional Interactions to Enhance Synapse Formation. eNeuro 3:e0074.
Xu K, Zhong G, Zhuang X (2013) Actin, spectrin, and associated proteins form a periodic cytoskeletal structure in axons. Science (80-) 339:452–456 Available at: http://www.pubmedcentral.nih.

gov/articlerender.fcgi?artid=3815867&tool=pmcentrez&rendertype=abstract.
Yamasaki T, Hoyos-Ramirez E, Martenson JS, Morimoto-Tomita M, Tomita S (2017) GARLH Family Proteins Stabilize GABAA Receptors at Synapses. Neuron 93:1138–1152.e6 Available at: http://dx.doi.org/10.1016/j.neuron.2017.02.023.
Zhou Y, Gunput RAF, Pasterkamp RJ (2008) Semaphorin signaling: progress made and promises ahead. Trends Biochem Sci 33:161–170.

Chapter 3

Axonal CB1 receptors mediate inhibitory bouton formation via cAMP increase and PKA

Abbreviated title: Inhibitory bouton formation via cAMP increase

Authors: Jian Liang[1], Dennis LH Kruijssen[1,2], Aniek CJ Verschuuren[1], Bas JB Voesenek[1], Feline Benavides[1], Maria Sáez Gonzalez[1], Marvin Ruiter[1], Corette J Wierenga[1]

Affiliation: [1] Cell Biology, Neurobiology and Biophysics, Department of Biology, Faculty of Science, Utrecht University, 3584 CH Utrecht, the Netherlands
[2] current address: College of Life Sciences, Faculty of Science, University of Amsterdam, 1098 XH, Amsterdam, The Netherlands

Corresponding author email: c.j.wierenga@uu.nl

This chapter has been published in the Journal of Neuroscience, Vol. 41, Issue 40, 6 Oct 2021

Abstract

Experience-dependent formation and removal of synapses are essential throughout life. For instance, GABAergic synapses are removed to facilitate learning, and strong excitatory activity is accompanied by formation of inhibitory synapses to maintain coordination between excitation and inhibition. We recently discovered that active dendrites trigger the growth of inhibitory synapses via CB1 receptor-mediated endocannabinoid signaling, but the underlying mechanism remained unclear. Using two-photon microscopy to monitor the formation of individual inhibitory boutons in hippocampal organotypic slices from mice (both sexes), we found that CB1 receptor activation mediated the formation of inhibitory boutons and promoted their subsequent stabilization. Inhibitory bouton formation did not require neuronal activity and was independent of $G_{i/o}$ protein signaling, but was directly induced by elevating cAMP levels using forskolin and by activating G_s proteins using DREADDs. Blocking PKA activity prevented CB1 receptor-mediated inhibitory bouton formation. Our findings reveal that axonal CB1 receptors signal via unconventional downstream pathways and that inhibitory bouton formation is triggered by an increase in axonal cAMP levels. Our results demonstrate an unexpected role for axonal CB1 receptors in axon-specific, and context-dependent, inhibitory synapse formation.

Significance statement

Coordination between excitation and inhibition is required for proper brain function throughout life. It was previously shown that new inhibitory synapses can be formed in response to strong excitation to maintain this coordination, and this was mediated by endocannabinoid signaling via CB1 receptors. As activation of CB1 receptors generally results in suppression of synaptic transmission, it remained unclear how CB1 receptors can mediate the formation of inhibitory synapses. Here we show that CB1 receptors on inhibitory axons signal via unconventional intracellular pathways and that inhibitory bouton formation is triggered by an increase in axonal cAMP levels and requires PKA activity. Our findings point to a central role for axonal cAMP signaling in activity-dependent inhibitory synapse formation.

Introduction

Synaptic plasticity, the strengthening and weakening of existing synapses, is often considered the physiological basis for learning and adaptation. In addition, the experience-dependent formation and removal of synapses is equally important (Bailey and Kandel, 1993; Caroni et al., 2012). Changes in the number of synaptic connections have been shown to be critical during learning *in vivo* (Bailey and Chen, 1989; Hofer et al., 2009; Ruediger et al., 2011; Caroni et al., 2012; Kozorovitskiy et al., 2012) and strongly determine postsynaptic function (Scholl et al., 2020). Plasticity of GABAergic synapses is particularly important for shaping and controlling brain activity throughout life (Flores and Méndez, 2014; Maffei et al., 2017; Chiu et al., 2019; Herstel and Wierenga, 2021) and GABAergic dysfunction is associated with multiple brain disorders, including schizophrenia and autism (Lewis et al., 2005; Mullins et al., 2016; Tang et al., 2021). For example, the number of inhibitory synapses is rapidly adjusted during learning (Bourne and Harris, 2011; Donato et al., 2013, 2015; Chen et al., 2015) or when sensory input is lost (Keck et al., 2011) to facilitate plasticity at nearby excitatory synapses. Vice versa, potentiation of excitatory synapses can trigger the formation of inhibitory synapses to maintain a local balance (Knott et al., 2002; Bourne and Harris, 2011; Hu et al., 2019). The formation, stabilization and removal of synapses likely requires local context-dependent signaling mechanisms (Kleindienst et al., 2011; Nishiyama and Yasuda, 2015; Oh et al., 2016; Niculescu et al., 2018; Hu et al., 2019; Kirchner and Gjorgjieva, 2019), but our current understanding of these processes, especially at inhibitory synapses, is far from complete.

We recently discovered that strong, clustered activation of excitatory synapses along dendrites of hippocampal CA1 pyramidal neurons can trigger the formation of a new inhibitory bouton onto the activated dendrite (Hu et al., 2019). We proposed that this dendritic mechanism serves to maintain local balance between excitatory and inhibitory inputs during ongoing synaptic plasticity. Inhibitory bouton formation required dendritic endocannabinoid synthesis and activation of CB1 receptors (Hu et al., 2019). Dendritic endocannabinoids are well-known to serve as retrograde signals to regulate synaptic plasticity (Alger, 2002; Chevaleyre and Castillo, 2003; Kano et al., 2009; Castillo et al., 2012; Katona and Freund, 2012), but it is unclear how CB1 receptors can trigger new inhibitory bouton formation.

CB1 receptors are G-protein coupled receptors and are widely abundant in the brain. They are expressed in both excitatory and inhibitory neurons,

as well as in glia cells (Navarrete et al., 2014; Hebert-Chatelain et al., 2016; Maroso et al., 2016; Bonilla-Del Río et al., 2021). Perhaps the most prominent CB1 expression is in a subset of inhibitory axons in the dendritic layer of the hippocampal CA1 area (Dudok et al., 2015; Bonilla-Del Río et al., 2021). Axonal CB1 signaling plays an important role during axon guidance (Berghuis et al., 2007; Argaw et al., 2011; Roland et al., 2014; Njoo et al., 2015), but axonal CB1 receptor expression remains high during adulthood. The best described actions of CB1 receptors in adulthood is to suppress neurotransmitter release (Alger, 2002; Kano et al., 2009; Castillo et al., 2012). However, CB1 receptors are not enriched in boutons, but freely diffuse within the entire axonal membrane (Dudok et al., 2015). It is possible that axonal CB1 receptors may function as replacement pool for internalized synaptic receptors at boutons as recently suggested for opioid receptors (Jullié et al., 2020), although synaptic enrichment would still be expected. In addition, GABA release at dendritic inhibitory synapses is not strongly modulated by CB1 receptors (Lee et al., 2010, 2015), and coupling between CB1 receptors and the active zone is weak (Dudok et al., 2015). This suggests that CB1 receptors in inhibitory axons serve an additional purpose. Interestingly, it was recently described that CB1 receptors can also mediate synaptic potentiation (Cui et al., 2016; Monday and Castillo, 2017; Wang et al., 2017). Although CB1 receptors typically signal via $G_{i/o}$-proteins, many additional downstream pathways, both dependent and independent of G-proteins, have been described (Glass and Felder, 1997; Berghuis et al., 2007; Flores-Otero et al., 2014; Roland et al., 2014; Cui et al., 2016; Zhou et al., 2019; Marti-Solano et al., 2020).

Here, we demonstrate that activation of axonal CB1 receptors can trigger the initial formation of inhibitory synapses. Using two-photon time lapse imaging we observed the formation of inhibitory boutons upon brief application of the CB1 receptor agonist WIN. We demonstrate that this requires the presence of CB1 receptors on inhibitory axons. Furthermore, we found that CB1-mediated inhibitory bouton formation is independent of $G_{i/o}$ protein signaling and neuronal activity. We find that new inhibitory boutons are formed in response to elevated cAMP levels or activation of G_s protein signaling in inhibitory axons. Our data indicate that activation of axonal CB1 receptors triggers inhibitory synapse formation via an atypical signaling pathway via G_s-proteins. Furthermore, our data identify an increase in axonal cAMP as a crucial second messenger for mediating inhibitory bouton formation.

Results

Repeated CB1 receptor activation increases functional presynaptic terminals

We previously demonstrated that new inhibitory boutons can form in response to brief CB1 receptor activation (Hu et al., 2019). Newly formed boutons often did not persist (Hu et al., 2019), suggesting that additional or repeated signaling is required to eventually form functional inhibitory synapses (Wierenga, 2017; Frias et al., 2019). It was recently reported that strong, but brief, CB1 receptor activation can induce synaptic potentiation, while longer CB1 activation induces synaptic depression (Cui et al., 2015, 2016). This suggests that CB1 activation pattern is an important factor in determining its downstream signaling. We therefore sought to employ repeated, short activation of CB1 receptors in order to induce the formation of inhibitory synapses. We activated CB1 receptors in hippocampal slice cultures by repeated short exposure to the CB1 receptor ligand 2-AG (100 µM; 3 times 20 minutes with 2 hours interval) (Fig. 1A). We verified that this treatment did not affect the distribution of CB1 receptors in these slices (data not shown). We recorded miniature inhibitory postsynaptic currents (mIPSCs) in CA1 pyramidal neurons to assess functional inhibitory synapses 24 hours after the start of the first 2-AG exposure (Fig. 1B). Repeated CB1 receptor activation resulted in an increase of the mean mIPSC frequency by 38% (control: 3.9 ± 0.3 Hz; 2-AG: 5.5 ± 0.4 Hz, p=0.013; Fig 1C), while mIPSC amplitudes were not affected (Fig. 1D). Continuous exposure to 2-AG for 24 hours did not alter frequency or amplitude of spontaneous IPSCs (Fig. 1E,F), consistent with the notion that activation pattern determines CB1 downstream signaling. Interestingly, mIPSCs after repeated 2-AG exposure appeared to have longer rise times (Fig. 1G), while decay times were not different (Fig. 1H). We separated mIPSCs with slow and fast rise times based on a double Gaussian fit of the distribution of rise times (Fig. 1I). When we then analyzed the interevent intervals of fast and slow mIPSCs separately, we observed that the interevent intervals of slow mIPSCs were decreased after repeated CB1 activation, while the interevent intervals of fast mIPSCs were not affected (Fig. 1J,K). This analysis revealed that the observed increase in mIPSC frequency was due to a specific increase in the frequency of slow mIPSCs with long rise times (Fig. 1L). The rise time of mIPSCs depends on synaptic maturation (Lazarus and Josh Huang, 2011; Gonzalez-Burgos et al., 2015; Pardo et al., 2018), but is also strongly influenced by subcellular location, as dendritic filtering attenuates mIPSCs originating from dendritic inhibitory synapses (Rall, 1967; Bekkers and Clements, 1999; Wierenga and

Wadman, 1999). This suggests that the increased mIPSC frequency after CB1 receptor activation may reflect an increase of inhibitory currents from dendritic locations, or from immature synapses.

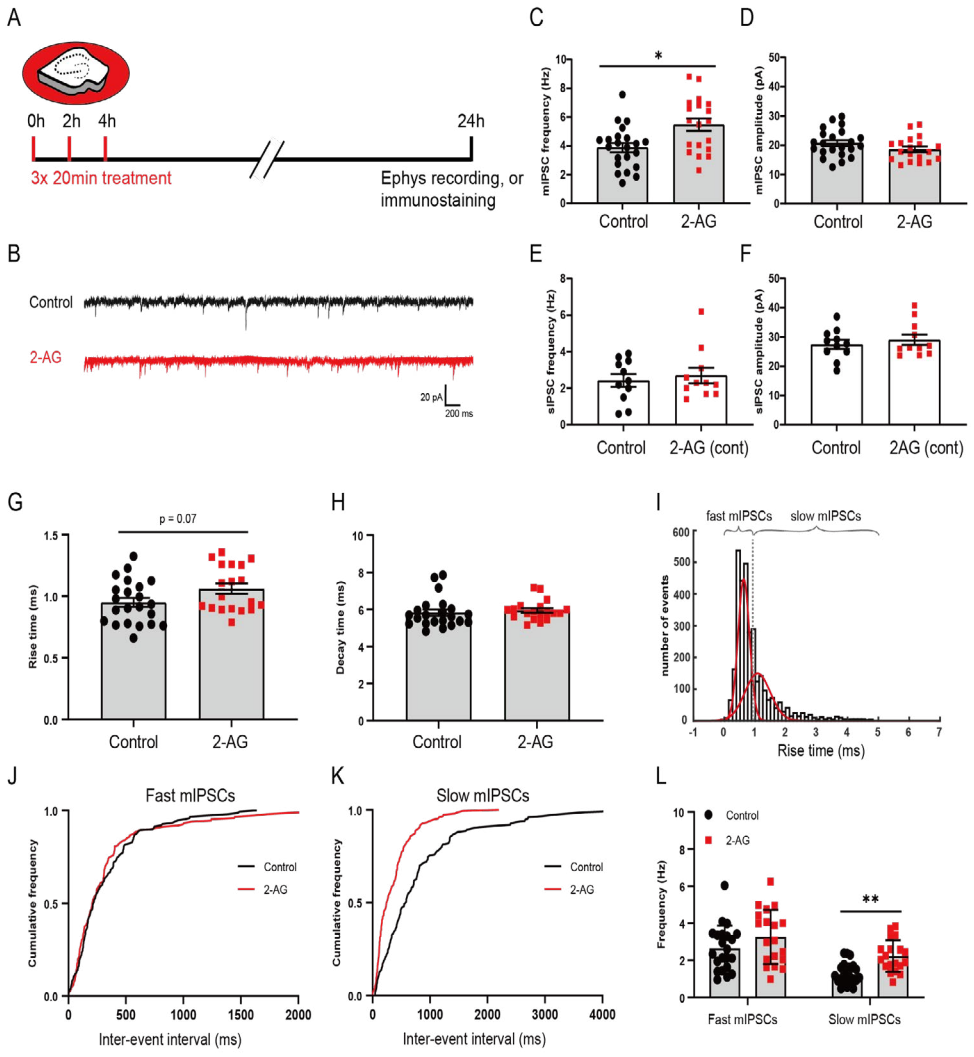

Figure 1. Repeated CB1 receptor activation results in increased mIPSC frequency.

(A) Organotypic hippocampal cultures were treated 3 times with culturing medium containing 100 µM 2-AG or DMSO (control) for 20 minutes with 2 hour intervals. After 24 hours, slices were used for electrophysiology and immunostaining experiments.

(B) Example traces of miniature inhibitory postsynaptic currents (mIPSCs) recordings from control (black) and 2-AG treated slice (red).

(C, D) Mean frequency (C) and amplitude (D) of mIPSCs in control and 2-AG treated slices (MW, p = 0.013 in C and p = 0.16 in D). Data from 22 cells in 6 control slices and 19 cells in

6 2-AG treated slices.

(E, F) Mean frequency (E) and amplitude (F) of sIPSCs in control and 2-AG treated slices, when 2-AG was continuously present for 24 hr (p = 0.99 in E and p = 0.95 in F; MW). Data from 11 cells in 5 control slices and 11 cells in 6 2-AG treated slices.

(G) Mean rise time of mIPSCs in control and 2-AG treated slices (MW, p = 0.073).

(H) Mean of mIPSC decay time in control and 2-AG treated slices (MW, p = 0.19).

(I) The distribution of rise times of mIPSCs was fitted with a double Gaussian to separate fast and slow mIPSCs.

(J,K) Cumulative distribution of interevent intervals of mIPSCs with fast (J) and slow (K) rise times (KS, p = 0.65 in J, and p < 0.0001 in K).

(L) Mean frequency of mIPSCs with fast and slow rise times (2w ANOVA Sidak, fast: p = 0.14; slow: p = 0.0095).

Data in G-L and C,D are from the same data set

To determine if the observed increase in mIPSCs was associated with an increase in the number of inhibitory synapses, we analyzed presynaptic VGAT and postsynaptic gephyrin puncta in the dendritic region of the CA1 area in parallel immunohistochemistry experiments (Fig. 2A). We observed that the density of VGAT puncta was slightly increased after repeated 2-AG application (Fig. 2B), while the VGAT puncta size was decreased (Fig. 2C). Gephyrin puncta density and size were not affected by repeated 2-AG exposure (Fig. 2D,E), and the density of inhibitory synapses, defined as VGAT-gephyrin associations, was also not different from control slices (Fig. 2F,G). We therefore made a distinction between VGAT puncta that were associated with gephyrin and VGAT puncta without gephyrin (Fig. 2A, last panel). We observed that the increase in VGAT density was due to a specific increase in VGAT puncta that were not associated with gephyrin (Fig. 2H). In contrast, the reduction in VGAT puncta size was mostly due to a reduction in size of VGAT puncta with gephyrin association (Fig. 2I). This suggests that repeated short activation of CB1 receptors has two separable effect on inhibitory synapses: on the one hand it leads to shrinkage of VGAT clusters at inhibitory synapses, possibly reflecting synaptic depression (Monday et al., 2020), while at the same time new VGAT clusters are formed which are not associated with the postsynaptic scaffold gephyrin. Live imaging experiments have shown that VGAT is rapidly recruited when new boutons are formed in inhibitory axons, and that gephyrin normally follows within a few hours (Wierenga et al., 2008; Dobie and Craig, 2011; Frias et al., 2019). Our data suggest that repeated CB1 receptor activation induces the formation of presynaptic VGAT clusters, likely reflecting immature inhibitory synapses.

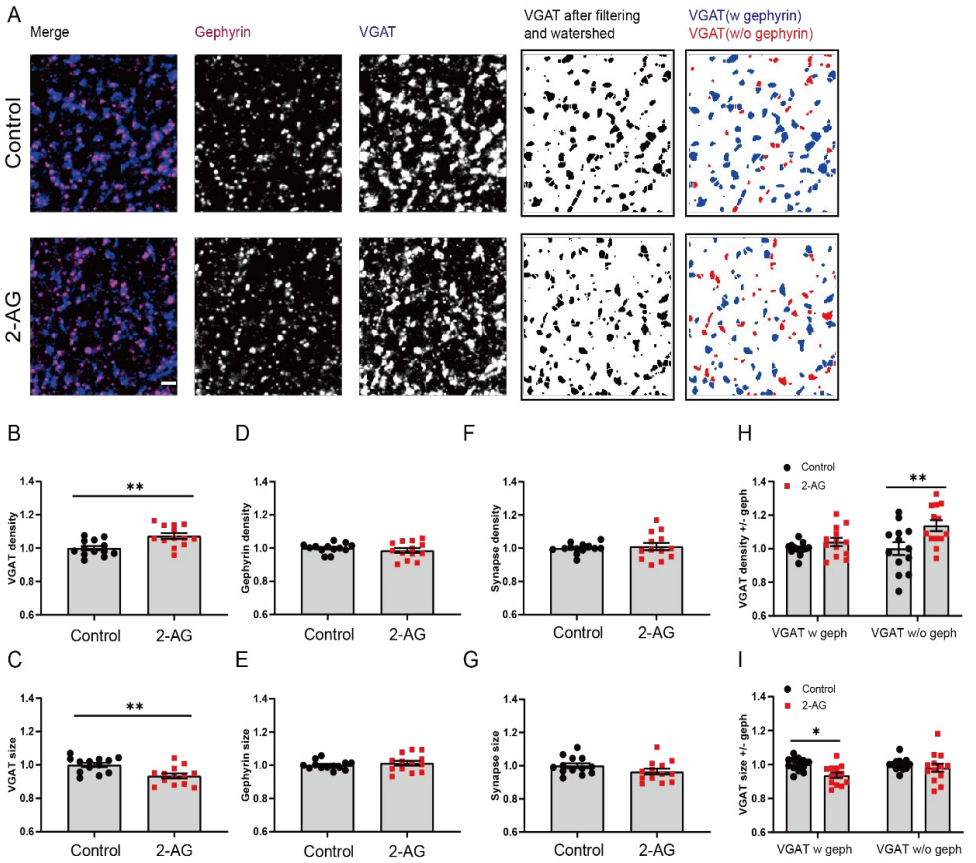

Figure 2. Repeated CB1 receptor activation induces the formation of partial inhibitory synapses.

(A) Representative immunostaining images showing the presynaptic VGAT (blue) and postsynaptic gephyrin (purple) in control (upper) and 2-AG (lower) slices. Individual VGAT puncta were identified using watershed segmentation and these were color coded to distinguish VGAT puncta associated with gephyrin (blue) and VGAT puncta without gephyrin (red).

(B, C) Normalized density (B) and size (C) of VGAT puncta in control and 2-AG slices (MW, p = 0. 0061 in B; p = 0.004 in C).

(D, E) Normalized density (D) and size (E) of gephyrin puncta in control and 2-AG slices (MW, p = 0.54 in D; p = 0. 64 in E).

(F, G) Normalized density (F) and size (G) of VGAT/gephyrin colocalizations in control and 2-AG slices (MW, p = 0.76 in F; p = 0.099 in G).

(H, I) Normalized density (F) and size (G) of VGAT puncta with and without gephyrin (2w ANOVA Sidak, p = 0.55 and p = 0.003 in H; p = 0.017 and p = 0.65 in I).

Data from 13 image stacks in 7 slices per group.

Acute activation of CB1 receptors affects non-persistent boutons density only slightly

To get further insight in the role of CB1 receptors in the formation of inhibitory synapses, we performed two-photon live imaging in organotypic hippocampal slices to monitor GFP-labeled inhibitory bouton dynamics in response to short activation of CB1 receptors. Here we used short applications (5 minutes) of CB1 receptor agonists to mimic retrograde endocannabinoid signaling (Hu et al., 2019), but we wanted to avoid inducing synaptic weakening (Monday et al., 2020). We used the endogenous CB1 receptor ligand 2-AG as well as the chemically synthesized agonist WIN552121-2 (WIN), which is widely used because of its high affinity and stability (Chevaleyre et al., 2007; Roland et al., 2014; Wang et al., 2017). We verified that brief WIN application only transiently and mildly suppressed inhibitory currents (data not shown). As previously reported (Frias et al., 2019), the majority of inhibitory boutons were present at all timepoints during the 140 minutes imaging period (persistent boutons), but a substantial fraction of inhibitory boutons appeared, disappeared, or reappeared, during the imaging period (Fig 3A) (Schuemann et al., 2013; Frias et al., 2019). We will refer to the latter as non-persistent (NP) boutons. Bath application of 100 µM 2-AG (5 minutes) did not affect overall bouton density (control: 30.8 ± 1.7 boutons per 100 µm; 2-AG: 29.8 ± 1.7 boutons per 100 µm, p=0.81). The density of NP boutons appeared slightly increased after 2-AG compared to DMSO control (Fig. 3B,C), but this was mainly due to a large effect in a single axon. We calculated for each axon the average fraction of NP boutons that are present over time (NP presence). In control slices there was a small decrease in NP presence over time, possibly reflecting a decrease in network activity level when the slices are transferred from the incubator to the microscope. After 2-AG application NP presence appeared slightly more stable (Fig. 3D), but this difference did not reach statistical significance. We assessed if this difference could be traced back to a more specific effect in a particular subgroup of NP boutons (see methods and (Frias et al., 2019)), but we could not detect any differences in the densities of NP bouton subgroups in slices treated with control DMSO or 2-AG (Fig. 3E). There was also no difference in bouton duration (data not shown).

The endocannabinoid 2-AG is rather unstable in solution and gets rapidly degraded in biological tissue (Savinainen et al., 2012; Dócs et al., 2017). To exclude the possibility that 2-AG gets degraded before it can activate CB1 receptors, we repeated these experiments using 20 µM WIN. Short activation (5 minutes) of CB1 receptors by bath application of WIN slightly increased in

NP bouton density (Fig. 3F,G). Although the increase appeared more robust compared to the 2-AG-induced effect, the effect was too small to reach statistical significance. Similar to 2-AG, the average NP presence appeared slightly increased (Fig. 3H), but we could not detect any changes in specific NP boutons subgroups (Fig. 3I). Together these observations indicate that short CB1 receptor activation by 2-AG or WIN leads to only a small (if any) increase in NP bouton density in GFP-labeled inhibitory axons.

Endocannabinoids are produced on demand in postsynaptic neurons (Alger and Kim, 2011; Hashimotodani et al., 2013; Piomelli, 2014), but an ambient level of endocannabinoids is always present, even in slices (Szabó et al., 2014; Lee et al., 2015; Lenkey et al., 2015). Tonic CB1 receptor activation by endocannabinoids affects mostly perisomatic inhibitory synapses, while dendritic inhibitory synapses are reported to be less sensitive (Lee et al., 2010, 2015). To address if tonic activation of CB1 receptors contributes to inhibitory bouton dynamics in our GFP-labeled axons (which mostly target dendrites (Wierenga et al., 2010)), we applied 5 µM AM251, an antagonist of CB1 receptors. However, AM251 had no effect on NP bouton density (Fig. 3J,K), NP presence or NP bouton subgroups (Fig. 3L,M).

Together our experimental findings indicate that inhibitory bouton dynamics of the GFP-labeled axons are not under strong tonic endocannabinoid control and that short CB1 receptor activation by 2-AG or WIN only slightly increases NP inhibitory bouton density.

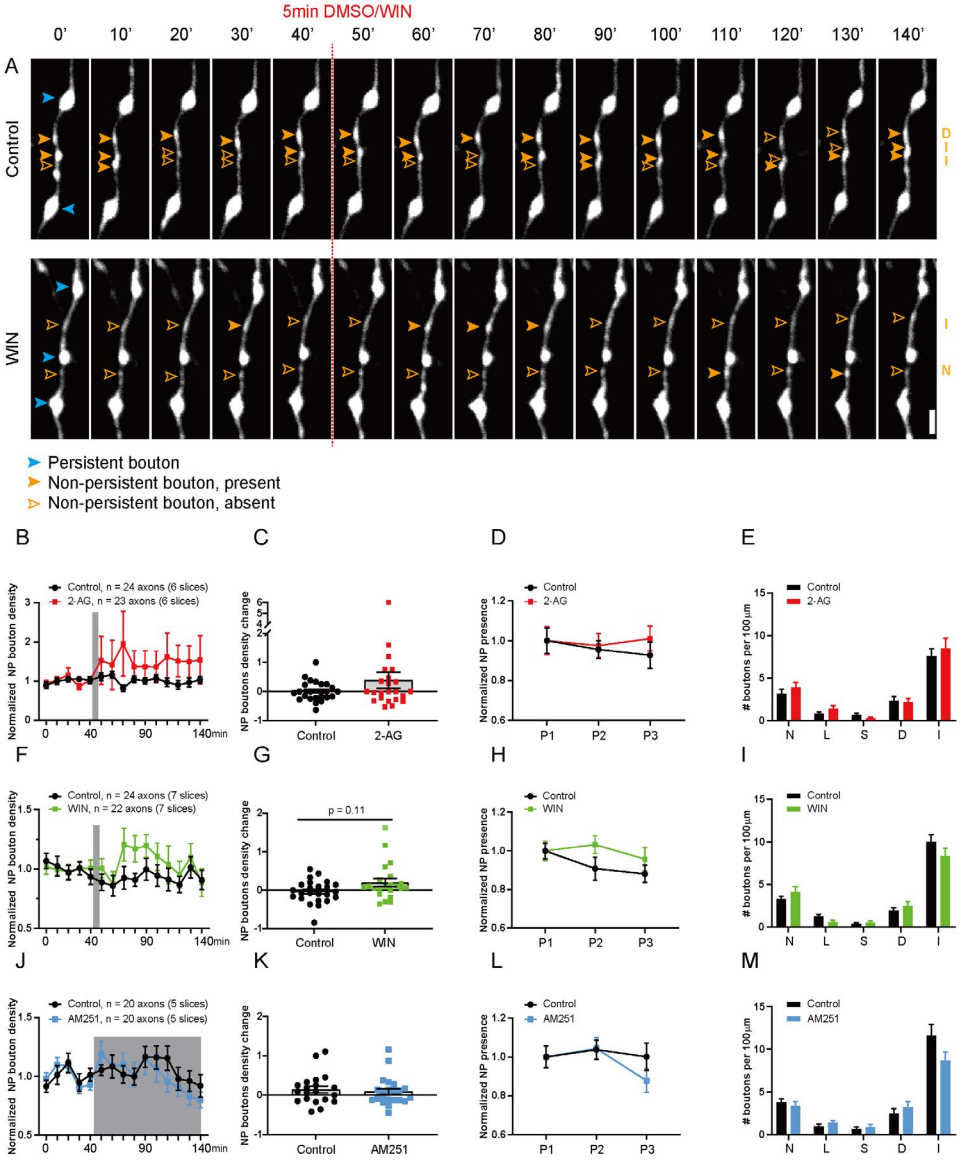

Figure 3. Brief activation of CB1 receptors slightly increases NP bouton density

(A) Representative two-photon time lapse images of GAD65-GFP labelled inhibitory axons in the dendritic region of the hippocampal CA1 area (maximal projections of 17 z-sections). After a baseline of five time points (40 minutes), CB1 receptor agonist or DMSO was washed in for 5 minutes. Imaging was continued for another ten time points (total imaging period is 140 minutes). Persistent boutons (blue) and non-persistent (NP) boutons (orange) are indicated by arrow heads. Empty arrow heads reflect a NP bouton which was absent at the time point. Scale bar is 2 µm.

(B) CB1 receptors were activated by bath application of 100 µM 2-AG for 5 minutes. Normalized NP bouton density over time in control (black) slices and after 2-AG (red) application (2w ANOVA, $p = 0.33$).
(C) Maximum change in NP bouton density in control slices and after 2-AG application (MW, $p = 0.54$).
(D) Normalized NP presence over time in control and 2-AG treated slices. P1= time points 1 to 5, P2= time points 6 to 10, and P3= time points 11 to 15) in control and 2-AG treated slices (2w ANOVA, $p = 0.61$).
(E) Mean density of NP bouton subgroups in control slices and after 2-AG application. N – new boutons (MW, $p = 0.35$); L – lost boutons (MW, $p = 0.44$); S – stabilizing boutons (MW, $p = 0.21$); D – destabilizing boutons (MW, $p = 0.91$); I – intermittent boutons (MW, $p = 0.87$).
(F) CB1 receptors were activated by bath application of 20 µM WIN for 5 minutes. Normalized NP bouton density over time in control (black) slices and after 2-AG (green) application (2w ANOVA, $p = 0.20$).
(G) Maximum change in NP bouton density in control slices and after WIN application (MW, $p = 0.11$).
(H) Normalized NP presence over time in control slices and after WIN application (2w ANOVA, $p = 0.20$).
(I) Mean density of NP bouton subgroups in control slices and after WIN application (MW, $p = 0.40$ (N); $p = 0.06$ (L); $p = 0.79$ (S); $p = 0.70$ (D); $p = 0.10$(I)).
(J) Slices were treated with the CB1 receptor antagonist AM251 (5 µM) after time point 5. Normalized NP bouton density over time in control (black) slices and during AM251 (blue) application (2w ANOVA, $p = 0.66$).
(K) Maximum change in NP bouton density in control slices and during AM251 application (MW, $p = 0.6$).
(L) Normalized NP presence over time in control slices and during AM251 application (2w ANOVA, $p = 0.56$).
(M) Mean density of NP bouton subgroups in control slices and during AM251 application (MW, $p = 0.46$ (N); $p = 0.23$ (L); $p = 0.94$ (S); $p = 0.29$ (D); $p = 0.10$(I)).
Data in A from 24 axons in 6 control slices and 23 axons in 6 2-AG slices. Data in B from 24 axons in 7 control slices and 22 axons in 7 WIN slices. Data in C from 20 axons in 5 control slices and 20 axons in 5 AM251 slices.

CB1 receptors regulate inhibitory bouton dynamics specifically in CB1R+ axons

The expression of CB1 receptors largely overlaps with the expression pattern of CCK in GABAergic interneurons (Katona et al., 1999, 2006). These interneurons are partially labeled in the GAD65-GFP mice which we use for our experiments (Wierenga et al., 2010). We previously estimated that ~50% of the GFP-labeled inhibitory axons express CB1 receptors in our slices (Hu et al., 2019), and this may significantly dilute an effect of CB1

receptor activation on bouton dynamics (Fig. 3). We therefore used *post-hoc* immunostaining immediately after two-photon live imaging to distinguish between axons with and without CB1 receptors (CB1R+ and CB1R- axons respectively; Fig. 4A, B). In accordance with previous reports (Mikasova et al., 2008; Dudok et al., 2015), CB1 receptors covered the entire surface of CB1R+ inhibitory axons and individual CB1R+ axons could be easily traced from the CB1 immunostainings (Fig. 4A, B). In addition, there was significant CB1 background staining, presumably reflecting CB1 receptors in pyramidal cells and glia cells (Bonilla-Del Río et al., 2021). CB1R- axons had a higher bouton density and higher bouton turnover compared to CB1R+ axons (Fig. 4C; see below), supporting the notion that CB1R+ and CB1R- GFP-labeled axons belong to separate subtypes of GABAergic cells.

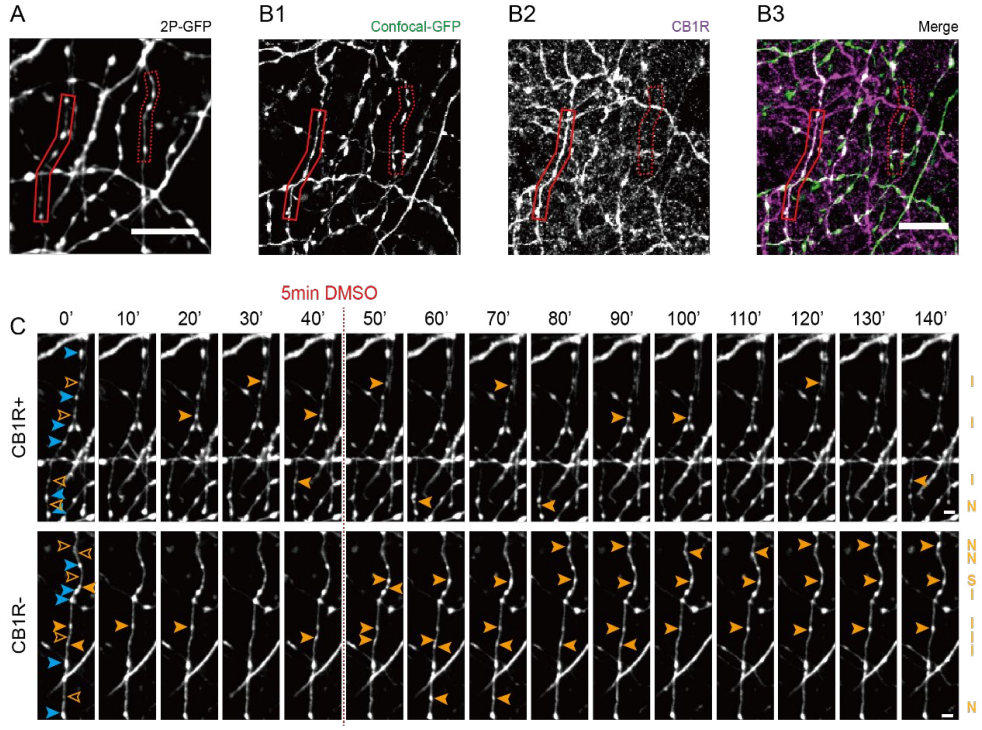

Figure 4. Distinction between CB1R+ and CB1R- axons using post hoc immunohistochemistry

(A) Z-projection of representative two-photon image of GFP-labeled inhibitory axons. After two-photon live imaging, the slice was immediately fixated and further processed for immunohistochemistry to assess CB1R expression.

(B) Confocal images of the same area after post hoc immunohistochemistry, showing the same GFP-labeled axons (B1) as in A (indicated with solid and dashed red boxes). Immunostaining against CB1 receptors (B2) show a clear distinction between CB1R+ axons

(solid red box), which express CB1 receptors, which cover the entire axonal surface, and CB1R- axons (dashed red box). Which do not express CB1 receptors.
(C) Two-photon time lapse imaging of bouton dynamics in the CB1R+ and CB1R- axons indicated in A and B. Arrow heads indicate P (blue) and NP (orange) boutons as in Fig. 3A. Scale bars are 10 μm in A,B and 2 μm in C,D.

We repeated the WIN application experiments, but now separately analyzed CB1R+ and CB1R- axons. In CB1R+ axons the density of NP boutons significantly increased after WIN application (Fig. 5A,B). WIN also increased average NP presence compared to control axons (Fig. 5C). When we analyzed the NP bouton subgroups we found a specific increase in the density of new and stabilizing boutons (Fig. 5D,F), whereas other NP subgroups were unaffected (Fig. 5D-H). New boutons reflect immature synapses, which start to recruit pre- and postsynaptic proteins, while levels of VGAT and gephyrin at stabilizing boutons at the end of the imaging period is comparable to persistent boutons (Schuemann et al., 2013; Frias et al., 2019). In clear contrast, WIN had no effect on bouton density or dynamics in CB1R- axons in the same slices (Fig. 5I-P). These results indicate that axonal CB1 receptors are required for mediating the WIN-induced changes in bouton dynamics in inhibitory axons, and exclude a role for CB1 receptors on other cells. Our results indicate that short activation of axonal CB1 receptors leads to an increase in NP bouton density by specifically promoting the formation and stabilization of inhibitory boutons.

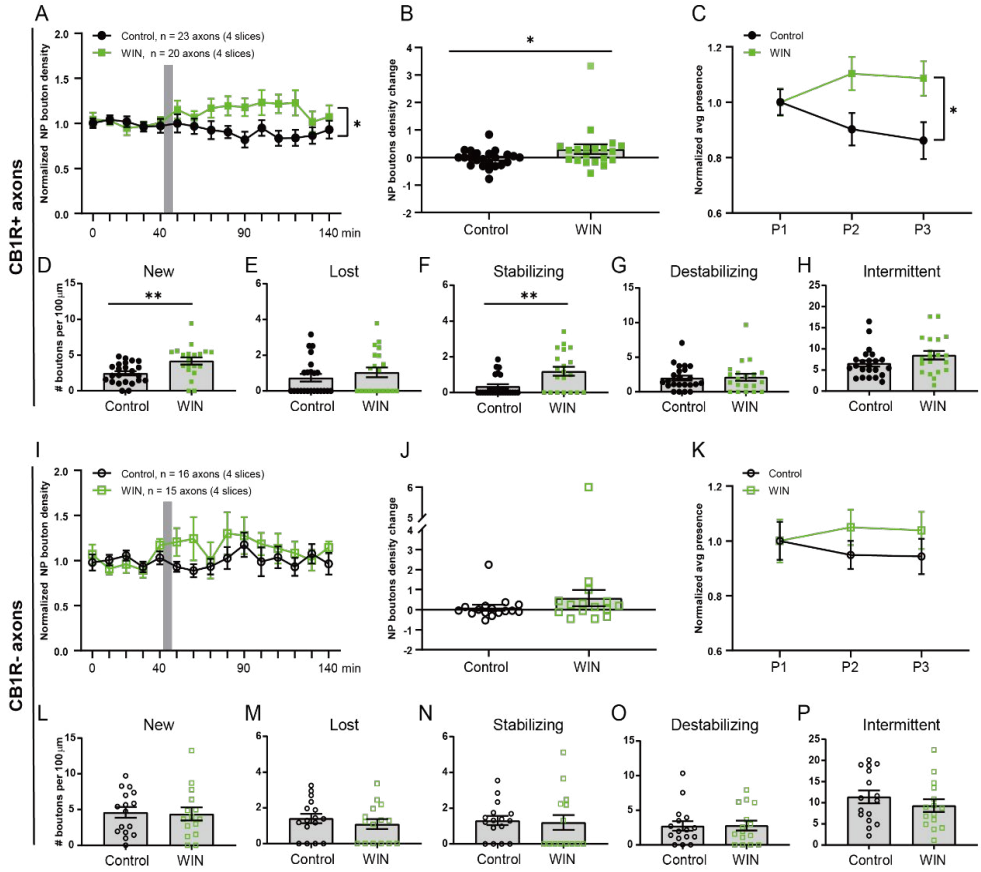

Figure 5. WIN promotes formation and stabilization of inhibitory boutons only in CB1R+ axons

(A) Normalized NP bouton density in CB1R+ axons over time in control (black) slices and after WIN (green) application (2w ANOVA, $p = 0.018$; interaction $p = 0.026$).

(B) Maximum change in NP bouton density in CB1R+ axons in control (black) slices and after WIN (green) application (MW, $p = 0.047$).

(C) Normalized NP presence in CB1R+ axons over time in control slices and after WIN application (2w ANOVA, $p = 0.022$; interaction $p = 0.045$).

(D-H) Mean density of NP bouton subgroups in CB1R+ axons in control slices and after WIN application. D, new boutons (MW, $p = 0.002$); E, lost boutons (MW, $p = 0.39$); F, stabilizing boutons (MW, $p = 0.005$); G, destabilizing boutons (MW, $p = 0.87$); H, intermittent boutons (MW, $p = 0.16$).

(I) Normalized NP bouton density in CB1R- axons over time in control (black) slices and after WIN (green) application (2w ANOVA, $p = 0.27$).

(J) Maximum change in NP bouton density in CB1R- axons in control (black) slices and after WIN (green) application (MW, $p = 0.21$).

(K) Normalized NP presence in CB1R- axons over time in control slices and after WIN application (2w ANOVA, $p = 0.37$).
(L-P) Mean density of NP bouton subgroups in CB1R- axons in control slices and after WIN application. L, new boutons (MW, $p = 0.77$); M, lost boutons (MW, $p = 0.46$); N, stabilizing boutons (MW, $p = 0.50$); O, destabilizing boutons (MW, $p = 0.99$); P, intermittent boutons (MW, $p = 0.34$).
Data from 25 CB1R+ and 16 CB1R- axons in 4 control slices and 20 CB1R+ and 15 CB1R- axons in 4 slices with WIN application.

WIN-induced bouton formation does not require $G_{i/o}$ signaling and neuronal activity

CB1 receptors are G-protein coupled receptors. Endocannabinoid signaling via CB1 receptors typically activates $G_{i/o}$ heterotrimeric proteins, resulting in a reduction of neurotransmitter release at presynaptic terminals (Lovinger, 2008; Castillo et al., 2012). We therefore tested whether WIN-induced bouton formation requires $G_{i/o}$ signaling. We pretreated the slices with pertussis toxin (PTX) (1 µg/ml) for 24 hours to eliminate $G_{i/o}$ signaling (Guo and Ikeda, 2004; Campbell and Smrcka, 2018), and then performed two-photon time-lapse live imaging as before. Axons with and without CB1R were distinguished using *post-hoc* immunostaining (Fig. 6A-C). PTX pretreatment had no major effect on CB1 receptor expression patterns.

Under control conditions, CB1R- axons had a higher bouton density compared to CB1R+ axons (Fig. 6D), which was mainly due to a higher density of NP boutons (Fig. 6E,F). The density for all NP bouton subgroups was almost twice as high in CB1R- axons compared to CB1R+ axons (Fig. 6G), showing that overall inhibitory bouton dynamics were more pronounced in CB1R- axons compared to CB1R+ axons. Unexpectedly, we observed that 24 hr pretreatment with PTX affected bouton density. PTX pretreatment specifically downregulated bouton density in CB1R- axons, while bouton density in CB1R+ axons was largely unaffected (Fig. 6D). PTX specifically reduced the density of non-persistent boutons in CB1R- axons (Fig. 6E,F). After PTX pretreatment there was no longer a difference in NP bouton subgroups between CB1R+ and CB1R- inhibitory axons (Fig. 6H). This suggests that under normal conditions CB1R- axons have a higher $G_{i/o}$ protein activity compared to CB1R+ axons in these slices. These data imply that $G_{i/o}$ signaling is an important regulator of inhibitory bouton dynamics.

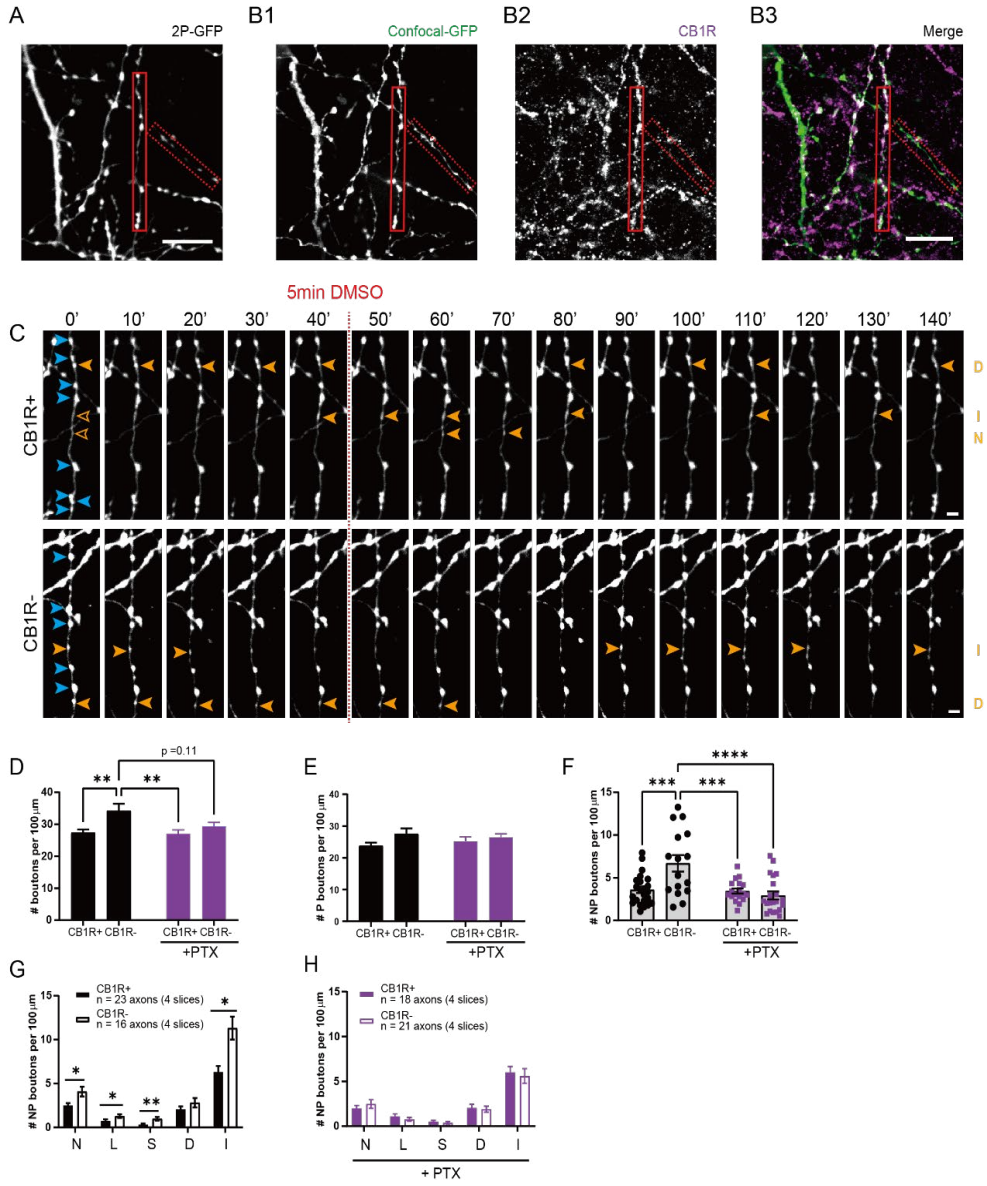

Figure 6. $G_{i/o}$ signaling is an important regulator of inhibitory bouton dynamics

(A) Z-projection of representative two-photon image of GFP-labeled inhibitory axons after PTX pretreatment.

(B) Confocal images of the same area after post hoc immunohistochemistry, showing the same GFP-labeled axons (B1) as in A (solid and dashed red boxes indicate CB1R+ and CB1R- axons).

(C) Two-photon time lapse imaging of bouton dynamics in the CB1R+ and CB1R- axons

indicated in A and B after PTX pretreatment. Arrow heads indicate P (blue) and NP (orange) boutons as in Fig. 3A.

(D) Average bouton density during baseline in CB1R+ and CB1R- axons in control slices and after PTX pretreatment. Comparisons between CB1R+ and CB1R- axons: $p = 0.0056$ for control, $p = 0.79$ after PTX; between control and PTX: $p = 0.11$ for CB1R- axons, $p > 0.99$ for CB1R+ axons; between CB1R+ (control) and CB1R- (PTX): $p = 0.86$ and between CB1R- (control) and CB1R+ (PTX): $p = 0.0057$ (2w ANOVA Sidak).

(E) Average density of persistent (P) boutons during baseline in CB1R+ and CB1R- axons in control slices and after PTX pretreatment (p=0.057 for axon type, 2w ANOVA Sidak).

(F) Average density of non-persistent (NP) boutons during baseline in CB1R+ and CB1R- axons in control slices and after PTX pretreatment. Comparisons between CB1R+ and CB1R- axons: $p = 0.0007$ for control, $p = 0.99$ after PTX; between control and PTX: $p < 0.0001$ for CB1R- axons, $p > 0.99$ for CB1R+ axons; between CB1R+ (control) and CB1R- (PTX): $p = 0.93$ and between CB1R- (control) with CB1R+ (PTX): $p = 0.0008$ (2w ANOVA Sidak).

(G) Mean density of NP bouton subgroups in CB1R+ and CB1R- axons in control slices. N – new boutons (MW, $p = 0.035$); L – lost boutons (MW, $p = 0.037$); S – stabilizing boutons (MW, $p = 0.002$); D – destabilizing boutons (MW, $p = 0.47$); I – intermittent boutons (MW, $p = 0.010$).

(H) Mean density of NP bouton subgroups in CB1R+ and CB1R- axons after PTX pretreatment (MW, $p = 0.45$ (N); $p = 0.41$ (L); $p = 0.36$ (S); $p = 0.88$ (D); $p = 0.40$(I)).

Data from 23 CB1R+ and 16 CB1R- axons in 4 control slices, and 18 CB1R+ and 21 CB1R- axons in 4 PTX-pretreated slices. Scale bars are 10 µm in A,B and 2 µm in C,D.

We then tested whether acute activation of CB1 receptors via WIN can induce changes in inhibitory bouton dynamics in the absence of $G_{i/o}$ signaling. We observed that short activation of CB1 receptors by WIN could still induce the formation of new inhibitory boutons in CB1R+ axons after pretreatment with PTX (Fig. 7A). This indicates that the formation of new inhibitory boutons by CB1 receptor activation is independent of $G_{i/o}$ signaling. However, in the absence of $G_{i/o}$ signaling WIN application no longer promoted bouton stabilization (Fig. 7B; compare with Fig. 5F), suggesting that bouton stabilization requires intact $G_{i/o}$ signaling. As before, other NP bouton subgroups were not affected (Fig. 7C) and WIN application did not affect bouton formation (density of new boutons was 81 ± 23 % of control; MW, p = 0.51) or bouton dynamics (data not shown) in CB1R- axons. These data indicate that short activation of CB1 receptors on inhibitory axons by WIN promotes the formation of new boutons via a $G_{i/o}$-independent signaling pathway.

$G_{i/o}$ protein signaling can hyperpolarize neurons via activation of K^+ channels

(Bacci et al., 2004; Guo and Ikeda, 2004). Blocking ongoing $G_{i/o}$ activity with PTX may therefore enhance neuronal activity in our slices, which may by itself affect inhibitory bouton dynamics. However, as enhancing neuronal activity is expected to promote overall inhibitory bouton turnover (Schuemann et al., 2013; Frias et al., 2019), this does not appear in line with the observed decrease in inhibitory bouton dynamics in CB1R- axons after PTX. To address if WIN-induced inhibitory bouton formation is affected by activity, we blocked network activity with TTX to reduce overall bouton dynamics (Schuemann et al., 2013; Frias et al., 2019). We observed that in the presence of TTX, brief activation of CB1 receptors with WIN still induced the specific increase in the density of new boutons (Fig. 7D). However, WIN did no longer induce a change in the density of stabilizing boutons (Fig. 7E), consistent with our earlier finding that inhibitory bouton stabilization requires activity (Frias et al., 2019). Other NP bouton subgroups were not affected (Fig. 7F) and WIN application did not significantly affect bouton formation (179 ± 216 % of control; MW, p = 0.11) or other bouton dynamics (data not shown) in CB1R- axons. Together these data demonstrate that CB1 receptor-mediated inhibitory bouton formation does not require $G_{i/o}$ protein signaling and is independent of activity.

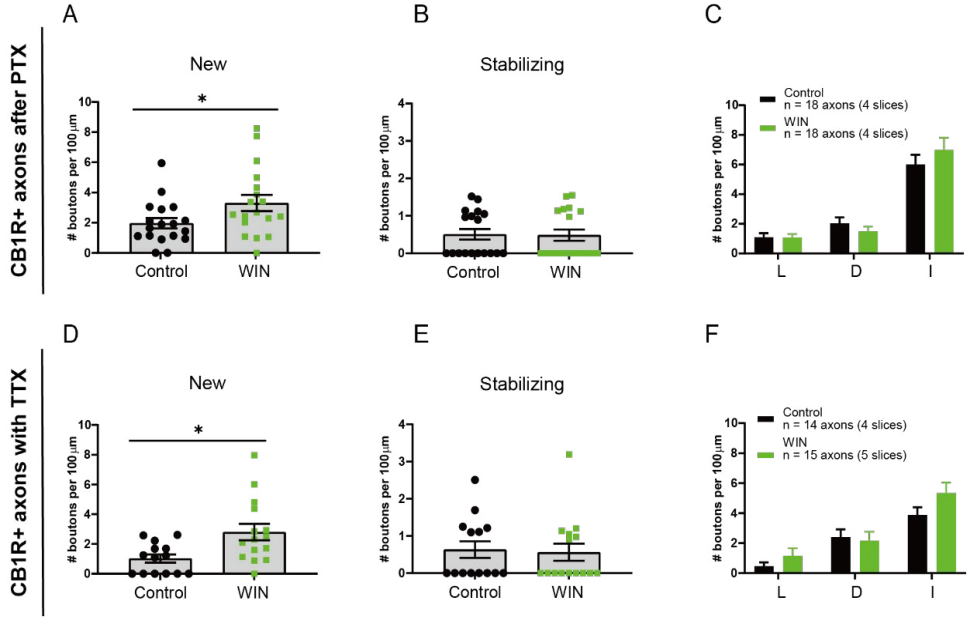

Figure 7. CB1-mediated bouton formation does not require $G_{i/o}$ signaling and is independent of activity.

(A) Mean density of new boutons in CB1R+ axons after control (black) and WIN (green) application in PTX-pretreated slices (MW, *p* = 0.047).

(B) Mean density of stabilizing boutons in CB1R+ axons after control and WIN application in

PTX-pretreated slices (MW, $p = 0.93$).
(C) Mean density of other NP bouton subgroups in CB1R+ axons after control and WIN application in PTX-pretreated slices. L – lost boutons (MW, $p = 0.82$); D – destabilizing boutons (MW, $p = 0.37$); I – intermittent boutons (MW, $p = 0.59$).
(D) Mean density of new boutons in CB1R+ axons after control (black) and WIN (green) application in the presence of TTX (MW, $p = 0.013$).
(E) Mean density of stabilizing boutons in CB1R+ axons after control and WIN application in the presence of TTX (MW, $p = 0.61$).
(F) Mean density of other NP bouton subgroups in CB1R+ axons after control and WIN application in the presence of TTX. L – lost boutons (MW, $p = 0.23$); D – destabilizing boutons (MW, $p = 0.56$); I – intermittent boutons (MW, $p = 0.16$).
Data in A-C from 18 axons in 4 slices with DMSO (control) application and 18 axons in 4 slices with WIN application. Data in D-F from 14 axons in 4 slices with DMSO (control) application and 15 axons in 5 slices with WIN application.

3

Acute elevation of cAMP levels promotes inhibitory bouton formation via PKA

Besides the typical downstream signaling pathway via $G_{i/o}$ proteins, CB1R activation can trigger several other signaling pathways, including via $G_{12/13}$ (Roland et al., 2014), G_q (Lauckner et al., 2005) and G_s proteins (Glass and Felder, 1997; Finlay et al., 2017). Intriguingly, a novel form of CB1 receptor-mediated synaptic potentiation was recently reported, which was shown to depend on activity of presynaptic protein kinase A (PKA) (Cui et al., 2016; Wang et al., 2017). This raises the attention to CB1 receptor-mediated G_s signaling, as G_s protein signaling enhances PKA activity via stimulation of cAMP production (Antoni, 2012; Taylor et al., 2013). We therefore tested if inhibitory bouton dynamics were affected when we directly elevated cAMP levels via activation of adenylyl cyclase (AC) by 25 µM forskolin (5 minutes) (Fig. 8A). We observed that brief application of forskolin induced the formation of new inhibitory boutons (Fig. 8B), while other NP subgroups were not affected (Fig. 8C,D). This suggests that the inhibitory bouton formation that we observed after CB1 receptor activation may be mediated by G_s signaling. The increase in inhibitory bouton formation after forskolin application appeared much stronger compared to WIN application (compare Fig. 8B to Fig. 3I), suggesting that most, if not all, GFP-labeled inhibitory axons responded to forskolin.

To directly test if downstream PKA activity is required, we blocked PKA activity with PKI 14-22 (Chevaleyre et al., 2007). We observed that in the presence of PKI 14-22 WIN did no longer trigger the formation or stabilization of inhibitory boutons (Fig. 8E,F). Interestingly, we observed a decrease in the density of destabilizing boutons after WIN treatment (Fig. 8G), suggesting

that PKA activity levels may be important for the maintenance of inhibitory boutons. Together these data show that the formation of new inhibitory boutons is promoted by increasing intracellular cAMP levels and PKA activity.

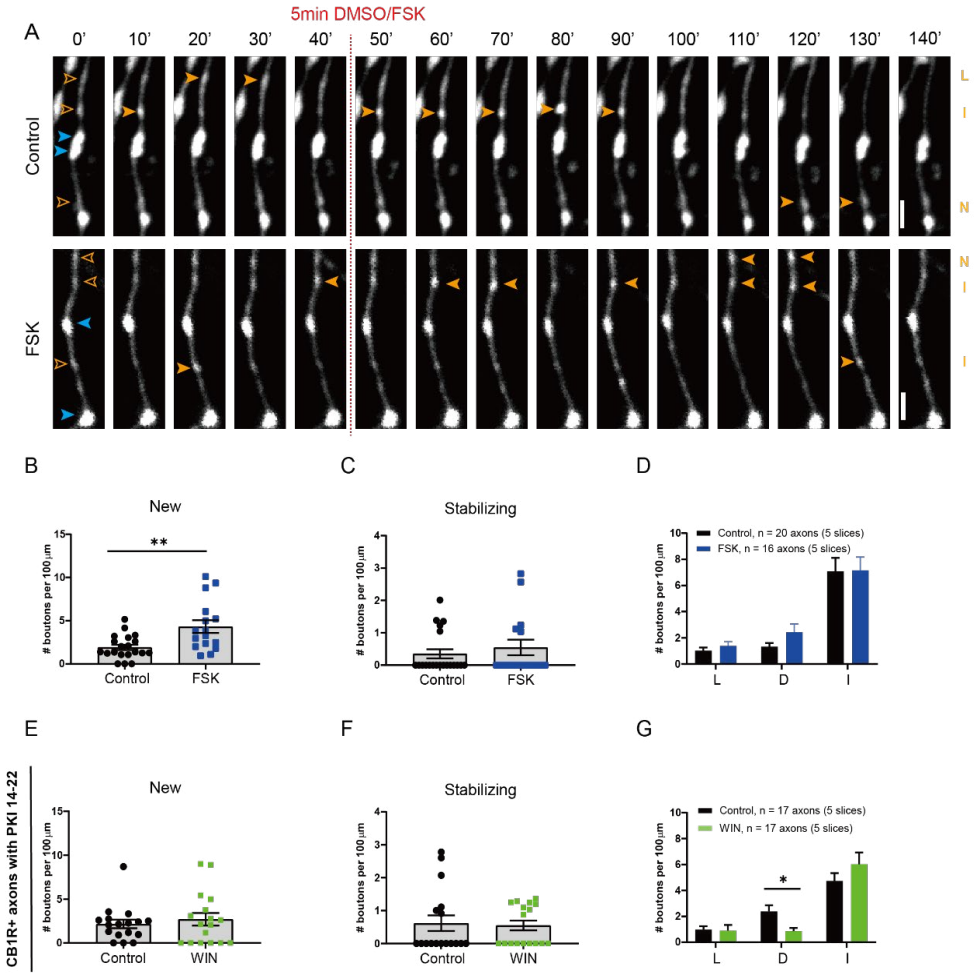

Figure 8. Inhibitory bouton formation is promoted by increasing intracellular cAMP levels with forskolin

(A) Representative two-photon time lapse images of bouton dynamics in GFP-labeled axons after control or forskolin application. Arrow heads indicate P (blue) and NP (orange) boutons as in Fig. 3A. Scale bar is 2 µm.

(B) Mean density of new boutons in control (black) slices and after forskolin (blue) application (MW, $p = 0.007$).

(C) Mean density of stabilizing boutons in control slices and after forskolin application (MW, $p = 0.67$).

(D) Mean density of other subgroup of NP boutons in control slices and after forskolin application. L – lost boutons (MW, $p = 0.46$); D – destabilizing boutons (MW, $p = 0.37$); I –

intermittent boutons (MW, $p = 0.81$).
Scale bars are 2 µm.
(E) Mean density of new boutons in control (black) slices and after WIN (green) application in the presence of PKA blocker PKI 14-22 (MW, $p = 0.81$).
(F) Mean density of stabilizing boutons in control slices and after WIN application in the presence of PKA blocker PKI 14-22 (MW, $p = 0.66$).
(G) Mean density of other subgroup of NP boutons in control slices and after WIN application in the presence of PKA blocker PKI 14-22. L – lost boutons (MW, $p = 0.29$); D – destabilizing boutons (MW, $p = 0.027$); I – intermittent boutons (MW, $p = 0.45$).
Scale bars are 2 µm.

G_s signaling in inhibitory axons promotes inhibitory bouton formation

Bath application of forskolin strongly increases neuronal activity (Mitoma and Konishi, 1996; Gekel and Neher, 2008) and will raise cAMP levels in all cells in the slice. The observed specific increase in new inhibitory bouton formation after forskolin, without affecting overall bouton dynamics, is therefore quite remarkable. However, we cannot conclude that the observed increase in inhibitory bouton formation is a direct effect of elevated cAMP levels in the inhibitory axons. We made use of DREADDs (Designer Receptors Exclusively Activated by Designer Drugs) (Urban and Roth, 2015; Roth, 2016) to achieve cell-specific manipulation of presynaptic cAMP levels. G_s-DREADDs allow the direct activation of the G_s-protein signaling pathway using the specific ligand CNO. To achieve sparse expression restricted to inhibitory neurons we infected hippocampal slices from VGAT-Cre mice with Cre-dependent AAVs. We used two AAVs: one containing a HA-tagged G_s-DREADD construct and one containing GFP (Fig. 9A; see methods for details). Infections with these two AAVs resulted in sparse GFP-labeling of inhibitory cells and their axons, which partially overlapped with G_s-HA expression (Fig. 9B). P*ost-hoc* immunostaining allowed us to identify GFP-labeled axons with and without G_s-HA (HA+ and HA- axons) in the same slice (Fig. 9C,D). We performed two-photon microscopy to monitor bouton dynamics in GFP-expressing HA+ and HA- inhibitory axons (Fig. 9E). Bouton dynamics in VGAT-Cre slices were in line with previous data (Frias et al., 2019), indicating that the AAV infections did not alter overall bouton dynamics in inhibitory axons. After a 40-minute baseline period, G_s-DREADDs were activated via bath application of CNO ligand. We found that CNO activation strongly increased the density of new boutons in G_s-HA positive axons compared to HA- axons (Fig. 9F). Other NP bouton subgroups were not affected, although the density of stabilizing boutons appeared to be somewhat increased (Fig. 9G,H). These data show that specific activation of G_s signaling in inhibitory axons mimics the WIN-induced inhibitory bouton formation.

Together, our results indicate that inhibitory bouton formation after brief CB1 receptor activation does not require $G_{i/o}$-signaling, and that it is mimicked by activation of G_s signaling in inhibitory axons. This suggests that CB1 receptors on inhibitory axons couple to G_s proteins rather than the conventional $G_{i/o}$ effectors to trigger inhibitory bouton formation.

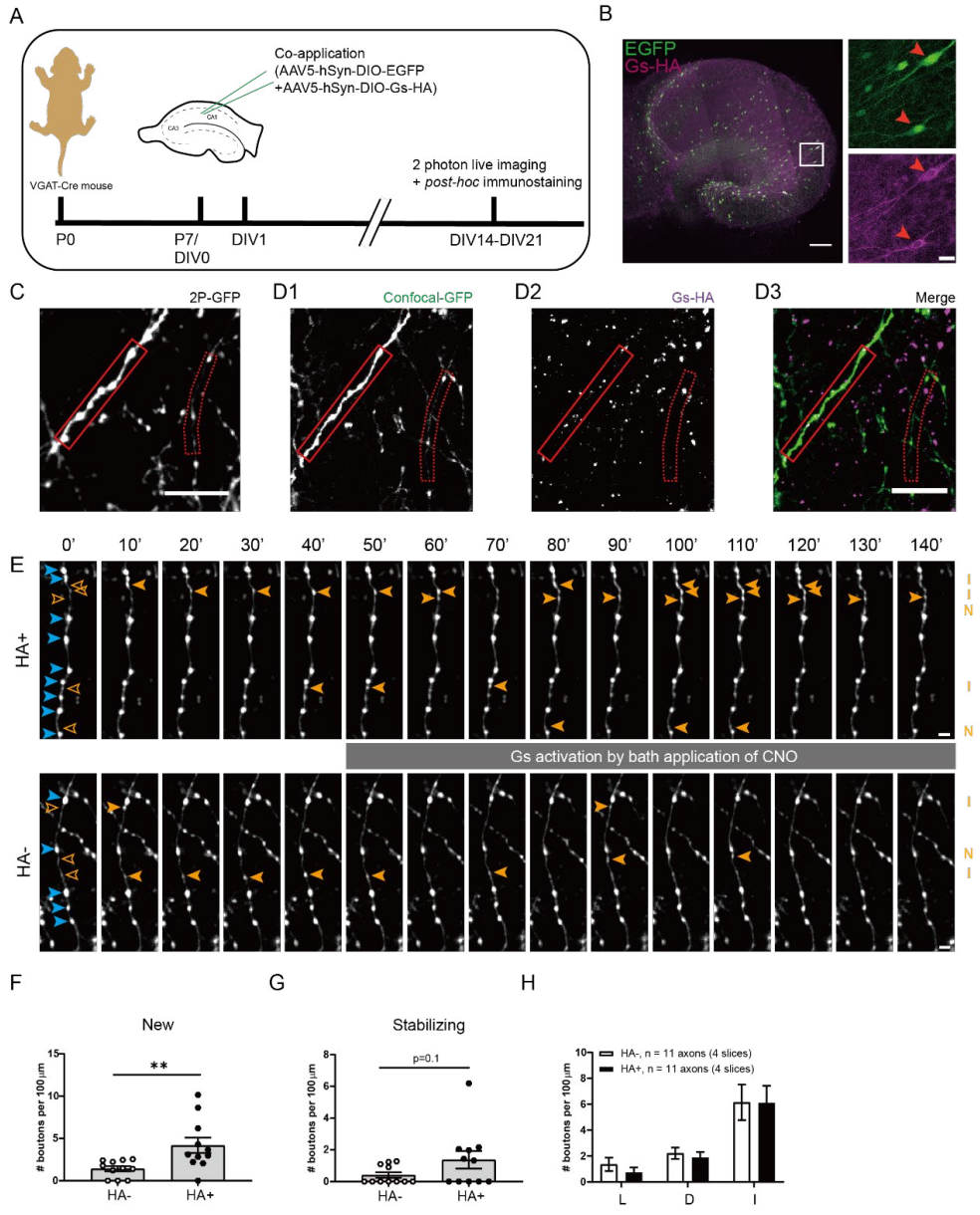

Figure 9. Specific activation of Gs at inhibitory axons induce new bouton formation.
(A) Experimental design. Hippocampal slice cultures are prepared from P7 VGAT-Cre mouse

pups. At DIV1 (days *in vitro*), AAV5-hSyn-DIO-EGFP and AAV5-hSyn-DIO-Gs-HA viruses are applied to the VGAT-Cre slice cultures. After 2-3 weeks (DIV 14-21) slices were used for two-photon live imaging and *post hoc* immunostaining to reveal Gs-HA expression.

(B) Representative example of VGAT-Cre slice culture at DIV20 showing sparse expression of GFP and Gs-HA in GABAergic cells. Right images (zoom from white box) show Gs-HA and EGFP co-expression in a subset of neurons (red arrow heads).

(C) Z-projection of representative two-photon image of GFP-labeled inhibitory axons in VGAT-Cre slice.

(D) Confocal images of the same area in C after post hoc immunohistochemistry against HA, showing the same GFP-labeled axons as in A (solid and dashed red boxes indicate HA+ and HA- axons).

(E) Two-photon time lapse imaging of bouton dynamics in the HA+ and HA- axons indicated in C and D. Gs-DREADDs were activated by bath application of 10 µM CNO after the 40 minutes baseline period. Arrow heads indicate P (blue) and NP (orange) boutons as in Fig. 3A.

(F) Mean density of new boutons at HA+ and HA- axons in response to Gs-DREADD activation (MW, $p = 0.003$).

(G) Mean density of stabilizing boutons at HA+ and HA- axons in response to Gs-DREADD activation (MW, $p = 0.10$).

(H) Mean density of other subgroup of NP boutons at HA+ and HA- axons in response to Gs-DREADD activation. L – lost boutons (MW, $p = 0.30$); D – destabilizing boutons (MW, $p = 0.44$); I – intermittent boutons (MW, $p = 0.85$)

Data from 11 HA+ and 11 HA- axons in 4 slices. Scale bars are 200 µm (overview) and 20 µm (zoom) in B, 10 µm in C,D and 2 µm in E.

Discussion

Here we examined the signaling pathway underlying the CB1 receptor-mediated formation of new inhibitory synapses. We made several important observations. First of all, repeated CB1 activation led to an increase in mIPSC frequency and an increase in the density of presynaptic VGAT clusters, which were not associated with postsynaptic gephyrin. Inhibitory synapses which do not contain gephyrin are immature and show reduced transmission (Danglot et al., 2003; Yu et al., 2007; Patrizi et al., 2008; Niwa et al., 2012; Nguyen et al., 2016). Our observations are in line with the notion that pre- and postsynaptic signaling pathways during synapse formation are largely independent (Wierenga, 2017; Jiang et al., 2021) and suggest that CB1 receptors act purely presynaptically. Second, brief activation of CB1 receptors specifically triggered the formation of inhibitory synapses in CB1R+ axons. This indicates that formation of inhibitory synapses is mediated by axonal CB1 receptors and our data exclude a prominent role for CB1 receptors in astrocytes or postsynaptic neurons. Third, bouton turnover in inhibitory axons was strongly reduced when $G_{i/o}$ protein signaling was blocked by PTX pretreatment. This suggests that modulation of axonal cAMP levels is an important regulator of bouton turnover in inhibitory axons. Fourth, CB1 receptor-mediated inhibitory bouton growth was independent of ongoing $G_{i/o}$ signaling and activity, suggesting that signaling pathways downstream of axonal CB1 receptors differ from presynaptic CB1 receptors. Finally, inhibitory synapse formation was induced in response to an increase in cAMP after forskolin application, and when G_s signaling was activated via G_s-DREADDs, which were expressed exclusively in inhibitory neurons. These findings revealed that an increase in cAMP is
the key second messenger signal for inhibitory bouton formation and suggest that axonal CB1 receptors trigger inhibitory bouton formation by enhancing PKA activity.

Our present study has limitations that are important to mention here. First of all, we use transgenic mice in which several inhibitory neuron subtypes are labeled with GFP (Wierenga et al., 2010). This unspecific labeling diluted and hampered the detection of axon-specific effects (Fig. 2). However, we used it to our advantage by performing posthoc immunostaining to distinguish between different inhibitory axon types. This allowed comparison between CB1R+ and CB1R-, or HA+ and HA- axons in the same slice and avoided comparison between slices from different GFP-labeled mouse lines. Another limitation of our study is that we have used bath application of CB1 agonist WIN to trigger inhibitory bouton formation. Under physiological

conditions, endocannabinoid signals are likely transient and highly localized (Hashimotodani et al., 2007; Monday and Castillo, 2017; Hu et al., 2019), providing spatial and temporal control over inhibitory synapse formation. We elevated cAMP levels to trigger inhibitory bouton formation by bath application of forskolin or by activation of G_s-DREADDs in inhibitory cells. While this allowed separation of formation and stabilization of inhibitory boutons, it likely abolished spatial modulations. Axons contain several phosphodiesterases, which rapidly degrade cAMP and provide spatiotemporal compartmentalization of cAMP signaling (Baillie, 2009; Argyrousi et al., 2020). Pretreatment with PTX will disturb these cAMP modulations and this strongly reduced inhibitory bouton dynamics and abolished the difference between CB1R+ and CB1R- axons (Fig. 6L). This indicates that CB1R- axons have higher $G_{i/o}$ baseline activity compared to CB1R+ axons and suggests that cAMP modulation is an important factor regulating inhibitory bouton dynamics. Future research should further assess the relationship between cAMP signaling and inhibitory bouton turnover.

Synapse formation is a multistep process, with each step regulated by specific signaling pathways (Wierenga, 2017; Jiang et al., 2021). Our detailed two-photon analysis allows dissecting these steps and addressing the involved signaling pathways. Inhibitory synapse formation starts with the growth of a new bouton at an axonal location where the inhibitory axon is in close proximity to a dendrite (Wierenga et al., 2008; Dobie and Craig, 2011; Villa et al., 2016; Hu et al., 2019). Our data indicate that axonal CB1 receptors can trigger bouton formation, which does not require neuronal activity. We observed that CB1 receptor-mediated inhibitory bouton formation was not affected in the presence of TTX (Fig. 7D). In addition, we observed that forskolin, which strongly raises neuronal activity (data not shown), did not affect overall bouton turnover (Fig. 8D). This was unexpected given our previous observations that inhibitory bouton turnover is enhanced by neuronal activity (Schuemann et al., 2013; Frias et al., 2019). On the other hand, we observed that blocking $G_{i/o}$ signaling strongly affected bouton turnover (Fig. 6F,H), which appeared independent of activity. These data suggest that axonal cAMP is the primary second messenger affecting inhibitory bouton formation, which is indirectly modulated by activity, possibly via changes in neuromodulatory signals.

Our data indicate that axonal CB1 receptors can directly trigger bouton formation via an increase in cAMP, while subsequent bouton stabilization and postsynaptic assembly requires additional signaling. WIN-induced bouton stabilization was prevented when $G_{i/o}$ signaling was blocked by PTX

(Fig. 7B), and bouton stabilization was not altered by increasing cAMP levels with forskolin (Fig. 8C), although it may be facilitated with longer elevations (Fig. 9H). These data suggest that after the initial formation, CB1 receptors may also promote bouton stabilization via a more indirect pathway. We previously showed that bouton stabilization requires neuronal activity and involves local actin remodeling via a reduction in ROCK activity (Frias et al., 2019). Interactions between CB1 receptor signaling and ROCK activity (Berghuis et al., 2007) and actin remodeling (Njoo et al., 2015; Zhou et al., 2019) have been reported, but future research should further clarify the precise nature of these interactions.

CB1 receptors are highly versatile and are involved in many neuronal processes via multiple downstream pathways, including axon guidance and synaptic plasticity (Berghuis et al., 2007; Roland et al., 2014; Njoo et al., 2015; Araque et al., 2017; Monday and Castillo, 2017). There are multiple factors, including interacting proteins (Guggenhuber et al., 2016), which determine which downstream signaling pathway is activated after CB1 receptor activation (Flores-Otero et al., 2014; Nogueras-Ortiz and Yudowski, 2016) and this functional selectivity of CB1 receptors may have important clinical relevance (Ibsen et al., 2017; Laprairie et al., 2017; Sholler et al., 2020). It was recently reported that the duration of CB1 receptor activation determines the direction of plasticity at corticostriatal synapses with brief activation inducing LTP, while prolonged activation induces LTD (Cui et al., 2015, 2016). Our data suggest that brief activation of axonal CB1 receptors promotes the formation of new inhibitory boutons via G_s-mediated elevation of cAMP levels, but we have not extensively tested longer activations or different ligand concentrations. An intriguing possibility is that the subcellular location of CB1 receptors affects downstream signaling pathway, or that different CB1 receptor isoforms are localized to different subcellular locations (Marti-Solano et al., 2020). CB1 receptors at presynaptic terminals couple to $G_{i/o}$ to affect GABA release (Guo and Ikeda, 2004; Lee et al., 2015), while CB1 receptors in the axonal shaft of the same inhibitory axons may couple to G_s proteins. Even though CB1 receptors prefer coupling to G_i-proteins, they can switch to G_s when G_i-proteins are not available or already occupied (Glass and Felder, 1997; Caballero-Florán et al., 2016; Eldeeb et al., 2016; Finlay et al., 2017). This may suggest that G_i proteins are only available at presynaptic terminals, while G_s protein coupling could be dominant in axons.

Our experiments indicate that PKA is an important effector downstream of cAMP to trigger inhibitory bouton formation. Presynaptic PKA activity is

also involved in CB1-mediated synaptic plasticity (Chevaleyre et al., 2007; Cui et al., 2016) and may act by altering local clustering and inter-bouton exchange of synaptic vesicles (Patzke et al., 2019; Chenouard et al., 2020). PKA resides close to the plasma membrane and preferably phosphorylates membrane proteins in its close proximity (Tillo et al., 2017). Potential PKA targets to mediate inhibitory bouton formation remain yet to be identified. In addition, PKA-independent pathways downstream of cAMP signaling may also play a role, for instance via Epac2 (Kawasaki et al., 1998). Epac2 activity can strongly increase synaptic transmission (Gekel and Neher, 2008; Fernandes et al., 2015), yet a role in synapse formation has not been reported. Interestingly, Epac2 was recently found to be downstream of G_s-coupled β adrenergic receptors to mediate presynaptic LTP at parallel fiber synapses to Purkinje cells (Martín et al., 2020). cAMP signaling via PKA, Epac2 or Rho GTPases may affect the axonal cytoskeleton. Actin is important in the formation, stabilization and maintenance of presynaptic terminals (Bednarek and Caroni, 2011; Pielage et al., 2011; Chia et al., 2013, 2014; Frias et al., 2019; Chenouard et al., 2020) and cAMP fluctuations may drive local modifications in the actin cytoskeleton (Bernier et al., 2019) underlying structural presynaptic changes.

Our findings suggest that axonal CB1 receptors serve an important role in local, on demand synapse formation. Our observation that inhibitory bouton formation was more prominent after cAMP elevation than after WIN application (compare Fig. 8B and 9F to 3I) suggests that axonal cAMP signaling is an important second messenger signal mediating bouton formation not only in CB1R+, but perhaps in all, inhibitory axons. Intriguingly, our observations are reminiscent of cAMP-mediated bouton formation in zebrafish (Yoshida and Mishina, 2005), Aplysia (Nazif et al., 1991; Bailey and Kandel, 1993; Upreti et al., 2019) and Drosophila axons (Zhong et al., 1992; Koon et al., 2011; Maiellaro et al., 2016). This raises the possibility that axonal cAMP signaling is a universal second messenger system for regulating structural plasticity in axons. Activation of CB1 receptors via dendritic endocannabinoid signaling (Hu et al., 2019) then represents one specific way to trigger cAMP-mediated bouton formation in CB1R+ axons in response to strong excitatory synaptic activity. Other axons may employ different axonal receptors to mediate bouton formation. Indeed, GABAergic interneurons express many different G-proteins (Cox et al., 2008; Helboe et al., 2015; Puighermanal et al., 2017), which often provide neuromodulatory context signals from other brain areas (Hattori et al., 2017). Our findings raise the intriguing possibility that neuromodulatory receptors on the

axonal surface provide the opportunity to build a new inhibitory bouton on demand, triggered by axon-specific and context-dependent signaling.

Materials and Methods

Animals

All animal experiments were performed in compliance with the guidelines for the welfare of experimental animals issued by the Federal Government of The Netherlands. All animal experiments were approved by the Animal Ethical Review Committee (DEC) of Utrecht University.

Mouse hippocampal slice culture

Organotypic mouse hippocampal slices were acquired from female and male GAD65-GFP mice at 6-7 days after birth. In these mice, ~20% interneurons are labelled by GFP from early embryonic developmental stage into adulthood (López-Bendito et al., 2004). Most GFP-labelled interneurons target dendrites of CA1 pyramidal cells and express VIP or reelin, while parvalbumin and somatostatin-positive neurons are not labelled (Wierenga et al., 2010). Slice culture preparation details are described previously (Frias et al., 2019; Hu et al., 2019). Mice were sacrificed and the isolated hippocampus was placed in ice-cold HEPES-GBSS (containing 1.5 mM $CaCl_2 \cdot 2H_2O$, 0.2 mM KH_2PO_4, 0.3 mM $MgSO_4 \cdot 7H_2O$, 5 mM KCl, 1 mM $MgCl_2 \cdot 6H_2O$, 137 mM NaCl, 0.85 mM Na_2HPO_4 and 12.5 mM HEPES) supplemented with 12.5 mM HEPES, 25 mM glucose and 1 mM kynurenic acid (pH set around 7.2, osmolarity set around 320 mOsm, sterile filtered). Slices were vertically chopped along the long axis of hippocampus at thickness of 400 µm. They were then quickly washed with culturing medium (consisting of 48% MEM, 25% HBSS, 25% horse serum, 30 mM glucose and 12.5 mM HEPES, pH set at 7.3-7.4 and osmolarity set at 325 mOsm), and transferred to Millicell cell culture inserts (Milipore) in 6-well plates. Slices were cultured in an incubator (35 °C, 5% CO_2) until use. Culturing medium was completely replaced twice a week. Slices were used after 2 to 3 weeks *in vitro*, when the circuitry is relatively mature and stable (De Simoni et al., 2003).

Pharmacological treatments

The following drugs were used: 20 µM WIN 55212-2 (WIN; Tocris Bioscience), 100 µM 2-AG (Tocris Bioscience), 25 µM forskolin (Abcam), Pertussis toxin 1 µg/ml (Tocris Bioscience), 10 µM CNO (Tocris Bioscience), 5 µM AM251 (Tocris Bioscience), 1 µM TTX (Abcam), 1 µM PKI 14-22 (Tocris Bioscience). For acute treatments, ACSF containing the drug or 0.1% DMSO vehicle was bath applied for 5 minutes. AM251 and CNO were bath applied after a baseline period (5 time points) and continued until the end of the experiment. TTX or PKI 14-22 were added to the ACSF and were present during the entire two-photon imaging period. Pertussis toxin was added to the slice culture

medium and a small drop was placed on top of the slice 24 hours before the start of the experiment. Treated slices were kept in the incubator.
CB1 receptor activation can result in different downstream signaling pathways, which depend on ligand concentration and duration (Cui et al., 2015, 2016). We used a relatively high concentration of WIN (20 µM) to aim for strong activation of CB1 receptors. We used relatively short applications to mimic CB1 receptor activation under physiological conditions (Hu et al., 2019) and to avoid the induction of synaptic depression which have been observed with longer applications (Cui et al., 2016; Monday et al., 2020). We expect that CB1 receptor activation under physiological conditions will be shorter, and therefore perhaps more efficient in triggering inhibitory bouton formation.
For repeated treatment of 2-AG, normal culturing medium was replaced by medium containing 100 µM 2-AG or 0.1% DMSO for 20 minutes. This was repeated 3 times with 2 hours intervals. At the start of each medium replacement, a small drop was placed on top of the slices to facilitate exchange. A treatment duration of 20 minutes (rather than 5) was chosen to ensure penetration in the entire slice as solution exchange may be slower in the incubator compared to the microscope bath. After the last treatment, the medium was replaced 3 times with fresh medium to ensure wash out. During and after the treatment slices were kept in the incubator and experiments (immunocytochemistry or electrophysiology) were performed 24 hours after the start of the first treatment.

Electrophysiology recording and analysis
Slices were transferred to a recording chamber which was continuously perfused with carbogenated artificial cerebrospinal fluid (ACSF; containing 126 mM NaCl, 3 mM KCl, 2.5 mM $CaCl_2$, 1.3 mM $MgCl_2$, 1.25 mM NaH_2PO_4, 26 mM $NaHCO_3$, 20 mM glucose and 1 mM Trolox) at 32 °C. Whole-cell patch clamp measurements were recorded with a MultiClamp 700B amplifier (Molecular Devices) and stored using pClamp 10 software. Recordings were filtered with a 3 kHz Bessel filter. Thick-walled borosilicate pipettes of 4–6 MΩ were filled with pipette solution containing (in mM): 70 K-gluconate, 70 KCl, 0.5 EGTA, 10 HEPES, 4 MgATP, 0.4 NaGTP, and 4 Na_2-phosphocreatine. Cells were discarded if series resistance was above 35 MΩ or if the resting membrane potential exceeded -50 mV. Recordings were excluded when the series resistance after the recording deviated more than 30% from its original value. To isolate miniature inhibitory postsynaptic currents (mIPSCs) TTX, AP5 and DNQX were added to the ACSF. The mIPSCs were analyzed in pClamp and Matlab with homemade scripts (Ruiter et al., 2020). Rise

time of mIPSCs were determined as the time between10% and 90% of the peak value. The distribution of the rise times of mIPSCs recorded in control conditions (generated from 150 mIPSCs per cell) were fitted with two Gaussians and their crossing point determined the separation between fast and slow mIPSCs (Ruiter et al., 2020). A double Gaussian fit for the rise time distribution in 2-AG conditions gave a similar separation value (control: 0.9 ms; 2-AG: 1.1 ms) and we verified that our conclusions did not change by taking the 2-AG separation value.

Two-photon time lapse imaging

Time-lapse two-photon imaging was performed in carbogenated, continuously perfused ACSF at 32 °C. Slices were transferred in a 3 cm dish containing ACSF. Two-photon imaging was performed on a customized two-photon laser scanning microscope (Femto2D, Femtonics, Budapest, Hungary) with a Ti-Sapphire femtosecond pulsed laser (MaiTai HP, Spectra-Physics) with a 60x water immersion objective (Nikon NIR Apochromat, NA = 1.0). A 4x objective (Nikon Plan Apochromat) was used to determine the location of the dendritic layer of the CA1 region. GFP was excited at 910 nm to visualize GFP-labelled axons. 3D image stacks were acquired at a size of 93.5 µm x 93.5 µm (1124 x 1124 pixels) with 50-63 z-steps (0.5 µm step size). Acquisition time per image stack was ~7 minutes. We acquired image stacks every 10 minutes, with a total of 15 time points (140 minutes). After a baseline of 5 time points, drugs were bath applied.

For slices in which we performed post-hoc immunostaining, an overview of the imaging region was made after the last time point (203 µm x 203 µm, ~50 z-steps of 1.0 µm step size), and a line scar was made using high intensity laser power at 910 nm at the edge of the zoomed out imaging area to facilitate alignment with post-hoc confocal microscopy.

Two-photon image analysis

Individual axons with at least 50 µm length were traced using the CellCounter plugin imbedded in Fiji for all time points (TPs). Individual boutons were identified with custom-built semi-automatic Matlab software, as described previously (Frias et al., 2019). In short, a 3D axonal intensity profile was reconstructed at each TP and individual boutons were selected based on a local threshold (0.5 standard deviation above mean axon intensity). Only boutons containing at least 5 pixels above threshold were included. All boutons at all time points were visually inspected and manual corrections were made if deemed necessary.

Persistent (P) boutons were defined as boutons which were present at all

TPs. Non-persistent (NP) boutons were absent at one or more TPs. Boutons which were present for only one time point were considered transport events and were excluded (Schuemann et al., 2013; Frias et al., 2019). Based on their presence or absence during baseline (first 5 TP) and after treatment, NP boutons were further classified into five subgroups (Frias et al., 2019; Ruiter et al., 2021): new boutons (only present after baseline), lost boutons (only present during baseline), stabilizing boutons (non-persistent during baseline, persistent after treatment), destabilizing boutons (persistent during baseline, non-persistent after treatment), intermittent boutons (non-persistent during baseline and after treatment).

Bouton density was calculated per axon as the average number of boutons at each TP divided by the 3D axon length. NP bouton density was determined for each TP as the number of NP boutons that were present divided by the 3D axon length. NP bouton densities were normalized to the average baseline value (first 5 TP) to allow comparison between axons. The maximum change in NP bouton density change was calculated as the maximum NP bouton density (average over 3TPs) divided by the baseline NP bouton density (average over TP2-4). NP presence was determined as the fraction of NP boutons that were present at each time point and these values were averaged for the first, second and third period of 5 TPs each. Changes in NP presence reflect changes in the density of NP bouton subgroups, as well as in bouton duration. However, differences in bouton duration (% of TPs present) of NP bouton subgroups were never observed in any of the conditions and we therefore only report NP bouton densities.

Immunocytochemistry and confocal microscopy

Fixation of the slices was performed in 4% paraformaldehyde (PFA) for 30 minutes at room temperature covered by aluminum foil. Following washing with phosphate-buffered saline (PBS; 3x 10 minutes), slices were permeabilized with 0.5% Triton X-100 (15 minutes), followed by PBS washing (3x 5 minutes), and 1 hour incubation in blocking solution (0.2% Triton X-100 and 10% goat serum). Application of primary antibodies in blocking solution was performed overnight at 4 °C. After PBS washing (3x 15 minutes), secondary antibodies were applied for 4 hours. After PBS washing (2x 15 minutes), slices were mounted in Vectashield solution.

We used the following primary antibodies: rabbit α-VGAT (Synaptic Systems, 131 003; 1:1000; RRID: AB 887869), mouse α-gephyrin (Synaptic Systems, 147 011; 1:1000; RRID: AB_887717), mouse α-CB1R (Synaptic Systems, 258 011; 1:1000; RRID: AB_2619969), rat α-HA (Roche, 11 867 423 001; 1:500; RRID: AB_390918), and the following secondary antibodies: anti-mouse Alex647

(Life Technologies, A21241, 1:500; RRID: AB_2535810) and anti-rabbit Alex405 (Life Technologies, A31556, 1:250; RRID: AB_221605) for VGAT and gephyrin staining, anti-mouse Alexa647 (Life Technologies, A21236, 1:500; RRID: AB_2535805) and anti-mouse Alexa568 (Life Technologies, A11031, 1:500; RRID: AB_144696) for CB1R staining, and anti-rat Alexa568 (Life Technologies, A11077, 1:500; RRID: AB_2534121) for HA staining.
Confocal imaging was performed using a Zeiss LSM-700 microscope system with a 63x oil-immersion objective. A 20x objective was used to find back the two-photon imaging area based on the line scar. Image size was 101.3 µm x 101.3 µm (1024 x 1024 pixels) with 0.3 µm z steps for synapse quantification, and up to 203 µm x 203 µm for post-hoc axon identification. Confocal images were analyzed in Fiji and corresponding axons in the confocal and two-photon images were identified using the line scar as a guide. Expression of CB1R or HA was determined by visual inspection. In some cases, the image was mirrored to confirm or reject positive staining. Negative axons were always chosen close to positive axons in the same imaging area, assuring that the absence of CB1R or HA expression was not due to low immunostaining quality. In addition, we verified that CB1R expression or staining levels did not affect our conclusion as we found the same results when we split CB1R+ axons in two separate groups with high and low CB1R levels. Per slice, 2-6 axons per group were included in the analysis.
For synapse quantification images were analyzed in Fiji using a custom macro (Ruiter et al., 2020). An average projection image was made from 5 z-planes, images were median filtered (1 pixel radius) and individual puncta were identified using watershed segmentation. VGAT and gephyrin puncta were analyzed separately and overlap was determined afterwards. Four independent experiments were performed with 1 or 2 image areas per slice. To compare between treatments, data were normalized per experiment.

AAV virus application in VGAT-Cre slices
Hippocampal slice cultures were prepared as described above from VGAT-Cre mice (JAX stock #028862) at 6-7 days after birth. Floxed AAV5 viruses to express GFP (ssAAV-5/2-hSyn1-dlox-EGFP(rev)-dlox-WPRE-hGHp(A), #v115-5, RRID: Addgene_50457; Viral Vector Facility, Zurich University) and HA-tagged G_s-DREADDs (pssAAV-2-hSyn1-dlox-HA_rM3D(Gs)_IRES_mCitrine(rev)-dlox-WPRE-hGHp(A), #v111-5, RRID: Addgene_50456; Viral Vector Facility, Zurich University) were applied at DIV1 on top of the hippocampal CA1 region by a microinjector (Eppendorf, FemtoJet) aided by a stereoscopic microscope (Leica, M80). This resulted in widespread, but sparse GFP and G_s-HA expression in GABAergic neurons, which partially

overlapped. Two-photon time lapse imaging was performed when slices were kept 2 to 3 weeks *in vitro*. After a baseline period (5 time points), G_s signaling was activated by bath application of 10 µM CNO (Tocris Bioscience), which was continued until the end of the experiment. P*ost hoc* immunostaining was performed using rat anti-HA primary antibodies (Roche, #11 867 423 001; 1:500; RRID: AB_390918) and anti-rat Alexa568 (Life Technologies, A11077, 1:500; RRID: AB_2534121) as secondary antibodies. We selected slices with good GFP labeling in the dendritic layer for the two-photon experiments and in 4 out of 13 slices we were able to identify up to 5 axons of each type within the imaging area. Identification of HA+ and HA- axons was performed in Fiji, bouton dynamics analysis in Matlab as described above.

Experimental Design and Statistical Analyses

All experiments were performed and analyzed blindly. Live imaging experiments for bouton dynamics analysis were performed in paired slices from the same animal and the same culture. Statistical analysis was performed using GraphPad Prism software. Data are reported as mean ± standard error unless stated otherwise. The variance between axons was larger than the variance between slices, indicating that individual axons are independent measurements. Results from treatment and control experiments were compared using the nonparametric Mann-Whitney U test (MW). Distributions were compared with Kolmogorov-Smirnov test (KS). Multiple comparisons were made using two-way ANOVA (2w ANOVA) followed by Sidak's test. Repeated two-way ANOVA analysis was used for comparing NP bouton density and NP presence over time. P-values (not adjusted for multiplicity) are indicated in the figure legends. Differences were considered significant when $p < 0.05$ ($^*p < 0.05$, $^{**}p < 0.01$, $^{***}p < 0.001$).

Acknowledgements:
This work was supported by a CSC scholarship (JL), by Alzheimer Nederland (MR; WE.03-2018-11) and by the Netherlands Organisation for Scientific Research (MSG; OCENW.KLEIN.150), and as part of the research program of the Foundation for Fundamental Research on Matter (FOM) (DLHK; #15PR3178; 16NEPH05). We thank Lotte Herstel for helping with experiments in Fig. 1E-F and René van Dorland for excellent technical support.

Author contributions:
JL, DLHK, CJW designed the experiments. JL, DLHK, MR, BJBV, ACJV, FB performed the experiments. JL, BJBV, ACJV, FB, MSG, MR analyzed the data. CJW wrote the manuscript with input from all other authors.

Conflict of Interest:
The authors declare no competing financial interests.

List of references

Alger BE (2002) Retrograde signaling in the regulation of synaptic transmission: Focus on endocannabinoids.

Alger BE, Kim J (2011) Supply and demand for endocannabinoids. Trends Neurosci 34:304–315 Available at: http://dx.doi.org/10.1016/j.tins.2011.03.003.

Antoni FA (2012) New paradigms in cAMP signalling. Mol Cell Endocrinol 353:3–9.

Araque A, Castillo PE, Manzoni OJ, Tonini R (2017) Synaptic functions of endocannabinoid signaling in health and disease. Neuropharmacology 124:13–24 Available at: http://dx.doi.org/10.1016/j.neuropharm.2017.06.017.

Argaw A, Duff G, Zabouri N, Cécyre B, Chainé N, Cherif H, Tea N, Lutz B, Ptito M, Bouchard JF (2011) Concerted action of CB1 cannabinoid receptor and deleted in colorectal cancer in axon guidance. J Neurosci 31:1489–1499.

Argyrousi EK, Heckman PRA, Prickaerts J (2020) Role of cyclic nucleotides and their downstream signaling cascades in memory function: Being at the right time at the right spot. Neurosci Biobehav Rev 113:12–38 Available at: https://doi.org/10.1016/j.neubiorev.2020.02.004.

Bacci A, Huguenard JR, Prince DA (2004) Long-lasting self-inhibition of neocortical interneurons mediated by endocannabinoids. Nature 431:1–5.

Bailey CH, Chen M (1989) Time course of structural changes at identified sensory neuron synapses during long-term sensitization in Aplysia. J Neurosci 9:1774–1780.

Bailey CH, Kandel ER (1993) Structural changes accompanying memory storage. Annu Rev Physiol 55:397–426 Available at: http://www.ncbi.nlm.nih.gov/pubmed/8466181 [Accessed January 24, 2013].

Baillie GS (2009) Compartmentalized signalling: Spatial regulation of cAMP by the action of compartmentalized phosphodiesterases. FEBS J 276:1790–1799 Available at: https://pubmed.ncbi.nlm.nih.gov/19243430/ [Accessed December 23, 2020].

Bednarek E, Caroni P (2011) B-Adducin Is Required for Stable Assembly of New Synapses and Improved Memory Upon Environmental Enrichment. Neuron 69:1132–1146 Available at: http://dx.doi.org/10.1016/j.neuron.2011.02.034.

Bekkers JM, Clements JD (1999) Quantal amplitude and quantal variance of strontium-induced asynchronous EPSCs in rat dentate granule neurons. J Physiol 516:227–248.

Berghuis P, Rajnicek AM, Morozov YM, Ross RA, Mulder J, Urban GM, Monory K, Marsicano G, Matteoli M, Canty A, Lrving AJ, Katona I, Yanagawa Y, Rakic P, Lutz B, Mackie K, Harkany T (2007) Hardwiring the Brain: Endocannabinoids Shape Neuronal Connectivity. Science (80-) 316:1212–1216.

Bernier L-P, Bohlen CJ, York EM, Choi HB, Kamyabi A, Dissing-Olesen L, Hefendehl JK, Collins HY, Stevens B, Barres BA, MacVicar BA (2019) Nanoscale Surveillance of the Brain by Microglia via cAMP-Regulated Filopodia. Cell Rep 27:2895–2908 Available at: https://linkinghub.elsevier.com/retrieve/pii/S2211124719306217.

Bonilla-Del Río I, Puente N, Mimenza A, Ramos A, Serrano M, Lekunberri L, Gerrikagoitia I, Christie BR, Nahirney PC, Grandes P (2021) Acute Δ9 -tetrahydrocannabinol prompts rapid changes in cannabinoid CB 1 receptor immunolabeling and subcellular structure in CA1 hippocampus of young adult male mice. J Comp Neurol:10.1002/cne.25098. Online ahead of print.

Bourne JN, Harris KM (2011) Coordination of size and number of excitatory and inhibitory synapses results in a balanced structural plasticity along mature hippocampal CA1 dendrites during LTP. Hippocampus 21:354–373 Available at: http://www.ncbi.nlm.nih.gov/pubmed/20101601 [Accessed May 21, 2013].

Caballero-Florán RN, Conde-Rojas I, Oviedo Chávez A, Cortes-Calleja H, Lopez-Santiago LF, Isom LL, Aceves J, Erlij D, Florán B (2016) Cannabinoid-induced depression of synaptic transmission is switched to stimulation when dopaminergic tone is increased in the globus pallidus of the rodent. Neuropharmacology 110:407–418 Available at: http://linkinghub.elsevier.com.sci-hub.cc/retrieve/pii/S0028390816303379.

Campbell AP, Smrcka A V (2018) Targeting G protein-coupled receptor signalling by blocking G proteins. Nat Rev Drug Discov 17:789–803.

Caroni P, Donato F, Muller D (2012) Structural plasticity upon learning: regulation and functions. Nat Rev Neurosci 13:478–490 Available at: http://dx.doi.org/10.1038/nrn3258.

Castillo PE, Younts TJ, Chávez AE, Hashimotodani Y (2012) Endocannabinoid signaling and synaptic

function. Neuron 76:70–81 Available at: http://www.ncbi.nlm.nih.gov/pubmed/23040807 [Accessed August 16, 2013].

Chen SX, Kim AN, Peters AJ, Komiyama T (2015) Subtype-specific plasticity of inhibitory circuits in motor cortex during motor learning. Nat Neurosci 18:1109–1115 Available at: http://www.nature.com/neuro/journal/v18/n8/full/nn.4049.html?WT.ec_id=NEURO-201508&spMailingID=49196618&spUserID=MTMyMDY4MzI3NDgzS0&spJobID=723694367&spReportId=NzIzNjk0MzY3S0%5Cnhttp://www.nature.com/neuro/journal/v18/n8/pdf/nn.4049.pdf.

Chenouard N, Xuan F, Tsien RW (2020) Synaptic vesicle traffic is supported by transient actin filaments and regulated by PKA and NO. Nat Commun 11.

Chevaleyre V, Castillo PE (2003) Heterosynaptic LTD of hippocampal GABAergic synapses: A novel role of endocannabinoids in regulating excitability. Neuron 38:461–472.

Chevaleyre V, Heifets BD, Kaeser PS, Südhof TC, Purpura DP, Castillo PE (2007) Endocannabinoid-Mediated Long-Term Plasticity Requires cAMP/PKA Signaling and RIM1α. Neuron 54:801–812.

Chia PH, Chen B, Li P, Rosen MK, Shen K (2014) Local F-actin network links synapse formation and axon branching. Cell 156:208–220 Available at: http://dx.doi.org/10.1016/j.cell.2013.12.009 [Accessed January 21, 2014].

Chia PH, Li P, Shen K (2013) Cellular and molecular mechanisms underlying presynapse formation. J Cell Biol 203:11–22 Available at: http://www.ncbi.nlm.nih.gov/pubmed/24127213 [Accessed January 28, 2014].

Chiu CQ, Barberis A, Higley MJ (2019) Preserving the balance: diverse forms of long-term GABAergic synaptic plasticity. Nat Rev Neurosci 20:272–281 Available at: http://dx.doi.org/10.1038/s41583-019-0141-5.

Cox DJ, Racca C, LeBeau FEN (2008) B-Adrenergic Receptors Are Differentially Expressed in Distinct Interneuron Subtypes in the Rat Hippocampus. J Comp Neurol 509:551–565.

Cui Y, Paille V, Xu H, Genet S, Delord B, Fino E, Berry H, Venance L (2015) Endocannabinoids mediate bidirectional striatal spike-timing-dependent plasticity. J Physiol 593:2833–2849 Available at: http://www.ncbi.nlm.nih.gov/pubmed/25873197.

Cui Y, Prokin I, Xu H, Delord B, Genet S, Venance L, Berry H (2016) Endocannabinoid dynamics gate spike- timing dependent depression and potentiation. Elife 5:1–32.

Danglot L, Triller A, Bessis A (2003) Association of gephyrin with synaptic and extrasynaptic GABAA receptors varies during development in cultured hippocampal neurons. Mol Cell Neurosci 23:264–278.

De Simoni A, Griesinger CB, Edwards FA (2003) Development of rat CA1 neurones in acute versus organotypic slices: role of experience in synaptic morphology and activity. J Physiol 550:135–147 Available at: http://www.ncbi.nlm.nih.gov/pubmed/12879864.

Dobie FA, Craig AM (2011) Inhibitory synapse dynamics: coordinated presynaptic and postsynaptic mobility and the major contribution of recycled vesicles to new synapse formation. J Neurosci 31:10481–10493 Available at: http://www.jneurosci.org/cgi/doi/10.1523/JNEUROSCI.6023-10.2011 [Accessed July 20, 2011].

Dócs K, Mészár Z, Gonda S, Kiss-Szikszai A, Holló K, Antal M, Hegyi Z (2017) The ratio of 2-AG to its isomer 1-AG as an intrinsic fine tuning mechanism of CB1 receptor activation. Front Cell Neurosci 11:1–13.

Donato F, Chowdhury A, Lahr M, Caroni P (2015) Early- and Late-Born Parvalbumin Basket Cell Subpopulations Exhibiting Distinct Regulation and Roles in Learning. Neuron 85:770–786 Available at: http://dx.doi.org/10.1016/j.neuron.2015.01.011.

Donato F, Rompani SB, Caroni P (2013) Parvalbumin-expressing basket-cell network plasticity induced by experience regulates adult learning. Nature 504:272–276 Available at: http://www.ncbi.nlm.nih.gov/pubmed/24336286 [Accessed January 9, 2014].

Dudok B et al. (2015) Cell-specific STORM super-resolution imaging reveals nanoscale organization of cannabinoid signaling. Nat Neurosci 18:75–86 Available at: http://www.ncbi.nlm.nih.gov/pubmed/25485758 [Accessed December 29, 2016].

Eldeeb K, Leone-kabler S, Howlett AC (2016) CB1 cannabinoid receptor-mediated increases in cyclic AMP accumulation are correlated with reduced Gi/o function. J Basic Clin Physiol Pharmacol 27:311–322.

Fernandes HB, Riordan S, Nomura T, Remmers CL, Kraniotis S, Marshall JJ, Kukreja L, Vassar R, Contractor A (2015) Epac2 mediates cAMP-dependent potentiation of neurotransmission in the hippocampus. J Neurosci 35:6544–6553.

Finlay DB, Cawston EE, Grimsey NL, Hunter MR, Korde A, Vemuri VK, Makriyannis A, Glass M (2017) Gαs signalling of the CB1 receptor and the influence of receptor number. Br J Pharmacol 174:2545–2562.

Flores-Otero J, Ahn KH, Delgado-Peraza F, Mackie K, Kendall DA, Yudowski GA (2014) Ligand-specific endocytic dwell times control functional selectivity of the cannabinoid receptor 1. Nat Commun 5:1–11 Available at: http://www.nature.com/doifinder/10.1038/ncomms5589.

Flores CE, Méndez P (2014) Shaping inhibition: activity dependent structural plasticity of GABAergic synapses. Front Cell Neurosci 8:1–13 Available at: http://journal.frontiersin.org/journal/10.3389/fncel.2014.00327/full [Accessed November 5, 2014].

Frias CP, Liang J, Bresser T, Scheefhals L, van Kesteren M, Dorland R van, Hu HY, Bodzeta A, Van Bergen en Henegouwen PMP, Hoogenraad CC, Wierenga CJ (2019) Semaphorin4D induces inhibitory synapse formation by rapid stabilization of presynaptic boutons via MET co-activation. J Neurosci 39:4221–4237 Available at: https://www.biorxiv.org/content/early/2018/02/22/100271.

Gekel I, Neher E (2008) Application of an Epac activator enhances neurotransmitter release at excitatory central synapses. J Neurosci 28:7991–8002.

Glass M, Felder CC (1997) Concurrent stimulation of cannabinoid CB1 and dopamine D2 receptors augments cAMP accumulation in striatal neurons: evidence for a Gs linkage to the CB1 receptor. J Neurosci 17:5327–5333 Available at: http://www.jneurosci.org/content/17/14/5327.short%5Cnpapers3://publication/uuid/B88F3EC1-F7CD-48E4-B2ED-E2A4D9FA0546.

Gonzalez-Burgos G, Miyamae T, Pafundo DE, Yoshino H, Rotaru DC, Hoftman G, Datta D, Zhang Y, Hammond M, Sampson AR, Fish KN, Ermentrout GB, Lewis DA (2015) Functional maturation of GABA synapses during postnatal development of the monkey dorsolateral prefrontal cortex. Cereb Cortex 25:4076–4093.

Guggenhuber S, Alpar A, Chen R, Schmitz N, Wickert M, Mattheus T, Harasta AE, Purrio M, Kaiser N, Elphick MR, Monory K, Kilb W, Luhmann HJ, Harkany T, Lutz B, Klugmann M (2016) Cannabinoid receptor-interacting protein Crip1a modulates CB1 receptor signaling in mouse hippocampus. Brain Struct Funct 221:2061–2074 Available at: http://dx.doi.org/10.1007/s00429-015-1027-6.

Guo J, Ikeda SR (2004) Endocannabinoids modulate N-type calcium channels and G-protein-coupled inwardly rectifying potassium channels via CB1 cannabinoid receptors heterologously expressed in mammalian neurons. Mol Pharmacol 65:665–674.

Hashimotodani Y, Ohno-shosaku T, Kano M (2007) Ca2+-assisted receptor-driven endocannabinoid release: mechanisms that associate presynaptic and postsynaptic activities. Curr Opin Neurobiol 17:360–365.

Hashimotodani Y, Ohno-Shosaku T, Tanimura A, Kita Y, Sano Y, Shimizu T, Di Marzo V, Kano M (2013) Acute inhibition of diacylglycerol lipase blocks endocannabinoid-mediated retrograde signalling: Evidence for on-demand biosynthesis of 2-arachidonoylglycerol. J Physiol 591:4765–4776.

Hattori R, Kuchibhotla K V., Froemke RC, Komiyama T (2017) Functions and dysfunctions of neocortical inhibitory neuron subtypes. Nat Neurosci 20:1199–1208.

Hebert-Chatelain E et al. (2016) A cannabinoid link between mitochondria and memory. Nature 539:555–559.

Helboe L, Egebjerg J, de Jong IEM (2015) Distribution of serotonin receptor 5-HT6 mRNA in rat neuronal subpopulations: A double in situ hybridization study. Neuroscience 310:442–454 Available at: http://dx.doi.org/10.1016/j.neuroscience.2015.09.064.

Herstel LJ, Wierenga CJ (2021) Network control through coordinated inhibition. Curr Opin Neurobiol 67:34–41.

Hofer SB, Mrsic-Flogel TD, Bonhoeffer T, Hübener M (2009) Experience leaves a lasting structural trace in cortical circuits. Nature 457:313–317 Available at: http://www.ncbi.nlm.nih.gov/pubmed/19005470 [Accessed November 13, 2012].

Hu HY, Kruijssen DL, Frias CP, Rózsa B, Hoogenraad CC, Wierenga CJ (2019) Endocannabinoid signaling mediates local dendritic coordination between excitatory and inhibitory synapses. Cell Rep 27:666–675.

Ibsen MS, Connor M, Glass M (2017) Cannabinoid CB 1 and CB 2 Receptor Signaling and Bias . Cannabis Cannabinoid Res 2:48–60 Available at: https://pubmed.ncbi.nlm.nih.gov/28861504/ [Accessed December 23, 2020].

Jiang X, Sando R, Südhof TC (2021) Multiple signaling pathways are essential for synapse formation induced by synaptic adhesion molecules. Proc Natl Acad Sci U S A 118.

Jullié D, Stoeber M, Sibarita J, Zieger HL, Bartol TM, Arttamangkul S, Sejnowski TJ, Hosy E, von Zastrow

M (2020) A Discrete Presynaptic Vesicle Cycle for Neuromodulator Receptors. Neuron 105:1–15.
Kano M, Ohno-Shosaku T, Hashimotodani Y, Watanabe MUM (2009) Endocannabinoid-mediated control of synaptic transmission. Physiol Rev 89:309–380 Available at: http://physrev.physiology.org/content/89/1/309.short.
Katona I, Freund TF (2012) Multiple functions of endocannabinoid signaling in the brain. Annu Rev Neurosci 35:529–558 Available at: http://www.annualreviews.org/doi/10.1146/annurev-neuro-062111-150420.
Katona I, Sperlágh B, Sík A, Käfalvi A, Vizi ES, Mackie K, Freund TF (1999) Presynaptically located CB1 cannabinoid receptors regulate GABA release from axon terminals of specific hippocampal interneurons. J Neurosci 19:4544–4558.
Katona I, Urban GM, Wallace M, Ledent C, Jung K-M, Piomelli D, Mackie K, Freund TF (2006) Molecular Composition of the Endocannabinoid System at Glutamatergic Synapses. J Neurosci 26:5628–5637 Available at: http://www.jneurosci.org/cgi/doi/10.1523/JNEUROSCI.0309-06.2006.
Kawasaki H, Springett GM, Mochizuki N, Toki S, Nakaya M, Matsuda M, Housman DE, Graybiel AM (1998) A family of cAMP-binding proteins that directly activate Rap1. Science (80-) 282:2275–2279.
Keck T, Scheuss V, Jacobsen RI, Wierenga CJ, Eysel UT, Bonhoeffer T, Hübener M (2011) Loss of sensory input causes rapid structural changes of inhibitory neurons in adult mouse visual cortex. Neuron 71:869–882 Available at: http://linkinghub.elsevier.com/retrieve/pii/S0896627311005642 [Accessed September 9, 2011].
Kirchner JH, Gjorgjieva J (2019) A unifying framework for synaptic organization on cortical dendrites. bioRxiv.
Kleindienst T, Winnubst J, Roth-alpermann C, Bonhoeffer T, Lohmann C (2011) Activity-Dependent Clustering of Functional Synaptic Inputs on Developing Hippocampal Dendrites. Neuron 72:1012–1024.
Knott GW, Quairiaux C, Genoud C, Welker E (2002) Formation of dendritic spines with GABAergic synapses induced by whisker stimulation in adult mice. Neuron 34:265–273 Available at: http://www.ncbi.nlm.nih.gov/pubmed/11970868.
Koon AC, Ashley J, Barria R, Dasgupta S, Brain R, Waddell S, Alkema MJ (2011) Autoregulatory and paracrine control of synaptic and behavioral plasticity by octopaminergic signaling. Nat Neurosci 14:190–199.
Kozorovitskiy Y, Saunders A, Johnson CA, Lowell BB, Sabatini BL (2012) Recurrent network activity drives striatal synaptogenesis. Nature 485:646–650 Available at: http://dx.doi.org/10.1038/nature11052 [Accessed July 15, 2012].
Laprairie RB, Bagher AM, Denovan-Wright EM (2017) Cannabinoid receptor ligand bias: implications in the central nervous system. Curr Opin Pharmacol 32:32–43 Available at: https://pubmed.ncbi.nlm.nih.gov/27835801/ [Accessed December 23, 2020].
Lauckner JE, Hille B, Mackie K (2005) The cannabinoid agonist WIN55,212-2 increases intracellular calcium via CB1 receptor coupling to Gq/11 G proteins. Proc Natl Acad Sci U S A 102:19144–19149.
Lazarus MS, Josh Huang Z (2011) Distinct maturation profiles of perisomatic and dendritic targeting GABAergic interneurons in the mouse primary visual cortex during the critical period of ocular dominance plasticity. J Neurophysiol 106:775–787.
Lee SH, Ledri M, Tóth B, Marchionni I, Henstridge CM, Dudok B, Kenesei K, Barna L, Szabó SI, Renkecz T, Oberoi M, Watanabe M, Limoli CL, Horvai G, Soltesz I, Katona I (2015) Multiple forms of endocannabinoid and endovanilloid signaling regulate the tonic control of GABA release. J Neurosci 35:10039–10057.
Lee SS-H, Földy C, Soltesz I (2010) Distinct Endocannabinoid Control of GABA Release at Perisomatic and Dendritic Synapses in the Hippocampus. J Neurosci 30:7993–8000 Available at: http://www.jneurosci.org/cgi/doi/10.1523/JNEUROSCI.6238-09.2010.
Lenkey N, Kirizs T, Holderith N, Mláte Z, Szabó G, Vizi ES, Hájos N, Nusser Z (2015) Tonic endocannabinoid-mediated modulation of GABA release is independent of the CB1 content of axon terminals. Nat Commun 6:6557.
Lewis DA, Hashimoto T, Volk DW (2005) Cortical inhibitory neurons and schizophrenia. Nat Rev Neurosci 6:312–324 Available at: http://www.ncbi.nlm.nih.gov/pubmed/15803162.
López-Bendito G, Sturgess K, Erdélyi F, Szabó G, Molnár Z, Paulsen O (2004) Preferential origin and layer destination of GAD65-GFP cortical interneurons. Cereb Cortex 14:1122–1133 Available at:

http://www.ncbi.nlm.nih.gov/pubmed/15115742.
Lovinger DM (2008) Presynaptic modulation by endocannabinoids. Handb Exp Pharmacol 184:435–477.
Maffei A, Charrier C, Caiati MD, Barberis A, Mahadevan V, Woodin MA, Tyagarajan SK (2017) Emerging mechanisms underlying dynamics of GABAergic synapses. J Neurosci 37:10792–10799.
Maiellaro I, Lohse MJ, Kittel RJ, Calebiro D (2016) cAMP Signals in Drosophila Motor Neurons Are Confined to Single Synaptic Boutons. Cell Rep 17:1238–1246 Available at: http://dx.doi.org/10.1016/j.celrep.2016.09.090.
Maroso M, Szabo GG, Kim HK, Alexander A, Bui AD, Lee SH, Lutz B, Soltesz I (2016) Cannabinoid Control of Learning and Memory through HCN Channels. Neuron 89:1059–1073 Available at: http://dx.doi.org/10.1016/j.neuron.2016.01.023.
Marti-Solano M, Crilly SE, Malinverni D, Munk C, Harris M, Pearce A, Quon T, Mackenzie AE, Wang X, Peng J, Tobin AB, Ladds G, Milligan G, Gloriam DE, Puthenveedu MA, Babu MM (2020) Combinatorial expression of GPCR isoforms affects signalling and drug responses. Nature 587:650–656 Available at: http://dx.doi.org/10.1038/s41586-020-2888-2.
Martín R, García-Font N, Suárez-Pinilla AS, Bartolomé-Martín D, Ferrero JJ, Luján R, Torres M, Sánchez-Prieto J (2020) β-adrenergic receptors/epac signaling increases the size of the readily releasable pool of synaptic vesicles required for parallel fiber LTP. J Neurosci 40:8604–8617.
Mikasova L, Groc L, Choquet D, Manzoni OJ (2008) Altered surface trafficking of presynaptic cannabinoid type 1 receptor in and out synaptic terminals parallels receptor desensitization. Proc Natl Acad Sci U S A 105:18596–18601.
Mitoma H, Konishi S (1996) Long-lasting facilitation of inhibitory transmission by monoaminergic and cAMP-dependent mechanism in rat cerebellar GABAergic synapses. Neurosci Lett 217:141–144.
Monday H, Bourdenx M, Jordan B, Castillo P (2020) CB 1 receptor-mediated inhibitory LTD triggers presynaptic remodeling via protein synthesis and ubiquitination. Elife 9:e54812.
Monday HR, Castillo PE (2017) Closing the gap: long-term presynaptic plasticity in brain function and disease. Curr Opin Neurobiol 45:106–112 Available at: http://www.sciencedirect.com/science/article/pii/S0959438816301878.
Mullins C, Fishell G, Tsien RW (2016) Unifying Views of Autism Spectrum Disorders: A Consideration of Autoregulatory Feedback Loops. Neuron 89:1131–1156 Available at: http://dx.doi.org/10.1016/j.neuron.2016.02.017.
Navarrete M, Díez A, Araque A (2014) Astrocytes in endocannabinoid signalling. Philos Trans R Soc B Biol Sci 369.
Nazif FA, Byrne JH, Cleary LJ (1991) cAMP induces long-term morphological changes in sensory neurons of Aplysia. Brain Res 539:324–327.
Nguyen QA, Horn ME, Nicoll RA (2016) Distinct roles for extracellular and intracellular domains in neuroligin function at inhibitory synapses. Elife 5:e19236.
Niculescu D, Michaelsen-Preusse K, Güner Ü, van Dorland R, Wierenga CJ, Lohmann C (2018) A BDNF-Mediated Push-Pull Plasticity Mechanism for Synaptic Clustering. Cell Rep 24:2063–2074.
Nishiyama J, Yasuda R (2015) Biochemical Computation for Spine Structural Plasticity. Neuron 87:63–75 Available at: http://dx.doi.org/10.1016/j.neuron.2015.05.043.
Niwa F, Bannai H, Arizono M, Fukatsu K, Triller A, Mikoshiba K (2012) Gephyrin-independent GABA(A)R mobility and clustering during plasticity. PLoS One 7:e36148 Available at: http://www.pubmedcentral.nih.gov/articlerender.fcgi?artid=3338568&tool=pmcentrez&rendertype=abstract [Accessed March 28, 2013].
Njoo C, Agarwal N, Lutz B, Kuner R (2015) The Cannabinoid Receptor CB1 Interacts with the WAVE1 Complex and Plays a Role in Actin Dynamics and Structural Plasticity in Neurons. PLoS Biol 13:e1002286 Available at: http://dx.doi.org/10.1371/journal.pbio.1002286.
Nogueras-Ortiz C, Yudowski GA (2016) The multiple waves of cannabinoid 1 receptor signaling. Mol Pharmacol 90:620–626 Available at: http://molpharm.aspetjournals.org/cgi/doi/10.1124/mol.116.104539.
Oh WC, Lutzu S, Castillo PE, Kwon H (2016) De novo synaptogenesis induced by GABA in the developing mouse cortex. Science (80-) 353:1037–1040.
Pardo GVE, Lucion AB, Calcagnotto ME (2018) Postnatal development of inhibitory synaptic transmission in the anterior piriform cortex. Int J Dev Neurosci 71:1–9.
Patrizi A, Scelfo B, Viltono L, Briatore F, Fukaya M, Watanabe M, Strata P, Varoqueaux F, Brose N, Fritschy J, Sassoè-Pognetto M, Sassoe M (2008) Synapse formation and clustering of neuroligin-2 in the

absence of GABAA receptors. Proc Natl Acad Sci U S A 105:13151–13156 Available at: http://www.ncbi.nlm.nih.gov/pubmed/18723687.

Patzke C, Brockmann MM, Dai J, Gan KJ, Grauel MK, Fenske P, Liu Y, Acuna C, Rosenmund C, Südhof TC (2019) Neuromodulator Signaling Bidirectionally Controls Vesicle Numbers in Human Synapses. Cell 179:498–513 Available at: http://www.ncbi.nlm.nih.gov/pubmed/31585084.

Pielage J, Bulat V, Zuchero JB, Fetter RD, Davis GW (2011) Hts/adducin controls synaptic elaboration and elimination. Neuron 69:1114–1131 Available at: http://www.ncbi.nlm.nih.gov/pubmed/21435557 [Accessed March 27, 2011].

Piomelli D (2014) More surprises lying ahead. The endocannabinoids keep us guessing. Neuropharmacology 76:228–234 Available at: http://dx.doi.org/10.1016/j.neuropharm.2013.07.026.

Puighermanal E, Cutando L, Boubaker-Vitre J, Honoré E, Longueville S, Hervé D, Valjent E (2017) Anatomical and molecular characterization of dopamine D1 receptor-expressing neurons of the mouse CA1 dorsal hippocampus. Brain Struct Funct 222:1897–1911.

Rall W (1967) Distinguishing theoretical synaptic potentials computed for different soma-dendritic distributions of synaptic input. J Neurophysiol 30:1138–1168.

Roland AB, Ricobaraza A, Carrel D, Jordan BM, Rico F, Simon A, Humbert-Claude M, Ferrier J, McFadden MH, Scheuring S, Lenkei Z (2014) Cannabinoid-induced actomyosin contractility shapes neuronal morphology and growth. Elife 3:e03159.

Roth BL (2016) DREADDs for Neuroscientists. Neuron 89:683–694 Available at: http://dx.doi.org/10.1016/j.neuron.2016.01.040.

Ruediger S, Vittori C, Bednarek E, Genoud C, Strata P, Sacchetti B, Caroni P (2011) Learning-related feedforward inhibitory connectivity growth required for memory precision. Nature 473:514–518 Available at: http://www.nature.com/doifinder/10.1038/nature09946 [Accessed May 2, 2011].

Ruiter M, Herstel LJ, Wierenga CJ (2020) Reduction of dendritic inhibition in CA1 pyramidal neurons in amyloidosis models of early Alzheimer's disease. J Alzheimer's Dis 78:951–964.

Ruiter M, Lützkendorf C, Liang J, Wierenga CJ (2021) Amyloid-β Oligomers Induce Only Mild Changes to Inhibitory Bouton Dynamics. J Alzheimer's Dis Reports:in press.

Savinainen JR, Saario SM, Laitinen JT (2012) The serine hydrolases MAGL, ABHD6 and ABHD12 as guardians of 2-arachidonoylglycerol signalling through cannabinoid receptors. Acta Physiol 204:267–276.

Scholl B, Thomas CI, Ryan MA, Kamasawa N, Fitzpatrick D (2020) Cortical neuron response selectivity derives from strength in numbers of synapses. Nature Available at: http://dx.doi.org/10.1038/s41586-020-03044-3.

Schuemann A, Klawiter A, Bonhoeffer T, Wierenga CJ (2013) Structural plasticity of GABAergic axons is regulated by network activity and GABAA receptor activation. Front Neural Circuits 7:1–16 Available at: http://journal.frontiersin.org/article/10.3389/fncir.2013.00113/abstract.

Sholler DJ, Huestis MA, Amendolara B, Vandrey R, Cooper ZD (2020) Therapeutic potential and safety considerations for the clinical use of synthetic cannabinoids. Pharmacol Biochem Behav 199 Available at: https://pubmed.ncbi.nlm.nih.gov/33086126/ [Accessed December 23, 2020].

Szabó GG, Lenkey N, Holderith N, Andrási T, Nusser Z, Hájos N (2014) Presynaptic calcium channel inhibition underlies CB1 cannabinoid receptor-mediated suppression of GABA release. J Neurosci 34:7958–7963.

Tang X, Jaenisch R, Sur M (2021) The role of GABAergic signalling in neurodevelopmental disorders. Nat Rev Neurosci 3:in press.

Taylor SS, Zhang P, Steichen JM, Keshwani MM, Kornev AP (2013) PKA: Lessons learned after twenty years. Biochim Biophys Acta - Proteins Proteomics 1834:1271–1278.

Tillo SE, Xiong WH, Takahashi M, Miao S, Andrade AL, Fortin DA, Yang G, Qin M, Smoody BF, Stork PJS, Zhong H (2017) Liberated PKA Catalytic Subunits Associate with the Membrane via Myristoylation to Preferentially Phosphorylate Membrane Substrates. Cell Rep 19:617–629 Available at: http://dx.doi.org/10.1016/j.celrep.2017.03.070.

Upreti C, Konstantinov E, Kassabov SR, Bailey CH, Kandel ER (2019) Serotonin Induces Structural Plasticity of Both Extrinsic Modulating and Intrinsic Mediating Circuits In Vitro in Aplysia Californica. Cell Rep 28:2955-2965.e3.

Urban DJ, Roth BL (2015) DREADDs (Designer Receptors Exclusively Activated by Designer Drugs): Chemogenetic Tools with Therapeutic Utility. Annu Rev Pharmacol Toxicol 55:399–417 Available

at: http://www.annualreviews.org/doi/10.1146/annurev-pharmtox-010814-124803.
Villa KL, Berry KP, Subramanian J, Cha JW, Oh WC, Kwon H-B, Kubota Y, So PTC, Nedivi E (2016) Inhibitory synapses are repeatedly assembled and removed at persistent sites in vivo. Neuron 89:756–769 Available at: http://linkinghub.elsevier.com/retrieve/pii/S0896627316000118.
Wang W, Jia Y, Pham DT, Palmer LC, Jung K-M, Cox CD, Rumbaugh G, Piomelli D, Gall CM, Lynch G (2017) Atypical endocannabinoid signaling initiates a new form of memory-related plasticity at a cortical input to hippocampus. Cereb Cortex:1–14 Available at: https://academic.oup.com/cercor/article-lookup/doi/10.1093/cercor/bhx126.
Wierenga CJ (2017) Live imaging of inhibitory axons: Synapse formation as a dynamic trial-and-error process. Brain Res Bull 129:43–49 Available at: http://dx.doi.org/10.1016/j.brainresbull.2016.09.018.
Wierenga CJ, Becker N, Bonhoeffer T (2008) GABAergic synapses are formed without the involvement of dendritic protrusions. Nat Neurosci 11:1044–1052 Available at: http://www.ncbi.nlm.nih.gov/pubmed/18711391.
Wierenga CJ, Müllner FE, Rinke I, Keck T, Stein V, Bonhoeffer T (2010) Molecular and electrophysiological characterization of GFP-expressing CA1 interneurons in GAD65-GFP mice. PLoS One 5:e15915 Available at: http://www.pubmedcentral.nih.gov/articlerender.fcgi?artid=3013138&tool=pmcentrez&rendertype=abstract [Accessed March 10, 2012].
Wierenga CJ, Wadman WJ (1999) Miniature inhibitory postsynaptic currents in CA1 pyramidal neurons after kindling epileptogenesis. J Neurophysiol 82:1352–1362 Available at: http://www.ncbi.nlm.nih.gov/pubmed/10482754.
Yoshida T, Mishina M (2005) Distinct roles of calcineurin-nuclear factor of activated T cells and protein kinase A - cAMP response element-binding protein signaling in presynaptic differentiation. J Neurosci 25:3067–3079.
Yu W, Jiang M, Miralles CP, Li R-W, Chen G, de Blas AL (2007) Gephyrin clustering is required for the stability of GABAergic synapses. Mol Cell Neurosci 36:484–500 Available at: http://www.pubmedcentral.nih.gov/articlerender.fcgi?artid=2464357&tool=pmcentrez&rendertype=abstract [Accessed January 23, 2013].
Zhong Y, Budnik V, Wu CF (1992) Synaptic plasticity in Drosophila memory and hyperexcitable mutants: Role of cAMP cascade. J Neurosci 12:644–651.
Zhou R, Han B, Xia C, Zhuang X (2019) Membrane-associated periodic skeleton is a signaling platform for RTK transactivation in neurons. Science (80-) 365:929–934 Available at: http://www.ncbi.nlm.nih.gov/pubmed/31467223.

Chapter 4

Agonist-induced changes in CB1 receptor distribution

Authors: Jian Liang, Bas JB Voesenek, Corette J Wierenga

Affiliation: Cell Biology, Neurobiology and Biophysics, Department of Biology, Faculty of Science, Utrecht University, 3584 CH Utrecht, the Netherlands

Corresponding author: Corette J. Wierenga

Abstract

Endocannabinoid type 1 (CB1) receptor is the most abundant G-protein coupled receptor in the brain. It is widely expressed in multiple regions of central nervous system and peripheral nervous system. Activation of CB1 receptors with endogenous or exogenous agonists induces receptor internalization and desensitization. Internalized CB1 receptors are located at endosomes, where they are sorted into lysosomes or recycled back to the plasma membrane. Newly synthesized CB1R are anterogradely transported from the soma to axonal terminals, but the regulation mechanism of CB1 receptor internalization and trafficking after activation remains unclear. In addition, agonist-induced bias signals are common for many GPCRs, including CB1 receptors. For instance, CB1 receptors have different dwell times at plasm membrane upon activation with endogenous cannabinoid 2-AG or with chemical agonist WIN 55212-2 (WIN) and distinct downstream effectors will be activated. However, it is unclear if biased signals affect receptor trafficking and distribution of CB1 receptors. Here we investigated CB1 receptor internalization in hippocampal slice cultures and primary cultures. We found that the synthetic agonist WIN induced CB1 receptor internalization and retrograde translocation of internalized CB1 receptors into the soma, while endogenous cannabinoid 2-AG resulted in recycling of internalized CB1 receptors back to the membrane. Furthermore, we found that WIN-induced CB1 receptor internalization and translocation was promoted by neuronal activity and G protein signals. Interestingly, the difference in CB1 receptor internalization between WIN and 2-AG was absent in cultured primary neurons. This demonstrates that CB1 receptor internalization or trafficking is a highly regulated process.

Introduction

Endocannabinoids in the central nerve system are widely distributed neuromodulators involved in brain development, synaptic plasticity, stress and learning (Tsou et al., 1998; Kano et al., 2009; Castillo et al., 2012). Most of these effects are mediated through cannabinoid receptor type 1 (CB1). CB1 receptors are G protein coupled receptors (GPCRs) and belong to the class A GPCRs. Heterotrimeric G proteins contain three subunits: α, β and γ. Activated CB1 receptors promote switching of the Gα subunits from the inactive guanosine diphosphate (GDP) state to the active guanosine triphosphate (GTP) state. Active Gα dissociates from the heteromeric G protein complex and can interact with multiple downstream effectors, including enzymes and ion channels. Typically, CB1 receptors are coupled to $G\alpha_{i/o}$ proteins (Howlett et al., 2002; Busquets-Garcia et al., 2018). Activated $G\alpha_{i/o}$ inhibits adenylyl cyclase (AC), the enzyme that converts ATP into cyclic adenosine monophosphate (cAMP). Activation of presynaptic CB1 receptors therefore typically results in a reduction of cellular cAMP levels, which reduces neurotransmitter release via a decrease in RIM phosphorylation by cAMP-dependent protein kinase A (PKA) (Chevaleyre et al., 2007). In parallel, the released Gβγ subunits directly inhibit voltage-dependent calcium channels (VGCC) and/or activate inward-rectifying K^+ channels, also resulting in short-term synaptic depression (Kano et al., 2009). There is accumulating evidence that activated CB1 receptors also interact with other downstream effectors mediating alternative signal transduction pathways, via other G-protein dependent effectors like $G\alpha_s$, G_q, $G_{12/13}$ (Lauckner et al., 2005; Roland et al., 2014; Cui et al., 2016; Finlay et al., 2017; Wang et al., 2017) as well as G protein independent effectors like β-arrestin (Nguyen et al., 2012; Delgado-Peraza et al., 2016).

The diversity of downstream signaling after CB1 receptor activation may result from functional selectivity induced by different agonists (Hua et al., 2016; Laprairie et al., 2017). CB1 receptors in the brain are activated by two major endogenous cannabinoids, 2-AG and AEA. In addition, there are many chemical synthetic agonists, including CP55 940 and WIN 55212-2 (WIN). WIN is widely used in endocannabinoid research because of its high affinity of CB1 receptors and high stability in biological conditions (Compton et al., 1992). Binding with different agonists can induce specific conformational changes of the CB1 receptor (Laprairie et al., 2014; Shao et al., 2016), resulting in the recruitment of different downstream effectors. For instance, it has been reported that CB1 receptor activation by WIN or 2-AG results in

a different dwell time at the membrane, which may result from different receptor conformations, and this biases downstream signaling (Flores-Otero et al., 2014; Delgado-Peraza et al., 2016).

CB1 receptors are not uniformly distributed in the central nervous system (Tsou et al., 1998). They are highly expressed at inhibitory neurons, where their distribution is polarized towards axonal shaft and terminals. Newly synthesized CB1 receptors undergo protein quality control through cis- and trans-Golgi modifications before they are inserted into to the plasma membrane (Leterrier et al., 2006). The axonal polarization of CB1 receptors is established through biased delivery via anterograde transport to the axon and continuous internalization of CB1 receptors at the somatodendritic region (Leterrier et al., 2006; Fletcher-Jones et al., 2019). The c-terminal of CB1 receptors contains a H9 domain, which plays an important role for maintaining polarity of the CB1 receptor distribution (Fletcher-Jones et al., 2019). Internalization and desensitization of activated CB1 receptors is regulated via interactions with GPCR kinases (GRKs) and β-arrestins (Jin et al., 1999; Kouznetsova et al., 2002). Internalized CB1 receptors are sorted into endosomes, and then they either recycle back to the membrane to continue signal transduction or traffic into lysosomes to be degraded. The distribution pattern of CB1 receptors can be regulated by receptor activity (Leterrier et al., 2006; Simon et al., 2013), also the precise mechanisms remain unresolved (Fletcher-Jones et al., 2020).

Here, we analyzed the CB1 receptor distribution in hippocampal slice cultures. We find that some CB1 receptors get localized to the somata of GABAergic cells after the acute WIN application that we used in our two photon live imaging experiments, while their localization remained strictly axonal in control slices. Blocking $G\alpha_{i/o}$ activity or reducing neuronal activity also increased CB1 receptor localization to GABAergic somata, and WIN enhanced this effect. This suggests that G protein activity and neuronal activated promote CB1 receptor internalization and/or retrograde transport after WIN activation. In addition, longer and repeated treatment with WIN further reduced CB1 receptor expression levels and enhanced retrograde trafficking. However, endogenous agonist 2-AG had no effect, suggesting functional selectivity of CB1 receptor signaling. Interestingly, CB1 receptor expression patterns are different at organotypic hippocampal slices and cultured dissociated neurons. WIN failed to induce CB1 receptor internalization and trafficking in cultured dissociated neurons. This suggests that the axonal distribution of CB1 receptor is largely dependent on intact

neuronal networks, and that functional selectivity determined the agonist-induced redistribution of CB1 receptors.

Results

CB1 receptor location in somata after short WIN treatment and activity block

As described in chapter 3, we performed *post-hoc* immunostaining of CB1 receptors in the slices that were used for the two-photon time lapse imaging. These slices were treated for 5 minutes (bath application) with 20 µM WIN or 0.1% DMSO control, followed by 1.5 hr imaging. We could clearly distinguish CB1- and CB1+ axons with similar certainty in control and WIN-treated slices, but we did notice a subtle difference in CB1 expression pattern between WIN-treated and control slices. In the hippocampus, C1B receptors are typically located at axonal shafts and in presynaptic terminals of GABAergic interneurons (Katona et al., 1999; Dudok et al., 2015). In agreement with the literature, we observed only a few CB1+ somata in control slices. However, we noticed that the number of CB1+ somata were significantly increased in WIN-treated slices (Fig. 1B). A substantial fraction of CB1R+ somata were also positive for GFP, indicating that they were GABAergic cells (Fig. 1A). We assume that also GFP- somata with CB1R+ staining were GABAergic cells, as they were located mostly outside of the pyramidal layer. We verified that the number of GFP+ cells were similar in the images taken from control and WIN-treated slices (Fig. 1C). These data suggest that activated CB1 receptors are partially internalized and translocated into the cell body, which agrees well with previous reports from literature (Coutts et al., 2001; Grimsey et al., 2010; Thibault et al., 2013).

We also analyzed the density of CB1+ somata in slices that were treated with PTX, a G_i protein blocker, or TTX, a sodium channel blocker which inhibits neuronal activity in the slice (see chapter 3). Interestingly, we found that the number of CB1 positive somata were slightly increased under PTX pretreatment and TTX conditions, and that CB1 activation by WIN did not result in a further increase (Fig. 1B). This suggests that G protein activity and neuronal activity play an important role in endocytosis and/or intracellular transport of CB1 receptors.

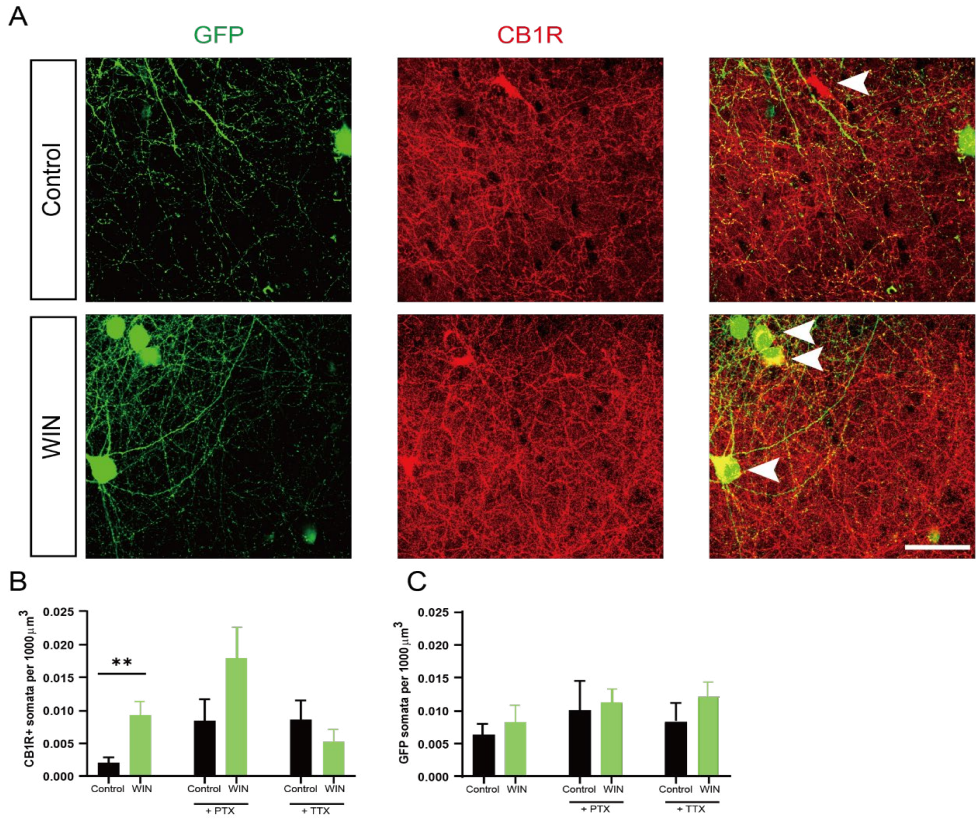

Figure 1. WIN induced CB1R accumulation at somata during acute treatment.
(A) Representative images of CB1R *post hoc* immunostaining (middle, red) after 5 minutes of DMSO (control) or WIN application in hippocampal slices. Arrows indicate CB1R+ somata. Scale bar 50µm
(B) Density of CB1R+ somata in slices treated for 5 minutes with DMSO or WIN. Shown are data from slices in normal ACSF, slices which were 24hr pretreated with PTX and slices which were in ACSF containing TTX. MW tests: $p = 0.0043$ for ACSF comparison; $p = 0.2$ for PTX comparison; $p = 0.8$ for TTX comparison. One-way ANOVA with Dunnett's test, $p = 0.14$ comparison for control and control with PTX; $p = 0.097$ comparison for control and control with TTX and $p = 0.14$ comparison between WIN and WIN with PTX; $p = 0.66$ comparison between WIN and WIN with TTX.
(C) Density of GFP somata in slices treated for 5 minutes with DMSO or WIN. Shown are data from slices in normal ACSF, slices which were 24hr pretreated with PTX and slices which were in ACSF containing TTX. MW tests: $p = 0.66$ for ACSF comparison; $p = 0.2$ for ACSF comparison; $p = 0.78$ for ACSF comparison.
Data from 7 slices in control group and 6 slices in WIN treated group. 4 paired slices under PTX pretreated groups. 5 slices in control under TTX treatment and 4 slices with WIN under TTX treatment.

CB1R translocation within axons after short WIN treatment

We further analyzed the CB1 receptor expression patterns in GFP-labeled

inhibitory axons in these slices in more detail. At first glance, there was no clear difference in CB1 receptor expression level in the axons in control and WIN-treated slices (Fig. 2A), but under PTX and TTX conditions the CB1 receptor expression level appeared decreased after WIN treatment (Fig. 2B, C). When we zoom in on individual axons, the CB1R staining is more dotty and the clear outline of CB1R+ axons is absent under PTX and TTX conditions (Fig. 2B, C). To quantify these changes, we made line profiles along GFP-labeled CB1R+ axons (Fig. 2D) and determined the coefficient of variation (CV) of the fluorescence profiles for GFP and CB1 signals. As expected, the CV of the GFP signal was similar for all groups (Fig. 2E), indicating that axon morphology was similar in all slices. However, the CV of CB1 receptor signal along the inhibitory axons was significantly reduced under PTX conditions (Fig. 2F). Unfortunately, we could not compare fluorescence intensities between slices as image acquisition parameters were not kept constants for all slices.

Under baseline conditions, the CB1R profile closely follows the GFP profile, in agreement with the notion that CB1 receptors are not enriched in presynaptic boutons, but evenly decorate the entire axonal membrane (Dudok et al., 2015). This close alignment with CB1R levels and axonal morphology is reflected in high Pearson's correlation coefficients of the GFP and CB1 fluorescence profiles (Fig. 2G). The PTX and TTX conditions did not affect this correlation, but we observed that CB1 activation by WIN strongly reduced Pearson's correlation coefficients under these conditions (Fig. 2G).

Together our data indicate that WIN induces CB1 receptor translocation towards the soma, probably after internalization (although we did not show this directly) and redistribution along the axon. Furthermore, Gi protein activity and neuronal activity appear to promote these processes, although CB1R levels in the axons closely correlated with axonal morphology. Under these conditions axonal CB1 receptors appear more sensitive to WIN-induced translocation within the axon.

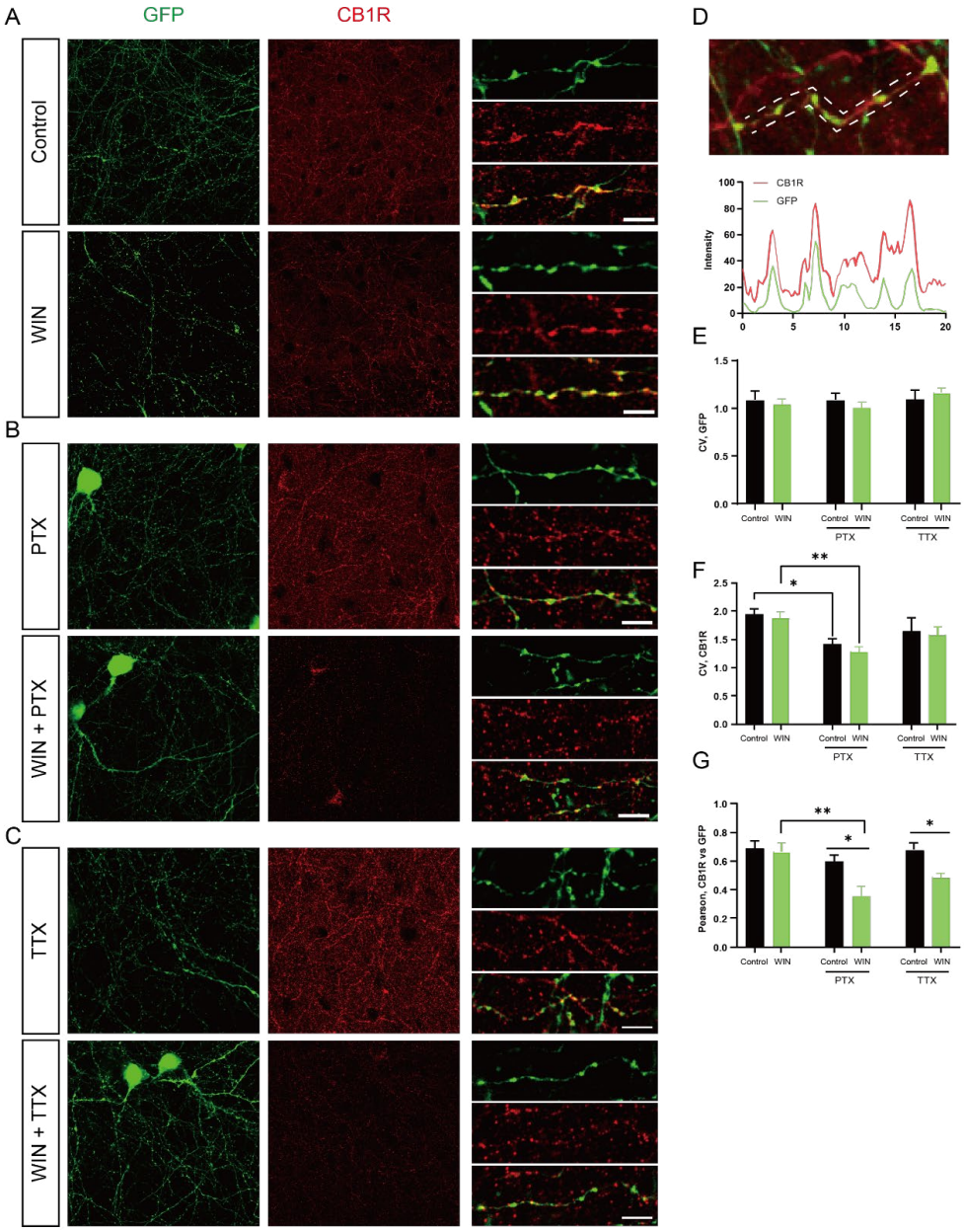

Figure 2. WIN induced CB1R internalization during acute treatment.

(A) Representative images of CB1R *post hoc* immunostaining (red) after 5 minutes application of DMSO (upper) or WIN (lower) application in slices in normal ACSF.

(B) Representative images of CB1R *post hoc* immunostaining (red) after 5 minutes application of DMSO (upper) or WIN (lower) application in slices after 24hr PTX pretreatment.

(C) Representative images of CB1R *post hoc* immunostaining (red) after 5 minutes application of DMSO (upper) or WIN (lower) application in slices in ACSF containing TTX.

(D) Individual GFP-labeled inhibitory axon showing CB1R immunostaining (upper panel),

and line profiles for GFP and CB1R signal (lower panel).
(E) Coefficient of variation (CV) of GFP signal. MW test: p = 0.93 for ACSF group; p = 0.55 for PTX group; p = 0.46 for TTX group. One-way ANOVA with Dunnett's test within control, p > 0.99 between DMSO and PTX; p > 0.99 between DMSO and TTX. One-way ANOVA with Dunnett's test within WIN treatment, p = 0.85 between WIN and WIN + PTX; p = 0.25 between WIN and WIN + TTX.
(F) Coefficient of variation (CV) of CB1R signal. MW tests: p = 0.73 for ACSF group; p = 0.34 for PTX group; p > 0.99 for TTX group. One-way ANOVA with Dunnett's test within control, p = 0.031 between DMSO and PTX; p = 0.27 between DMSO and TTX. One-way ANOVA with Dunnett's test within WIN treatment, p = 0.002 between WIN and WIN + PTX; p = 0.15 between WIN and WIN + TTX.
(G) Pearson correlation coefficient of CB1R vs GFP from acute DMSO/WIN group, p = 0.62 MW test; p = 0.014 at acute DMSO/WIN group under PTX treatment; p = 0.14 under TTX treatment. One-way ANOVA with Dunnett's test within control, p = 0.35 between DMSO and PTX; p = 0.99 between DMSO and TTX. One-way ANOVA with Dunnett's test within WIN treatment, p = 0.002 between WIN and WIN + PTX; p = 0.097 between WIN and WIN + TTX. Data from 9 axons of 3 individual slices per each group.

WIN induced CB1R translocation towards the soma after repeated treatment

We next asked whether repeated agonists treatment further enhances CB1 receptor internalization. We therefore performed repeated treatments (3 times, 20 minutes, interval 2 hours), followed by immunostainings after 24 hours. Here we compared repeated CB1R activation with 2-AG and with WIN. These are both agonists of CB1 receptors, but 2-AG is expected to degrade rapidly in biological tissue, while WIN will stay active. We observed that CB1R expression levels appeared unaffected by the repeated 2-AG treatment (Fig. 3A, B). However, we observed a clear reduction in overall CB1R immunofluorescence level and an increased accumulation into somata after repeated WIN treatment (Fig. 3C). WIN induced CB1 receptors internalization and translocation is consisted with previous studies (Thibault et al., 2013).

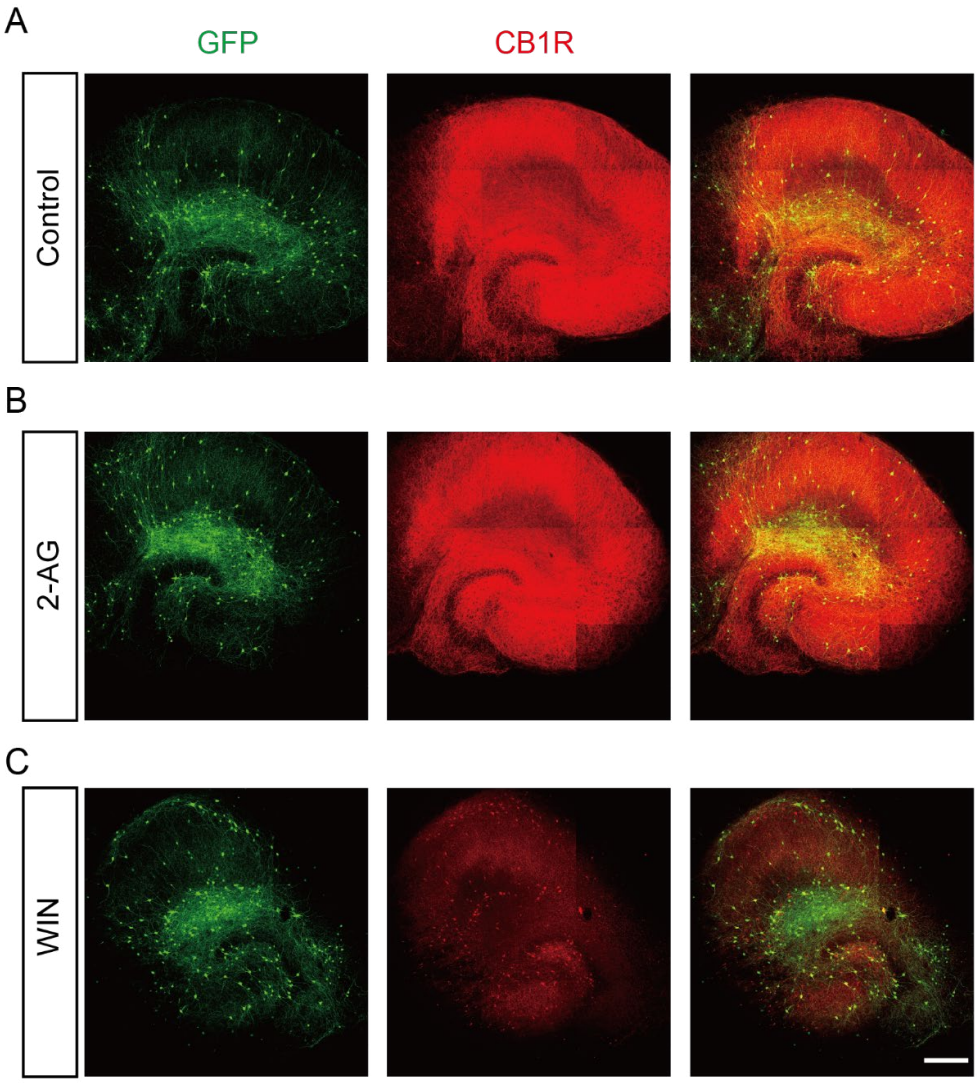

Figure 3. Agonists alters distribution of CB1 receptors after repeated treatment.
(A-C) Representative images of CB1R immunostaining in GAD65-GFP slices 24 hours after repeated (3x 20min treatment) DMSO (A), WIN (B) or 2-AG (C) treatment in hippocampal slices. Scale bar 50µm

In addition, we determined fluorescence profiles of CB1 receptors along GFP-labeled axons in these slices (Fig. 4A). After repeated activation by WIN, but not by 2-AG, axonal CB1 receptor levels were dramatically reduced compared to control and the remaining CB1 receptors appeared accumulated at boutons (Fig. 4A). Indeed, quantification of the mean intensity of the axonal profiles of VGAT (Fig. 4B), GFP (Fig. 4C) and gephyrin (Fig. 4E), were similar in

all slices, but CB1R intensity was strongly reduced in WIN-treated slices (Fig 4D). We analyzed the coefficient of variation (CV) of the fluorescent profiles along the GFP-labeled axons. The CV of CB1 receptor signals were significant decreased after repeated WIN treatment (Fig. 4H). In contrast, there was no effect on CV of VGAT, gephyrin or GFP profiles (Fig. 4F, G, I), indicating that the effect was specific for CB1 receptors. Furthermore, the correlation between CB1 receptors and axonal morphology (GFP profile) also was significantly decreased (Fig. 4J). Interestingly, we also observed a decrease in correlation between CB1R and gephyrin, which may result from loss of CB1 receptors in boutons. (Fig. 4K). These data indicate that repeated activation of CB1 receptors by WIN, but not by 2-AG, induce a significant reduction in axonal receptor levels and possible translocation of CB1 receptors towards boutons. The loss of axonal CB1 receptors appears to represent a loss of function, as we observed, in clear contrast with our earlier observations after 2-AG (Fig. 2 in chapter 3), that the presynaptic VGAT and postsynaptic gephyrin puncta density at dendritic area of CA1 were not affected after repeated WIN application (Fig. 4L, M).

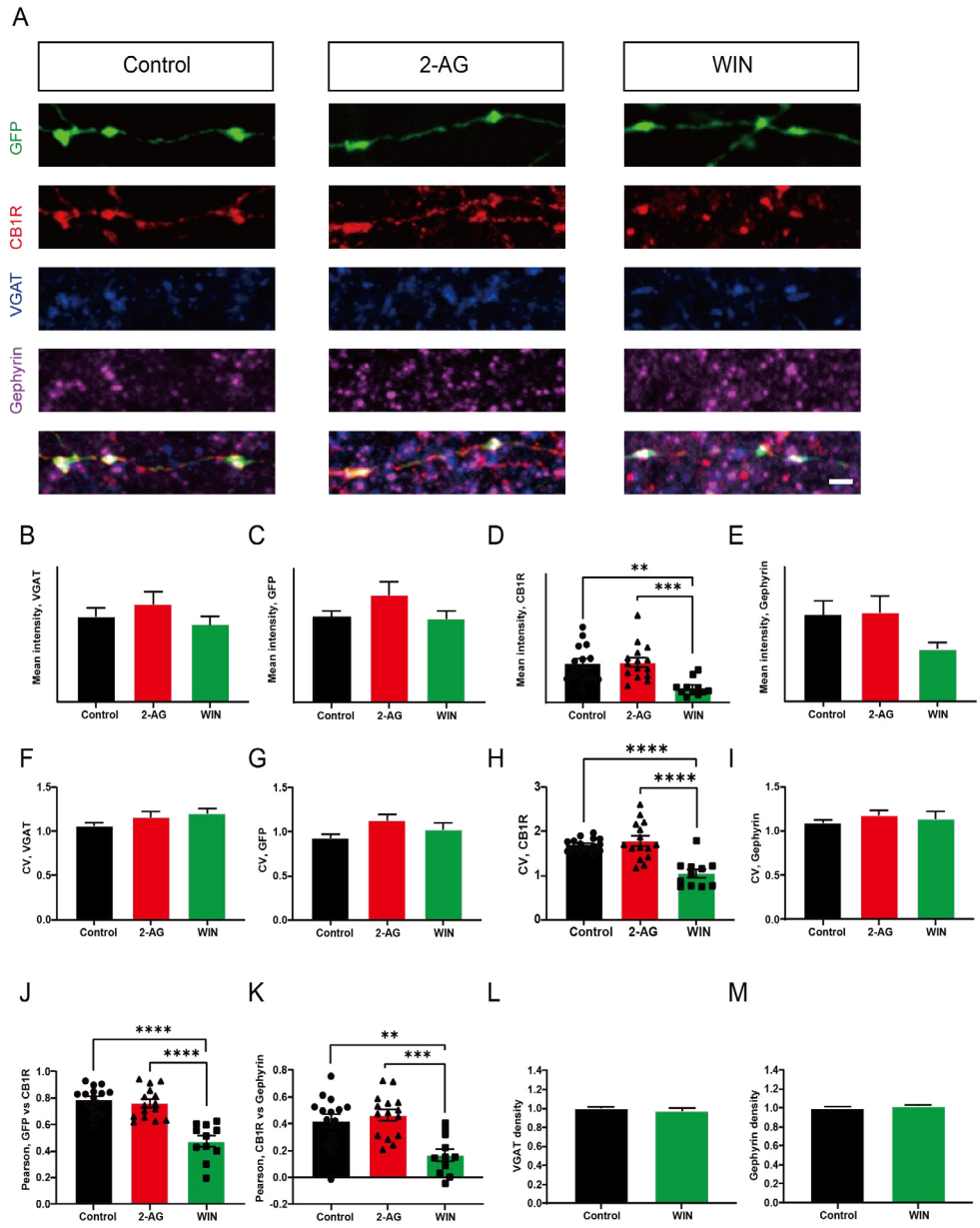

Figure 4. **Agonists induced CB1R internalization after repeated treatment.**
(A) Representative axon images of CB1R (red), VGAT (blue), Gephyrin (magenta) after repeated DMSO, WIN or 2-AG treatment in hippocampal slices. Scale bar 50µm
(B) Mean intensity of VGAT, one-way ANOVA with Turkey's test, p = 0.87 between DMSO and WIN; p = 0.65 between DMSO and 2-AG; p = 0.39 between WIN and 2-AG.
(C) Mean intensity of GFP, one-way ANOVA with Turkey's test, p = 0.99 between DMSO and WIN; p = 0.25 between DMSO and 2-AG; p = 0.26 between WIN and 2-AG.
(D) Mean intensity of GFP, one-way ANOVA with Turkey's test, p = 0.0016 between DMSO

and WIN; p = 0.96 between DMSO and 2-AG; p = 0.0008 between WIN and 2-AG.
(E) Mean intensity of GFP, one-way ANOVA with Turkey's test, p = 0.23 between DMSO and WIN; p = 0.99 between DMSO and 2-AG; p = 0.19 between WIN and 2-AG.
(F) Coefficient of variation (CV) of VGAT, one-way ANOVA with Turkey's test, p = 0.22 between DMSO and WIN; p = 0.46 between DMSO and 2-AG; p = 0.82 between WIN and 2-AG.
(G) Coefficient of variation (CV) of GFP, one-way ANOVA with Turkey's test, p = 0.57 between DMSO and WIN; p = 0.052 between DMSO and 2-AG; p = 0.46 between WIN and 2-AG.
(H) Coefficient of variation (CV) of CB1R, one-way ANOVA with Turkey's test, p < 0.0001 between DMSO and WIN; p = 0.77 between DMSO and 2-AG; p < 0.0001 between WIN and 2-AG.
(I) Coefficient of variation (CV) of Gephyrin, one-way ANOVA with Turkey's test, p = 0.86 between DMSO and WIN; p = 0.51 between DMSO and 2-AG; p = 0.87 between WIN and 2-AG.
(J) Pearson correlation coefficient of CB1R vs GFP, one-way ANOVA with Turkey's test, p < 0.0001 between DMSO and WIN; p = 0.75 between DMSO and 2-AG; p < 0.0001 between WIN and 2-AG.
(K) Pearson correlation coefficient of CB1R vs Gephyrin, one-way ANOVA with Turkey's test, p = 0.0016 between DMSO and WIN; p = 0.79 between DMSO and 2-AG; p = 0.0003 between WIN and 2-AG.
(L) Normalized VGAT puncta density under repeated WIN (20μM) treatment; p = 0.49 (MW).
(M) Normalized gephyrin puncta density under repeated WIN (20μM) treatment; p = 0.64 (MW).
Data from 13 image stacks in seven slices in control and 2-AG treated group, and 11 image stacks in six slices in WIN treated group.

4

Different CB1R distributions in organotypic hippocampal slices and cultured primary neurons

The molecular mechanisms underlying the observed differences in CB1R translocation after 2-AG vs WIN activation are unclear. Molecular mechanisms of receptor internalization and translocation are often studied in more simple systems, such as cell lines. We therefore wondered if we could further study these processes in cultured primary neurons. CB1 receptors are well expressed in primary hippocampal neurons (Roland et al., 2014; Fletcher-Jones et al., 2019).

We compared the CB1 receptor distribution in organotypic hippocampal slices and cultured neurons. In slices, CB1 receptors are highly abundant in the CA1 cell layer, and CB1R staining closely overlaps well with VGAT staining, beautifully outlining the somata of the CA1 pyramidal cells. In addition, it is easy to follow CB1R+ axons in the imaging field (Fig. 5A). As described above, repeated WIN application results in a loss of CB1 receptor staining at axons and VGAT terminals, and a gain of CB1R staining in (presumably) GABAergic

stomata (Fig. 5A). In clear contrast, CB1 receptors appeared much more abundant in cultures of primary hippocampal neurons. CB1R staining was present in many (if not all) somata and neurites, including axons, which can be identified with Tau immunostaining (Fig. 5B). The staining pattern was not strongly affected by WIN activation. These data indicate that CB1 receptor distributions are very different in these two culture systems.

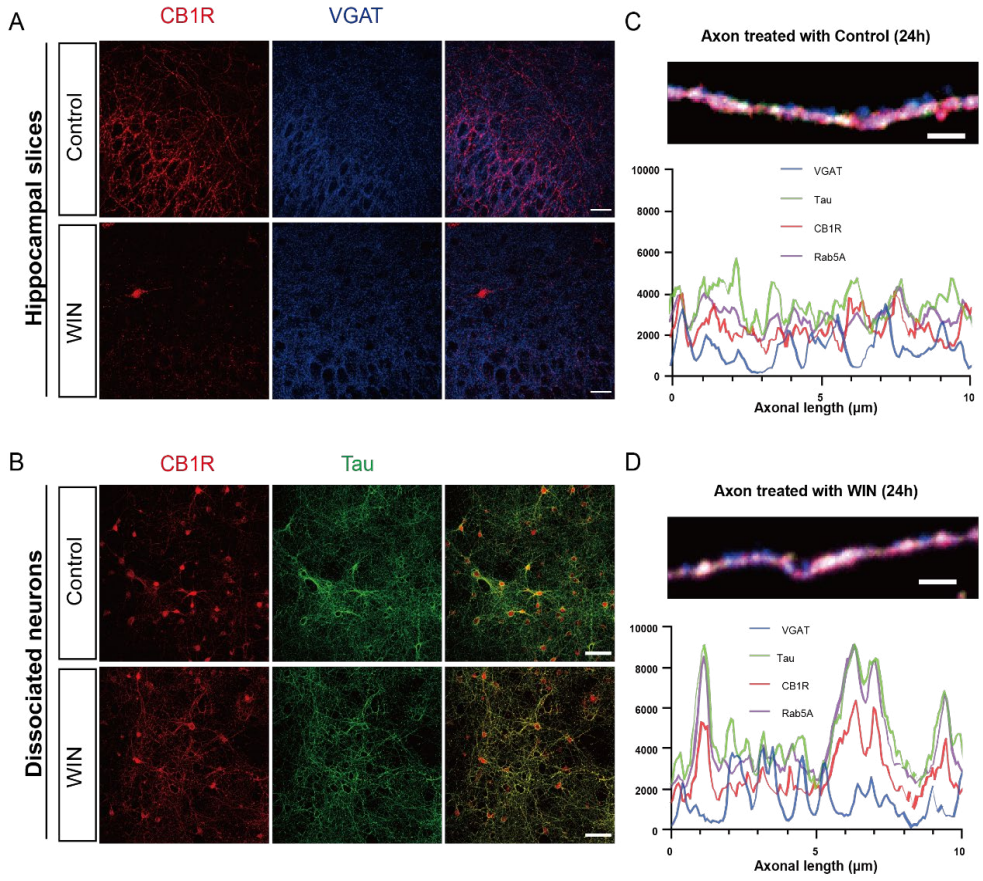

Figure 5. Different CB1R distributions in organotypic slices and cultured primary neurons.
(A) Representative images of CB1R and VGAT immunostaining in organotypic hippocampal slices after repeated DMSO (control) of WIN treatment (3x 20 min treatment, 24 hours later fixation). Scale bar is 25 µm.
(B) Representative image of CB1R and Tau immunostaining in cultured primary hippocampal neurons after 24 hours treatment with DMSO or WIN. Scale bar is 100 µm.
(C, D) Representative image of axonal intensity profile of VGAT, Tau, CB1R and Rab5A immunostaining in cultured primary neurons treated with DMSO (C) or WIN (D) for 24 hours. Bottom: Axonal line profile of fluorescence intensities. Scale bar is 1.5 µm.

We analyzed axonal intensity profiles for VGAT, tau and CB1R and Rab5a in

primary cultures after WIN treatment to address if CB1R translocation was similar compared to slice cultures (Fig. 5C, D). Here we included the endosome marker Rab5a to examine if activated CB1R get located to endosomes (Irving et al., 2000). We examined three different WIN treatments: 5 minutes treatment followed by 1.5 hrs washout and recovery (similar to the short WIN treatment during the two-photon live imaging experiments in chapter 3), and continuous WIN treatment for 1 hr and for 24 hrs. In cultures that were treated for only 5 minutes with WIN, we observed an increased intensity of VGAT, Tau and Rab5A profiles, while CB1R immunofluorescence levels remained unaffected (Fig. 6A-D).

When we compared these results with the 1 hr and 24 hrs WIN treatments, we found that the changes in VGAT and Tau immunofluorescence intensity were somewhat variable between the different WIN treatments and not very pronounced (Fig. 6E-L). In fact, the intensity of VGAT profiles was decreased after 24 hours WIN treatment, possibly reflecting synaptic weakening after prolonged CB1R activation (Monday et al., 2020). Interestingly, we consistently observed an increase in Rab5A intensity profiles in WIN treated versus control cultures (Fig. D, H, L), suggesting that CB1R activation results in an increase in endosomes in axons.

In addition to the change in Rab5a intensity, we consistently observed an increased correlation between the axonal Rab5A profiles with CB1 receptors and Tau immunostaining profiles after all WIN treatments (Fig. 6M-R). These data suggests that CB1R activation mobilizes Rab5A endosomes into axons, and that activated CB1R may translocate to endosomes after WIN application. However, drawing conclusions from these data should be done with great care as CB1R translocation after WIN activation was not very strong and we could not detect any clear difference between VGAT+ and VGAT- axons in any of these parameters (data not shown). Furthermore, the clear differences between CB1R localization in organotypic slices and cultured primary neurons prevents generalization of these observations to our previous findings in intact tissue.

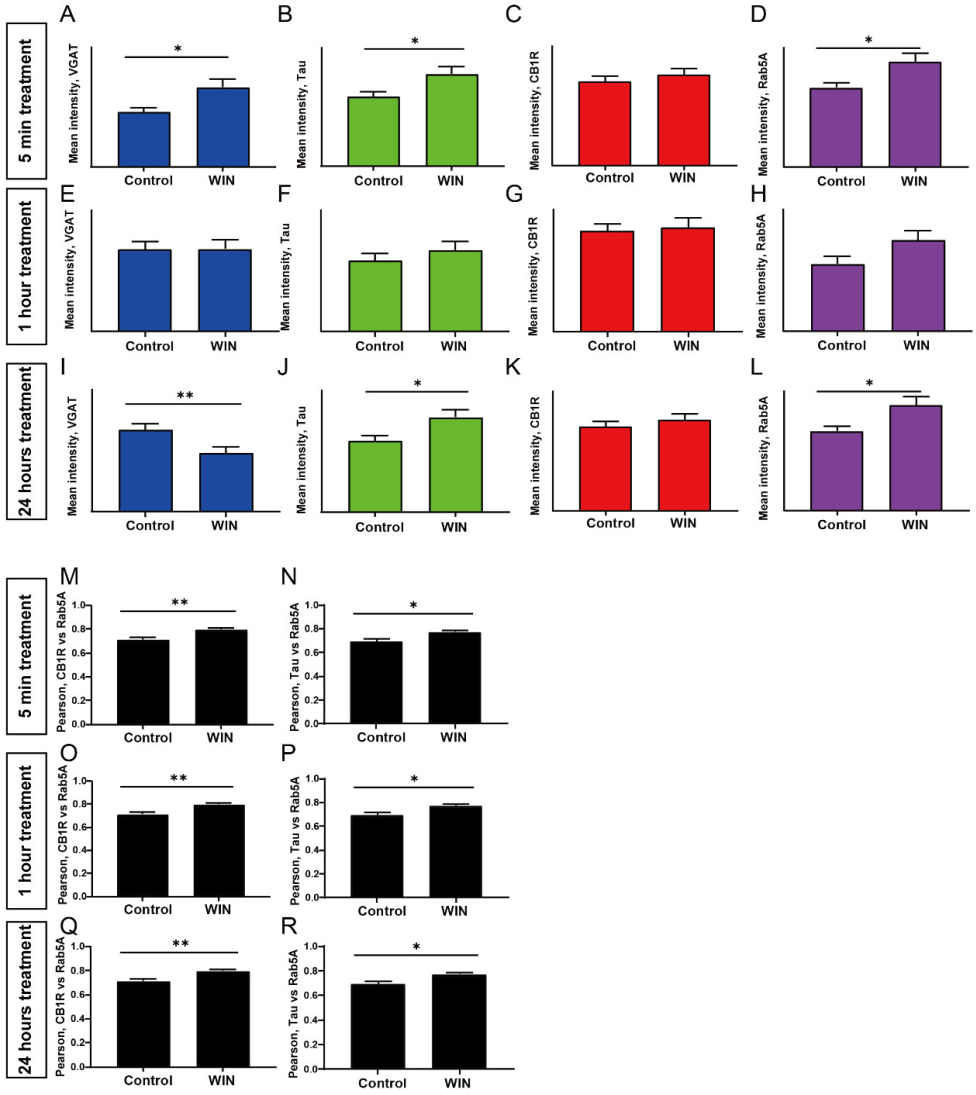

Figure 6. WIN has no effect on CB1R internalization during acute, short or long-term treatment in disassociated neuron culture.

(A-L) Mean density of VGAT (blue), Tau (green), CB1R (red) and Rab5 (magenta) from acute 5 minutes WIN treatment, then fixation after 1.5 hours (A-D). Mean intensity of VGAT in A, p = 0.017 (MW); mean intensity of Tau in B, p = 0.04 (MW); mean intensity of CB1R in C, p = 0.62 (MW); mean intensity of Rab5A in D, p = 0.042 (MW). Mean density of VGAT (blue), Tau (green), CB1R (red) and Rab5 (magenta) from 1 hour WIN treatment (E-H). Mean intensity of VGAT in E, p = 0.66 (MW); mean intensity of Tau in F, p = 0.65 (MW); mean intensity of CB1R in G, p = 0.82 (MW); mean intensity of Rab5A in H, p = 0.09 (MW). Mean density of VGAT (blue), Tau (green), CB1R (red) and Rab5 (magenta) from 24 hours WIN treatment (I-L). Mean intensity of VGAT in I, p = 0.0058 (MW); mean intensity of Tau in J, p = 0.036 (MW);

mean intensity of CB1R in K, p = 0.85 (MW); mean intensity of Rab5A in L, p = 0.038 (MW). (M-R) M is the Pearson's correlation coefficient of CB1R vs Rab5A, p = 0.0016 (MW). N is the Pearson's correlation coefficient of Tau vs Rab5A, p = 0.017 (MW). O is the Pearson's correlation coefficient of CB1R vs Rab5A, p = 0.0088 (MW). P is the Pearson's correlation coefficient of Tau vs Rab5A, p = 0.039 (MW). Q is the Pearson's correlation coefficient of CB1R vs Rab5A, p < 0.0001 (MW). R is the Pearson's correlation coefficient of Tau vs Rab5A, p < 0.0001 (MW). Data from 36 axons in 4 cultures per groups (only repeated 2 round).

Discussion

In the present study, we found that the synthetic CB1R agonist WIN promotes CB1 receptor translocation within axons and towards the soma in organotypic hippocampal slices. Although we did not address this directly, this translocation likely requires receptor internalization, followed by intracellular transport (Coutts et al., 2001; Grimsey et al., 2010; Winckler and Mellman, 2010; Simon et al., 2013). Surprisingly, activation of CB1 receptors with the endogenous agonist 2-AG did not induce any prominent translocation of CB1 receptors, not even after repeated 2-AG application. Finally, we observed that CB1 receptor expression patterns were dramatically different between organotypic hippocampal slices and cultured primary hippocampal neurons.

We observed two different translocations of CB1 receptors, towards the soma and within axons. First of all, we observed that WIN treatment resulted in CB1 receptor localization in somata. These somata presumably belong to CB1R+ GABAergic cells, as a substantial overlap with GFP was found, and most CB1R+ somata were located outside of the pyramidal cell layer. This fits well with the reported expression of CB1 receptors by a subset of GABAergic cells (Klausberger et al., 2005; Dudok et al., 2015), which only partially overlaps with GFP expression in GAD65-GFP mice (Wierenga et al., 2010). This suggests that WIN treatment did not induce aberrant CB1R expression in cells that normally do not express CB1R. In vivo, CB1 receptors are restricted to the axons of these cells (Katona et al., 1999, 2006; Dudok et al., 2015). CB1 receptors have fast turnover in vivo (Garzón et al., 2009; Ogasawara et al., 2015). CB1R location in the somata of CB1R+ cells may reflect translocation of receptors from the axons back in the soma (Thibault et al., 2013), possibly to undergo lysosomal degradation. However, our data does not exclude that CB1 receptors in the soma reflect buildup of newly synthesized CB1 receptors, for instance by impaired transport towards the axon (Fletcher-Jones et al., 2019).

We observed that under certain circumstances (not in control slices) WIN treatment resulted in a more subtle reorganization of CB1 receptors within the axon, in which the perfect alignment with CB1 receptors and axonal morphology was disturbed. This suggests that activation of axonal CB1 receptors lead to local recycling of receptors to and from the axonal membrane. It is possible that this reflects clustering at presynaptic boutons, similar to what has been described for other G-protein coupled receptors

(Jullié et al., 2020). It remains unclear if this reorganization towards boutons does not occur under control conditions, or if it remains undetectable. If only a portion of axonal CB1 receptors get reorganized after WIN treatment, the overall density of axonal CB1 receptors will determine if changes are detectable.

An important observation from the present study is that CB1R translocation was strongly influenced by PTX and TTX. When PTX or TTX was present in the ACSF, CB1 receptors were already present in somata in the absence of WIN treatment (Fig. 1). Furthermore, in PTX and TTX conditions WIN induced significant CB1R reorganization within axons that was not observed under normal conditions. These observations appear to directly contradict previous studies, which reported that PTX is not involved in agonist-induced CB1 receptor internalization in cultured primary neurons (Hsieh et al., 1999; Coutts et al., 2001). The apparent contradiction may be explained by the difference in model system. Interestingly, we previously observed that CB1R-mediated bouton formation was maintained in PTX and TTX conditions (Figures 7Aand 7D in chapter 3), indicating that the WIN-induced translocation of axonal CB1 receptors, either within axons or towards the soma, does not interfere with the CB1R signaling pathways required for bouton formation. Unfortunately, we could not determine overall CB1R density in our slices and this will be an important parameter to determine in future experiments. Overall CB1R expression levels appeared not extensively affected, as overall CB1R immunostaining appeared comparable to control conditions and CB1R+ and CB1R- axons could be clearly distinguished (Fig. 2A). One possibility is that under PTX and TTX conditions, CB1R delivery to axons may be impaired, resulting in a buildup of CB1Rs in the soma and a reduced level of CB1Rs in the axons. This may explain the reduced CV of CB1R intensity profiles in axons (Fig. 2D) and the impaired correlation of CB1 receptor profiles with axonal morphology (Fig. 2E), without the need for a direct effect on the internalization process (Hsieh et al., 1999; Coutts et al., 2001). At this point, we do not have any good explanation how PTX and TTX may interfere with delivery of CB1 receptors into axons. Alternatively, PTX and TTX may have a direct effect on CB1R translocation, for instance via decreasing phosphorylation of CB1 receptors, which is required for receptor recycling, which may alter post-endocytic trafficking (Bradbury et al., 2009; Flores-Otero et al., 2014; Kunselman et al., 2019).

The total number of CB1 receptors present at the cell surface determines the potential for a physiological response to an endocannabinoid signal.

Here, we found that two widely used agonists affect the distribution of CB1 receptor differentially (Fig. 3A). Prolonged activation of CB1 receptor by WIN significantly reduced axonal CB1 receptor expression, while axonal CB1 receptors remained in place after repeated activation by the endogenous agonist 2-AG. This is an important observation as many electrophysiology studies use WIN instead of 2-AG in experiments. Interestingly, anandamide (the other endocannabinoid in the brain) showed similar effects as WIN on CB1 receptor distribution (Hsieh et al., 1999). This difference may reflect functional selectivity of CB1 receptors, a bias towards downstream signaling pathways after activation that is determined by the specific agonist. Indeed, a clear difference in dwell time at the plasma membrane was reported when CB1 receptors are activated by WIN or by 2-AG (Flores-Otero et al., 2014). As 2-AG prolongs the receptor dwell time, it may bias towards β-arrestin signaling cascades participating in CB1 receptor internalization. However, one should be careful with this interpretation, as the duration and strength of CB1R activation are also important determinants of effective CB1R signaling (Cui et al., 2016, 2018). Even though we applied both agonists for 20 minutes to our slices, the efficient CB1R activation in these slices is likely different between 2-AG and WIN treatment. 2-AG gets rapidly degraded in neural tissue by degradation enzymes such as MAGL (Lee et al., 2015; Lenkey et al., 2015), which is expected to substantially shorten CB1R activation. WIN is a synthetic agonist and will remain stable and active during the entire 20 minutes.

Another important observation in this study is that translocation of CB1 receptors is different in cultured primary neurons and organotypic slices. In primary cultures, we found that WIN-induced activation of CB1 receptors increases the Rab5a-containing endosomes in axons (Irving et al., 2000) and that WIN increased the colocalization of CB1 receptors with Rab5a. However, we observed that CB1 receptors were localized to many, if not all, somata and neurites of cultured primary neurons. This is in clear contrast to organotypic slices and in vivo, where CB1 receptors are selectively localized to axons of GABAergic CB1R+ cells. This polarized distribution is very important for CB1R function. The nonselective distribution of CB1 receptor in cultured primary neurons may reflect the relative immature state of these neurons, or a difference in ambient endocannabinoid levels and ongoing CB1 receptor activation. However, this significantly limits the interpretation of our findings in cultured primary neurons.

It is important to realize that WIN-induced bouton formation appears largely

independent of the CB1R reorganization or translocation that we studied in this chapter. Under control conditions, 5 minutes of WIN treatment induces rapid bouton formation without any detectable receptor reorganization or translocation of CB1R receptors in the inhibitory axons (Fig. 2). Also after repeated 2-AG treatment, which induces the formation of new inhibitory presynaptic terminals (Liang et al., 2021), CB1R profiles remained unchanged (Fig. 4). Even more, under PTX and TTX conditions in which CB1R expression was altered, WIN continued to induce bouton formation. In this case, axonal receptor levels may be reduced, but receptors remain evenly distributed over the axonal membrane. This would be consistent with a specific role for extrasynaptic, axonal CB1 receptors in inhibitory synapse formation. A translocation of extrasynaptic CB1 receptor into presynaptic boutons after local CB1 receptor activation may represent a mechanism to limit further inhibitory bouton formation.

Materials and Methods

Transgenic GAD65-GFP mice from both sexes were used in these experiments. All animal experiments were performed in compliance with the guidelines for the welfare of experimental animals issued by the Federal Government of the Netherlands. All animal experiments were approved by the Animal Ethical Review Committee (DEC) of Utrecht University

Mouse organotypic hippocampal slice culture

Organotypic mouse hippocampal slices were acquired from female and male GAD65-GFP mice at 6-7 days after birth. In these mice, ~20% interneurons are labelled by GFP from early embryonic developmental stage into adulthood (López-Bendito et al., 2004). Most GFP-labelled interneurons target dendrites of CA1 pyramidal cells and express VIP or reelin, while parvalbumin and somatostatin-positive neurons are not labelled. Slice culture preparation details are described previously (Frias et al., 2019; Hu et al., 2019) . Mice were sacrificed and the isolated hippocampus was placed in ice-cold HEPES-GBSS (containing 1.5 mM $CaCl_2 \cdot 2H_2O$, 0.2 mM KH_2PO_4, 0.3 mM $MgSO_4 \cdot 7H_2O$, 5 mM KCl, 1 mM $MgCl_2 \cdot 6H_2O$, 137 mM NaCl, 0.85 mM Na_2HPO_4 and 12.5 mM HEPES) supplemented with 12.5 mM HEPES, 25 mM glucose and 1 mM kynurenic acid (pH set around 7.2, osmolarity set around 320 mOsm, sterile filtered). Slices were vertically chopped along the long axis of hippocampus at thickness of 400 µm. They were then quickly washed with culturing medium (consisting of 48% MEM, 25% HBSS, 25% horse serum, 30 mM glucose and 12.5 mM HEPES, pH set at 7.3-7.4 and osmolarity set at 325 mOsm) and transferred to Millicell cell culture inserts (Milipore) in 6-well plates. Slices were cultured in an incubator (35 °C, 5% CO_2) until use. Culturing medium was completely replaced twice a week. Slices were used after 2 to 3 weeks *in vitro*, when the circuitry is relatively mature and stable (De Simoni et al., 2003).

Primary neuron cultures

Primary neurons were acquired from rat hippocampi at embryonic day 18, which were dissected and dissociated in trypsin in 37°C water bath. Neurons were plated on coverslips pre-coated with poly-L-lysine (37.5µg/mL) and laminin (1.25µg/mL). Neurobasal medium (NB) contained 1% B27 (GIBCO), 0.5mM glutamine (GIBCO), 15.6µM glutamate (Sigma), and 1% penicillin/ streptomycin (GIBCO) under controlled temperature and CO2 conditions (37°C, 5% CO2) was used for neuron culture (Pan et al., 2019). Treatments started at DIV 22.

Immunocytochemistry and confocal microscopy of organotypic slices
Fixation of the slices was performed in 4% paraformaldehyde (PFA) for 30 minutes at room temperature covered by aluminum foil. Following washing with phosphate-buffered saline (PBS; 3x 10 minutes), slices were permeabilized with 0.5% Triton X-100 (15 minutes), followed by PBS washing (3x 5 minutes), and 1 hour incubation in blocking solution (0.2% Triton X-100 and 10% goat serum). Application of primary antibodies in blocking solution was performed overnight at 4 °C. After PBS washing (3x 15 minutes), secondary antibodies were applied for 4 hours. After PBS washing (2x 15 minutes), slices were mounted in Vectashield solution.
We used the following primary antibodies: rabbit α-VGAT (Synaptic Systems, 131 003; 1:1000; RRID: AB 887869), mouse α-gephyrin (Synaptic Systems, 147 011; 1:1000; RRID: AB_887717), mouse α-CB1R (Synaptic Systems, 258 011; 1:1000; RRID: AB_2619969), and the following secondary antibodies: anti-mouse Alex647 (Life Technologies, A21241, 1:500; RRID: AB_2535810) and anti-rabbit Alex405 (Life Technologies, A31556, 1:250; RRID: AB_221605) for VGAT and gephyrin staining, anti-mouse Alexa647 (Life Technologies, A21236, 1:500; RRID: AB_2535805) and anti-mouse Alexa568 (Life Technologies, A11031, 1:500; RRID: AB_144696) for CB1R staining.
Acquisition of confocal images was performed under Zeiss LSM-700 microscope system with a 20x (Plan-Apochromat 20x/0.8 M27) and a 63x oil-immersion objective (Plan-Apochromat; NA=1.4). Image size was 101.3 µm x 101.3 µm (1024 x 1024 pixels) with 0.3 µm z steps for axon reorganization, and up to 203 µm x 203 µm for somata identification. Tile scans with customized z-stack imaging was used for analyzing CB1 receptor distribution at organotypic hippocampal slices. Fluorescence intensity profiles were measured using line profiles in Fiji with a line width of 15 pixels.

Immunohistochemistry and confocal imaging of cultured primary neurons
Cultured primary neurons were treated by transferring the coverslips in a new well containing half new medium and half old medium with 20µM WIN-552112-2 or DMSO. After the 5 minutes treatment, neurons were put back in the incubator in control medium for 1.5 hours and then they were fixed. For 1 hr and 24 hrs WIN treatments, neurons were immediately fixed after 60 minutes or 24 hours WIN treatment respectively. Neurons were fixed with 200 µL 4% PFA for 10 minutes. Subsequently, the neurons were washed for 3 times for 5 minutes in PBS, then 1XGDB buffer was used as blocking buffer for 30 minutes. Primary antibodies (Synaptic Systems 258011; mouse anti-CB1R 1:500, Synaptic Systems 131006; chicken anti-VGAT 1:500, Chemicon mouse anti-tau 1:500, and Invitrogen rabbit anti-Rab5a 1:500) were added

to the neurons in blocking buffer for 1 hour. The neurons were then washed again 3 times for 5 minutes with PBS, Secondary antibodies (Life Technologies A21236 anti-mouse Alexa 647 1:500, BioConnect ab175675 anti-chicken Alexa 405 1:500, Life Technologies A21141 anti-ms-IgG2B Alexa 488 1:500, and Life Technologies A21135 anti-msIgG2A 1:500) were added into blocking buffer for 3 hours incubation. Finally, neurons were washed 3 times for 10 minutes in PBS and mounted in Vectashield solution. Neurons were kept at 4 degrees in the dark for storage.

All image acquisition was performed under a Zeiss LSM-700 microscope system with a 20x (Plan-Apochromat 20x/0.8 M27) and a 63x oil-immersion objective (Plan-Apochromat; NA=1.4). The 20x objective was used to make an overview of the neurons, while the 63x objective was used to image a single neuron and axons. Around 11 steps z-stack imaging (step size 0.3 um) was made for acquiring intact information. Fluorescence intensity profiles were measured as described above.

For synapse quantification images were analyzed in Fiji using a custom macro (Ruiter et al., 2020; Liang et al., 2021). An average projection image was made from 5 z-planes, images were median filtered (1 pixel radius) and individual puncta were identified using watershed segmentation.

Experimental Design and Statistical Analyses

All experiments were performed and analyzed blindly. Statistical analysis was performed using GraphPad Prism software. Data are reported as mean ± standard error unless stated otherwise. Results from treatment and control experiments were compared using the nonparametric Mann-Whitney U test (MW). One-way ANOVA with Dunnett's test was used for comparing difference among multiple groups/treatment.

Author contributions:

JL and CJW conceived the research and designed the experiments. JL performed and analyzed all experiments, with pilot experiments performed by BJBV. JL and CJW wrote the manuscript. CJW supervised the research.

Reference

Bradbury FA, Zelnik JC, Traynor JR (2009) G Protein independent phosphorylation and internalization of the δ-opioid receptor. J Neurochem 109:1526–1535.

Busquets-Garcia A, Bains J, Marsicano G (2018) CB 1 Receptor Signaling in the Brain: Extracting Specificity from Ubiquity. Neuropsychopharmacology 43:4–20 Available at: http://dx.doi.org/10.1038/npp.2017.206.

Castillo PE, Younts TJ, Chávez AE, Hashimotodani Y (2012) Endocannabinoid Signaling and Synaptic Function. Neuron 76:70–81.

Chevaleyre V, Heifets BD, Kaeser PS, Südhof TC, Purpura DP, Castillo PE (2007) Endocannabinoid-Mediated Long-Term Plasticity Requires cAMP/PKA Signaling and RIM1α. Neuron 54:801–812.

Compton DR, Gold LH, Ward SJ, Balster RL, Martin BR (1992) Aminoalkylindole analogs: cannabimimetic activity of a class of compounds structurally distinct from delta 9-tetrahydrocannabinol. J Pharmacol Exp Ther 263:1118 LP – 1126 Available at: http://jpet.aspetjournals.org/content/263/3/1118.abstract.

Coutts AA, Anavi-Goffer S, Ross RA, MacEwan DJ, Mackie K, Pertwee RG, Irving AJ (2001) Agonist-induced internalization and trafficking of cannabinoid CB1 receptors in hippocampal neurons. J Neurosci 21:2425–2433.

Cui Y, Perez S, Venance L (2018) Endocannabinoid-LTP Mediated by CB1 and TRPV1 Receptors Encodes for Limited Occurrences of Coincident Activity in Neocortex. Front Cell Neurosci 12:1–14.

Cui Y, Prokin I, Xu H, Delord B, Genet S, Venance L, Berry H (2016) Endocannabinoid dynamics gate spike- timing dependent depression and potentiation. Elife 5:1–32.

De Simoni A, Griesinger CB, Edwards FA (2003) Development of rat CA1 neurones in acute versus organotypic slices: role of experience in synaptic morphology and activity. J Physiol 550:135–147.

Delgado-Peraza F, Ahn KH, Nogueras-Ortiz C, Mungrue IN, Mackie K, Kendall DA, Yudowski GA (2016) Mechanisms of Biased β -Arrestin-Mediated Signaling Downstream from the Cannabinoid 1 Receptor. Mol Pharmacol 89.

Dudok B et al. (2015) Cell-specific STORM super-resolution imaging reveals nanoscale organization of cannabinoid signaling. Nat Neurosci 18:75–86.

Finlay DB, Cawston EE, Grimsey NL, Hunter MR, Korde A, Vemuri VK, Makriyannis A, Glass M (2017) Gαs signalling of the CB1 receptor and the influence of receptor number. Br J Pharmacol 174:2545–2562.

Fletcher-Jones A, Hildick KL, Evans AJ, Nakamura Y, Henley JM, Wilkinson KA (2020) Protein Interactors and Trafficking Pathways That Regulate the Cannabinoid Type 1 Receptor (CB1R). Front Mol Neurosci 13.

Fletcher-Jones A, Hildick KL, Evans AJ, Nakamura Y, Wilkinson KA, Henley JM (2019) The C-Terminal helix 9 motif in rat cannabinoid receptor type 1 regulates axonal trafficking and surface expression. Elife 8:1–26.

Flores-Otero J, Ahn KH, Delgado-Peraza F, Mackie K, Kendall DA, Yudowski GA (2014) Ligand-specific endocytic dwell times control functional selectivity of the cannabinoid receptor 1. Nat Commun 5.

Frias CP, Liang J, Bresser T, Scheefhals L, Van Kesteren M, Van Dorland R, Yin Hu H, Bodzeta A, Van Bergen En Henegouwen PMP, Hoogenraad CC, Wierenga CJ (2019) Semaphorin4D induces inhibitory synapse formation by rapid stabilization of presynaptic boutons via MET coactivation. J Neurosci 39:4221–4237.

Garzón J, de la Torre-Madrid E, Rodríguez-Muñoz M, Vicente-Sánchez A, Sánchez-Blázquez P (2009) Gz mediates the long-lasting desensitization of brain CB1 receptors and is essential for cross-tolerance with morphine. Mol Pain 5:1–22.

Grimsey NL, Graham ES, Dragunow M, Glass M (2010) Cannabinoid Receptor 1 trafficking and the role of the intracellular pool: Implications for therapeutics. Biochem Pharmacol 80:1050–1062.

Howlett AC, Barth F, Bonner TI, Cabral G, Casellas P, Devane WA, Felder CC, Herkenham M, Mackie K, Martin BR, Mechoulam R, Pertwee RG (2002) International Union of Pharmacology. XXVII. Classification of cannabinoid receptors. Pharmacol Rev 54:161–202.

Hsieh C, Brown S, Derleth C, Mackie K (1999) Internalization and recycling of the CB1 cannabinoid receptor. J Neurochem 73:493–501.

Hu HY, Kruijssen DLH, Frias CP, Rózsa B, Hoogenraad CC, Wierenga CJ (2019) Endocannabinoid Signaling Mediates Local Dendritic Coordination between Excitatory and Inhibitory Synapses. Cell Rep 27:666-675.e5.

Hua T et al. (2016) Crystal Structure of the Human Cannabinoid Receptor CB1. Cell 167:750-762.e14.

Irving AJ, Coutts AA, Harvey J, Rae MG, Mackie K, Bewick GS, Pertwee RG (2000) Functional expression of cell surface cannabinoid CB1 receptors on presynaptic inhibitory terminals in cultured rat hippocampal neurons. Neuroscience 98:253–262.

Jin W, Brown S, Roche JP, Hsieh C, Celver JP, Kovoor A, Chavkin C, Mackie K (1999) Distinct domains of the CB1 cannabinoid receptor mediate desensitization and internalization. J Neurosci 19:3773–3780.

Jullié D, Stoeber M, Sibarita JB, Zieger HL, Bartol TM, Arttamangkul S, Sejnowski TJ, Hosy E, von Zastrow M (2020) A Discrete Presynaptic Vesicle Cycle for Neuromodulator Receptors. Neuron 105:663-677.e8.

Kano M, Ohno-Shosaku T, Hashimotodani Y, Uchigashima M, Watanabe M (2009) Endocannabinoid-mediated control of synaptic transmission. Physiol Rev 89:309–380.

Katona I, Sperlágh B, Sík A, Käfalvi A, Vizi ES, Mackie K, Freund TF (1999) Presynaptically located CB1 cannabinoid receptors regulate GABA release from axon terminals of specific hippocampal interneurons. J Neurosci 19:4544–4558.

Katona I, Urban GM, Wallace M, Ledent C, Jung K-M, Piomelli D, Mackie K, Freund TF (2006) Molecular Composition of the Endocannabinoid System at Glutamatergic Synapses. J Neurosci 26:5628–5637.

Klausberger T, Marton LF, O'Neill J, Huck JHJ, Dalezios Y, Fuentealba P, Suen WY, Papp E, Kaneko T, Watanabe M, Csicsvari J, Somogyi P (2005) Complementary roles of cholecystokinin- and parvalbumin-expressing GABAergic neurons in hippocampal network oscillations. J Neurosci 25:9782–9793.

Kouznetsova M, Kelley B, Shen M, Thayer SA (2002) Desensitization of cannabinoid-mediated presynaptic inhibition of neurotransmission between rat hippocampal neurons in culture. Mol Pharmacol 61:477–485.

Kunselman JM, Zajac AS, Weinberg ZY, Puthenveedu MA (2019) Homologous regulation of mu opioid receptor recycling by Gβγ, protein kinase C, and receptor phosphorylation. Mol Pharmacol 96:702–710.

Laprairie RB, Bagher AM, Denovan-Wright EM (2017) Cannabinoid receptor ligand bias: implications in the central nervous system. Curr Opin Pharmacol 32:32–43 Available at: http://dx.doi.org/10.1016/j.coph.2016.10.005.

Laprairie RB, Bagher AM, Kelly MEM, Dupré DJ, Denovan-Wright EM (2014) Type 1 cannabinoid receptor ligands display functional selectivity in a cell culture model of striatal medium spiny projection neurons. J Biol Chem 289:24845–24862.

Lauckner JE, Hille B, Mackie K (2005) The cannabinoid agonist WIN55,212-2 increases intracellular calcium via CB1 receptor coupling to Gq/11 G proteins. Proc Natl Acad Sci U S A 102:19144–19149.

Lee SH, Ledri M, Tóth B, Marchionni I, Henstridge CM, Dudok B, Kenesei K, Barna L, Szabó SI, Renkecz T, Oberoi M, Watanabe M, Limoli CL, Horvai G, Soltesz I, Katona I (2015) Multiple forms of endocannabinoid and endovanilloid signaling regulate the tonic control of GABA release. J Neurosci 35:10039–10057.

Lenkey N, Kirizs T, Holderith N, Máté Z, Szabó G, Vizi ES, Hájos N, Nusser Z (2015) Tonic endocannabinoid-mediated modulation of GABA release is independent of the CB1 content of axon terminals. Nat Commun 6.

Leterrier C, Lainé J, Darmon M, Boudin H, Rossier J, Lenkei Z (2006) Constitutive activation drives compartment-selective endocytosis and axonal targeting of type 1 cannabinoid receptors. J Neurosci 26:3141–3153.

Liang J, Kruijssen DL, Verschuuren AC, Voesenek BJ, Benavides F, Sáez Gonzalez M, Ruiter M, Wierenga CJ (2021) Axonal CB1 receptors mediate inhibitory bouton formation via cAMP increase. J Neurosci:https://doi.org/10.1523/JNEUROSCI.0851-21.2021.

López-Bendito G, Sturgess K, Erdélyi F, Szabó G, Molnár Z, Paulsen O (2004) Preferential origin and layer destination of GAD65-GFP cortical interneurons. Cereb Cortex 14:1122–1133.

Monday H, Bourdenx M, Jordan B, Castillo P (2020) CB 1 receptor-mediated inhibitory LTD triggers presynaptic remodeling via protein synthesis and ubiquitination.

Nguyen PT, Schmid CL, Raehal KM, Selley DE, Bohn LM, Sim-Selley LJ (2012) β-Arrestin2 regulates cannabinoid CB 1 receptor signaling and adaptation in a central nervous system region-dependent manner. Biol Psychiatry 71:714–724 Available at: http://dx.doi.org/10.1016/j.biopsych.2011.11.027.

Ogasawara D et al. (2015) Rapid and profound rewiring of brain lipid signaling networks by acute diacylglycerol lipase inhibition. Proc Natl Acad Sci 113:26–33.

Pan X, Cao Y, Stucchi R, Hooikaas PJ, Portegies S, Will L, Martin M, Akhmanova A, Harterink M, Hoogenraad CC (2019) MAP7D2 Localizes to the Proximal Axon and Locally Promotes Kinesin-1-Mediated Cargo Transport into the Axon. Cell Rep 26:1988-1999.e6 Available at: https://doi.org/10.1016/j.celrep.2019.01.084.

Roland AB, Ricobaraza A, Carrel D, Jordan BM, Rico F, Simon A, Humbert-Claude M, Ferrier J, McFadden MH, Scheuring S, Lenkei Z (2014) Cannabinoid-induced actomyosin contractility shapes neuronal morphology and growth. Elife 3:e03159.

Ruiter M, Herstel LJ, Wierenga CJ (2020) Reduction of Dendritic Inhibition in CA1 Pyramidal Neurons in Amyloidosis Models of Early Alzheimer's Disease. J Alzheimer's Dis 78:1–14.

Shao Z, Yin J, Chapman K, Grzemska M, Clark L, Wang J, Rosenbaum DM (2016) High-resolution crystal structure of the human CB1 cannabinoid receptor. Nature 540:602–606 Available at: http://dx.doi.org/10.1038/nature20613.

Simon AC, Loverdo C, Gaffuri AL, Urbanski M, Ladarre D, Carrel D, Rivals I, Leterrier C, Benichou O, Dournaud P, Szabo B, Voituriez R, Lenkei Z (2013) Activation-dependent plasticity of polarized GPCR distribution on the neuronal surface. J Mol Cell Biol 5:250–265.

Thibault K, Carrel D, Bonnard D, Gallatz K, Simon A, Biard M, Pezet S, Palkovits M, Lenkei Z (2013) Activation-dependent subcellular distribution patterns of CB1 Cannabinoid Receptors in the Rat Forebrain. Cereb Cortex 23:2581–2591.

Tsou K, Brown S, Sañudo-Peña M., Mackie K, Walker J. (1998) Immunohistochemical distribution of cannabinoid CB1 receptors in the rat central nervous system. Neuroscience 83.

Wang W, Jia Y, Pham DT, Palmer LC, Jung K-M, Cox CD, Rumbaugh G, Piomelli D, Gall CM, Lynch G (2017) Atypical endocannabinoid signaling initiates a new form of memory-related plasticity at a cortical input to hippocampus. Cereb Cortex:1–14.

Wierenga CJ, Müllner FE, Rinke I, Keck T, Stein V, Bonhoeffer T (2010) Molecular and electrophysiological characterization of GFP-expressing CA1 interneurons in GAD65-GFP mice. PLoS One 5:e15915.

Winckler B, Mellman I (2010) Trafficking guidance receptors. Cold Spring Harb Perspect Biol 2:1–18.

Chapter 5

General discussion

Jian Liang

Cell Biology, Department of Biology, Faculty of Science, Utrecht University, 3584 CH Utrecht, The Netherlands

Dysfunction of synaptic inhibition is associated with a wide spectrum of brain diseases. In this thesis, I have shown that the formation of inhibitory boutons is a dynamic process. Multiple proteins and signal modulators are involved in this process. It is crucial to explore the molecular mechanisms of inhibitory bouton dynamics and inhibitory synapse formation to develop experimental tools to address how altered synaptic inhibition influences neuronal circuit activity and behavioral state. This may yield new insights into dysfunction of inhibition in diseases.

Inhibitory bouton formation is a dynamic, multi-step process. One of the key questions is which signaling pathways and proteins are involved in different stages of inhibitory bouton formation. This thesis forms a start to answering this question. In chapter 2 we demonstrated that the secreted protein Sema4D plays a specific role in stabilizing non-persistent boutons. We found that Sema4D-induced bouton stabilization requires receptor tyrosine kinase MET, and that this process involves actin depolymerization and is dependent on neuronal network activity. Multiple intrinsic and external factors including aging, neuronal activity, neuromodulators could affect bouton dynamics, and we will discuss some of these in this final chapter.

In chapter 3 we found that activation of CB1 receptors induced new bouton formation and stabilizing boutons. CB1 receptors are G-protein coupled receptor (GPCR), and highly abundant at axons and axonal terminals of inhibitory neurons. We demonstrated that endocannabinoids mediated bouton formation involves an unconventional Gs dependent signal pathway. However, the precise downstream effector pathways after receptor activation are still unclear, and we will deliberate potential targets after activation of CB1 receptors involved in bouton formation.

Typically, GPCRs are internalized and then recycled back to the membrane after activation. Interestingly, in chapter 4 we observed that activation by WIN, but not by the endogenous cannabinoid 2-AG induces CB1 receptor clustering in the somata of GFP-labeled GABAergic neurons. The mechanism underlying this internalization and trafficking of axonal CB1 receptors remains unresolved. However, the ligand dependence suggests functional selectivity, i.e., biased signal cascades downstream of CB1 receptors, resulting in ligand-dependent CB1 receptor distribution. Functional selectivity of CB1 receptors makes endocannabinoid signal highly complex, and we will discuss this in more detail in this final chapter.

Molecular identity of inhibitory non-persistent boutons

The neuronal synapse is the place for neuronal information exchange and transfer. A change in synapses - synaptic plasticity - alters information processing and is therefore tightly associated with learning and memory (Stuchlik, 2014; Takeuchi et al., 2014; Abraham et al., 2019). The structure of synapses has been described in detail (Harris and Weinberg, 2012; Liu et al., 2019) and modern superresolution microscopy has recently revealed the molecular organization of mature inhibitory synapses (Specht et al., 2013; Pennacchietti et al., 2017). However, we do not yet have a complete list of all molecular components at these synapses and we also do not know in what order they have to assemble to form new inhibitory synapses (Dobie and Craig, 2011; Frias and Wierenga, 2013). Our live imaging approach revealed that inhibitory synapse formation is a highly dynamic process: the transition from an empty axon-dendrite crossing to a functional inhibitory synapse involves specific molecular steps including initial bouton formation, bouton stabilization, and synaptic protein clustering (Wierenga et al., 2008; Dobie and Craig, 2011; Frias and Wierenga, 2013; Wierenga, 2017).

The vast majority of boutons (~80%) of an inhibitory axon is persistent. We showed in chapter 2 that these are occupied with presynaptic VAGT and faced along with postsynaptic protein gephyrin and they represent mature, and stable inhibitory synapses. However, ~20% of inhibitory boutons are non-persistent boutons and their identity cannot be seen from a single snapshot. Only by following the dynamics of boutons over time using live imaging, we could identify the developmental stage of individual boutons.

By characterizing the sequence of events that occurs during inhibitory synapse formation, it should be possible to find markers for specific developmental stages of boutons. For instance, in chapter 2 we found that presynaptic VGAT occurs at an earlier stage during synapse formation compared to postsynaptic gephyrin. We used this knowledge in chapter 3, where we observed that repeated CB1 receptor activation increases the number of VGAT puncta that are not associated with gephyrin. This suggested that inhibitory bouton formation was ‘stuck’ at an early stage. Indeed, detailed live imaging revealed that cAMP/PKA signaling downstream of axonal CB1 receptors promotes the initial bouton formation, but that additional, probably activity-dependent processes are required for subsequent bouton stabilization and gephyrin recruitment.

It will be very useful to have immunohistochemical markers for inhibitory synapses at different developmental stages. For instance, in several diseases, inhibitory synapse development is impaired or delayed (Milosevic et al., 2018; Davenport et al., 2019; Shimojo et al., 2020; Kurucu et al., 2021). Having a good marker for synapse development would allow comparing inhibitory synapse development in different conditions and brain areas. As it is much harder to chemically isolate inhibitory synapses compared to excitatory synapses, the molecular components of inhibitory synapses remained largely unknown for a long time. However, with advanced mass spectrometry, numerous bouton proteins have now been identified, including synaptic vesicle proteins, active zone proteins, and synaptic adhesion proteins that are specific for inhibitory synapses (Ken H. Loh et al., 2016). Some of these proteins may be good candidates for markers of different developmental stages of non-persistent boutons. For instance, Mdga1 is a well-known ligand for Neuroligin 2 and Mdga1 inhibits inhibitory synapse formation by disrupting the interaction between neurexin and neuroligin 2 (Lee et al., 2013; Pettem et al., 2013). Additionally, Mdga1 is highly colocalized with VGAT, which suggests a potential role in inhibitory synapse pruning (Ken H. Loh et al., 2016). This would mean that Mdga1 could be a marker for destabilizing boutons or boutons that will be removed. It will be important to determine at which stage which molecules get recruited to inhibitory synapses.

As we showed in chapter 2, it is well possible to combine two photon time-lapse imaging with *post hoc* immunostaining, to determine during which developmental stage some of these components are recruited. However, establishing the sequence of molecular events by performing live imaging followed by *post hoc* immunostaining for every protein of interest would be very time-consuming. In addition, such an analysis can only be performed for the small number of proteins for which excellent antibodies are available. An alternative method would be to label proteins in living brain tissue and to follow their recruitment during bouton formation under the two-photon microscope. However, genetic encoding strategies to tag proteins of interest with fluorescent labels have the considerable disadvantage that they usually result in overexpression of the protein of interest. Especially in small compartments like axons and boutons, even a small overexpression may severely disturb cellular context and protein function (Shiraiwa et al., 2020). Interestingly, the newest CRISPR (clustered regularly interspaced short palindromic repeats) mediated knock-in approaches, like HITI (Homology Independent Targeted Integration) or TKIT (Targeted Knock-In with Two), provide a unique possibility to label endogenous proteins in post-mitotic

neurons (Suzuki et al., 2016; Willems et al., 2020; Fang et al., 2021). In this way, labeled proteins are expressed at endogenous levels and they can be observed in their natural cellular environment. Importantly, there is no real limitation in which proteins can be labeled, and the group of Harold MacGillavry has already generated a library of synaptic proteins that includes relevant candidates for inhibitory synapses (Willems2020). The use of self-labeling proteins like Halo Tags or SNAP tags provide additional flexibility to label endogenous proteins with diverse selective organic fluorophores (Gautier et al., 2008; Los et al., 2008; Erdmann et al., 2019). When specific molecular markers are identified, these can then be used to further characterize the molecular components of the different developmental stages of inhibitory bouton formation.

Factors implicated in inhibitory bouton dynamics

Inhibitory bouton dynamics are important so that neuronal networks are flexible and can rapidly adapt to changing circumstances. Inhibitory synapses can be adapted during learning and adaptation (Keck et al., 2011; Chéreau et al., 2017; Sun et al., 2019). For instance, when mice were trained to learn a complicated motor task, it was found that somatic inhibitory bouton density was increased, while dendritic inhibitory bouton density was decreased during the training period (Chen et al., 2015). The decrease in dendritic inhibitory boutons is thought to facilitate the plasticity of the local excitatory connections at dendritic spines that is required for learning the task. Indeed, when the researchers interfered with inhibitory plasticity, motor learning was impaired (Chen et al., 2015). A similar observation was made during the reorganization of the visual cortex after a lesion in the eye. The density of inhibitory boutons was quickly reduced (within 48 hr), allowing for a massive turnover of excitatory connections during the next 2-3 months (Keck et al., 2011). In our research group, we showed that if excitatory synapses get overactive, endocannabinoids get produced which led to the rapid formation of inhibitory synapses via CB1 receptors to reinstate (Hu, Kruijssen 2019). These example studies show how the dynamic character of inhibitory synapses allows continuous updating of synaptic connections. These dynamics are therefore essential for experience-dependent learning and adaptation of brain function.

Inhibitory presynaptic bouton dynamics reflect the dynamic processes of inhibitory synapse formation and removal. Changes in cell shape and the morphology of synapses likely indiacte modifications of the intracellular

cytoskeleton (Basu and Lamprecht, 2018; Luxenburg and Zaidel-Bar, 2019). Cytoskeleton filaments are present in boutons and play an important role in synaptic versicles clustering. Actin is highly enriched at boutons, both as monomeric G-actin and filamentous F-actin. F-actin is continuously polymerizing and depolymerizing. By engaging with synapsins and other actin-binding proteins, actin can serve as presynaptic scaffolding protein and it maintains and organizes the size of synaptic vesicle pool, vesicle docking and priming, and eventually regulates synaptic efficacy and morphology. In chapter 2 we showed that actin depolymerization promotes inhibitory bouton stabilization, but it is unclear if actin also influences bouton formation and elimination (Wierenga, 2017; Frias et al., 2019). We showed in chapter 3 that cAMP/PKA signaling is important in mediating initial bouton formation after CB1 receptor activation, but it is well possible that, either in parallel or subsequentially, CB1 receptors also signal to the actin cytoskeleton. For instance, it is known that activation of postsynaptic CB1 receptors in dendritic spines can result in actin depolymerization via the WAVE complex, which results in spine loss (Njoo et al., 2015). A similar downstream pathway is involved in CB1-mediated axonal growth cone collapse, demonstrating that the interactions between the actin cytoskeleton and CB1 receptors are common within axons (Njoo et al., 2015). It is therefore well possible that axonal CB1 receptors regulate actin dynamics in nascent boutons via a similar mechanism to promote bouton stabilization. Interestingly, CB1-mediated actin depolymerization was shown to be G_i-dependent (Njoo et al., 2015). This underscores the capacity of CB1 receptors to activate multiple, Gi-dependent and Gi-independent, downstream signaling pathways. It will be interesting to establish in the future if CB1 receptors in the axonal shaft activate both signaling pathways (via cAMP and via actin) in parallel during inhibitory synapse formation. Alternatively, axonal CB1 receptors first generate a bouton in a Gi-independent manner via cAMP/PKA. When this bouton has recruited synaptic vesicles (VGAT) and possibly Gi proteins, subsequent activation of CB1 receptors can now lead to bouton stabilization via actin remodeling.

Neurexins are cell adhesion proteins located at presynaptic terminals, which have crucial roles in synapse development and function. Mammalian cells have three neurexin genes, Nrx1-3, which are synthesized from two independent promoters (Craig and Kang, 2007). α-neurexins have longer extracellular domains containing six LNS domains and three EGF-like domains, while β-neurexins have short extracellular domains containing only one LNS domain. Additionally, neurexins have intensively conserved

splicing sites to generate various isoforms. Neurexins have diverse pre- and postsynaptic partners, such as neuroligins and leucine-rich repeat transmembrane proteins (LRRTMs) (Graf et al., 2004; Craig and Kang, 2007; Huang and Scheiffele, 2008). Interestingly, α-neurexins are distributed diffusely along inhibitory axons, while β-neurexins are more restricted at inhibitory boutons via postsynaptic anchoring to NL2 (Fu and Huang, 2010). Particularly, β-neurexins have high turnover rates at inhibitory synapse, which provides a potential mechanism to influence synapse formation via rapid recruitment of neurexins. Surprisingly, loss-of-function mutations of presynaptic neurexins were shown to enhance tonic endocannabinoid signaling via promotion of postsynaptic 2-AG synthesis (Anderson et al., 2015). In contrast, loss-of-function mutations of postsynaptic neuroligin 3 decreased tonic endocannabinoids signal (Földy et al., 2013). Neurexins can form nanoclusters at individual synapse, and loss-of-function mutations of neurexins alter presynaptic $GABA_B$ receptor localization and thereby modify synaptic release (Trotter et al., 2019; Luo et al., 2021). Whether neurexins can also affect CB1 receptor activation or location at axonal shafts and terminals is not clear. It will be interesting to investigate whether neurexins physically interact with axonal CB1 receptors. The dynamics of neurexins are regulated by neuronal activity and cAMP/PKA activity(Fu and Huang, 2010; Klatt et al., 2021), but it has not been examined if activation of CB1 receptors influence the distribution of neurexins inside and outside of synapses . It will be important to further explore the precise roles of neurexin-neuroligin interactions in endocannabinoid-mediated synapse development and plasticity.

Bouton dynamics are affected in disease conditions (Grillo et al., 2013; Mostany et al., 2013; Liebscher et al., 2014; Ash et al., 2018; Ruiter et al., 2021). Ageing is a risk factor for many neurodegenerative diseases. In aged mice brain, excitatory boutons are more dynamic—bouton turnover is increased and large boutons get destabilized, which may contribute to cognitive decline (Grillo et al., 2013; Mostany et al., 2013). In an Alzheimer's disease (AD) mouse model, boutons in excitatory axons have a higher turnover rate and lower survival fraction, and this has been linked to synapse loss and dysfunction of memory and cognition (Liebscher et al., 2014). We have examined inhibitory bouton dynamics in Aβ-treated slices and a mouse model for Alzheimer's disease (Ruiter et al., 2021). However, we found only minor changes in bouton dynamics, which was consistent with our earlier finding that Aβ affects release properties of GABAergic synapses, but not the number of inhibitory synapses, at this very early stage of the disease.

However, at a later stage of Alzheimer's disease, specific inhibitory axons are affected and they even get degraded (Schmid Neuron 2016). Together, these data suggest that excitatory and inhibitory synapses display differential sensitivity to amyloid β.

Downstream effectors upon CB1 receptors activation

In this thesis, we demonstrated that endocannabinoids could induce inhibitory bouton formation via activation of axonal CB1 receptors (chapter 3). We found that axonal CB1 receptors use a rather unconventional downstream signaling pathway in this process. In general, CB1 receptors can interact with different G proteins to transduce extracellular signals upon activation. Typically, CB1 receptors recruit heterometric G_i proteins to inhibit cAMP/PKA level (Kano et al., 2009; Argaw et al., 2011; Castillo et al., 2012). However, more and more evidence shows that CB1 receptors also interact with other G proteins, including G_q (Lauckner et al., 2005), $G_{12/13}$ (Roland et al., 2014), and G_s (Finlay et al., 2017). Additionally, CB1 receptors can interact with β-arrestins to exert G-protein independent signaling pathways (Turu and Hunyady, 2010). Activated CB1 receptors can signal via multiple intracellular effectors, including GRKs, β-arrestins, factor associated with neutral sphingomyelinase, and cannabinoid receptor-interacting protein 1a (CRIP1a) to induce extracellular signal-regulated kinases (ERK) activation and regulate the activity of many other kinases (Blume et al., 2017).

In most cases, signal transduction via GPCRs starts with activation of receptors that are present in the membrane. However, the density of GPCRs in the membrane is regulated by GPCR activation itself. For instance, activated CB1 receptors can recruit GPCR kinases (GRKs), and β-arrestins which mediate internalization and desensitization of CB1 receptors (Smith et al., 2010). CRIP1a competes with β-arrestins to bind to the C-terminal of CB1 receptors, and attenuates CB1 receptors internalization (Howlett et al., 2010; Blume et al., 2017). In addition to signaling at the plasma membrane, signaling also occurs via intracellular CB1 receptors (Hebert-Chatelain et al., 2016), or from endocytosed CB1 receptors (Smith et al., 2010; Rozenfeld, 2011). There is a wide variety of cytoplasmic effectors, which make endocannabinoid signaling highly complex (Harkany et al., 2007; Keimpema et al., 2011).

In chapter 3 we found that endocannabinoids can induce inhibitory bouton formation via an increase in cAMP/PKA activity. We showed that axonal CB1 receptors are mediating this signaling. However, the further downstream

cascades mediating inhibitory bouton formation remain unresolved. Under physiological circumstances, when endocannabinoids are produced by an active dendrite, only the CB1 receptors on a nearby inhibitory axon will be activated, which is expected to produce a local increase in cAMP/PKA signaling. An important next challenge will be to resolve how local this signal is at the subcellular level. Fortunately, there are recent exciting developments in engineering of sensitive biosensors. For instance, a highly sensitive new biosensor for PKA was recently developed. This sensor, called tAKARα, is a FRET-based fluorescent lifetime sensor, which reports PKA activity by a decrease in lifetime (Ma et al., 2018). Even more recently, a novel cAMP sensor, called cAMPFIRE, was developed, which shows significantly improved sensitivity compared to previous sensors (Massengill et al., 2021a). These new tools make it possible to answer our questions in the near future by monitoring cAMP/PKA activity in axonal shaft or boutons of inhibitory axons (Chen et al., 2014; Patel and Gold, 2015; Koschinski and Zaccolo, 2017; Massengill et al., 2021b). Identification of the downstream effectors of cAMP/PKA signaling will be the next challenge. Some potential effectors attract our attention, including the cytoskeleton. Just underneath the plasma membrane actin, spectrin and associated proteins form a membrane-associated periodic skeleton (MPS) of rings. This rather rigid structure may secure structural integrity of the thin axons in the densely packed neuronal tissue (Leterrier et al., 2017; Leterrier, 2021). The MPS may provide a platform for CB1 receptor mediated signaling at the membrane. Interestingly, a recent paper showed that CB1 receptor activation results in colocalization of these receptors with the MPS (Zhou et al., 2019). This then leads to transactivation of the ERK pathway via tropomyosin receptor kinase B (TrkB) or fibroblast growth factor receptors (FGFRs), which both have been previously linked to inhibitory synaptic plasticity (Frias and Wierenga, 2013; Zhou et al., 2019). ERK signaling actually results in degradation of the MPS and thereby ERK signaling is halted. It is interesting to speculate that this brief ERK signaling after CB1 receptor activation could provide the opportunity to form a new bouton through local reorganization of cytoskeleton structure including spectrin and actin (Zhou et al., 2019; Li et al., 2020). However, it should be noted that these data were all acquired in primary cultures, where CB1 receptors are ubiquitously expressed at high levels. As we describe in chapter 4, this is very different from the in vivo situation. These results may therefore reflect a role for the ERK signaling pathway in redistribution of CB1 receptors away from the membrane.

Other interactions between the CB1 receptors and the cytoskeleton have also

been described. For instance, it has been shown that CB1 receptor activation by WIN can induce rapid growth cone retraction via actomyosin contractions during structural plasticity (Roland et al., 2014). In addition, activated CB1 receptors can regulate actin indirectly via the WAVE complex during spine shrinking and removal (Njoo et al., 2015). Intriguingly, CB1 signaling via the cytoskeleton may be partially dependent on Rho-GTPase and Rho-associated kinase (ROCK) activity. In chapter 2, we showed that ROCK-dependent actin depolymerization is required for bouton stabilization (Frias et al., 2019). Together, this literature suggests an intriguing link between CB1 receptor activation, and the intracellular cytoskeleton and it suggests that multiple downstream pathways may be activated in parallel during CB1 receptor-mediated inhibitory bouton formation.

Most of the molecular mechanism upon CB1 receptors activation is investigated in cultured neurons, but we should pay attention that CB1 receptors are ubiquitously expressed at high levels in all cultured primary neurons, including excitatory neurons, while in vivo, CB1 receptors are mostly restricted to inhibitory axons. It is unclear if axonal polarization of CB1 receptors can also occur in cultured primary neurons, for instance when activity levels are raised. This raises doubt that the molecular mechanisms downstream of CB1 receptor activation in cultured primary neurons and *in vivo* will be comparable. Indeed, we observed clear differences that have been described in chapter 4. For instance, we observed that WIN induced CB1 receptor clustering at somata in slices, which was absent, or at least undetectable, in cultured primary neurons. It is therefore well plausible that the results described by Zhou et al. (Zhou et al., 2019) may reflect a role for the ERK signaling pathway in activity-dependent redistribution of CB1 receptors away from the membrane. This illustrates well the advantages and the limitations of the primary culturing system to study molecular mechanisms.

Functional selectivity of endocannabinoid's signal

G-protein coupled receptors (GPCRs) are the largest group of membrane proteins. As described above, the downstream signaling via G proteins is highly diverse. Ligand-induced conformational changes are the basis for GPCR-mediated signal transduction (Wang et al., 2018b). However, dependent on the specific ligand, the conformational change in the receptor may be slightly different, thereby affecting downstream recruitment of effectors and signaling cascades. This selective activation of the downstream

signaling by different ligands is termed “functional selectivity” or “ligand bias”. This phenomenon is not specific for CB1 receptors, but commonly described in the GPCR research field (Bosier et al., 2010; Zhou and Bohn, 2014). For instance, the heptahelical serotonin 2A receptor (5-HT_{2A}) exerts distinct signal transductions upon different agonists activation. For instance, psychoactive agonists of 5-HT_{2A} like lysergic acid diethylamide (LSD) induce hallucinations through distinct G_q and G_i signaling pathways, while other nonhallucinogenic agonists lisuride and serotonin lack this psychoactive effect. (González-Maeso et al., 2007; Abbas and Roth, 2008; Schmid et al., 2008; Raote et al., 2013).

These diverse functions are mediated via multiple intracellular downstream signaling cascades. Typically, ligands induce CB1 receptor conformational changes to activate heterotrimeric $G_{i/o}$ proteins and activated $G_{i/o}$ subunits dissociate away from the receptor-protein complex. The activated Giα subunit interfaces with adenylyl cyclase (AC) to inhibit cAMP production (Kano et al., 2009; Castillo et al., 2012). At presynaptic terminals, where high levels of CB1 receptors are present, activated CB1 receptors result in a decrease of release probability and therefore a suppression of synaptic transmission (Castillo et al., 2012). Rather unexpectedly, recent studies showed that CB1 receptors in the striatum and lateral perforant path (LPP) can also potentiate neurotransmitter releasing (Cui et al., 2016; Wang et al., 2018a). In these studies, presynaptic PKA signaling was implied, suggesting that CB1 receptors signal via unconventional downstream pathways, possibly via G_s proteins. In chapter 3 of this thesis, we found that WIN-induced bouton formation is also dependent on an increase in PKA signaling, which seems consistent with a G_s-protein coupling of axonal CB1 receptors.

Endocannabinoid signaling can also involve G protein independent signaling. Recent studies showed that CB1 receptors interact with β-arrestin1 and β-arrestin2 to induce receptor internalization, and to activate kinases including MAPKs and ERKs (Delgado-Peraza et al., 2016; Jagla et al., 2019). β-arrestins are scaffold proteins regulating receptor internalization and desensitization, and are well-known to mediate biased signaling of GPCRs. The balance between G protein-dependent and-independent signaling appears to be determined by the agonist (Laprairie et al., 2014, 2017; Lu et al., 2019). CB1 receptor activation by endogenous cannabinoid 2-AG results in a long dwell time of the receptor at the membrane, and downstream signaling biased towards β-arrestins. However, after activation by the exogenous synthetic agonist WIN, CB1 receptors display a shorter dwell time, which

biases signaling towards G proteins (Flores-Otero et al., 2014). Interaction of CB1 receptors with β-arrestin1 biases downstream signaling towards the ERK1/2 pathway, while β-arrestin2 is required for rapid internalization of CB1 receptors (Flores-Otero et al., 2014; Nogueras-Ortiz and Yudowski, 2016). Moreover, β-arrestin2 deletion attenuates internalization of CB1 receptors and reduces endocannabinoid tolerance *in vivo* (Nguyen et al., 2012). The precise role of β-arrestin1/2 in functional selectivity of CB1 receptor signaling still requires further research.

Another layer of complexity of GPCRs signaling results from the variety of isoforms that are expressed in different tissue or organisms (Shire et al., 1995; Ryberg et al., 2005). CB1 receptors are encoded by the *CNR* gene. Although this gene does not have many introns, CNR undergoes splicing which results in different CB1 receptor isoforms (Marti-Solano et al., 2020). Different isoforms may have bias towards specific downstream signaling pathways (Marti-Solano et al., 2020). In addition, the subcellular location of CB1 receptors may determine downstream signaling, perhaps due to limited availability of downstream effectors. For instance, CB1 receptors are located in the mitochondria membrane, which regulate synaptic plasticity and neuronal energy metabolism (Bénard et al., 2012).

It is also of interest to note that CB1 receptors may form heterodimers with other GPCRs, something which is well described for other GPCRs (Borroto-Escuela et al., 2013). It is already reported that CB1 receptors can interact with opioid receptors, A2A adenosine receptors, and D2 dopamine receptors (Ferré et al., 2010; Terzian et al., 2011; Borroto-Escuela et al., 2013; Befort, 2015). These mosaic heterodimeric receptor complexes can provide a signal platform to exert unique information transduction.

Trafficking of CB1 receptors in neurons

As described above, CB1 receptors are strongly enriched in inhibitory axons and inhibitory axonal terminals (Katona et al., 2006; Dudok et al., 2015). Newly synthesized CB1 receptors undergo protein quality control checks before they can form functional proteins. This process involves cis- and trans-Golgi modifications and newly synthesized CB1 receptors are then inserted into the plasma membrane (Winckler and Mellman, 2010). The axonal enrichment of CB1 receptors is the result of continuous endocytosis at somatodendritic compartments, while endocytosis of CB1 receptors does not occur in axons (Leterrier et al., 2006; Simon et al., 2013). The C-terminal

of CB1 receptors, and especially the H9 helix, is important for CB1 receptor trafficking from the soma to axonal terminals (Fletcher-Jones et al., 2019, 2020).

Initiation of the GPCR signal transduction always happens at the plasma membrane, but translocation of receptors can play an important role in signal amplification and transduction (Weinberg et al., 2019). Upon ligand binding, CB1 receptors recruit GRKs and β-arrestins to initiate fast receptor internalization and desensitization (Grimsey et al., 2010). Typically, internalized receptors will be packed into endosomes and recycled back to the plasma membrane to maintain a dynamic equilibrium. In parallel, CB1 receptors can also be transported into lysosomes to be degraded (Grimsey et al., 2010). β-arrestins play an important role in mediating subcellular internalization and translocation of CB1 receptors via endocytosis. Interestingly, there is some evidence that CB1 receptors are transported back to the soma via retrograde trafficking in neurons (Thibault et al., 2013). We also found that CB1 receptors are internalized and translocated from the axon to the soma upon activation by WIN (chapter 4). However, we observed that activation by the endogenous cannabinoid 2-AG did not induce CB1 receptor translocation. We found that in both cases internalized CB1 receptors were colocalized with the endosomal protein Rab5A. This suggests that internalized CB1 receptors were packed into endosomes in the axon, and that an agonist-dependent mechanism exists to direct CB1 receptors to be recycled back to the membrane or be translocated to the soma (Rozenfeld, 2011). In the future, it would be interesting to monitor this process with live imaging via new proteins labelling strategies as we described before.

Future perspective

The super family of GPCRs is the largest family of membrane proteins and consist of more than 800 proteins. GPCRs contain more than 50% of current drug targets against many diseases including various brain disorders. Functional selectivity of GPCRs hampers the identification of novel drug targets for treatment. However, recent advances in revealing the crystal structures of several GPCRs has already provided new insights in functional selectivity (Zhou and Bohn, 2014; Hua et al., 2016; Li et al., 2020). This is promising for the search to new therapies targeted at GPCRs. It will be important to better understand the relationship between the conformational state of the GPCRs and the interaction with either G proteins or arrestins. In the future, it may be possible to identify or even design agonists which can induce a certain downstream signaling cascade by stabilizing a specific receptor conformation. It may be possible to selectively activate CB1 receptors to either suppress inhibitory transmission or to induce inhibitory synapse formation. This could have an enormous therapeutic impact.

Reference

Abbas A, Roth BL (2008) Arresting serotonin. Proc Natl Acad Sci U S A 105:831–832.

Abraham WC, Jones OD, Glanzman DL (2019) Is plasticity of synapses the mechanism of long-term memory storage? npj Sci Learn 4 Available at: http://dx.doi.org/10.1038/s41539-019-0048-y.

Anderson GR, Aoto J, Tabuchi K, Földy C, Covy J, Yee AX, Wu D, Lee SJ, Chen L, Malenka RC, Südhof TC (2015) β-Neurexins Control Neural Circuits by Regulating Synaptic Endocannabinoid Signaling. Cell 162:593–606.

Argaw A, Duff G, Zabouri N, Cecyre B, Chaine N, Cherif H, Tea N, Lutz B, Ptito M, Bouchard J-F (2011) Concerted Action of CB1 Cannabinoid Receptor and Deleted in Colorectal Cancer in Axon Guidance. J Neurosci 31:1489–1499.

Ash RT, Fahey PG, Park J, Zoghbi HY, Smirnakis SM (2018) Increased axonal bouton stability during learning in the mouse model of MECP2 duplication syndrome. eNeuro 5.

Basu S, Lamprecht R (2018) The role of actin cytoskeleton in dendritic spines in the maintenance of long-term memory. Front Mol Neurosci 11:1–9.

Befort K (2015) Interactions of the opioid and cannabinoid systems in reward: Insights from knockout studies. Front Pharmacol 6:1–15.

Bénard G et al. (2012) Mitochondrial CB 1 receptors regulate neuronal energy metabolism. Nat Neurosci 15:558–564.

Blume LC, Patten T, Eldeeb K, Leone-Kabler S, Ilyasov AA, Keegan BM, O'Neal JE, Bass CE, Hantgan RR, Lowther WT, Selley DE, Howlett AC (2017) Cannabinoid receptor interacting protein 1a competition with β-arrestin for CB1 receptor binding sites. Mol Pharmacol 91:75–86.

Borroto-Escuela DO, Romero-Fernandez W, Rivera A, Van Craenenbroeck K, Tarakanov AO, Agnati LF, Fuxe K (2013) On the G-protein-coupled receptor heteromers and their allosteric receptor-receptor interactions in the central nervous system: Focus on their role in pain modulation. Evidence-based Complement Altern Med 2013.

Bosier B, Muccioli GG, Hermans E, Lambert DM (2010) Functionally selective cannabinoid receptor signalling: Therapeutic implications and opportunities. Biochem Pharmacol 80:1–12.

Castillo PE, Younts TJ, Chávez AE, Hashimotodani Y (2012) Endocannabinoid Signaling and Synaptic Function. Neuron 76:70–81.

Chen SX, Kim AN, Peters AJ, Komiyama T (2015) Subtype-specific plasticity of inhibitory circuits in motor cortex during motor learning. Nat Neurosci 18:1109–1115.

Chen Y, Saulnier JL, Yellen G, Sabatini BL (2014) A PKA activity sensor for quantitative analysis of endogenous GPCR signaling via 2-photon FRET-FLIM imaging. Front Pharmacol 5 APR:1–12.

Chéreau R, Saraceno GE, Angibaud J, Cattaert D, Nägerl UV (2017) Superresolution imaging reveals activity-dependent plasticity of axon morphology linked to changes in action potential conduction velocity. Proc Natl Acad Sci U S A 114:1401–1406.

Craig AM, Kang Y (2007) Neurexin-neuroligin signaling in synapse development. Curr Opin Neurobiol 17:43–52.

Cui Y, Prokin I, Xu H, Delord B, Genet S, Venance L, Berry H (2016) Endocannabinoid dynamics gate spike- timing dependent depression and potentiation. Elife 5:1–32.

Davenport EC, Szulc BR, Drew J, Taylor J, Morgan T, Higgs NF, López-Doménech G, Kittler JT (2019) Autism and Schizophrenia-Associated CYFIP1 Regulates the Balance of Synaptic Excitation and Inhibition. Cell Rep 26:2037-2051.e6.

Delgado-Peraza F, Ahn KH, Nogueras-Ortiz C, Mungrue IN, Mackie K, Kendall DA, Yudowski GA (2016) Mechanisms of Biased *β* -Arrestin-Mediated Signaling Downstream from the Cannabinoid 1 Receptor. Mol Pharmacol 89.

Dobie FA, Craig AM (2011) Inhibitory synapse dynamics: Coordinated presynaptic and postsynaptic mobility and the major contribution of recycled vesicles to new synapse formation. J Neurosci 31:10481–10493.

Dudok B et al. (2015) Cell-specific STORM super-resolution imaging reveals nanoscale organization of cannabinoid signaling. Nat Neurosci 18:75–86.

Erdmann RS, Baguley SW, Richens JH, Wissner RF, Xi Z, Allgeyer ES, Zhong S, Thompson AD, Lowe N, Butler R, Bewersdorf J, Rothman JE, St Johnston D, Schepartz A, Toomre D (2019) Labeling Strategies Matter for Super-Resolution Microscopy: A Comparison between HaloTags and SNAP-tags. Cell Chem Biol 26:584-592.e6 Available at: https://doi.org/10.1016/j.chembiol.2019.01.003.

Fang H, Bygrave AM, Roth RH, Johnson RC, Huganir RL (2021) An optimized crispr/cas9 approach for precise genome editing in neurons. Elife 10:1–25.
Ferré S, Lluís C, Justinova Z, Quiroz C, Orru M, Navarro G, Canela EI, Franco R, Goldberg SR (2010) Adenosine-cannabinoid receptor interactions. Implications for striatal function. Br J Pharmacol 160:443–453.
Finlay DB, Cawston EE, Grimsey NL, Hunter MR, Korde A, Vemuri VK, Makriyannis A, Glass M (2017) Gαs signalling of the CB1 receptor and the influence of receptor number. Br J Pharmacol 174:2545–2562.
Fletcher-Jones A, Hildick KL, Evans AJ, Nakamura Y, Henley JM, Wilkinson KA (2020) Protein Interactors and Trafficking Pathways That Regulate the Cannabinoid Type 1 Receptor (CB1R). Front Mol Neurosci 13.
Fletcher-Jones A, Hildick KL, Evans AJ, Nakamura Y, Wilkinson KA, Henley JM (2019) The C-Terminal helix 9 motif in rat cannabinoid receptor type 1 regulates axonal trafficking and surface expression. Elife 8:1–26.
Flores-Otero J, Ahn KH, Delgado-Peraza F, Mackie K, Kendall DA, Yudowski GA (2014) Ligand-specific endocytic dwell times control functional selectivity of the cannabinoid receptor 1. Nat Commun 5.
Földy C, Malenka RC, Südhof TC (2013) Autism-associated neuroligin-3 mutations commonly disrupt tonic endocannabinoid signaling. Neuron 78:498–509.
Frias CP, Liang J, Bresser T, Scheefhals L, Van Kesteren M, Van Dorland R, Yin Hu H, Bodzeta A, Van Bergen En Henegouwen PMP, Hoogenraad CC, Wierenga CJ (2019) Semaphorin4D induces inhibitory synapse formation by rapid stabilization of presynaptic boutons via MET coactivation. J Neurosci 39:4221–4237.
Frias CP, Wierenga CJ (2013) Activity-dependent adaptations in inhibitory axons. Front Cell Neurosci 7:1–16.
Fu Y, Huang ZJ (2010) Differential dynamics and activity-dependent regulation of α- and β-neurexins at developing GABAergic synapses. Proc Natl Acad Sci U S A 107:22699–22704.
Gautier A, Juillerat A, Heinis C, Corrêa IR, Kindermann M, Beaufils F, Johnsson K (2008) An Engineered Protein Tag for Multiprotein Labeling in Living Cells. Chem Biol 15:128–136.
González-Maeso J, Weisstaub N V., Zhou M, Chan P, Ivic L, Ang R, Lira A, Bradley-Moore M, Ge Y, Zhou Q, Sealfon SC, Gingrich JA (2007) Hallucinogens Recruit Specific Cortical 5-HT2A Receptor-Mediated Signaling Pathways to Affect Behavior. Neuron 53:439–452.
Graf ER, Zhang X, Jin SX, Linhoff MW, Craig AM (2004) Neurexins induce differentiation of GABA and glutamate postsynaptic specializations via neuroligins. Cell 119:1013–1026.
Grillo FW, Song S, Teles-Grilo Ruivo LM, Huang L, Gao G, Knott GW, MacO B, Ferretti V, Thompson D, Little GE, De Paola V (2013) Increased axonal bouton dynamics in the aging mouse cortex. Proc Natl Acad Sci U S A 110.
Grimsey NL, Graham ES, Dragunow M, Glass M (2010) Cannabinoid Receptor 1 trafficking and the role of the intracellular pool: Implications for therapeutics. Biochem Pharmacol 80:1050–1062.
Harkany T, Guzmán M, Galve-Roperh I, Berghuis P, Devi LA, Mackie K (2007) The emerging functions of endocannabinoid signaling during CNS development. Trends Pharmacol Sci 28:83–92.
Harris KM, Weinberg RJ (2012) Ultrastructure of synapses in the mammalian brain. Cold Spring Harb Perspect Biol 4:7.
Hebert-Chatelain E et al. (2016) A cannabinoid link between mitochondria and memory. Nature 539:555–559.
Howlett A, Blume L, Dalton G (2010) CB1 Cannabinoid Receptors and their Associated Proteins. Curr Med Chem 17:1382–1393.
Hua T et al. (2016) Crystal Structure of the Human Cannabinoid Receptor CB1. Cell 167:750-762.e14.
Huang ZJ, Scheiffele P (2008) GABA and neuroligin signaling: linking synaptic activity and adhesion in inhibitory synapse development. Curr Opin Neurobiol 18:77–83.
Jagla CAD, Scott CE, Tang Y, Qiao C, Mateo-Semidey GE, Yudowski GA, Lu D, Kendall DA (2019) Pyrimidinyl biphenylureas act as allosteric modulators to activate cannabinoid receptor 1 and initiate b-arrestin–dependent responses S. Mol Pharmacol 95:1–10.
Kano M, Ohno-Shosaku T, Hashimotodani Y, Uchigashima M, Watanabe M (2009) Endocannabinoid-mediated control of synaptic transmission. Physiol Rev 89:309–380.
Katona I, Urban GM, Wallace M, Ledent C, Jung K-M, Piomelli D, Mackie K, Freund TF (2006) Molecular Composition of the Endocannabinoid System at Glutamatergic Synapses. J Neurosci 26:5628–

5637.
Keck T, Scheuss V, Jacobsen RI, Wierenga CJ, Eysel UT, Bonhoeffer T, Hübener M (2011) Loss of sensory input causes rapid structural changes of inhibitory neurons in adult mouse visual cortex. Neuron 71:869–882.
Keimpema E, MacKie K, Harkany T (2011) Molecular model of cannabis sensitivity in developing neuronal circuits. Trends Pharmacol Sci 32:551–561 Available at: http://dx.doi.org/10.1016/j.tips.2011.05.004.
Ken H. Loh, Stawski PS, Draycott AS, Udeshi ND, Lehrman EK, Wilton DK, Svinkina T, Deerinck TJ, Ellisman MH, Stevens B, Carr SA, Ting AY (2016) Proteomic Analysis of Unbounded Cellular Compartments: Synaptic Clefts. Cell 166:1295-1307.e21.
Klatt O, Repetto D, Brockhaus J, Reissner C, El khallouqi A, Rohlmann A, Heine M, Missler M (2021) Endogenous β-neurexins on axons and within synapses show regulated dynamic behavior. Cell Rep 35.
Koschinski A, Zaccolo M (2017) Activation of PKA in cell requires higher concentration of cAMP than in vitro: Implications for compartmentalization of cAMP signalling. Sci Rep 7:1–12 Available at: http://dx.doi.org/10.1038/s41598-017-13021-y.
Kurucu H, Colom-Cadena M, Davies C, Wilkins L, King D, Rose J, Tzioras M, Tulloch JH, Smith C, Spires-Jones TL (2021) Inhibitory synapse loss and accumulation of amyloid beta in inhibitory presynaptic terminals in Alzheimer's disease. Eur J Neurol:1–13.
Laprairie RB, Bagher AM, Denovan-Wright EM (2017) Cannabinoid receptor ligand bias: implications in the central nervous system. Curr Opin Pharmacol 32:32–43 Available at: http://dx.doi.org/10.1016/j.coph.2016.10.005.
Laprairie RB, Bagher AM, Kelly MEM, Dupré DJ, Denovan-Wright EM (2014) Type 1 cannabinoid receptor ligands display functional selectivity in a cell culture model of striatal medium spiny projection neurons. J Biol Chem 289:24845–24862.
Lauckner JE, Hille B, Mackie K (2005) The cannabinoid agonist WIN55,212-2 increases intracellular calcium via CB1 receptor coupling to Gq/11 G proteins. Proc Natl Acad Sci U S A 102:19144–19149.
Lee K, Kima Y, Lee SJ, Qiang Y, Lee D, Lee HW, Kim H, Je HS, Südhof TC, Ko J (2013) MDGAs interact selectively with neuroligin-2 but not other neuroligins to regulate inhibitory synapse development. Proc Natl Acad Sci U S A 110:336–341.
Leterrier C (2021) Putting the axonal periodic scaffold in order. Curr Opin Neurobiol 69:33–40 Available at: https://doi.org/10.1016/j.conb.2020.12.015.
Leterrier C, Dubey P, Roy S (2017) The nano-architecture of the axonal cytoskeleton. Nat Rev Neurosci 18:713–726 Available at: http://dx.doi.org/10.1038/nrn.2017.129.
Leterrier C, Lainé J, Darmon M, Boudin H, Rossier J, Lenkei Z (2006) Constitutive activation drives compartment-selective endocytosis and axonal targeting of type 1 cannabinoid receptors. J Neurosci 26:3141–3153.
Li H, Yang J, Tian C, Diao M, Wang Q, Zhao S, Li S, Tan F, Hua T, Qin Y, Lin CP, Deska-Gauthier D, Thompson GJ, Zhang Y, Shui W, Liu ZJ, Wang T, Zhong G (2020) Organized cannabinoid receptor distribution in neurons revealed by super-resolution fluorescence imaging. Nat Commun 11 Available at: http://dx.doi.org/10.1038/s41467-020-19510-5.
Liebscher S, Page RM, Käfer K, Winkler E, Quinn K, Goldbach E, Brigham EF, Quincy D, Basi GS, Schenk DB, Steiner H, Bonhoeffer T, Haass C, Meyer-Luehmann M, Hübener M (2014) Chronic γ-secretase inhibition reduces amyloid plaque-associated instability of pre- and postsynaptic structures. Mol Psychiatry 19:937–946.
Liu YT, Tao CL, Lau PM, Zhou ZH, Bi GQ (2019) Postsynaptic protein organization revealed by electron microscopy. Curr Opin Struct Biol 54:152–160 Available at: https://doi.org/10.1016/j.sbi.2019.02.012.
Los G V. et al. (2008) HaloTag: A Novel Protein Labeling Technology for Cell Imaging and Protein Analysis. ACS Chem Biol 3.
Lu D, Immadi SS, Wu Z, Kendall DA (2019) Translational potential of allosteric modulators targeting the cannabinoid CB 1 receptor. Acta Pharmacol Sin 40:324–335 Available at: http://dx.doi.org/10.1038/s41401-018-0164-x.
Luo F, Sclip A, Merrill S, Südhof TC (2021) Neurexins regulate presynaptic GABAB-receptors at central synapses. Nat Commun 12:1–13 Available at: http://dx.doi.org/10.1038/s41467-021-22753-5.
Luxenburg C, Zaidel-Bar R (2019) From cell shape to cell fate via the cytoskeleton — Insights from the

epidermis. Exp Cell Res 378:232–237 Available at: https://doi.org/10.1016/j.yexcr.2019.03.016.
Ma L, Jongbloets BC, Xiong WH, Melander JB, Qin M, Lameyer TJ, Harrison MF, Zemelman B V., Mao T, Zhong H (2018) A Highly Sensitive A-Kinase Activity Reporter for Imaging Neuromodulatory Events in Awake Mice. Neuron 99:665-679.e5 Available at: https://doi.org/10.1016/j.neuron.2018.07.020.
Marti-Solano M, Crilly SE, Malinverni D, Munk C, Harris M, Pearce A, Quon T, Mackenzie AE, Wang X, Peng J, Tobin AB, Ladds G, Milligan G, Gloriam DE, Puthenveedu MA, Babu MM (2020) Combinatorial expression of GPCR isoforms affects signalling and drug responses. Nature 587:650–656 Available at: http://dx.doi.org/10.1038/s41586-020-2888-2.
Massengill CI, Bayless-Edwards L, Ceballos CC, Cebul ER, Qin M, Whorton MR, Ye B, Mao T, Zhong H (2021a) Highly sensitive genetically-encoded sensors for population and subcellular imaging of cAMP in vivo. bioRxiv:2021.08.27.457999 Available at: https://www.biorxiv.org/content/10.1101/2021.08.27.457999v1%0Ahttps://www.biorxiv.org/content/10.1101/2021.08.27.457999v1.abstract.
Massengill CI, Day-Cooney J, Mao T, Zhong H (2021b) Genetically encoded sensors towards imaging cAMP and PKA activity in vivo. J Neurosci Methods 362:109298 Available at: https://doi.org/10.1016/j.jneumeth.2021.109298.
Milosevic L, Kalia SK, Hodaie M, Lozano AM, Fasano A, Popovic MR, Hutchison WD (2018) Neuronal inhibition and synaptic plasticity of basal ganglia neurons in Parkinson's disease. Brain 141:177–190.
Mostany R, Anstey JE, Crump KL, Maco B, Knott G, Portera-Cailliau C (2013) Altered synaptic dynamics during normal brain aging. J Neurosci 33:4094–4104.
Nguyen PT, Schmid CL, Raehal KM, Selley DE, Bohn LM, Sim-Selley LJ (2012) β-Arrestin2 regulates cannabinoid CB 1 receptor signaling and adaptation in a central nervous system region-dependent manner. Biol Psychiatry 71:714–724 Available at: http://dx.doi.org/10.1016/j.biopsych.2011.11.027.
Njoo C, Agarwal N, Lutz B, Kuner R (2015) The Cannabinoid Receptor CB1 Interacts with the WAVE1 Complex and Plays a Role in Actin Dynamics and Structural Plasticity in Neurons. PLoS Biol 13:1–36.
Nogueras-Ortiz C, Yudowski GA (2016) The multiple waves of cannabinoid 1 receptor signaling. Mol Pharmacol 90:620–626.
Patel N, Gold MG (2015) The genetically encoded tool set for investigating cAMP: More than the sum of its parts. Front Pharmacol 6:1–11.
Pennacchietti F, Vascon S, Nieus T, Rosillo C, Das S, Tyagarajan SK, Diaspro A, del Bue A, Petrini EM, Barberis A, Zanacchi FC (2017) Nanoscale molecular reorganization of the inhibitory postsynaptic density is a determinant of gabaergic synaptic potentiation. J Neurosci 37:1747–1756.
Pettem KL, Yokomaku D, Takahashi H, Ge Y, Craig AM (2013) Interaction between autism-linked MDGAs and neuroligins suppresses inhibitory synapse development. J Cell Biol 200:321–336.
Raote I, Bhattacharyya S, Panicker MM (2013) Functional selectivity in serotonin receptor 2A (5-HT2A) endocytosis, recycling, and phosphorylation. Mol Pharmacol 83:42–50.
Roland AB, Ricobaraza A, Carrel D, Jordan BM, Rico F, Simon A, Humbert-Claude M, Ferrier J, McFadden MH, Scheuring S, Lenkei Z (2014) Cannabinoid-induced actomyosin contractility shapes neuronal morphology and growth. Elife 3:e03159.
Rozenfeld R (2011) Type I cannabinoid receptor trafficking: All roads lead to lysosome. Traffic 12:12–18.
Ruiter M, Lützkendorf C, Liang J, Wierenga CJ (2021) Amyloid-β Oligomers Induce Only Mild Changes to Inhibitory Bouton Dynamics. J Alzheimer's Dis Reports 5.
Ryberg E, Vu HK, Larsson N, Groblewski T, Hjorth S, Elebring T, Sjögren S, Greasley PJ (2005) Identification and characterisation of a novel splice variant of the human CB1 receptor. FEBS Lett 579:259–264.
Schmid CL, Raehal KM, Bohn LM (2008) Agonist-directed signaling of the serotonin 2A receptor depends on β-arrestin-2 interactions in vivo. Proc Natl Acad Sci U S A 105:1079–1084.
Shimojo M, Takuwa H, Takado Y, Tokunaga M, Tsukamoto S, Minatohara K, Ono M, Seki C, Maeda J, Urushihata T, Minamihisamatsu T, Aoki I, Kawamura K, Zhang MR, Suhara T, Sahara N, Higuchi M (2020) Selective disruption of inhibitory synapses leading to neuronal hyperexcitability at an early stage of tau pathogenesis in a mouse model. J Neurosci 40:3491–3501.
Shiraiwa K, Cheng R, Nonaka H, Tamura T, Hamachi I (2020) Chemical Tools for Endogenous Protein

Labeling and Profiling. Cell Chem Biol 27:970–985 Available at: https://doi.org/10.1016/j.chembiol.2020.06.016.
Shire D, Carillon C, Kaghad M, Calandra B, Rinaldi-Carmona M, Le Fur G, Caput D, Ferrara P (1995) An amino-terminal variant of the central cannabinoid receptor resulting from alternative splicing. J Biol Chem 270:3726–3731.
Simon AC, Loverdo C, Gaffuri AL, Urbanski M, Ladarre D, Carrel D, Rivals I, Leterrier C, Benichou O, Dournaud P, Szabo B, Voituriez R, Lenkei Z (2013) Activation-dependent plasticity of polarized GPCR distribution on the neuronal surface. J Mol Cell Biol 5:250–265.
Smith TH, Sim-Selley LJ, Selley DE (2010) Cannabinoid CB 1 receptor-interacting proteins: Novel targets for central nervous system drug discovery? Br J Pharmacol 160:454–466.
Specht CG, Izeddin I, Rodriguez PC, ElBeheiry M, Rostaing P, Darzacq X, Dahan M, Triller A (2013) Quantitative nanoscopy of inhibitory synapses: Counting gephyrin molecules and receptor binding sites. Neuron 79:308–321 Available at: http://dx.doi.org/10.1016/j.neuron.2013.05.013.
Stuchlik A (2014) Dynamic learning and memory, synaptic plasticity and neurogenesis: An update. Front Behav Neurosci 8:1–6.
Sun YJ, Sebastian Espinosa J, Hoseini MS, Stryker MP (2019) Experience-dependent structural plasticity at pre- And postsynaptic sites of layer 2/3 cells in developing visual cortex. Proc Natl Acad Sci U S A 116:21812–21820.
Suzuki K et al. (2016) In vivo genome editing via CRISPR/Cas9 mediated homology-independent targeted integration. Nature 540:144–149.
Takeuchi T, Duszkiewicz AJ, Morris RGM (2014) The synaptic plasticity and memory hypothesis: Encoding, storage and persistence. Philos Trans R Soc B Biol Sci 369.
Terzian AL, Drago F, Wotjak CT, Micale V (2011) The dopamine and cannabinoid interaction in the modulation of emotions and cognition: Assessing the role of cannabinoid CB1 receptor in neurons expressing dopamine D1 receptors. Front Behav Neurosci 5:1–10.
Thibault K, Carrel D, Bonnard D, Gallatz K, Simon A, Biard M, Pezet S, Palkovits M, Lenkei Z (2013) Activation-dependent subcellular distribution patterns of CB1 Cannabinoid Receptors in the Rat Forebrain. Cereb Cortex 23:2581–2591.
Trotter JH, Hao J, Maxeiner S, Tsetsenis T, Liu Z, Zhuang X, Südhof TC (2019) Synaptic neurexin-1 assembles into dynamically regulated active zone nanoclusters. J Cell Biol 218:2677–2698.
Turu G, Hunyady L (2010) Signal transduction of the CB1 cannabinoid receptor. J Mol Endocrinol 44:75–85.
Wang W, Jia Y, Pham DT, Palmer LC, Jung KM, Cox CD, Rumbaugh G, Piomelli D, Gall CM, Lynch G (2018a) Atypical Endocannabinoid Signaling Initiates a New Form of Memory-Related Plasticity at a Cortical Input to Hippocampus. Cereb Cortex 28:2253–2266.
Wang W, Qiao Y, Li Z (2018b) New Insights into Modes of GPCR Activation. Trends Pharmacol Sci 39:367–386 Available at: http://dx.doi.org/10.1016/j.tips.2018.01.001.
Weinberg ZY, Crilly SE, Puthenveedu MA (2019) Spatial encoding of GPCR signaling in the nervous system. Curr Opin Cell Biol 57:83–89 Available at: https://doi.org/10.1016/j.ceb.2018.12.006.
Wierenga CJ (2017) Live imaging of inhibitory axons: Synapse formation as a dynamic trial-and-error process. Brain Res Bull 129:43–49 Available at: http://dx.doi.org/10.1016/j.brainresbull.2016.09.018.
Wierenga CJ, Becker N, Bonhoeffer T (2008) GABAergic synapses are formed without the involvement of dendritic protrusions. Nat Neurosci 11:1044–1052.
Willems J, de Jong APH, Scheefhals N, Mertens E, Catsburg LAE, Poorthuis RB, de Winter F, Verhaagen J, Meye FJ, MacGillavry HD (2020) Orange: A CRISPR/Cas9-based genome editing toolbox for epitope tagging of endogenous proteins in neurons. Available at: http://dx.doi.org/10.1371/journal.pbio.3000665.
Winckler B, Mellman I (2010) Trafficking guidance receptors. Cold Spring Harb Perspect Biol 2:1–18.
Zhou L, Bohn LM (2014) Functional selectivity of GPCR signaling in animals. Curr Opin Cell Biol 27:102–108 Available at: http://dx.doi.org/10.1016/j.ceb.2013.11.010.
Zhou R, Han B, Xia C, Zhuang X (2019) Membrane-associated periodic skeleton is a signaling platform for RTK transactivation in neurons. Science (80-) 365:929–934.

Appendix

About the author

Jian was born on the 5th of December of 1989 in Sichuan province (Southwestern of China). He started biological research as a bachelor student in Chinese West Normal University since 2009. After graduated from 2013, he continued to a further training in plant cell biology with Dr. Shingo Nagawa at Shanghai Center for Plant Stress Biology (PSC), then he got his master degree in 2016. In the autumn of the same year, Jian joined Dr. Corette Wierenga's Lab at Utrecht University, where he investigated the mechanism of endocannabinoids modulates inhibitory bouton dynamics via high resolution two-photon microscopy. Since 2021, Jian moved back to China, worked as a postdoctoral researcher in the group of Dr. Bo Zhang at Shenzhen Bay Laboratory (SZBL), where he will continue to explore the function and mechanism of endocannabinoids' receptors and other orphan GPCRs in synapse development and in brain diseases.

List of presentations

(1) **Jian Liang**, Corette Wierenga. Regulation of inhibitory presynaptic bouton dynamics by endocannabinoid signaling, CAPBS meeting, Nijmegen 2018. (**Oral presentation**)

(2) **Jian Liang**, Corette Wierenga. Regulation of inhibitory presynaptic bouton dynamics by endocannabinoid signaling. Dutch Neuroscience Meeting, Lunteren 2018, 2019 **(poster)**

(3) **Jian Liang**, Corette Wierenga. Regulation of inhibitory presynaptic bouton dynamics by endocannabinoid signaling, 3rd axon meeting, Alicante, Spain, 2019 (**poster**)

(4) **Jian Liang**, 26th Annual PhD meeting, ONWAR 2019. Regulation of inhibitory presynaptic bouton dynamics by endocannabinoid signaling, Zeist, Utrecht, 2019 (**Oral presentation**)

(5) **Jian Liang,** 2020 IB College Tour, Atypical endocannabinoid signal mediates new inhibitory bouton formation. (**Online oral presentation**)

List of publications

(1) Frias CP, **Liang J,** Bresser T, Scheefhals L, van Kesteren M, van Dorland R, Hu HY, Bodzeta A, van Bergen En Henegouwen PMP, Hoogenraad CC, Wierenga CJ. Semaphorin4D Induces Inhibitory Synapse Formation by Rapid Stabilization of Presynaptic Boutons via MET Coactivation. J Neurosci. 2019 May 29;39(22):4221-4237.

(2) Ruiter M, Lützkendorf C, **Liang J**, Wierenga CJ. Amyloid-β Oligomers Induce Only Mild Changes to Inhibitory Bouton Dynamics. J Alzheimers Dis Rep. 2021 Feb 27;5(1):153-160.

(3) **Liang J**, Kruijssen DLH, Verschuuren ACJ, Voesenek BJB, Benavides FFW, Sáez Gonzalez M, Ruiter M, Wierenga CJ. Axonal CB1 Receptors Mediate Inhibitory Bouton Formation via cAMP Increase and PKA. J Neurosci. 2021 Oct 6;41(40):8279-8296. doi: 10.1523/JNEUROSCI.0851-21.2021.

(4) **Jian Liang**, Corette J Wierenga. Endocannabinoid signaling at excitatory and inhibitory synapses, 2022.(book chapter, under review)

English Summary

The synapse is a basic subcellular unit for neural communication. Synaptic changes such as synaptic potentiation or depression, are recognized to be the underlying mechanism for learning and memory. Defects in synapse development are associated with various brain diseases. Although the mechanism for excitatory synapse development is intensively investigated in past decades, the molecular mechanism underneath of inhibitory synapse development is less understood. The development of a single synapse goes through multiple phases including axons and dendrites are closed to each other, initiation of axon-dendrite contact, recruitment of synaptic proteins, synaptic pruning and maturation, and ultimately to be a functional synapse. With high resolution microscopy, the dynamic process of synapse formation can be monitored. For instance, during my PhD, I used two-photon microscopy to trace the dynamics of inhibitory bouton. These boutons dynamically disappear and reappear or new bouton formation. Inhibitory bouton dynamics might be tightly regulated by various intrinsic or extrinsic factors including secreted proteins, modulators, and neuronal activity. In the present thesis, I aimed to explore the molecular mechanism for inhibitory bouton formation and stabilization.

In chapter 2, we showed that secreted semaphorin Sema4D plays a crucial role in stabilization of inhibitory boutons. Exogeneous application of Sema4D promotes bouton stabilization and this process can be inhibited by either blocking neuronal activity or MET receptor activity. Additionally, Sema4D mediates bouton stabilization requires actin depolymerization and ROCK activity, which is supposed to be the downstream of MET receptor. Mutations in MET are recognized as a risk factor for autism spectrum disorder (ASD), but the function of MET was not fully understood. Here we proposed that Sema4D interacts with MET to mediate inhibitory bouton stabilization. This novel insight may shed a new light on the mechanism of ASD.

In chapter 3, we investigated the molecular mechanism of endocannabinoids signaling in inhibitory bouton formation. Endogenous cannabinoids are synthesized and released from the post-synapse to activate G-protein coupled receptors located on the presynaptic axon, such as the CB1 receptor. We described that the activation of CB1 receptors promotes bouton formation and stabilization, which is consistent with our previous reports. Interestingly, we further explore that the atypical G_s signal pathway is underlying axonal CB1 receptor mediated new bouton formation. In addition, this process is not affected by neuronal activity or the G_i protein

pathway. Endocannabinoid signaling is tightly implicated in learning and memory, and additions and dysfunction of endocannabinoid signaling is associated with multiple brain diseases, including Alzheimer's disease and Parkinson's disease. Our investigations provide new insights into the endocannabinoid signaling system. Furthermore, **in chapter 4**, we assessed the internalization of activated CB1 receptors via different agonists. We observed that the distribution pattern of CB1 receptors is changed upon activation by two distinct agonists, 2-AG and WIN. Consequently, repeated activation via WIN but not 2-AG induced CB1 receptor clustering at somata. We hypothesized that this difference probably results from functional selectivity which is less studied in endocannabinoid receptors. Additionally, we observed that CB1 receptor expression patterns are different between cultured slices and cultured neurons. The functional selectivity couldn't be reproduced in cultured neurons, which indicates that the distribution of CB1 receptors may need neuronal network activity. The distribution of CB1 receptor determines their function. The mechanism related to functional selectivity of CB1 receptor is still needed to be investigated in the future.

Here we used multiple techniques including high-resolution two live photon imaging, and electrophysiology, combined with pharmacology, chemogenetics, and viruses to investigate the factors or modulators involved in inhibitory bouton development. My thesis clearly broads our understanding of inhibitory synapse development.

Nederlandse Samenvatting

De synaps is dé subcellulaire eenheid voor neuronale communicatie. Het veranderen van synapsen , zoals synaptische potentiëring of depressie, wordt gezien als het mechanisme achter leren en geheugen. Defecten in de ontwikkeling van synapsen worden in verband gebracht met verschillende hersenziekten. Hoewel het mechanisme voor de ontwikkeling van stimulerende synapsen de afgelopen decennia intensief onderzocht is, is het moleculaire mechanisme achter de ontwikkeling van remmende synapsen nog minder bekend. Synapsontwikkeling doorloopt verschillende stappen, die begint met dicht bij elkaar liggende axonen en dendrieten, de initiatie van axon-dendrietcontact, de rekrutering van synaptische eiwitten, de snoei en rijping van synapsen, en tenslotte om de functionele synaps. Met hoge resolutie microscopie kan het dynamische proces van synapsvorming worden gevolgd. Zo heb ik tijdens mijn doctoraat twee-fotonenmicroscopie gebruikt om de remmende bouton-dynamiek te bestuderen. Remmende boutons zijn dynamisch; ze verdwijnen en verschijnen weer en er worden nieuwe boutons gevormd. Remmende bouton-dynamiek kan strak worden gereguleerd door verschillende intrinsieke of extrinsieke factoren, waaronder uitgescheiden eiwitten, modulatoren en neuronale activiteit. In dit proefschrift odnerzocht ik het moleculaire mechanisme achter de vorming en stabilisatie van remmende boutons.

In hoofdstuk 2 hebben we laten zien dat de door hersencellen afgegeven semaphorin Sema4D een cruciale rol speelt bij het stabiliseren van de remmende boutons. Exogene Sema4D bevordert de stabilisatie van de boutons en dit proces kan worden geremd door neuronale activiteit of MET-receptoractiviteit te blokkeren. Bovendien zijn door Sema4D stabiliserende boutons vereist voor actine depolymerisatie en ROCK-activiteit, die de afhankelijk van de MET-receptor zijn. Er zijn mutaties in MET bekend die een risicofactor voor autisme vormen), maar de functie van MET was nog niet bekend. Wij stellen dat Sema4D een interactie aangaat met MET-gemedieerde, stabiliserende, remmende boutons om een functionele synapsen te vormen. Dit nieuwe onderzoek kan een nieuw licht werpen op het mechanisme van autisme.

In hoofdstuk 3 onderzochten we het moleculaire mechanisme waarmee signalering door endocannabinoïden leidt tot de vorming van remmende boutons. Endogene cannabinoïden worden gesynthetiseerd en vrijgegeven uit postsynaps om presynaptische, op het axon-gelokaliseerde G-eiwit-gekoppelde receptoren, zoals CB1-receptor, te activeren. We hebben

beschreven dat activering van de CB1-receptor de vorming en stabilisatie van bouton bevordert, wat consistent is met ons eerdere werk. Interessant is dat de CB1-receptor-gemedieerde nieuwe bouton-vorming gebruik maakt van atypische Gs-signalering . Bovendien is dit proces onafhankelijk door neuronale activiteit of Gi-signalering. Endocannabinoïd signalering is belangrijk voor bij leren en geheugen. Een disfunctie van de signalering door endocannabinoïden wordt in verband gebracht met meerdere hersenziekten, waaronder de ziekte van Alzheimer en de ziekte van Parkinson. Ons onderzoek biedt nieuwe inzichten in het signaleringssysteem van endocannabinoïden. Verder hebben we **in hoofdstuk 4** de internalisatie van geactiveerde CB1-receptoren via verschillende agonisten beoordeeld. We hebben waargenomen dat de distributie van CB1-receptoren verandert bij activering door twee verschillende agonisten, 2-AG en WIN. De CB1-receptor clustert op cellichamen door, herhaalde activering via WIN maar niet door 2-AG. We veronderstelden dat dit komt door functionele selectiviteit van endocannabinoïde-receptoren die nog niet veel bestudeerd is. Bovendien hebben we waargenomen dat expressiepatronen van CB1-receptoren verschillen tussen gekweekte plakjes en gekweekte neuronen. De functionele selectiviteit kon niet worden gereproduceerd in gekweekte neuronen, wat aangeeft dat de distributie van CB1-receptoren mogelijk neuronale netwerkactiviteit nodig heeft. De verdeling van de CB1-receptor bepaalt de functie ervan. Het mechanisme achter de functionele selectiviteit van de CB1-receptor moet in de toekomst nog worden onderzocht.

Hier hebben we meerdere technische gebruikt, waaronder twee-fotonenmicroscopie, en elektrofysiologie, gecombineerd met farmacologische, chemogeneticische virusmethoden om de factoren te onderzoeken die betrokken zijn bij de ontwikkeling van remmende bouton. Mijn proefschrift verbreedt ons begrip van de ontwikkeling van remmende synapsen.

Acknowledgements

Finally, I got here. My PhD has been like a long journey, and I have gained many different experiences. I still remember that I was scared and made phone calls to a lot of people when I departed from Shanghai Pudong international airport. But I was very excited when I arrived in the Netherlands in the morning. Immediately, I knew it was the right place, as it was just like what I had seen in my textbooks. I have shared my experiences with many people and told them that Netherlands is such a beautiful country. During my master program I was involved in plant research. At the beginning in Utrecht, it was often frustrating to learn new concepts in electrophysiology, also because my English was very poor at that moment. But I didn't give up, and somehow, I managed. Eventually, I got a full training in neuroscience research and synaptic physiology in the Wierenga Lab at Utrecht University. Therefore, I would like to give my big thanks to a lot of people and a few organizations here.

First of all, I would like to thank my supervisor Dr. Corette Wierenga. Without her help, I am sure that I would not have finished my project and get my PhD. Corette is such a passionate and ambitious scientist. She always encouraged me to reach out, talk and discuss with colleagues in the field, go to conferences to share my work and discover new things, even though I am shy and feel like a don't have many ideas. She showed me to be critical at the bouton analysis and to be critical when reading papers, from which I benefited a lot. She established a great working environment in the lab, in which everyone just liked to share and discuss the projects, but also the life without science. I also really enjoyed the science weekend for the public. I remember so many funny and happy moments in our lab, our New Year part, the dinners… It's my great honor to work with you and get help from you.

Then I would like to thank Prof. Dr. Anna Akhmanova and Prof. dr. Casper Hoogenraad. Anna is such an experienced scientist that I am always astonished with her wealth of knowledge. All the comments you gave me in department meeting were very helpful. Casper, I still remember you were the first people who said "welcome" to me. I also thank you for sharing lab space and antibodies with us. I also like to thank the other faculty members in Cell Biology and Development Biology department, including Dr. Harold MacGillavry, Dr. Florian Berger, Dr. Ginny G. Farías, Prof. Dr. Lukas C. Kapitein, Prof. dr. Sander van den Heuvel, Prof. dr. Mike Boxem, Dr. Esther de Graaffand and Dr. Martin Harterink. Your comments and discussions about my project during our regularly meeting helped me a lot. I always enjoyed

our Friday borrels, lab outings and the New year party with you guys.

I would like to thank my committee members spending such long time reading and accepting my thesis. Particularly, I want to thank my paranymphs Carlijn and Fangrui. Carlijn is a great and warm-heatedness person. Your suggestions and comments to improve my thesis really were great. Fangrui, we are really close friends. It is very nice to meet you here and you are such a nice person. I witnessed that you changed from one person to a family of three, which is amazing. I was very surprised that Momo still remembered me when I came back to China. She is just so cute. The food from you and Yuanjie is so great that I am missing it a lot, even when I am in China.

Importantly, I want to thank the former and current members in Wierenga Lab. René, I can tell you are a nice person. I appreciated all your assistance in the lab. It is my great honor that you invited me to your house and your wedding (it was cancelled caused by COVID19, unfortunately). I would like to give my best wishes to you and your wife. I know you like to travel around the world. I hope you will travel to China and visit me one day. Dennis was the first person I met in the lab after Corette. Dennis introduced the lab to me and helped me to register in the service desk at the faculty of science. You are such a great person, and my discussions with you in the lab always helped me grow. Thank you so much and I wish you the best with your career at the University of Amsterdam. Hai Yin, you are such a smart person. You did the computer software and established the inflow and outflow system of the 2 photon setups for us. Thank you for all your help and suggestions. Cátia, thank you for all your bouton knowledge and for introducing me to the analysis method and bouton definitions. Marvin, you are a nice guy who likes to help other people. Thank you for your help with the puncta analysis, ephys data and suggestions for supervising master students. Thank you, Lotte, for organizing all the 2-photon microscope maintenance. Good luck with your PhD. Ate and Bart, it was my pleasure meeting you at the end of my PhD, thank you for organizing the online party! Maria, a big thanks to your help with the ephys data, I know it took a long time to reanalysis. And finally, I want to give a big thanks to the master students who worked with me. Aniek, I am proud that you managed to finish your thesis report. Congratulations to you on your great job. Bas, you are quiet and smart, and you work very efficient. I am very happy to have worked with you. I am convinced that you will do great in science, and I know that you will go for a PhD. Feline, thank for your help with the ephys data, good luck with your PhD in Rotterdam. Marijn, thank you for introducing me to Friesland, for being

such a very nice person. Matthijs, thank you for sharing your knowledge about bouton analysis at the beginning of my PhD, which was very helpful. And I also like to give thanks to Christine, Elske, Joe, Claudia and Iris. It was amazing that we could meet in Utrecht and work together for a while. All my best wishes to your career and life.

I would like to thank my officemates. Ilya, you are absolutely a humorous person, and I have enjoyed the non-science discussions between you and Fangrui. I will never forget your outfit on Easter Day, it was very impressive. And thank you for sharing your knowledge about the historic relationship between China and Russia. Cyntha Babet and Milena, I was happy to have you as officemates. Our office clearly gained vitality when you joined. I felt everyone was happier. And Fangrui, you are definitely a great person with humor and enthusiasm. Karin and Mithila, nice to meet you at the beginning of my PhD. Thank for Karin's gift and the plant on my desk grows well. I also like to thank Bart and Ha. I was happy to be your officemate during the pandemic of COVID19.

Our lab shared the wet lab room with the Casper group. I occasionally used stuff including some antibodies from the Casper group. Here, I appreciate and respect the Casper group and everyone who worked in N525, thank you for your generosity and help. Importantly, a big thanks goes out to Phebe. You organize the lab and the department very well. I also would like to thank Ilya and Eugene for introducing me to confocal microscopy and Wilco for organizing the virus room.

I met a lot of wonderful people in Netherlands. Eitan, you are such a great person, with a lot of humor. Thank you very much that you invited me to your parties. I know that you moved back to Israel. All my best wishes to you and your girlfriend. Riccardo, thank you for sharing funny stories during lunch time, good luck in Switzerland. I spent most of my PhD time on the fifth floor of the Kruytgebouw building. It was my great pleasure to meet everyone on the fifth floor, including Ankit Rai, Arthur de Jong, Anna Bodzeta, Inês, Manon, Nicky, Lisa, Jelmer, Peter Jan, York, Chiung-Yi, Roderick, Sybren, Robin, Robbelien, Feline, Vincent, Katerina, Vida, Thomanai, Sara, Mai Dai, Dipti, Funso, Boris, Joyce, Jessica, Mai Dan Nazmiye and many other members from Anna's lab, Casper's lab, Lucas's lab, Harold's lab, Ginny's lab, Florian's lab, Sabrina's lab, Paul's lab, Sander's lab, and Mike's lab.

Especially, I would like to thank my many Chinese friends in China and in the

Netherlands. Zhi Liu, Qi Zhou, Shasha in Sichuan, Xin Zhou in Dongguan city, Chunlei, Guokai, Jialin and Yong in Shanghai, and so on…, thank you for your ongoing help and support. I also met a lot of Chinese students like me who came to study neuroscience here. Yi Qin, Miao Chen, Yongbing, Jian Dong and Jing in Amsterdam, and Chao Guo in Nijmegen. You guys did great jobs, and congratulations and good luck with your scientific careers. Jingchao and Kai did great work here which inspired me and Fangrui (I guess). Chao also did a great job, and I would like to say thanks to Chao and Lilin, who invited me to their house to enjoy Chinese food, which is super memorable. Time flies, and you are now a father of two children. Liu, it is always great to talk with you, and you are doing absolutely nice work here. You are smart and you work hard. I believe that you will achieve a lot. Yujie and Xingxiu, you guys are like my big brother and sister, thanks for taking care of me. I very much appreciated this, and I hope to visit you in California one day. Tianshu and Bo - the "running men" - it is always a great pleasure to go cycling with you. Wenjuan, you did great work here, and inspired me to work hard. I am really glad to be your friend. Yuanjie, Qingkang, Hui Wang, Yuhao, Yang Xu, Jing Gan, Bohui, Muge, Wentao, it is my great pleasure to meet you here.

I want to give a big thank to my landlord in Utrecht, Mr. Dapei Hu. I also call you "Uncle Hu". Thank you and your family for taking care of me in the past four years. I am very grateful that I was so lucky to meet you in the Netherlands. I still remember how astonished you were when I came ringing your doorbell, alone with two big suitcases, which was the first time we met. Thank for you sharing tips on living in Utrecht, introducing the supermarkets and restaurants, and for sharing your story about that why and when you moved to the Netherlands in 1980s. I know you got ill, which gives you trouble hard to walk around. I pray it will not become worse, and I hope your family will take care of you very well. I also like to thank your son, Mr Shaowei Hu, and your daughter-in-law Mrs Hu (Qun Lin). You two are so warm-hearted. Please feel always welcome to visit me when you are in China. The past years, I had many housemates, Ting Yu, Min Shen, Dr. Jiwen Xia, Dr. Wenjie Fang, Yumeng Yang, Wu Li, Dr Bo Lou, Yang Cheng, Dr. Xincun Wang, Jiali, Siluo. It was my great pleasure to meet you in Utrecht.

I want to give a big thank to China Scholarship Council (CSC), which provided the finances to support my study abroad, and to Utrecht University, for having this cooperation scholarship with the Chinese government. I also thank Utrecht city. I have lived here for more than four years, and I always felt happy and comfortable. Utrecht is a historical city with many old buildings,

churches, old streets, which occupies a persistent piece of my memory. I will always remember the fireworks on the New Year Eve, the Christmas market and the activities at King's Day…

Last but not the least, I want to express my thanks to my family. It was hard for all of us when I studied abroad. My parents always worried about me as I am short and I don't have Kungfu, especially when I lived alone in another country. I also missed China and my family a lot. Right now, it is great that I am working in China, so I can spend more time with my parents. In the end, I would like to offer my special thank to Ms Joya Cai for her always encouragement and support. You are just so gorgeous!

Jian in Shenzhen, China
2021

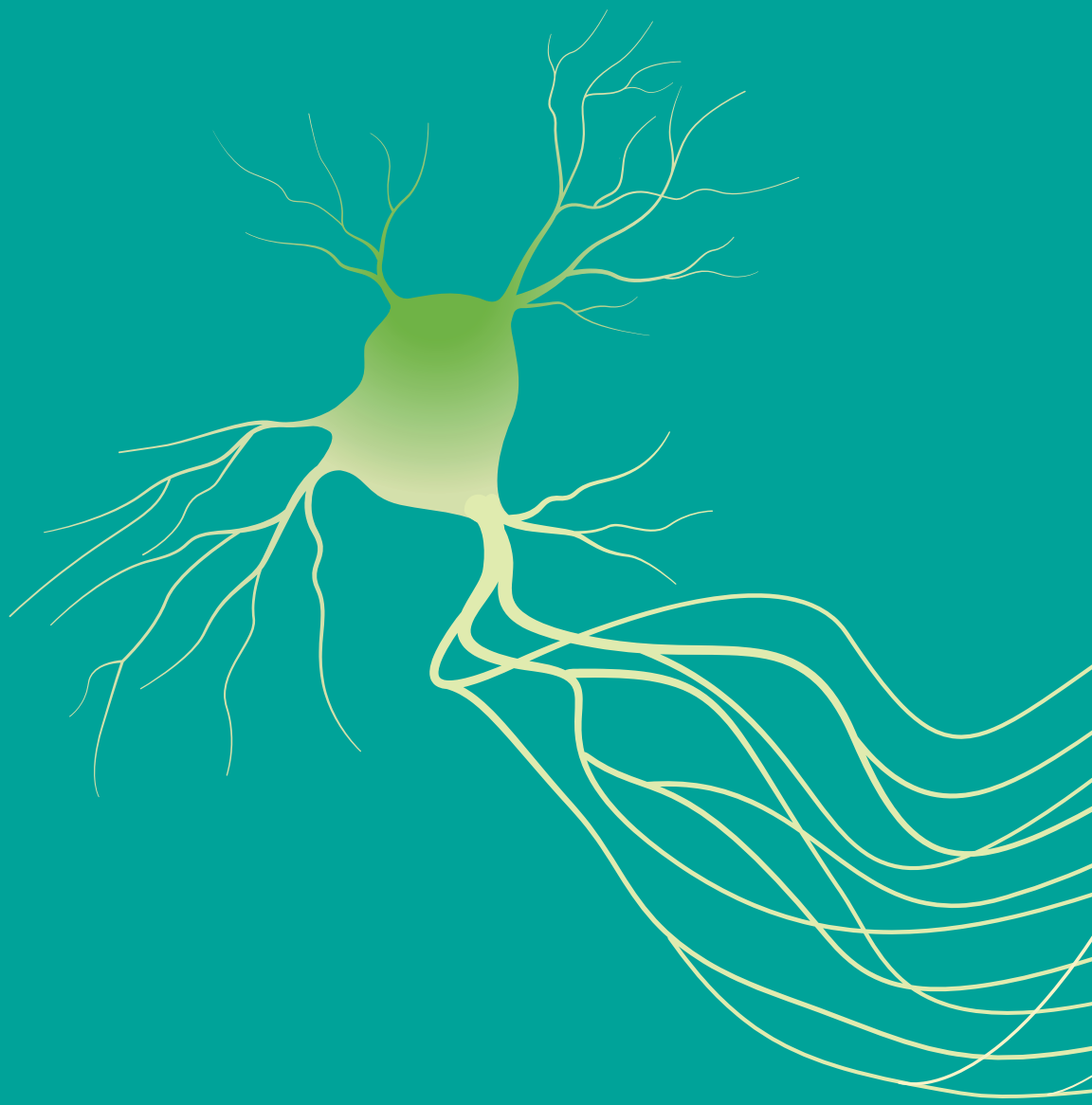

UMC Utrecht

Universiteit Utrecht

ISBN: 978-94-6458-148-5